A fresh look at AMPK signaling: multiple functions of novel interacting proteins

Sarah Zorman

UNIVERSITÉ DE GRENOBLE

LBFA U 1055

THÈSE

Pour obtenir le grade de

DOCTEUR DE L'UNIVERSITÉ DE GRENOBLE

Spécialité : **Biologie Moléculaire & Cellulaire**

Arrêté ministériel : 7 août 2006

Présentée par

Sarah ZORMAN

Thèse dirigée par **Uwe SCHALTTNER**

Préparée au sein du **Laboratoire de Bioénergétique Fondamentale et Appliquée**, dans **l'École Doctorale de Chimie et Sciences du Vivant**

Nouveau regard sur la signalisation AMPK : multiples fonctions de nouveaux interacteurs

Thèse soutenue publiquement le **8 novembre 2013**,
Devant le jury composé de :

Theo WALLIMANN
Professeur émérite de l'Université ETH Zurich, Rapporteur
Philippe ROUET
Directeur de recherche INSERM, Rapporteur
Jérôme GARIN
Directeur de recherche INSERM, Examinateur
Marc BILLAUD
Directeur de recherche CNRS, Examinateur
Michel SEVE
Professeur de l'Université Joseph Fourier, Président
Uwe SCHLATTNER
Professeur de l'Université Joseph Fourier, Directeur de Thèse

Université Joseph Fourier / Université Pierre Mendès France /
Université Stendhal / Université de Savoie / Grenoble INP

Remerciements

Avant d'aborder le travail scientifique qui fait l'objet de mon doctorat, je voudrais remercier ceux qui ont participé à différents niveaux à sa maturation. Je tiens à remercier Uwe Schlattner pour son accompagnement tout au long de ces trois ans, sa confiance, son écoute et la pertinence de ses conseils scientifiques.

Je remercie les membres du jury, Theo Walliman, Philippe Rouet, Jérôme Garin, Marc Billaud ainsi que Michel Sève pour avoir donné de leur temps et de leur compétence afin de juger ce travail.

Merci aux membres du laboratoire, en particulier Evangelia Mourmoura et Marie Le Guen pour leur soutien et leur amitié tout au long de ces trois années, mais aussi à Clovis Chabert, Fecal Ounnas et Martin Pelosse qui m'auront beaucoup fait rire. Cette thèse s'est déroulée au LBFA, où j'ai bénéficié de l'excellente qualité du service technique. Pour cela merci Sarah Hamant et Gérard Larmurier toujours disponibles et sérieux vous avez facilité ma vie au quotidien. Merci également à Stéphane Attia pour son assistance ainsi qu'à Hervé Dubouchaud pour sa gentillesse et son aide avec mon indispensable collègue, l'ordinateur. Finalement je voudrais remercier Christine Demeilliers qui m'a introduit au sein de ce laboratoire.

J'ai eu la chance de collaborer avec Pascual Sanz (IBV, Valencia, Espagne) qui m'a accueillie au sein de son laboratoire pendant trois mois. Merci à lui et toute son équipe très chaleureuse, auprès de qui j'ai beaucoup appris.

Je tiens à associer à ces remerciements le ministère de la recherche pour le financement de mon doctorat.

Pour terminer, mes pensées vont à ceux qui sont la clé de qui je suis aujourd'hui : Mick et Michel. Merci de m'avoir tout donné et même un peu plus. Cyril, Laurent, Sylvain mais aussi Virginie, ces 27 ans à grandir à vos côté m'ont énormément apporté. Un grand merci à chacun des petit zormans pour leurs rires qui rendent la vie plus douce.

Je ne pourrais finir sans remercier Alex pour son amour et son humour qui m'accompagnent chaque jour.

Abstract. AMP-activated protein kinase (AMPK) is a central energy sensor and regulator of cellular energy state, but the AMPK signaling network is still incompletely understood. Two earlier non-biased screens for AMPK interaction partners and substrates performed in the laboratory identified several candidate proteins, but functional and physiological roles remained unclear. Here we characterized the functional relationship of AMPK with four different protein interaction partners: gluthatione S-transferases (GSTP1 and GSTM1), fumarate hydratase (FH), an E3 ubiquitin-ligase (NRDP1), and vesicle-associated membrane proteins (VAMP2 and VAMP3). Each of these interaction partners seems to have a different function in AMPK signaling, either acting up- or down-stream of AMPK. GSTP1 and GSTM1 can contribute to AMPK activation by facilitating S-glutathionylation of AMPK under mildly oxidative conditions. This non-canonical regulation suggests AMPK as a sensor of cellular redox state. Mitochondrial FH was identified as the only clear AMPK downstream substrate, but surprisingly the phosphorylation site is present in the mitochondrial targeting prepeptide, possibly affecting mitochondrial import. NRDP1, whose expression as a full-length soluble protein was achieved here for the first time, is phosphorylated by AMPK only at low levels. The interaction does neither serve for AMPK ubiquitinylation, but rather affects NRDP1 turnover. Finally, interaction of VAMP2/3 with AMPK does not involve phosphorylation or activation events of one of the partners. Instead, we propose VAMP2/3 as scaffolding proteins that recruit AMPK to exocytotic vesicles which could favor phosphorylation of vesicular AMPK substrates for exocytosis. Collectively, our results add some new elements to the AMPK signaling network, suggesting that it is much more complex than anticipated. In addition to upstream kinases and downstream substrates, regulation of AMPK signaling occurs by secondary protein modifications other than phosphorylation, by effects on protein turnover, and probably also by specific subcellular recruitment of AMPK.

Résumé. La protéine kinase activée par AMP (AMPK) est un senseur et régulateur central de l'état énergétique cellulaire, mais ces voies de signalisation ne sont pour le moment que partiellement comprises. Deux criblages non-biaisés pour la recherche de partenaires d'interaction et de substrats d'AMPK ont précédemment été réalisés dans le laboratoire. Ces derniers ont permis l'identification de plusieurs candidats (protéines), mais leur rôle fonctionnel et physiologique n'était pas encore établi. Ici nous avons caractérisé la fonction de la relation entre AMPK et quatre partenaires d'interaction : gluthation S-transferases (GSTP1 and GSTM1), fumarate hydratase (FH), l'E3 ubiquitine-ligase (NRDP1), et les protéines associées à la membrane (VAMP2 and VAMP3). Chacune de ces interactions parait avoir un rôle différent dans la signalisation AMPK, agissant en amont ou en aval de la protéine AMPK. GSTP1 et GSTM1 contribueraient à l'activation d'AMPK en facilitant la S-glutathionylation d'AMPK en conditions oxydatives moyennes. Cette régulation non-canonique suggère que l'AMPK peut être un senseur de l'état redox cellulaire. FH mitochondrial est l'unique substrat AMPK clairement identifié. Etonnamment le site de phosphorylation se trouve dans le peptide signal mitochondrial, ce qui pourrait affecter l'import mitochondrial. NRDP1, protéine pour laquelle nous avons pour la première fois développé un protocole de production de la protéine soluble, est faiblement phosphorylée par l'AMPK. L'interaction ne sert pas à l'ubiquitination d'AMPK, mais affecte le renouvellement de NRDP1. Finalement, l'interaction de VAMP2/3 avec AMPK n'implique pas d'évènement de phosphorylation ou d'activation d'un des partenaires. Nous proposons un mécanisme de recrutement d'AMPK par VAMP2/3 (« scaffold ») au niveau des vésicules en exocytose. Ce recrutement favoriserait la phosphorylation de substrats de l'AMPK à la surface des vésicules en exocytoses. Une fois mis en commun, nos résultats enrichissent les connaissances sur les voies de signalisation AMPK, et suggèrent une grande complexité de ces dernières. Plus que les kinases en amont et des substrats en aval, la régulation de la signalisation d'AMPK se fait *via* des modifications secondaires autres que la phosphorylation, *via* des effets sur le renouvellement de protéines, et probablement *via* un recrutement spécifique de l'AMPK dans certains compartiments cellulaires.

Table of contents

PART 1

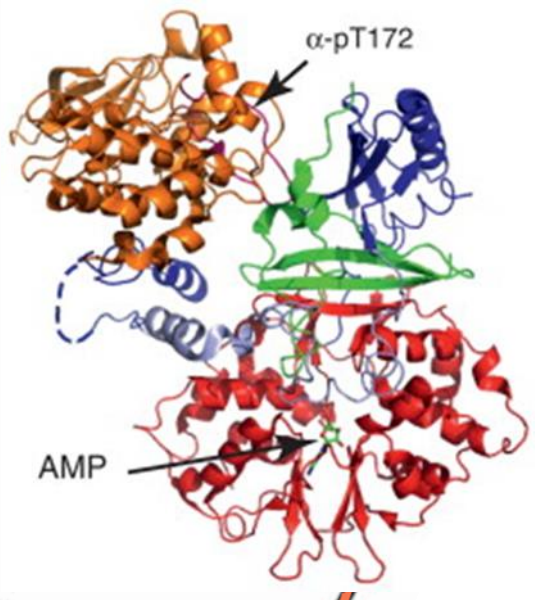

An introduction to AMP-activated protein kinase (AMPK)

Abstract. AMP-activated protein kinase (AMPK) is a heterotrimeric serine/threonine kinase. It is the most relevant kinase in the context of metabolic stability and energy homeostasis, playing a central role in sensing and regulating energy homeostasis at the cellular, organ and whole-body level. Activation involves covalent phosphorylation and allosteric binding of AMP or ADP that cooperate in a complex manner. Once activated, AMPK phosphorylates a broad range of downstream targets, resulting in the inhibition of anabolism and activation of catabolism, to maintain high levels of cellular ATP. Disturbance of energy homeostasis underlie a number of disease such as cardiovascular pathologies, neurodegenerative disease, cancer and type 2 diabetes. Since few years AMPK has emerged as a potential therapeutic target for some of these pathologies.

Résumé. La protéine kinase activée par l'AMP (AMPK) est une serine/thréonine kinase hétérotrimérique. Cette kinase est la plus importante dans le cadre de la stabilité métabolique, jouant un rôle central de senseur et régulateur de l'homéostasie énergétique au niveau de la cellule, de l'organe et de l'individu. Son activation requiert une phosphorylation covalente et une régulation allostérique par l'AMP ou l'ADP. Une fois activée, l'AMPK phosphoryle un grand nombre de cibles en aval, provoquant une inhibition de l'anabolisme et une activation du catabolisme, permettant le maintien d'un haut niveau d'ATP. Un grand nombre de pathologies sont sous-jacentes à des perturbations de l'homéostasie énergétique, telles les maladies cardiovasculaires, les maladies neurodégénératives, les cancers et le diabète de type 2. Depuis maintenant quelques années l'AMPK est considérée comme une cible thérapeutique potentielle.

Homeostasis of cell metabolism

Metabolism

Without external input of energy, entropy of a system will tend to a maximum; for living organisms, this disorder corresponds to death. Living organisms are highly organized, thus they need to constantly struggle against disorder. Oxidation of macromolecules generates a free energy reservoir in form of “high energy” compounds such as nucleotide triphosphates, which serves as fuel to maintain biological order. The overall metabolism process consists in coupling exergonic to endergonic reactions to maintain life, in other words metabolism utilizes the free energy to carry out vital functions such as biosynthesis of complex molecules, active transport, or mechanical work. (Atkins, 1984; Voet, 2011)

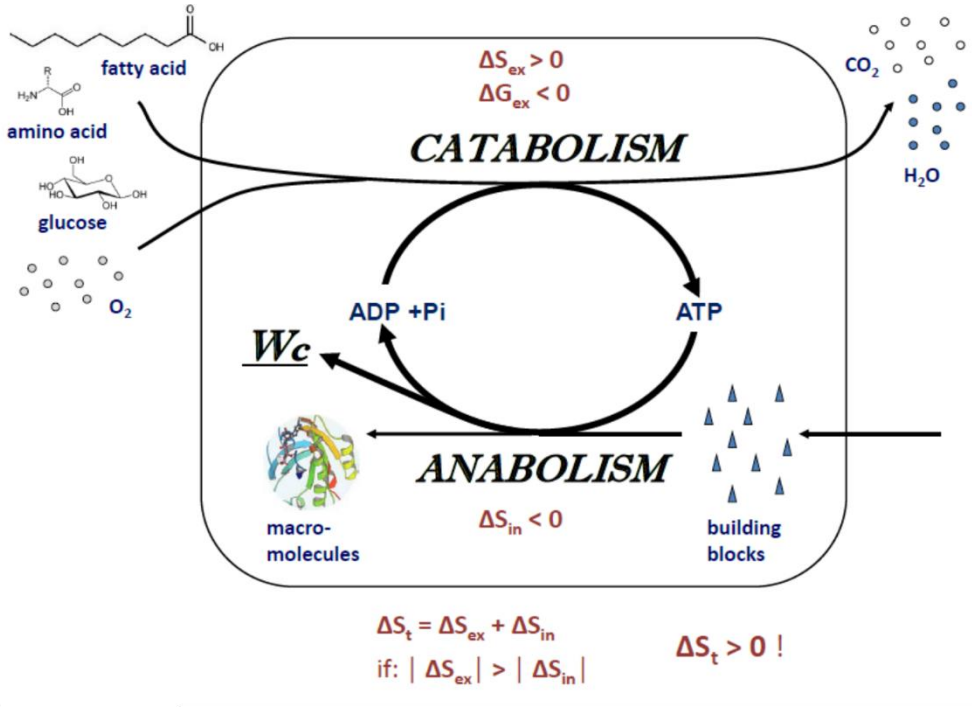

***Figure 1*. General scheme of cellular metabolism.** Catabolic reactions generating ATP (top), through coupling to anabolic reactions (biosynthesis, bottom) using ATP, maintain cell structural organization as an expression of the decrease of internal entropy (ΔSin < 0) and are also the source of energy for cellular work (Wc). Abbreviations: ΔSex, excess entropy; ΔSin, input entropy; ΔSt, total entropy; ΔGex, excess Gibbs free energy. For further details see text. Reproduced from (Saks, 2007).

The chemical reactions of metabolism are organized into metabolic pathways, in which a macromolecule is transformed into another one by a series of consecutive enzymatic

reactions. (Alberts, 2002; Atkins, 1984; Voet, 2011). Their reactants, intermediates, and product are referred to as metabolites. There are two subfamilies of enzymatic reactions composing the metabolic pathway (*Figure 1*).

(1) Catabolism, which breaks down complex molecules (nutrients and cell constituents) into more simple ones to generate building blocks and conserve free energy in form of a small number of compounds. The latter occurs mainly through the synthesis of ATP from ADP and phosphate and the reduction of the coenzyme $NADP^+$ to NADPH. Proteins, lipids and polysaccharides are broken down by enzymatic digestion into smaller molecules, such as amino acids, sugar, fatty acids and glycerol, respectively. Such small units can be taken up into the cell and oxidized.

(2) Anabolism, which uses the free energy sources and building blocks provided by catabolic processes to synthesize again more complex molecules needed to sustain a living cell. Anabolic processes are powered by the hydrolysis of ATP. Processes such as gluconeogenesis, glycogenesis, lipogenesis and protein synthesis are all anabolic processes which tend towards “building up” organs and tissues.

Metabolic reactions are accelerated by enzymes which are among the more effective catalysts known, capable of accelerating reactions up to a factor of 10^{14}. They thereby allow reactions that would otherwise not proceed rapidly at cell temperatures. More than 4500 enzymatic reaction are listed to date. (Alberts, 2002; Fruton, 1999; Kornberg, 1991)

Post-translational modification of proteins

Post-translational modifications (PTMs) are all chemical protein modifications that occur after translation. Mostly, these are covalent modifications of amino acid residues. Reversible PTMs can occur rapidly and have regulatory roles in different physiological responses. Multiple PTMs on a single protein create a large combinatorial pattern or “mod-forms”. Distinct mod-forms can elicit distinct downstream responses and thus knowledge of PTMs is the most informative measure of a protein’s state (Khoury et al., 2011).

Over 200 types of PTM have been identified (Jensen, 2006), which can be divided in two kinds of processes. A first type of PTMs are polypeptide modifications such as covalent binding of ubiquitin (ubiquitinylation) and ubiquitin-like moieties (e.g. sumoylation, neddylation) (Schwartz and Hochstrasser, 2003). Addition of these polypeptide molecules requires an entire group of specific enzymes. A second type of PTMs is based on a group of smaller molecules (e.g. acetyl, ADP-ribosyl, phosphoryl) which are provided by metabolic donors (e.g. acetyl-CoA, NAD, ATP) that are derived from basic cell metabolism. The final covalent binding is processed by single enzymes (Prabakaran et al., 2012).

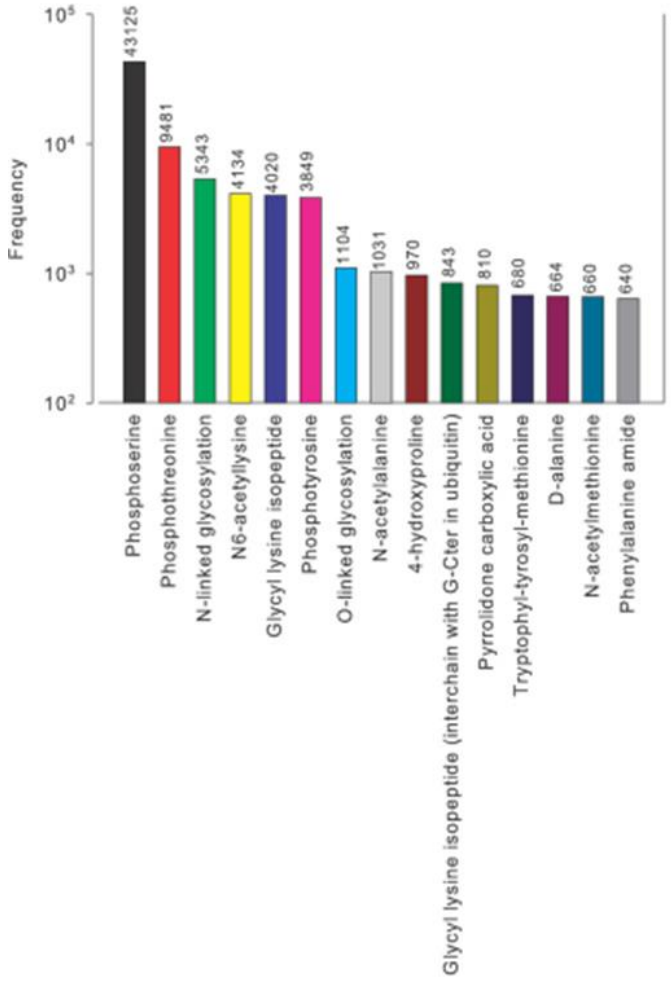

***Figure 2*. Top experimentally observed post-translational modifications.** Occurrence of experimentally detected PTMs, as curated from SwissProt. Figure from (Khoury et al., 2011).

Phosphorylation events dominate by large the number of experimentally observed PTMs (*Figure 2*). However, these numbers probably do not reflect the physiological proportion of these PTMs, but rather the preponderance of phosphorylation studies in literature.

Phosphorylation plays a key role in cell signaling for a wide range of cellular processes by providing a simple “on”/“off” switch for enzymes or receptors. This PTM is catalyzed by protein kinases and reversed by protein phosphatases. AMPK is an important effector of cellular protein phosphorylation.

AMPK, structure and localization

Role of AMPK in metabolism

Adenosine monophosphate-activated protein kinase (AMPK) is the most relevant kinase in the context of metabolic stability and energy homeostasis. AMPK is phylogenetically one of the most ancient eukaryotic protein kinases, conserved in all eukaryotic genomes that have been sequence to date, from protozoa and yeast to plants and human (Hardie, 2003). AMPK participates in sensing and controlling cellular and whole-body energy balance by its sensitivity to AMP and ADP. AMPK is allosterically activated by increasing AMP:ATP and ADP:ATP ratios (Hardie et al., 2012a), and its covalent phosphorylation by upstream kinases. It operates as a “metabolic master switch” at cellular, organ and whole-body levels (Hardie and Carling, 1997; Winder and Hardie, 1999). Activation of AMPK generally aims at compensating ATP loss via acceleration of catabolism and inhibition of anabolism.

AMPK structure

AMPK is part of a structurally related family of serine/threonine protein kinases (the AMPK-related-kinases [ARKs]) comprising around 14 members (Lizcano et al., 2004). It is a heterotrimeric complex consisting of a catalytic α-subunit and regulatory β- and γ-subunits (*Figure 3*). Further complexity is added by the existence of multiple subunit genes encoding each different isoforms of each subunit. In mammals, there are two genes encoding the AMPK α catalytic subunit (α1 and α2), two β genes (β1 and β2) and three γ subunit genes (γ1,γ2 and γ3) with γ2 and γ3 existing as splice variants (Hardie, 2007). Each of these subunit takes on a specific role in both the stability and activity of AMPK (Stapleton et al., 1996).

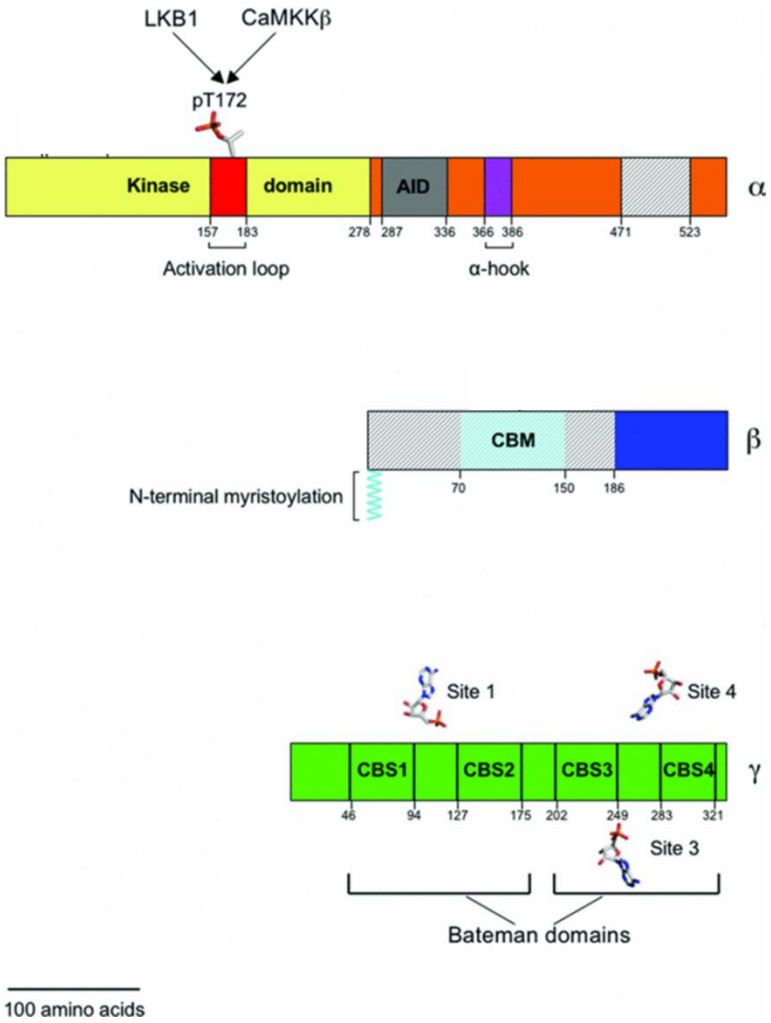

Figure 3. **Schematic representation of AMPK subunits.** Cartoon of the three AMPK subunits, highlighting key amino acid residues and regions implicated in the regulation of AMPK activity. The major upstream kinases phosphorylating Thr172 are LKB1 and CaMKKβ. AMP is shown bind to each of the three nucleotide-binding sites in the γ subunit. CBM, carbohydrate binding module; CBS, cystathionine β-synthetase. Figure from (Carling et al., 2012).

The α-subunit contains the catalytic domain and an inhibitory activation loop involved in its regulation (Crute et al., 1998; Pang et al., 2007). The key site for AMPK activation is found on the activation loop as threonine 172 (Thr172) which is phosphorylated by upstream kinases. The C-terminal α-domain is interacting with both the β-subunit and loop(s) contacting the γ-subunit (Pang et al., 2007)

The β-subunit tethers both α- and the γ-subunits (Iseli et al., 2005) as a scaffold protein with it C-terminal domain (aa 187 to 272) and also bears a carbohydrate binding module (CBM) (Hudson et al., 2003; Polekhina et al., 2003), that is found in a number of enzymes that metabolize polysaccharides, such as glycogen or starch (Hudson et al., 2003; Polekhina et al.,

2003). Consistent with the presence of a CBM, AMPK can bind to glycogen *in vitro* (Hudson et al., 2003; Polekhina et al., 2003). Functions in subcellular targeting to glycogen granules and regulation of glycogen metabolism have been proposed (McBride et al., 2009).

The γ-subunits Conserved in all γ-subunit are the four cystathionine β-synthetase (CBS) domains forming pairs called Bateman domains (Kemp, 2004) assembled in a head to head manner. The two Bateman domain bear four cavities to bind ligands, but since one site is non-functional, there are only three binding sites for nucleotide (AMP, ADP and ATP). These three functional sites have different affinity for nucleotides and play different roles in allosteric activation of AMPK (Hardie et al., 2011; Xiao et al., 2007).

AMPK subcellular localization

There is some evidence that AMPK isoforms determine intracellular distribution, protein recognition or tissue-specific functions, and especially provide selectivity for specific subsets of substrates within the ever increasing list of AMPK substrates (Carling et al., 2012; Hardie et al., 2012a, 2012b). AMPK is generally observed as a soluble complex with diffuse cytosolic localization. Functional differences are reported for the two catalytic α subunits, particularly for their responsiveness to AMP and upstream kinases, as well as their nuclear localization (Hedbacker and Carlson, 2008). In fact, α2-containning complexes, when activated, can translocate into the nucleus to phosphorylate important substrates (transcription factors, histones, and histone deacetylases) as seen after exercise in skeletal muscle (McGee et al., 2003; Suzuki et al., 2007). Also, α1 subunit has been shown to localize to the nucleus under some conditions (diurnal regulation) (Lamia et al., 2009). The β-subunit is post-translationally modified by myristoylation and phosphorylation, which has been shown to be required for proper activation of AMPK or its localization to membranes (Oakhill et al., 2010) which might favor membrane bound complex. AMPK may also be recruited into specific complexes via interaction with its upstream kinases, downstream substrates, or more general scaffolding proteins. Scaffolding proteins can provide specificity in cell signaling by isolating activated kinases from bulk signaling and directing the information flow into specific pathways.

Upstream regulation of AMPK

The requirement of biological systems to maintain high cellular ATP:ADP ratios and concomitantly ATP:AMP ratios at all times, even under conditions of high metabolic workload, is reflected by the dynamic and stringent control of AMPK activity. Regulation of AMPK activity is an elaborate process involving at least two upstream kinases and one protein phosphatase, as well as allosteric mechanisms (Hardie and Sakamoto, 2006; Hardie et al., 2006).

Allosteric regulation

AMPK is a highly conserved sensor of intracellular adenosine nucleotide levels that is activated when even modest decreases in ATP production results in relative increases in AMP or ADP (Carling et al., 1989; Hardie et al., 1998). Under these conditions, AMP or ADP bind to the two tandem Bateman domains (Kemp, 2004; Oakhill et al., 2011; Xiao et al., 2011) on the regulatory γ-subunit, leading to a conformational change that allosterically activates the kinase and protects the activating phosphorylation of AMPK at Thr172 (Bland and Birnbaum, 2011; Hardie et al., 2011; Oakhill et al., 2011; Xiao et al., 2011) against dephosphorylation by protein phosphatases (Davies et al., 1995; Suter et al., 2006). It was originally reported that AMP also promoted phosphorylation of AMPK by an upstream kinase (Hawley et al., 1995), later identified as LKB1 (Hawley et al., 2003; Woods et al., 2003).

Regulation by upstream kinases

Full activation of AMPK requires phosphorylation of the Thr172 residue in the α-subunit by different upstream kinases (Hawley et al., 1996; Stein et al., 2000). So far, two protein kinases are certain to phosphorylate this residue *in vivo*, namely liver kinase B1 (LKB1) (Hawley et al., 1995; Shaw et al., 2004a; Woods et al., 2003) and Ca^{2+}/Calmodulin-dependent kinase, especially the β isoform (CaMKKβ) (Hawley et al., 2005; Hurley et al., 2005; Woods et al., 2005).

LKB1 is a serine/threonine kinase which plays vital roles maintaining cell polarity thereby inhibiting inappropriate expansion of tumor cells. Germinal mutations in the LKB1 gene have

been associated with Peutz-Jeghers cancer syndrome (PJS), characterized by the development of polyps in the gastrointestinal tract (Hemminki et al., 1997; Scott et al., 2008). More recent studies show a large number of somatic mutations of the LKB1 gene present in lung, cervical, breast, intestinal, testicular, pancreatic and skin cancer (Forbes et al., 2010; Sanchez-Cespedes, 2007). LKB1 is an important upstream kinase of AMPK, thus suggesting an unexpected connection between AMPK and cancer (Luo et al., 2005; Motoshima et al., 2006; Shackelford and Shaw, 2009). LKB1 suppresses growth and proliferation by activating a group of 14 protein kinases, comprising AMPK and AMPK-related kinases (Ark) (Jaleel et al., 2005; Lizcano et al., 2004). Available evidence suggests that the tumor suppressor function of LKB1 is related to AMPK activation, in particular the ability of the latter to inhibit mTor signaling that triggers cell growth and proliferation (Alessi et al., 2006; Inoki et al., 2003; Shaw et al., 2004b).

CaMKKβ is also capable of phosphorylating and activating AMPK, thereby linking cytoplasmic Ca^{2+} levels to AMPK activity (Hawley et al., 2005; Hurley et al., 2005; Woods et al., 2005). Modest elevation of intracellular Ca^{2+} provoked by K^{+}-depolarization in neural tissue leads to a threefold activation of AMPK (Hawley et al., 2005). The tissue distribution of CaMKKs, with the highest levels in brain, suggests that they may play important roles in the nervous system. For example, brain AMPK may contribute to the survival of neurons under stress condition (Culmsee et al., 2001). Thus preservation of ATP levels by signaling from CaMKK to AMPK may represent a neuronal survival pathway.

In addition some other kinases seem to phosphorylate AMPK. The mammalian transforming growth factor β-activated kinase (**TAK1**), in complex with its accessory protein TAB1, was identified as a third possible upstream kinase capable of phosphorylating AMPK at Thr172 for activation (Herrero-Martín et al., 2009; Momcilovic et al., 2006; Xie et al., 2006). Also phosphorylation of AMPK at other sites has been reported, such as Ser485 (in α1) or Ser491 (in α2) by **Akt/PKB** (Horman et al., 2006; Kovacic et al., 2003), α-Ser173 by **PKA** (Hurley et al., 2006) or even by autophosphorylation reactions which reduce the accessibility of Thr172 to upstream kinases (Horman et al., 2006; Hurley et al., 2006).

Inactivation by protein phosphatases

Less known but not less important for the α-Thr172 phosphorylation state is regulation by protein phosphatases. Different phosphatases can dephosphorylate AMPK at Thr172 *in vitro* like protein phosphatase 2Cα (PP2Cα), protein phosphatase 2A (PP2A), and protein phosphatase 1 (PP1) (Davies et al., 1995; Marley et al., 1996). In heart and endothelial cells, the expression level of PP2A and PP2Cα are correlated with AMPK activation (Wang and Unger, 2005; Wu et al., 2007).

AMPK consensus recognition motif

AMPK phosphorylation sites have been described so far in more than 50 substrate proteins, especially during recent years. Many more sites may exist in substrate candidates resulting from large-scale screenings that are not yet characterized. Generally, to ascertain specificity in cell signaling, protein kinases recognize a specific motif on the surface of the substrate that is primarily defined by a particular amino acid sequence. In case of AMPK, a stringent motif has been proposed with the first substrates over 20 years ago: Φ(β,X)XXS/TXXXΦ, where ϕ is a hydrophobic residue (predominantly M, V, L, I or F), β is a basic residue (R, K or H) and the parentheses indicate that the order of residues at the P-4 and P-3 positions is not critical (Dale et al., 1995).

Detailed analysis of available data on AMPK phosphorylation sites reveals the presence of this stringent motif in about half of the described sites (*Figure 4*). However, another half of the identified sites corresponds only partially to this motif, either lacking one of the hydrophobic residues at P-5 and P+4, or the basic residue at P-3 or P-4 (*Figure 5*). With two sites, the motif is so N- or C-terminal in the sequence that part of the motif is missing. Also an AMPK phospho-motif screen using a library of synthetic peptides indicated lower conservation of the original AMPK motif, in particular for the positions from -1 to +4 (Gwinn et al., 2008). These data indicate that substrate recognition by AMPK may be less stringent than thought earlier.

UniProt	Name	Ref.	Abbr., P-site	5	4	3		0		4	
				Φ	β			*P*		Φ	
Q9BZL4	Protein phosphatase 1 regulatory subunit 12C	(Banko et al., 2011)	hPP12c-Ser452	G	L	Q	R	S	A	S	S	S	W	L	E	G
Q07866	Kinesin light chain 1	(McDonald et al., 2010)	hKLC1-Ser521	N	M	E	K	R	R	S	R	E	S	L	N	V
Q16875	6-phosphofructo-2-kinase	(Marsin et al., 2002)	hF262-Ser461	P	L	M	R	R	N	S	V	T	P	L	A	S
P49815	Tuberin	(Inoki et al., 2003)	hTSC2-Ser1387	P	L	S	K	S	S	S	S	P	E	L	Q	T
P49815	Tuberin	(Inoki et al., 2003)	hTSC2-Thr1271	P	L	P	R	S	N	T	V	A	S	F	S	S
Q53ET0	CREB-regulated transcription coactivator 2	(Koo et al., 2005; Screaton et al., 2004)	hCRTC2-Ser171	A	L	N	R	T	S	S	D	S	A	L	H	T
Q06210	Glucosamine-fructose-6-phosphate aminotransferase 1	(Li et al., 2007)	hGFPT1-Ser261	N	L	S	R	V	D	S	T	T	C	L	F	P
P41235	Hepatocyte nuclear factor 4-alpha	(Hong et al., 2003)	hHNF4A-Ser313	K	I	K	R	L	R	S	Q	V	Q	V	S	L
O70405	Serine/threonine-protein kinase ULK1	(Egan et al., 2011; Shang et al., 2011)	hULK1-Ser638	D	F	P	K	T	P	S	S	Q	N	L	L	A
P04049	RAF proto-oncogene serine/threonine-protein kinase	(Sprenkle et al., 1997)	hRAF1-Ser621	K	I	N	R	S	A	S	E	P	S	L	H	R
P13834	Glycogen synthase, muscle	(Carling et al., 1989)	rbGYS1-Ser8	P	L	S	R	T	L	S	V	S	S	L	P	G
A2RRU1	Glycogen synthase, muscle	(Jørgensen et al., 2004)	rGYS1-Ser8	P	L	S	R	S	L	S	V	S	S	L	P	G
Q95XA8	Protein CRTC-1	(Mair et al., 2011)	ceCRTC1-Ser179	Q	I	N	R	A	R	S	D	P	A	I	H	N
P51639	3-hydroxy-3-methylglutaryl-coenzyme A reductase	(Clarke and Hardie, 1990)	rHMDH-Ser871	H	M	V	H	N	R	S	K	I	N	L	Q	D
P04035	3-hydroxy-3-methylglutaryl-coenzyme A reductase	(Ching et al., 1996)	hHMDH-Ser871	H	M	I	H	N	R	S	K	I	N	L	Q	D
Q09472	Histone acetyltransferase p300	(Yang et al., 2001)	hEP300-Ser89	E	L	L	R	S	G	S	S	P	N	L	N	M
P50552	Vasodilator-stimulated phosphoprotein	(Blume et al., 2007)	hVASP-Ser322	T	L	P	R	M	K	S	S	S	S	V	T	T
Q62600	Nitric oxide synthase, endothelial	(Chen et al., 1999)	hNOS3-Thr495	G	I	T	R	K	K	T	F	K	E	V	A	N
Q9UQL6	Histone deacetylase 5	(McGee et al., 2008)	hHDAC5-Ser259	P	L	R	K	T	A	S	E	P	N	L	K	V
O70405	Serine/threonine-protein kinase ULK1	(Egan et al., 2011)	hULK1-Ser467	A	I	R	R	S	G	S	T	S	P	L	G	F
Q05469	Hormone-sensitive lipase	(Garton and Tonks, 1994)	rLIPS-Ser565	S	M	R	R	S	V	S	E	A	A	L	A	Q
Q16526	Cryptochrome-1	(Lamia et al., 2009)	hcry1-Ser71	N	L	R	K	L	N	S	R	L	F	V	I	R
P13569	Cystic fibrosis transmembrane conductance regulator	(King et al., 2009)	hCFTR-Ser768	Q	A	R	R	R	Q	S	V	L	N	L	M	T
Q8N122	Regulatory-associated protein of mTOR	(Gwinn et al., 2008)	hRPTOR-Ser792	K	M	R	R	A	S	S	Y	S	S	L	N	S
Q92538	Golgi-specific GTP/GDP exchange factor 1	(Miyamoto et al., 2008)	hGBF1-Thr1337	K	I	H	R	S	A	T	D	A	D	V	V	N
Q8VIP2	Carbohydrate-responsive element-binding protein	(Kawaguchi et al., 2002)	rChREBP-Ser568	L	L	R	P	P	E	S	P	D	A	V	P	E
O00763	Acetyl-CoA carboxylase 2	(Merrill et al., 1997)	hACC2-Ser222	T	M	R	P	S	M	S	G	L	H	L	V	K
P35570	Insulin receptor substrate 1	(Jakobsen et al., 2001)	rIRSI-Ser794	H	L	R	L	S	S	S	S	G	R	L	R	Y
P11497	Acetyl-CoA carboxylase 1	(Munday et al., 1988)	rACC1-Ser79	H	M	R	S	S	M	S	G	L	H	L	V	K
Q8N122	Regulatory-associated protein of mTOR	(Gwinn et al., 2008)	hRPTOR-Ser722	R	L	R	S	V	S	S	Y	G	N	I	R	A

Figure 4. AMPK substrates with the stringent AMPK consensus recognition motif. Phospho-sites of published AMPK substrates were analyzed for their compliance with the consensus sequence of AMPK substrate recognition (Dale et al., 1995; Scott et al., 2002) which is Φ(β,X)XXS/TXXXΦ (Φ being a hydrophobic residue and β any basic residue). Top: Sequences including six amino acids N- and C-terminal of the Ser or Thr phosphoacceptor (P) were aligned (UniProt identifiers, protein name and phosphosites are given; amino acids corresponding to the consensus sequence are color coded – orange: A,F,I,L,M,V,W; blue: K,R,H: green: S,T). **Right:** The frequency of individual amino acids at a specific position was calculated using the sequence logo algorithm (Crooks et al., 2004; Schneider and Stephens, 1990).

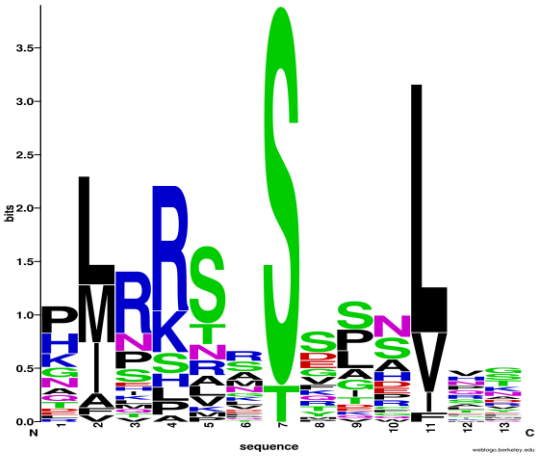

UniProt	Name	Ref.	Abbr., P-site	5 4 3 0 4
				Φ β P Φ
Q9UQB8	Brain-specific angiogenesis inhibitor 1-assoc. protein 2	(Banko et al., 2011)	hBAIP2-Ser366	T L P R S S S M A A G L E
O70405	Serine/threonine-protein kinase ULK1	(Egan et al., 2011)	hULK1-Thr575	K L P K P P T D P L G A V
Q9UQL6	Histone deacetylase 5	(McGee et al., 2008)	hHDAC5_Ser498	P L S R T Q S S P L P Q S
P30260	Cell division cycle protein 27 homolog	(Banko et al., 2011)	hCDC27-Ser379	A L P R R S S R L F T S D
O43524	Forkhead box protein O3	(Greer et al., 2007)	hFOXO3-Ser413	L M Q R S S S F P Y T T K
P52292	Importin subunit alpha-2	(Wang et al., 2004)	hIMA2-Ser105	A A R K L L S R E K Q P P
P46527	Cyclin-dependent kinase inhibitor 1B	(Liang et al., 2007)	hCDN1B-Thr198	G L R R R Q T - - - - - -
O70405	Serine/threonine-protein kinase ULK1	(Egan et al., 2011)	hULK1-Ser556	L G C R L H S A P N L S D
Q16526	Cryptochrome-1	(Lamia et al., 2009)	hCRY1-Ser280	K K V K K N S S P P L S L
O60343	TBC1 domain family member 4	(Geraghty et al., 2007)	hTBC1D4-Ser588	M R G R L G S V D S F E R
O60343	TBC1 domain family member 4	(Geraghty et al., 2007)	hTBC1D4-Thr642	F R R R A H T F S H P P S
Q14654	ATP-sensitive inward rectifier potassium channel 11	(Chang et al., 2009)	Hirk11-Ser385	K P K F S I S P D S L S -
Q9UBS5	Gamma-aminobutyric acid type B receptor subunit 1	(Terunuma et al., 2010)	hGABR1-Ser912	L R H Q L Q S R Q Q L R S
Q9BU19	Zinc finger protein 692	(Inoue and Yamauchi, 2006)	hZN692-Ser470	A H R S S K S H P A L L L
Q9NYV6	Transcription initiation factor IA	(Hoppe et al., 2009)	hTIFIA-Ser635	T H F R S P S S S V G S P
Q62600	Nitric oxide synthase, endothelial	(Chen et al., 1999)	hNOS3-Ser1177	S R I R T Q S F S L Q E R
P42345	Serine/threonine-protein kinase mTOR	(Cheng et al., 2004)	hMTOR-Thr2446	K R S R T R T D S Y S A G
P50552	Vasodilator-stimulated phosphoprotein	(Blume et al., 2007)	hVASP-Thr278	A R R R K A T Q V G E K T
Q07866	Kinesin light chain 1	(McDonald et al., 2010)	hKLC1-Ser524	K R R S R E S L N V D V V
P04637	Cellular tumor antigen p53	(Jones et al., 2005)	hP53-Ser15	S V E P P L S Q E T F S D
O95278	Laforin	(Romá-Mateo et al., 2011)	hEPM2A-Ser25	E L L V V G S R P E L G R
P49674	Casein kinase I isoform epsilon	(Um et al., 2007)	hKC1E-Ser389	G A P A N V S S S D L T G
P13405	Retinoblastoma-associated protein	(Dasgupta and Milbrandt, 2009)	hRB-Ser804	Y I S P L K S P Y K I S E
O00418	Eukaryotic elongation factor 2 kinase	(Browne et al., 2004)	hEFK2-Ser398	S L P S S P S S A T P H S
Q9UQK1	Protein phosphatase 1 regulatory subunit 3C	(Vernia et al., 2009)	hPPR36-Ser33	R L C L A H S P P V K S F
O75899	Gamma-aminobutyric acid type B receptor subunit 2	(Terunuma et al., 2010)	hGABR2-Ser783	T S V N Q A S T S R L E G
Q13621	Kidney-specific Na-K-Cl symporter	(Fraser et al., 2007)	hNKCC2-Ser126	P K V N R P S L L E I H E
Q95XA8	Protein CRTC-1	(Mair et al., 2011)	ceCRTC1-Ser76	G H N L G G S L P N V H Q
Q9UQK1	Protein phosphatase 1 regulatory subunit 3C	(Vernia et al., 2009)	hPPR36-Ser293	E S T I F D S P R L A S G
Q13177	Serine/threonine-protein kinase PAK 2	(Banko et al., 2011)	hPAK2-Ser20	A P P V R M S T I F S T G
P26285	6-phosphofructo-2-kinase	(Rider et al., 2004)	bF262-Ser466	V R M R R N S V T P L A S
P12277	B-type creatine kinase	*Ramirez unpubl.*	hBCK-Ser9	M P F S N S H N A L K L

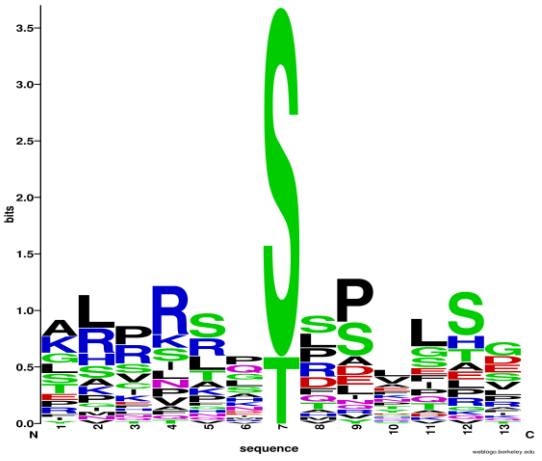

Figure 5. AMPK substrates with non-consensus recognition motifs. Phospho-sites of published AMPK substrates were analyzed for their compliance with the consensus sequence of AMPK substrate recognition (Dale et al., 1995; Scott et al., 2002) which is Φ(β,X)XXS/TXXXΦ (Φ being any hydrophobic residue and β any basic residue). Top: Sequences including six amino acids N- and C-terminal of the Ser or Thr phosphoacceptor (*P*) were aligned (UniProt identifiers, protein name and phosphosites are given; amino acids corresponding to the consensus sequence are color coded – orange: A,F,I,L,M,V,W; blue: K,R,H; green: S,T). **Right:** The frequency of individual amino acids at a specific position was calculated using the sequence logo algorithm (Crooks et al., 2004; Schneider and Stephens, 1990).

AMPK signaling downstream

Once activated, AMPK regulates a large number of downstream targets (*Figure 6*), shutting down anabolic pathways and stimulating catabolic pathways. Metabolic changes induced by AMPK are both acute changes due to direct phosphorylation of metabolic enzymes and chronic changes due to effect on gene expression by phosphorylation of transcription (co)factors and histone deacetylases (HDACs). Both result in the preservation of ATP levels (Carling, 2005; Hardie and Sakamoto, 2006). AMPK also participates in the control of non-metabolic processes such as cell proliferation and cell cycle (Beevers et al., 2006; Browne et al., 2004; Hay and Sonenberg, 2004).

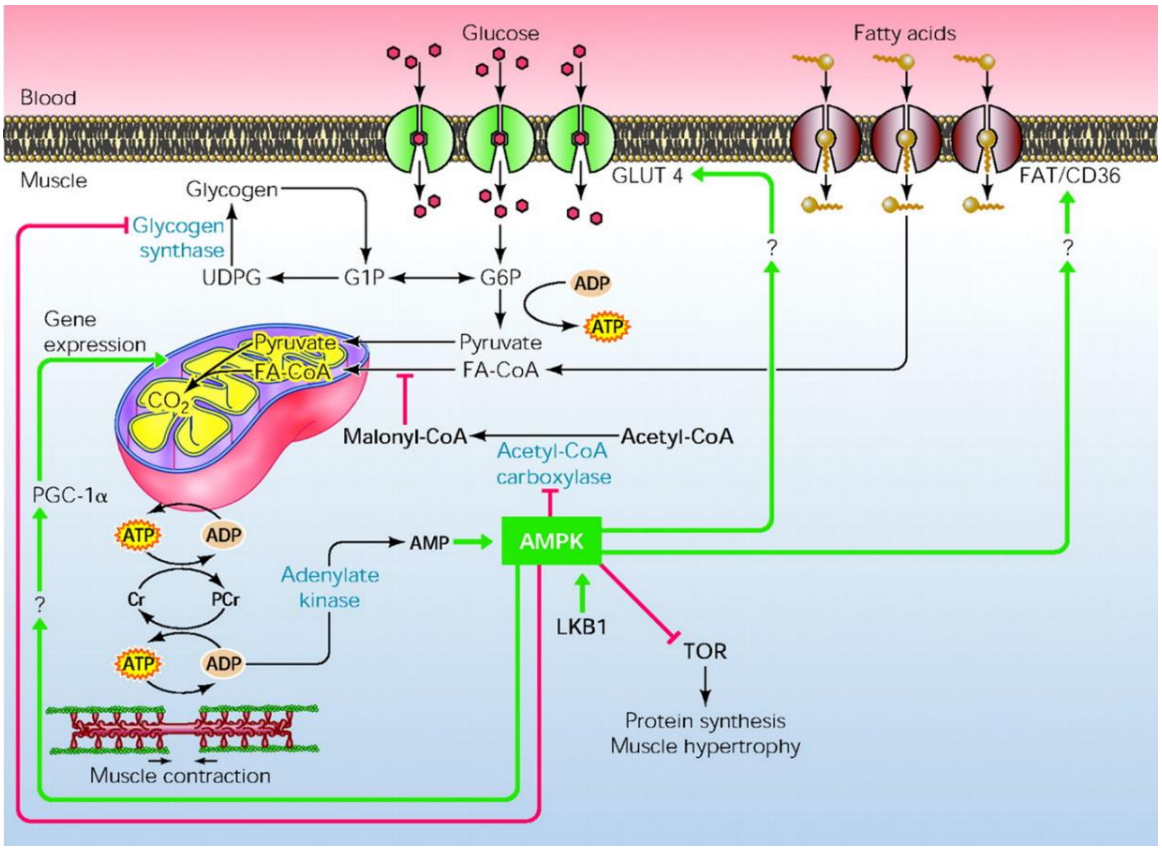

***Figure 6*. Metabolic changes known to be induced by AMPK in muscle.** Question marks indicate that the direct target for AMPK responsible for the observed downstream is not known. (Hardie and Sakamoto, 2006).

AMPK regulates carbohydrate metabolism

Glucose uptake across the plasma membrane is dependent on the glucose gradient as well as a family of transmembrane glucose transporters (GLUT). GLUTs are stored in cytosolic vesicles that translocate to the plasma membrane in response to triggers like muscle contraction, AMPK activation and insulin. Importantly, during exercise, glucose uptake increases independent of the insulin signaling pathway (Jørgensen et al., 2006) due to AMPK activation. Active AMPK increases GLUT4 translocation in muscle, cardiomyocytes and adipocytes (Kurth-Kraczek et al., 1999; Webster et al., 2010; Yamaguchi et al., 2005) and also increases GLUT3 translocation in neurons (Weisová et al., 2009). The signaling events, by which activation of AMPK leads to the translocation of these transporters remain unclear. Some studies revealed a critical role for the Rab GTPases Akt substrate of 160 kDa (AS160) (Cartee and Wojtaszewski, 2007; Sakamoto and Holman, 2008; Zaid et al., 2008). AMPK was shown to directly phosphorylate AS160, an effect which directly enhances binding to 14-3-3 (Geraghty et al., 2007), which in turn regulates vesicle translocation (Sakamoto and Holman, 2008; Treebak et al., 2006). Finally, AMPK increases the subsequent glycolytic flux via phosphorylation and activation of 6-phosphofructosekinase-2 (PFK2) (Marsin et al., 2000).

AMPK affects carbohydrate metabolism also in the long-term via transcriptional regulation. Phosphorylation of both peroxisome proliferator-activated receptor gamma co-activator-1 alpha (PGC-1α) (Horman et al., 2006) and histone deacetylase (HDAC) 5 (McGee et al., 2008) mediates transcriptional up-regulation of rate-limiting enzymes for the uptake of glucose, such as GLUT4 (Steinberg and Kemp, 2009) and hexokinase II (HKII) (Stoppani et al., 2002).

Hepatic glucose production, is negatively regulated by AMPK activation. Active AMPK downregulates the transcription of the gluconeogenic enzymes, L-type pyruvate kinase (L-PK) (Leclerc et al., 1998; da Silva Xavier et al., 2000), phosphoenol pyruvate carboxykinase (PEPCK) (Lochhead et al., 2000), and glucose-6-phosphatase (G-6-Pase) (Woods et al., 2000) by phosphorylation of transcription factor HNF-4α and transcriptional activator CREB (Steinberg and Kemp, 2009).

AMPK regulates lipid metabolism

Uptake of fatty acids (FA), similar as in case of glucose, depends on a transmembrane transporter (FAT/CD36) that is stored in cytosolic vesicles and translocated to the plasma membrane after AMPK activation (van Oort et al., 2009; Schwenk et al., 2010), thus increasing FA uptake (Shearer et al., 2004, 2005). It is unknown whether AMPK acts directly on CD36 or indirectly as is the case of regulation of glucose uptake.

AMPK is a main regulator of Acetyl-coA carboxylase (ACC), able to phosphorylate a number of serine residues on both cytosolic and mitochondrial ACC isoforms, (ACC1 and ACC2, respectively). The function of ACC is to regulate the metabolism of fatty acids. ACC catalyzes the carboxylation of acetyl-CoA to malonyl-CoA, a building block for FA synthesis and an allosteric inhibitor of mitochondrial carnitine palmitoyltransferase 1 (CPT1), a rate limiting enzyme for FA import and β-oxydation in the mitochondria (Bianchi et al., 1990; Merrill et al., 1997; Munday, 2002; Merrill et al., 1997). AMPK-mediated short term inhibition of ACC suppresses FA synthesis and increases FA β-oxydation by relieving the inhibitory effect of malonyl CoA on CPT1 (Munday, 2002).

The regulation of triglyceride (TG) turnover is a balance between biosynthesis and hydrolysis of TG, and AMPK is suggested to inhibit both. AMPK regulates TG synthesis via reducing activity of glycerol-3-phosphate acyl transferase (GPAT), which regulate one of the first steps of TG synthesis (Muoio et al., 1999). AMPK also appears to negatively regulate hormone-sensitive-kinase (HSL) activity and thus TG degradation (Watt et al., 2006).

Finally, AMPK phosphorylates and inhibits the rate-limiting enzyme for isoprenoid and cholesterol synthesis, the 3-hydroxy-3-methylglutaryl-CoA reductase (HMGR), thus preventing energy consuming cholesterol synthesis (Clarke and Hardie, 1990).

AMPK regulates protein metabolism, cell polarity, growth and apoptosis

Protein synthesis accounts for a large proportion of cellular ATP use. AMPK-mediated inhibition of protein synthesis is thus an important mechanism to maintain high ATP level. AMPK blocks the ribosomal elongation step by phosphorylation and activation of the eukaryote elongation factor 2 kinase (eEF2K) which in turn inhibits eEF2 (Browne et al., 2004).

AMPK also acts via cross-talk with other major cellular signaling hubs like the mammalian target of rapamycin complex (mTORC) which is inhibited by activated AMPK via two major distinct mechanism. The first involves the phosphorylation of the tuberous sclerosis complex protein-2 (TSC2) (Inoki et al., 2003) upstream of mTORC. The second mechanism involves direct phosphorylation of the mTORC subunit Raptor, causing mTORC inactivation (Gwinn et al., 2008). mTORC is a serine/threonine protein kinase which controls many aspects of metabolism, peptide translation, ribosome biogenesis, but also cell growth, cell proliferation, cell motility, and apoptosis, suggesting that AMPK-mediated modulation of mTORC is involved in regulation of these pathway (Beevers et al., 2006; Hay and Sonenberg, 2004).

AMPK regulates whole body energy metabolism

AMPK is established since long as a cellular energy sensor. The finding that hormones (e.g. leptin, adiponectin) activate AMPK in muscle and liver provides evidence for AMPK regulation of whole body energy status (Orci et al., 2004; Wang et al., 2007, 2005). Hypothalamic AMPK regulates food intake (Minokoshi et al., 2004) by the anorexigenic hormone leptin which leads to a reduction in food intake and the orexigenic hormone ghrelin as well as pharmacological activation of AMPK in hypothalamus which both leads to increased food intake (Andersson et al., 2004).

AMPK in human disease and as a therapeutic target

Cardiovascular pathologies

Several mutations in Bateman domains of the AMPK γ-subunits have been mapped and lead to a glycogen storage disorder and a related hereditary heart disease (Wolff-Parkinson-White syndrome), involving cardiac hypertrophy, contractile dysfunction and arrhythmias (Blair et al., 2001; Davies et al., 2006; Gollob et al., 2001; Milan et al., 2000; Scott et al., 2004). These mutations have been found to impair both the binding of AMP to the isolated Bateman domains and the activation of the heterotrimeric complex by AMP (Burwinkel et al., 2005; Scott et al., 2004). These mutations affect not only AMP binding, but also reduce ATP binding,

an inhibitory nucleotide (Burwinkel et al., 2005; Scott et al., 2004), resulting in increased basal activity of the mutated AMPK complexes (Arad et al., 2002; Burwinkel et al., 2005; Hamilton et al., 2001). The higher basal activity appears to cause excessive storage of glycogen in cardiac myocytes, possibly through increased basal glucose uptake (Arad et al., 2002; Burwinkel et al., 2005). In cardiac myocytes, this excessive glycogen storage is harmful and leads to improper development and function of the heart muscle. Interestingly, a similar mutation (R200Q) affecting a conserved basic residue in the first CBS motif of the γ3 isoform (which is expressed at the highest levels in skeletal muscle) leads to abnormal deposition of glycogen in skeletal muscle of pigs (Milan et al., 2000).

AMPK related neurodegenerative diseases

Brain is the most energy-consuming organ in our body, but specific functions of AMPK in this organ have only recently been studied. The kinase is widely expressed in the brain, and AMPK activity is tightly coupled to the energy status of both neuronal and whole-body levels. Recent studies revealed an important role of AMPK in neurodegenerative disease.

AMPK is particularly implicated in Alzheimer disease (AD) (Salminen et al., 2011)), which is characterized by accumulation of pathological protein aggregates like extracellular amyloid β (Aβ) plaques and intracellular neurofibrillary tangles, as well as by neuronal loss (Bettens et al., 2010; Bürklen et al., 2006; Jellinger, 2006). Aβ is the key molecule in AD, and it has been shown to be down-regulated by AMPK in primary cortical neurons and N2a neuroblastoma cells (Chen et al., 2009; Marambaud et al., 2005; Won et al., 2010). AMPK also has an inhibitory effect on Aβ production (Vingtdeux et al., 2010) and regulates Aβ degradation and removal from neurons (Vingtdeux et al., 2011).

Although studies on the involvement of the AMPK signaling cascade in other neurodegenerative disorders are still scarce, the role of AMPK does not seem to be limited to AD. In Hutington disease (HD), the AMPKα1 subunit was selectively activated and enriched in the nucleus of striatal neurons. AMPK over-activation enhanced neuronal death and formation of Huntington aggregates. In contrast, suppression of AMPK activity showed a neuroprotective effect (Ju et al., 2011). Similar effects of AMPK activation has been observed in Parkinson disease (PD), (Choi et al., 2010).

AMPK is related to cancer

Cancer is a broad group of pathologies involving unregulated cell growth. Cancer cells have a huge demand for energy to allow rapid growth and division. A large number of evidence suggests that basal AMPK activity, as well as its activation under energy-limiting conditions, antagonize cancer cell growth. First, activation of AMPK causes a reduction in anabolic pathways, ultimately leading to reduced cell growth (reviewed in (Shackelford and Shaw, 2009)). Second, the AMPK signaling cascade contains a number of tumor suppressors including its upstream kinase LKB1 and its downstream targets p53, TSC1/2 and mTOR. AMPK activation affects these targets to decrease cell growth, thus acting as a tumor suppressor. Another pathway by which AMPK can affect tumors growth is via its impact on lipid synthesis. Cancer cells exhibit high rates of de novo fatty acid synthesis (Alò et al., 1999; Milgraum et al., 1997; Swinnen et al., 2000) and a number of studies have shown that inhibition of FA synthesis result in significant anti-tumor activity, by inhibiting growth and increasing apoptosis (Kuhajda, 2000; Pizer et al., 2000). In the liver, FA synthase (FAS) gene expression is downregulated by AMPK (Foretz et al., 1998; Woods et al., 2000). As mentioned above, AMPK phosphorylates and inhibits also acetyl-CoA carboxylase (ACC), an important step in FA synthesis (Chajès et al., 2006; Hardie and Carling, 1997).

All of these mechanisms imply that AMPK acts as a tumor suppressor and that activation of AMPK would be advantageous in treating cancer. However, more recent studies have emerged that lead to the opposite conclusion. In certain cancer cells (e.g. prostate), increased AMPK activity provides the cells with an advantage by increasing the rate of glucose uptake and glycolysis (Banko et al., 2011; Massie et al., 2011), increasing mitosis (Banko et al., 2011), and increasing cell migration (Frigo et al., 2011). Cells lacking AMPK can be resistant to oncogenic transformation (Laderoute et al., 2006). The levels of AMPK subunits α, β, and γ are elevate in 2% to 25% of human cancers (cancergenome.nih.gov) and cancer cell lines. There is now solid proof for AMPK supporting tumor proliferation (Liang and Mills, 2013).

To date, it is difficult to reconcile these apparently opposing effects of AMPK on cell growth. Possibly, AMPK acts as a tumor suppressor only during the early events of oncogenic transformation, while in more developed, in particular solid tumors, its anti-stress effect facilitates tumor growth. More research is required to determine the precise role of AMPK in cancer.

AMPK a potential target for treatment of type 2 diabetes

Type 2 diabetes is a metabolic disorder characterized by hyperglycemia and altered lipid metabolism, caused by the islet β cells being unable to secrete adequate amounts of insulin. Regular exercise is an effective method of treating insulin resistance and type 2 diabetes (Saltiel and Kahn, 2001), and this beneficial effect is at least partly mediated by AMPK activation (Fujii et al., 2008). Metformin, the most widely prescribed Type 2 diabetes drug, has been shown to activate AMPK (Zhou et al., 2001) and to do so in an LKB1 dependent manner (Shaw et al., 2005). In intact cells, metformin increases AMPK activity, resulting in increased fatty acid oxidation, downregulation of lipogenic genes, decreased hepatic glucose production and stimulation of glucose uptake (Zhou et al., 2001). Nonetheless, metformin, AICAR (AICAriboside, an indirect AMPK activator) (Halseth et al., 2002), and A769662 (a direct AMPK activator (Cool et al., 2006), as well as genetic expression of constitutively active AMPK in liver (Foretz et al., 2005) all lower blood glucose levels, suggesting AMPK activation as a primary target for diabetes prevention and therapy (Zhang et al., 2009).

References

Alberts, B. (2002). Molecular biology of the cell (New York: Garland Science).

Alessi, D.R., Sakamoto, K., and Bayascas, J.R. (2006). LKB1-dependent signaling pathways. Annu. Rev. Biochem. *75*, 137–163.

Alò, P.L., Visca, P., Trombetta, G., Mangoni, A., Lenti, L., Monaco, S., Botti, C., Serpieri, D.E., and Di Tondo, U. (1999). Fatty acid synthase (FAS) predictive strength in poorly differentiated early breast carcinomas. Tumori *85*, 35–40.

Andersson, U., Filipsson, K., Abbott, C.R., Woods, A., Smith, K., Bloom, S.R., Carling, D., and Small, C.J. (2004). AMP-activated protein kinase plays a role in the control of food intake. J. Biol. Chem. *279*, 12005–12008.

Arad, M., Benson, D.W., Perez-Atayde, A.R., McKenna, W.J., Sparks, E.A., Kanter, R.J., McGarry, K., Seidman, J.G., and Seidman, C.E. (2002). Constitutively active AMP kinase mutations cause glycogen storage disease mimicking hypertrophic cardiomyopathy. J. Clin. Invest. *109*, 357–362.

Atkins, P.W. (1984). The second law (New York, N.Y.: Scientific American Books).

Banko, M.R., Allen, J.J., Schaffer, B.E., Wilker, E.W., Tsou, P., White, J.L., Villén, J., Wang, B., Kim, S.R., Sakamoto, K., et al. (2011). Chemical genetic screen for AMPKα2 substrates uncovers a network of proteins involved in mitosis. Mol. Cell *44*, 878–892.

Beevers, C.S., Li, F., Liu, L., and Huang, S. (2006). Curcumin inhibits the mammalian target of rapamycin-mediated signaling pathways in cancer cells. Int. J. Cancer J. Int. Cancer *119*, 757–764.

Bettens, K., Sleegers, K., and Van Broeckhoven, C. (2010). Current status on Alzheimer disease molecular genetics: from past, to present, to future. Hum. Mol. Genet. *19*, R4–R11.

Bianchi, A., Evans, J.L., Iverson, A.J., Nordlund, A.C., Watts, T.D., and Witters, L.A. (1990). Identification of an isozymic form of acetyl-CoA carboxylase. J. Biol. Chem. *265*, 1502–1509.

Blair, E., Redwood, C., Ashrafian, H., Oliveira, M., Broxholme, J., Kerr, B., Salmon, A., Ostman-Smith, I., and Watkins, H. (2001). Mutations in the gamma(2) subunit of AMP-activated protein kinase cause familial hypertrophic cardiomyopathy: evidence for the central role of energy compromise in disease pathogenesis. Hum. Mol. Genet. *10*, 1215–1220.

Bland, M.L., and Birnbaum, M.J. (2011). Cell biology. ADaPting to energetic stress. Science *332*, 1387–1388.

Blume, C., Benz, P.M., Walter, U., Ha, J., Kemp, B.E., and Renné, T. (2007). AMP-activated protein kinase impairs endothelial actin cytoskeleton assembly by phosphorylating vasodilator-stimulated phosphoprotein. J. Biol. Chem. *282*, 4601–4612.

Browne, G.J., Finn, S.G., and Proud, C.G. (2004). Stimulation of the AMP-activated protein kinase leads to activation of eukaryotic elongation factor 2 kinase and to its phosphorylation at a novel site, serine 398. J. Biol. Chem. *279*, 12220–12231.

Bürklen, T.S., Schlattner, U., Homayouni, R., Gough, K., Rak, M., Szeghalmi, A., and Wallimann, T. (2006). The creatine kinase/creatine connection to Alzheimer's disease: CK-inactivation, APP-CK complexes and focal creatine deposits. J. Biomed. Biotechnol. *2006*, 35936.

Burwinkel, B., Scott, J.W., Bührer, C., van Landeghem, F.K.H., Cox, G.F., Wilson, C.J., Grahame Hardie, D., and Kilimann, M.W. (2005). Fatal congenital heart glycogenosis caused by a recurrent activating R531Q mutation in the gamma 2-subunit of AMP-activated protein kinase (PRKAG2), not by phosphorylase kinase deficiency. Am. J. Hum. Genet. *76*, 1034–1049.

Carling, D. (2005). AMP-activated protein kinase: balancing the scales. Biochimie *87*, 87–91.

Carling, D., Clarke, P.R., Zammit, V.A., and Hardie, D.G. (1989). Purification and characterization of the AMP-activated protein kinase. Copurification of acetyl-CoA carboxylase kinase and 3-hydroxy-3-methylglutaryl-CoA reductase kinase activities. Eur. J. Biochem. FEBS *186*, 129–136.

Carling, D., Thornton, C., Woods, A., and Sanders, M.J. (2012). AMP-activated protein kinase: new regulation, new roles? Biochem. J. *445*, 11–27.

Cartee, G.D., and Wojtaszewski, J.F.P. (2007). Role of Akt substrate of 160 kDa in insulin-stimulated and contraction-stimulated glucose transport. Appl. Physiol. Nutr. Metab. Physiol. Appliquée Nutr. Métabolisme *32*, 557–566.

Chajès, V., Cambot, M., Moreau, K., Lenoir, G.M., and Joulin, V. (2006). Acetyl-CoA carboxylase alpha is essential to breast cancer cell survival. Cancer Res. *66*, 5287–5294.

Chang, T.-J., Chen, W.-P., Yang, C., Lu, P.-H., Liang, Y.-C., Su, M.-J., Lee, S.-C., and Chuang, L.-M. (2009). Serine-385 phosphorylation of inwardly rectifying K+ channel subunit (Kir6.2) by AMP-dependent protein kinase plays a key role in rosiglitazone-induced closure of the K(ATP) channel and insulin secretion in rats. Diabetologia *52*, 1112–1121.

Chen, Y., Zhou, K., Wang, R., Liu, Y., Kwak, Y.-D., Ma, T., Thompson, R.C., Zhao, Y., Smith, L., Gasparini, L., et al. (2009). Antidiabetic drug metformin (GlucophageR) increases biogenesis of Alzheimer's amyloid peptides via up-regulating BACE1 transcription. Proc. Natl. Acad. Sci. U. S. A. *106*, 3907–3912.

Chen, Z.P., Mitchelhill, K.I., Michell, B.J., Stapleton, D., Rodriguez-Crespo, I., Witters, L.A., Power, D.A., Ortiz de Montellano, P.R., and Kemp, B.E. (1999). AMP-activated protein kinase phosphorylation of endothelial NO synthase. FEBS Lett. *443*, 285–289.

Cheng, S.W.Y., Fryer, L.G.D., Carling, D., and Shepherd, P.R. (2004). Thr2446 is a novel mammalian target of rapamycin (mTOR) phosphorylation site regulated by nutrient status. J. Biol. Chem. *279*, 15719–15722.

Ching, Y.P., Davies, S.P., and Hardie, D.G. (1996). Analysis of the specificity of the AMP-activated protein kinase by site-directed mutagenesis of bacterially expressed 3-hydroxy 3-methylglutaryl-CoA reductase, using a single primer variant of the unique-site-elimination method. Eur. J. Biochem. FEBS *237*, 800–808.

Choi, J.-S., Lee, M.S., and Jeong, J.-W. (2010). Ethyl pyruvate has a neuroprotective effect through activation of extracellular signal-regulated kinase in Parkinson's disease model. Biochem. Biophys. Res. Commun. *394*, 854–858.

Clarke, P.R., and Hardie, D.G. (1990). Regulation of HMG-CoA reductase: identification of the site phosphorylated by the AMP-activated protein kinase in vitro and in intact rat liver. EMBO J. *9*, 2439–2446.

Cool, B., Zinker, B., Chiou, W., Kifle, L., Cao, N., Perham, M., Dickinson, R., Adler, A., Gagne, G., Iyengar, R., et al. (2006). Identification and characterization of a small molecule AMPK activator that treats key components of type 2 diabetes and the metabolic syndrome. Cell Metab. *3*, 403–416.

Crooks, G.E., Hon, G., Chandonia, J.-M., and Brenner, S.E. (2004). WebLogo: a sequence logo generator. Genome Res. *14*, 1188–1190.

Crute, B.E., Seefeld, K., Gamble, J., Kemp, B.E., and Witters, L.A. (1998). Functional domains of the alpha1 catalytic subunit of the AMP-activated protein kinase. J. Biol. Chem. *273*, 35347–35354.

Culmsee, C., Monnig, J., Kemp, B.E., and Mattson, M.P. (2001). AMP-activated protein kinase is highly expressed in neurons in the developing rat brain and promotes neuronal survival following glucose deprivation. J. Mol. Neurosci. MN *17*, 45–58.

Dale, S., Wilson, W.A., Edelman, A.M., and Hardie, D.G. (1995). Similar substrate recognition motifs for mammalian AMP-activated protein kinase, higher plant HMG-CoA reductase kinase-A, yeast SNF1, and mammalian calmodulin-dependent protein kinase I. FEBS Lett. *361*, 191–195.

Dasgupta, B., and Milbrandt, J. (2009). AMP-activated protein kinase phosphorylates retinoblastoma protein to control mammalian brain development. Dev. Cell *16*, 256–270.

Davies, J.K., Wells, D.J., Liu, K., Whitrow, H.R., Daniel, T.D., Grignani, R., Lygate, C.A., Schneider, J.E., Noël, G., Watkins, H., et al. (2006). Characterization of the role of gamma2 R531G mutation in AMP-activated protein kinase in cardiac hypertrophy and Wolff-Parkinson-White syndrome. Am. J. Physiol. Heart Circ. Physiol. *290*, H1942–1951.

Davies, S.P., Helps, N.R., Cohen, P.T., and Hardie, D.G. (1995). 5'-AMP inhibits dephosphorylation, as well as promoting phosphorylation, of the AMP-activated protein kinase. Studies using bacterially expressed human protein phosphatase-2C alpha and native bovine protein phosphatase-2AC. FEBS Lett. *377*, 421–425.

Egan, D.F., Shackelford, D.B., Mihaylova, M.M., Gelino, S., Kohnz, R.A., Mair, W., Vasquez, D.S., Joshi, A., Gwinn, D.M., Taylor, R., et al. (2011). Phosphorylation of ULK1 (hATG1) by AMP-activated protein kinase connects energy sensing to mitophagy. Science *331*, 456–461.

Forbes, S.A., Tang, G., Bindal, N., Bamford, S., Dawson, E., Cole, C., Kok, C.Y., Jia, M., Ewing, R., Menzies, A., et al. (2010). COSMIC (the Catalogue of Somatic Mutations in Cancer): a resource to investigate acquired mutations in human cancer. Nucleic Acids Res. *38*, D652–657.

Foretz, M., Carling, D., Guichard, C., Ferré, P., and Foufelle, F. (1998). AMP-activated protein kinase inhibits the glucose-activated expression of fatty acid synthase gene in rat hepatocytes. J. Biol. Chem. *273*, 14767–14771.

Foretz, M., Ancellin, N., Andreelli, F., Saintillan, Y., Grondin, P., Kahn, A., Thorens, B., Vaulont, S., and Viollet, B. (2005). Short-term overexpression of a constitutively active form of AMP-activated protein kinase in the liver leads to mild hypoglycemia and fatty liver. Diabetes *54*, 1331–1339.

Fraser, S.A., Gimenez, I., Cook, N., Jennings, I., Katerelos, M., Katsis, F., Levidiotis, V., Kemp, B.E., and Power, D.A. (2007). Regulation of the renal-specific Na+-K+-2Cl- co-transporter NKCC2 by AMP-activated protein kinase (AMPK). Biochem. J. *405*, 85–93.

Frigo, D.E., Howe, M.K., Wittmann, B.M., Brunner, A.M., Cushman, I., Wang, Q., Brown, M., Means, A.R., and McDonnell, D.P. (2011). CaM kinase kinase beta-mediated activation of the growth regulatory kinase AMPK is required for androgen-dependent migration of prostate cancer cells. Cancer Res. *71*, 528–537.

Fruton, J.S. (1999). Proteins, enzymes, genes: the interplay of chemistry and biology (New Haven, CT: Yale University Press).

Fujii, N., Ho, R.C., Manabe, Y., Jessen, N., Toyoda, T., Holland, W.L., Summers, S.A., Hirshman, M.F., and Goodyear, L.J. (2008). Ablation of AMP-activated protein kinase alpha2 activity exacerbates insulin resistance induced by high-fat feeding of mice. Diabetes *57*, 2958–2966.

Garton, A.J., and Tonks, N.K. (1994). PTP-PEST: a protein tyrosine phosphatase regulated by serine phosphorylation. EMBO J. *13*, 3763–3771.

Geraghty, K.M., Chen, S., Harthill, J.E., Ibrahim, A.F., Toth, R., Morrice, N.A., Vandermoere, F., Moorhead, G.B., Hardie, D.G., and MacKintosh, C. (2007). Regulation of multisite phosphorylation and 14-3-3 binding of AS160 in response to IGF-1, EGF, PMA and AICAR. Biochem. J. *407*, 231–241.

Gollob, M.H., Seger, J.J., Gollob, T.N., Tapscott, T., Gonzales, O., Bachinski, L., and Roberts, R. (2001). Novel PRKAG2 mutation responsible for the genetic syndrome of ventricular preexcitation and conduction system disease with childhood onset and absence of cardiac hypertrophy. Circulation *104*, 3030–3033.

Greer, E.L., Oskoui, P.R., Banko, M.R., Maniar, J.M., Gygi, M.P., Gygi, S.P., and Brunet, A. (2007). The energy sensor AMP-activated protein kinase directly regulates the mammalian FOXO3 transcription factor. J. Biol. Chem. *282*, 30107–30119.

Gwinn, D.M., Shackelford, D.B., Egan, D.F., Mihaylova, M.M., Mery, A., Vasquez, D.S., Turk, B.E., and Shaw, R.J. (2008). AMPK phosphorylation of raptor mediates a metabolic checkpoint. Mol. Cell *30*, 214–226.

Halseth, A.E., Ensor, N.J., White, T.A., Ross, S.A., and Gulve, E.A. (2002). Acute and chronic treatment of ob/ob and db/db mice with AICAR decreases blood glucose concentrations. Biochem. Biophys. Res. Commun. *294*, 798–805.

Hamilton, S.R., Stapleton, D., O'Donnell, J.B., Jr, Kung, J.T., Dalal, S.R., Kemp, B.E., and Witters, L.A. (2001). An activating mutation in the gamma1 subunit of the AMP-activated protein kinase. FEBS Lett. *500*, 163–168.

Hardie, D.G. (2003). Minireview: the AMP-activated protein kinase cascade: the key sensor of cellular energy status. Endocrinology *144*, 5179–5183.

Hardie, D.G. (2007). AMP-activated/SNF1 protein kinases: conserved guardians of cellular energy. Nat. Rev. Mol. Cell Biol. *8*, 774–785.

Hardie, D.G., and Carling, D. (1997). The AMP-activated protein kinase--fuel gauge of the mammalian cell? Eur. J. Biochem. FEBS *246*, 259–273.

Hardie, D.G., and Sakamoto, K. (2006). AMPK: a key sensor of fuel and energy status in skeletal muscle. Physiol. Bethesda Md *21*, 48–60.

Hardie, D.G., Carling, D., and Carlson, M. (1998). The AMP-activated/SNF1 protein kinase subfamily: metabolic sensors of the eukaryotic cell? Annu. Rev. Biochem. *67*, 821–855.

Hardie, D.G., Hawley, S.A., and Scott, J.W. (2006). AMP-activated protein kinase--development of the energy sensor concept. J. Physiol. *574*, 7–15.

Hardie, D.G., Carling, D., and Gamblin, S.J. (2011). AMP-activated protein kinase: also regulated by ADP? Trends Biochem. Sci. *36*, 470–477.

Hardie, D.G., Ross, F.A., and Hawley, S.A. (2012a). AMPK: a nutrient and energy sensor that maintains energy homeostasis. Nat. Rev. Mol. Cell Biol. *13*, 251–262.

Hardie, D.G., Ross, F.A., and Hawley, S.A. (2012b). AMP-activated protein kinase: a target for drugs both ancient and modern. Chem. Biol. *19*, 1222–1236.

Hawley, S.A., Selbert, M.A., Goldstein, E.G., Edelman, A.M., Carling, D., and Hardie, D.G. (1995). 5'-AMP activates the AMP-activated protein kinase cascade, and Ca2+/calmodulin activates the calmodulin-dependent protein kinase I cascade, via three independent mechanisms. J. Biol. Chem. *270*, 27186–27191.

Hawley, S.A., Davison, M., Woods, A., Davies, S.P., Beri, R.K., Carling, D., and Hardie, D.G. (1996). Characterization of the AMP-activated protein kinase kinase from rat liver and identification of threonine 172 as the major site at which it phosphorylates AMP-activated protein kinase. J. Biol. Chem. *271*, 27879–27887.

Hawley, S.A., Boudeau, J., Reid, J.L., Mustard, K.J., Udd, L., Mäkelä, T.P., Alessi, D.R., and Hardie, D.G. (2003). Complexes between the LKB1 tumor suppressor, STRAD alpha/beta and MO25 alpha/beta are upstream kinases in the AMP-activated protein kinase cascade. J. Biol. *2*, 28.

Hawley, S.A., Pan, D.A., Mustard, K.J., Ross, L., Bain, J., Edelman, A.M., Frenguelli, B.G., and Hardie, D.G. (2005). Calmodulin-dependent protein kinase kinase-beta is an alternative upstream kinase for AMP-activated protein kinase. Cell Metab. *2*, 9–19.

Hay, N., and Sonenberg, N. (2004). Upstream and downstream of mTOR. Genes Dev. *18*, 1926–1945.

Hedbacker, K., and Carlson, M. (2008). SNF1/AMPK pathways in yeast. Front. Biosci. J. Virtual Libr. *13*, 2408–2420.

Hemminki, A., Tomlinson, I., Markie, D., Järvinen, H., Sistonen, P., Björkqvist, A.M., Knuutila, S., Salovaara, R., Bodmer, W., Shibata, D., et al. (1997). Localization of a susceptibility locus for Peutz-Jeghers syndrome to 19p using comparative genomic hybridization and targeted linkage analysis. Nat. Genet. *15*, 87–90.

Herrero-Martín, G., Høyer-Hansen, M., García-García, C., Fumarola, C., Farkas, T., López-Rivas, A., and Jäättelä, M. (2009). TAK1 activates AMPK-dependent cytoprotective autophagy in TRAIL-treated epithelial cells. EMBO J. *28*, 677–685.

Hong, Y.H., Varanasi, U.S., Yang, W., and Leff, T. (2003). AMP-activated protein kinase regulates HNF4alpha transcriptional activity by inhibiting dimer formation and decreasing protein stability. J. Biol. Chem. *278*, 27495–27501.

Hoppe, S., Bierhoff, H., Cado, I., Weber, A., Tiebe, M., Grummt, I., and Voit, R. (2009). AMP-activated protein kinase adapts rRNA synthesis to cellular energy supply. Proc. Natl. Acad. Sci. U. S. A. *106*, 17781–17786.

Horman, S., Vertommen, D., Heath, R., Neumann, D., Mouton, V., Woods, A., Schlattner, U., Wallimann, T., Carling, D., Hue, L., et al. (2006). Insulin antagonizes ischemia-induced Thr172 phosphorylation of AMP-activated protein kinase alpha-subunits in heart via hierarchical phosphorylation of Ser485/491. J. Biol. Chem. *281*, 5335–5340.

Hudson, E.R., Pan, D.A., James, J., Lucocq, J.M., Hawley, S.A., Green, K.A., Baba, O., Terashima, T., and Hardie, D.G. (2003). A novel domain in AMP-activated protein kinase causes glycogen storage bodies similar to those seen in hereditary cardiac arrhythmias. Curr. Biol. CB *13*, 861–866.

Hurley, R.L., Anderson, K.A., Franzone, J.M., Kemp, B.E., Means, A.R., and Witters, L.A. (2005). The Ca2+/calmodulin-dependent protein kinase kinases are AMP-activated protein kinase kinases. J. Biol. Chem. *280*, 29060–29066.

Hurley, R.L., Barré, L.K., Wood, S.D., Anderson, K.A., Kemp, B.E., Means, A.R., and Witters, L.A. (2006). Regulation of AMP-activated protein kinase by multisite phosphorylation in response to agents that elevate cellular cAMP. J. Biol. Chem. *281*, 36662–36672.

Inoki, K., Zhu, T., and Guan, K.-L. (2003). TSC2 mediates cellular energy response to control cell growth and survival. Cell *115*, 577–590.

Inoue, E., and Yamauchi, J. (2006). AMP-activated protein kinase regulates PEPCK gene expression by direct phosphorylation of a novel zinc finger transcription factor. Biochem. Biophys. Res. Commun. *351*, 793–799.

Iseli, T.J., Walter, M., van Denderen, B.J.W., Katsis, F., Witters, L.A., Kemp, B.E., Michell, B.J., and Stapleton, D. (2005). AMP-activated protein kinase beta subunit tethers alpha and gamma subunits via its C-terminal sequence (186-270). J. Biol. Chem. *280*, 13395–13400.

Jakobsen, S.N., Hardie, D.G., Morrice, N., and Tornqvist, H.E. (2001). 5'-AMP-activated protein kinase phosphorylates IRS-1 on Ser-789 in mouse C2C12 myotubes in response to 5-aminoimidazole-4-carboxamide riboside. J. Biol. Chem. *276*, 46912–46916.

Jaleel, M., McBride, A., Lizcano, J.M., Deak, M., Toth, R., Morrice, N.A., and Alessi, D.R. (2005). Identification of the sucrose non-fermenting related kinase SNRK, as a novel LKB1 substrate. FEBS Lett. *579*, 1417–1423.

Jellinger, K.A. (2006). Alzheimer 100--highlights in the history of Alzheimer research. J. Neural Transm. Vienna Austria 1996 *113*, 1603–1623.

Jensen, O.N. (2006). Interpreting the protein language using proteomics. Nat. Rev. Mol. Cell Biol. *7*, 391–403.

Jones, R.G., Plas, D.R., Kubek, S., Buzzai, M., Mu, J., Xu, Y., Birnbaum, M.J., and Thompson, C.B. (2005). AMP-activated protein kinase induces a p53-dependent metabolic checkpoint. Mol. Cell *18*, 283–293.

Jørgensen, S.B., Nielsen, J.N., Birk, J.B., Olsen, G.S., Viollet, B., Andreelli, F., Schjerling, P., Vaulont, S., Hardie, D.G., Hansen, B.F., et al. (2004). The alpha2-5'AMP-activated protein kinase is a site 2 glycogen synthase kinase in skeletal muscle and is responsive to glucose loading. Diabetes *53*, 3074–3081.

Jørgensen, S.B., Richter, E.A., and Wojtaszewski, J.F.P. (2006). Role of AMPK in skeletal muscle metabolic regulation and adaptation in relation to exercise. J. Physiol. *574*, 17–31.

Ju, T.-C., Chen, H.-M., Lin, J.-T., Chang, C.-P., Chang, W.-C., Kang, J.-J., Sun, C.-P., Tao, M.-H., Tu, P.-H., Chang, C., et al. (2011). Nuclear translocation of AMPK-alpha1 potentiates striatal neurodegeneration in Huntington's disease. J. Cell Biol. *194*, 209–227.

Kawaguchi, T., Osatomi, K., Yamashita, H., Kabashima, T., and Uyeda, K. (2002). Mechanism for fatty acid "sparing" effect on glucose-induced transcription: regulation of carbohydrate-responsive element-binding protein by AMP-activated protein kinase. J. Biol. Chem. *277*, 3829–3835.

Kemp, B.E. (2004). Bateman domains and adenosine derivatives form a binding contract. J. Clin. Invest. *113*, 182–184.

Khoury, G.A., Baliban, R.C., and Floudas, C.A. (2011). Proteome-wide post-translational modification statistics: frequency analysis and curation of the swiss-prot database. Sci. Reports *1*.

King, J.D., Jr, Fitch, A.C., Lee, J.K., McCane, J.E., Mak, D.-O.D., Foskett, J.K., and Hallows, K.R. (2009). AMP-activated protein kinase phosphorylation of the R domain inhibits PKA stimulation of CFTR. Am. J. Physiol. Cell Physiol. *297*, C94–101.

Koo, S.-H., Flechner, L., Qi, L., Zhang, X., Screaton, R.A., Jeffries, S., Hedrick, S., Xu, W., Boussouar, F., Brindle, P., et al. (2005). The CREB coactivator TORC2 is a key regulator of fasting glucose metabolism. Nature *437*, 1109–1111.

Kornberg, A. (1991). For the love of enzymes: the odyssey of a biochemist (Cambridge, Mass.: Harvard University Press).

Kovacic, S., Soltys, C.-L.M., Barr, A.J., Shiojima, I., Walsh, K., and Dyck, J.R.B. (2003). Akt activity negatively regulates phosphorylation of AMP-activated protein kinase in the heart. J. Biol. Chem. *278*, 39422–39427.

Kuhajda, F.P. (2000). Fatty-acid synthase and human cancer: new perspectives on its role in tumor biology. Nutr. Burbank Los Angeles Cty. Calif *16*, 202–208.

Kurth-Kraczek, E.J., Hirshman, M.F., Goodyear, L.J., and Winder, W.W. (1999). 5' AMP-activated protein kinase activation causes GLUT4 translocation in skeletal muscle. Diabetes *48*, 1667–1671.

Laderoute, K.R., Amin, K., Calaoagan, J.M., Knapp, M., Le, T., Orduna, J., Foretz, M., and Viollet, B. (2006). 5'-AMP-activated protein kinase (AMPK) is induced by low-oxygen and glucose deprivation conditions found in solid-tumor microenvironments. Mol. Cell. Biol. *26*, 5336–5347.

Lamia, K.A., Sachdeva, U.M., DiTacchio, L., Williams, E.C., Alvarez, J.G., Egan, D.F., Vasquez, D.S., Juguilon, H., Panda, S., Shaw, R.J., et al. (2009). AMPK regulates the circadian clock by cryptochrome phosphorylation and degradation. Science *326*, 437–440.

Leclerc, I., Kahn, A., and Doiron, B. (1998). The 5'-AMP-activated protein kinase inhibits the transcriptional stimulation by glucose in liver cells, acting through the glucose response complex. FEBS Lett. *431*, 180–184.

Li, Y., Roux, C., Lazereg, S., LeCaer, J.-P., Laprévote, O., Badet, B., and Badet-Denisot, M.-A. (2007). Identification of a novel serine phosphorylation site in human glutamine:fructose-6-phosphate amidotransferase isoform 1. Biochemistry (Mosc.) *46*, 13163–13169.

Liang, J., and Mills, G.B. (2013). AMPK: a contextual oncogene or tumor suppressor? Cancer Res. *73*, 2929–2935.

Liang, J., Shao, S.H., Xu, Z.-X., Hennessy, B., Ding, Z., Larrea, M., Kondo, S., Dumont, D.J., Gutterman, J.U., Walker, C.L., et al. (2007). The energy sensing LKB1-AMPK pathway regulates p27(kip1) phosphorylation mediating the decision to enter autophagy or apoptosis. Nat. Cell Biol. *9*, 218–224.

Lizcano, J.M., Göransson, O., Toth, R., Deak, M., Morrice, N.A., Boudeau, J., Hawley, S.A., Udd, L., Mäkelä, T.P., Hardie, D.G., et al. (2004). LKB1 is a master kinase that activates 13 kinases of the AMPK subfamily, including MARK/PAR-1. EMBO J. *23*, 833–843.

Lochhead, P.A., Salt, I.P., Walker, K.S., Hardie, D.G., and Sutherland, C. (2000). 5-aminoimidazole-4-carboxamide riboside mimics the effects of insulin on the expression of the 2 key gluconeogenic genes PEPCK and glucose-6-phosphatase. Diabetes *49*, 896–903.

Luo, Z., Saha, A.K., Xiang, X., and Ruderman, N.B. (2005). AMPK, the metabolic syndrome and cancer. Trends Pharmacol. Sci. *26*, 69–76.

Mair, W., Morantte, I., Rodrigues, A.P.C., Manning, G., Montminy, M., Shaw, R.J., and Dillin, A. (2011). Lifespan extension induced by AMPK and calcineurin is mediated by CRTC-1 and CREB. Nature *470*, 404–408.

Marambaud, P., Zhao, H., and Davies, P. (2005). Resveratrol promotes clearance of Alzheimer's disease amyloid-beta peptides. J. Biol. Chem. *280*, 37377–37382.

Marley, A.E., Sullivan, J.E., Carling, D., Abbott, W.M., Smith, G.J., Taylor, I.W., Carey, F., and Beri, R.K. (1996). Biochemical characterization and deletion analysis of recombinant human protein phosphatase 2C alpha. Biochem. J. *320 (Pt 3)*, 801–806.

Marsin, A.S., Bertrand, L., Rider, M.H., Deprez, J., Beauloye, C., Vincent, M.F., Van den Berghe, G., Carling, D., and Hue, L. (2000). Phosphorylation and activation of heart PFK-2 by AMPK has a role in the stimulation of glycolysis during ischaemia. Curr. Biol. CB *10*, 1247–1255.

Marsin, A.-S., Bouzin, C., Bertrand, L., and Hue, L. (2002). The stimulation of glycolysis by hypoxia in activated monocytes is mediated by AMP-activated protein kinase and inducible 6-phosphofructo-2-kinase. J. Biol. Chem. *277*, 30778–30783.

Massie, C.E., Lynch, A., Ramos-Montoya, A., Boren, J., Stark, R., Fazli, L., Warren, A., Scott, H., Madhu, B., Sharma, N., et al. (2011). The androgen receptor fuels prostate cancer by regulating central metabolism and biosynthesis. EMBO J. *30*, 2719–2733.

McBride, A., Ghilagaber, S., Nikolaev, A., and Hardie, D.G. (2009). The glycogen-binding domain on the AMPK beta subunit allows the kinase to act as a glycogen sensor. Cell Metab. *9*, 23–34.

McDonald, A., Fogarty, S., Leclerc, I., Hill, E.V., Hardie, D.G., and Rutter, G.A. (2010). Cell-wide analysis of secretory granule dynamics in three dimensions in living pancreatic beta-cells: evidence against a role for AMPK-dependent phosphorylation of KLC1 at Ser517/Ser520 in glucose-stimulated insulin granule movement. Biochem. Soc. Trans. *38*, 205–208.

McGee, S.L., Howlett, K.F., Starkie, R.L., Cameron-Smith, D., Kemp, B.E., and Hargreaves, M. (2003). Exercise increases nuclear AMPK alpha2 in human skeletal muscle. Diabetes *52*, 926–928.

McGee, S.L., van Denderen, B.J.W., Howlett, K.F., Mollica, J., Schertzer, J.D., Kemp, B.E., and Hargreaves, M. (2008). AMP-activated protein kinase regulates GLUT4 transcription by phosphorylating histone deacetylase 5. Diabetes *57*, 860–867.

Merrill, G.F., Kurth, E.J., Hardie, D.G., and Winder, W.W. (1997). AICA riboside increases AMP-activated protein kinase, fatty acid oxidation, and glucose uptake in rat muscle. Am. J. Physiol. *273*, E1107–1112.

Milan, D., Jeon, J.T., Looft, C., Amarger, V., Robic, A., Thelander, M., Rogel-Gaillard, C., Paul, S., Iannuccelli, N., Rask, L., et al. (2000). A mutation in PRKAG3 associated with excess glycogen content in pig skeletal muscle. Science *288*, 1248–1251.

Milgraum, L.Z., Witters, L.A., Pasternack, G.R., and Kuhajda, F.P. (1997). Enzymes of the fatty acid synthesis pathway are highly expressed in in situ breast carcinoma. Clin. Cancer Res. Off. J. Am. Assoc. Cancer Res. *3*, 2115–2120.

Minokoshi, Y., Alquier, T., Furukawa, N., Kim, Y.-B., Lee, A., Xue, B., Mu, J., Foufelle, F., Ferré, P., Birnbaum, M.J., et al. (2004). AMP-kinase regulates food intake by responding to hormonal and nutrient signals in the hypothalamus. Nature *428*, 569–574.

Miyamoto, T., Oshiro, N., Yoshino, K., Nakashima, A., Eguchi, S., Takahashi, M., Ono, Y., Kikkawa, U., and Yonezawa, K. (2008). AMP-activated protein kinase phosphorylates Golgi-specific brefeldin A resistance factor 1 at Thr1337 to induce disassembly of Golgi apparatus. J. Biol. Chem. *283*, 4430–4438.

Momcilovic, M., Hong, S.-P., and Carlson, M. (2006). Mammalian TAK1 activates Snf1 protein kinase in yeast and phosphorylates AMP-activated protein kinase in vitro. J. Biol. Chem. *281*, 25336–25343.

Motoshima, H., Goldstein, B.J., Igata, M., and Araki, E. (2006). AMPK and cell proliferation--AMPK as a therapeutic target for atherosclerosis and cancer. J. Physiol. *574*, 63–71.

Munday, M.R. (2002). Regulation of mammalian acetyl-CoA carboxylase. Biochem. Soc. Trans. *30*, 1059–1064.

Munday, M.R., Carling, D., and Hardie, D.G. (1988). Negative interactions between phosphorylation of acetyl-CoA carboxylase by the cyclic AMP-dependent and AMP-activated protein kinases. FEBS Lett. *235*, 144–148.

Muoio, D.M., Seefeld, K., Witters, L.A., and Coleman, R.A. (1999). AMP-activated kinase reciprocally regulates triacylglycerol synthesis and fatty acid oxidation in liver and muscle: evidence that sn-glycerol-3-phosphate acyltransferase is a novel target. Biochem. J. *338 (Pt 3)*, 783–791.

Oakhill, J.S., Chen, Z.-P., Scott, J.W., Steel, R., Castelli, L.A., Ling, N., Macaulay, S.L., and Kemp, B.E. (2010). β-Subunit myristoylation is the gatekeeper for initiating metabolic stress sensing by AMP-activated protein kinase (AMPK). Proc. Natl. Acad. Sci. U. S. A. *107*, 19237–19241.

Oakhill, J.S., Steel, R., Chen, Z.-P., Scott, J.W., Ling, N., Tam, S., and Kemp, B.E. (2011). AMPK is a direct adenylate charge-regulated protein kinase. Science *332*, 1433–1435.

Van Oort, M.M., van Doorn, J.M., Hasnaoui, M.E., Glatz, J.F.C., Bonen, A., van der Horst, D.J., Rodenburg, K.W., and P Luiken, J.J.F. (2009). Effects of AMPK activators on the sub-cellular distribution of fatty acid transporters CD36 and FABPpm. Arch. Physiol. Biochem. *115*, 137–146.

Orci, L., Cook, W.S., Ravazzola, M., Wang, M.-Y., Park, B.-H., Montesano, R., and Unger, R.H. (2004). Rapid transformation of white adipocytes into fat-oxidizing machines. Proc. Natl. Acad. Sci. U. S. A. *101*, 2058–2063.

Pang, T., Xiong, B., Li, J.-Y., Qiu, B.-Y., Jin, G.-Z., Shen, J.-K., and Li, J. (2007). Conserved alpha-helix acts as autoinhibitory sequence in AMP-activated protein kinase alpha subunits. J. Biol. Chem. *282*, 495–506.

Pizer, E.S., Thupari, J., Han, W.F., Pinn, M.L., Chrest, F.J., Frehywot, G.L., Townsend, C.A., and Kuhajda, F.P. (2000). Malonyl-coenzyme-A is a potential mediator of cytotoxicity induced by fatty-acid synthase inhibition in human breast cancer cells and xenografts. Cancer Res. *60*, 213–218.

Polekhina, G., Gupta, A., Michell, B.J., van Denderen, B., Murthy, S., Feil, S.C., Jennings, I.G., Campbell, D.J., Witters, L.A., Parker, M.W., et al. (2003). AMPK beta subunit targets metabolic stress sensing to glycogen. Curr. Biol. CB *13*, 867–871.

Prabakaran, S., Lippens, G., Steen, H., and Gunawardena, J. (2012). Post-translational modification: nature's escape from genetic imprisonment and the basis for dynamic information encoding. Wiley Interdiscip. Rev. Syst. Biol. Med. *4*, 565–583.

Rider, M.H., Bertrand, L., Vertommen, D., Michels, P.A., Rousseau, G.G., and Hue, L. (2004). 6-phosphofructo-2-kinase/fructose-2,6-bisphosphatase: head-to-head with a bifunctional enzyme that controls glycolysis. Biochem. J. *381*, 561–579.

Romá-Mateo, C., Solaz-Fuster, M.D.C., Gimeno-Alcañiz, J.V., Dukhande, V.V., Donderis, J., Worby, C.A., Marina, A., Criado, O., Koller, A., Rodriguez De Cordoba, S., et al. (2011). Laforin, a dual-specificity phosphatase involved in Lafora disease, is phosphorylated at Ser25 by AMP-activated protein kinase. Biochem. J. *439*, 265–275.

Sakamoto, K., and Holman, G.D. (2008). Emerging role for AS160/TBC1D4 and TBC1D1 in the regulation of GLUT4 traffic. Am. J. Physiol. Endocrinol. Metab. *295*, E29–37.

Saks, V. (2007). Introduction: From the Discovery of Biological Oxidation to Molecular System Bioenergetics. In Molecular System Bioenergetics, V. Saks, ed. (Weinheim, Germany: Wiley-VCH Verlag GmbH & Co. KGaA), pp. 1–8.

Salminen, A., Kaarniranta, K., Haapasalo, A., Soininen, H., and Hiltunen, M. (2011). AMP-activated protein kinase: a potential player in Alzheimer's disease. J. Neurochem. *118*, 460–474.

Saltiel, A.R., and Kahn, C.R. (2001). Insulin signalling and the regulation of glucose and lipid metabolism. Nature *414*, 799–806.

Sanchez-Cespedes, M. (2007). A role for LKB1 gene in human cancer beyond the Peutz-Jeghers syndrome. Oncogene *26*, 7825–7832.

Schneider, T.D., and Stephens, R.M. (1990). Sequence logos: a new way to display consensus sequences. Nucleic Acids Res. *18*, 6097–6100.

Schwartz, D.C., and Hochstrasser, M. (2003). A superfamily of protein tags: ubiquitin, SUMO and related modifiers. Trends Biochem. Sci. *28*, 321–328.

Schwenk, R.W., Dirkx, E., Coumans, W.A., Bonen, A., Klip, A., Glatz, J.F.C., and Luiken, J.J.F.P. (2010). Requirement for distinct vesicle-associated membrane proteins in insulin- and AMP-activated protein kinase (AMPK)-induced translocation of GLUT4 and CD36 in cultured cardiomyocytes. Diabetologia *53*, 2209–2219.

Scott, J.W., Norman, D.G., Hawley, S.A., Kontogiannis, L., and Hardie, D.G. (2002). Protein kinase substrate recognition studied using the recombinant catalytic domain of AMP-activated protein kinase and a model substrate. J. Mol. Biol. *317*, 309–323.

Scott, J.W., Hawley, S.A., Green, K.A., Anis, M., Stewart, G., Scullion, G.A., Norman, D.G., and Hardie, D.G. (2004). CBS domains form energy-sensing modules whose binding of adenosine ligands is disrupted by disease mutations. J. Clin. Invest. *113*, 274–284.

Scott, R., Crooks, R., and Meldrum, C. (2008). Gene symbol: STK11. Disease: Peutz-Jeghers Syndrome. Hum. Genet. *124*, 300.

Screaton, R.A., Conkright, M.D., Katoh, Y., Best, J.L., Canettieri, G., Jeffries, S., Guzman, E., Niessen, S., Yates, J.R., 3rd, Takemori, H., et al. (2004). The CREB coactivator TORC2 functions as a calcium- and cAMP-sensitive coincidence detector. Cell *119*, 61–74.

Shackelford, D.B., and Shaw, R.J. (2009). The LKB1-AMPK pathway: metabolism and growth control in tumour suppression. Nat. Rev. Cancer *9*, 563–575.

Shang, L., Chen, S., Du, F., Li, S., Zhao, L., and Wang, X. (2011). Nutrient starvation elicits an acute autophagic response mediated by Ulk1 dephosphorylation and its subsequent dissociation from AMPK. Proc. Natl. Acad. Sci. U. S. A. *108*, 4788–4793.

Shaw, R.J., Kosmatka, M., Bardeesy, N., Hurley, R.L., Witters, L.A., DePinho, R.A., and Cantley, L.C. (2004a). The tumor suppressor LKB1 kinase directly activates AMP-activated kinase and regulates apoptosis in response to energy stress. Proc. Natl. Acad. Sci. U. S. A. *101*, 3329–3335.

Shaw, R.J., Bardeesy, N., Manning, B.D., Lopez, L., Kosmatka, M., DePinho, R.A., and Cantley, L.C. (2004b). The LKB1 tumor suppressor negatively regulates mTOR signaling. Cancer Cell *6*, 91–99.

Shaw, R.J., Lamia, K.A., Vasquez, D., Koo, S.-H., Bardeesy, N., Depinho, R.A., Montminy, M., and Cantley, L.C. (2005). The kinase LKB1 mediates glucose homeostasis in liver and therapeutic effects of metformin. Science *310*, 1642–1646.

Shearer, J., Fueger, P.T., Vorndick, B., Bracy, D.P., Rottman, J.N., Clanton, J.A., and Wasserman, D.H. (2004). AMP kinase-induced skeletal muscle glucose but not long-chain fatty acid uptake is dependent on nitric oxide. Diabetes *53*, 1429–1435.

Shearer, J., Wilson, R.J., Battram, D.S., Richter, E.A., Robinson, D.L., Bakovic, M., and Graham, T.E. (2005). Increases in glycogenin and glycogenin mRNA accompany glycogen resynthesis in human skeletal muscle. Am. J. Physiol. Endocrinol. Metab. *289*, E508–514.

Da Silva Xavier, G., Leclerc, I., Salt, I.P., Doiron, B., Hardie, D.G., Kahn, A., and Rutter, G.A. (2000). Role of AMP-activated protein kinase in the regulation by glucose of islet beta cell gene expression. Proc. Natl. Acad. Sci. U. S. A. *97*, 4023–4028.

Sprenkle, A.B., Davies, S.P., Carling, D., Hardie, D.G., and Sturgill, T.W. (1997). Identification of Raf-1 Ser621 kinase activity from NIH 3T3 cells as AMP-activated protein kinase. FEBS Lett. *403*, 254–258.

Stapleton, D., Mitchelhill, K.I., Gao, G., Widmer, J., Michell, B.J., Teh, T., House, C.M., Fernandez, C.S., Cox, T., Witters, L.A., et al. (1996). Mammalian AMP-activated protein kinase subfamily. J. Biol. Chem. *271*, 611–614.

Stein, S.C., Woods, A., Jones, N.A., Davison, M.D., and Carling, D. (2000). The regulation of AMP-activated protein kinase by phosphorylation. Biochem. J. *345 Pt 3*, 437–443.

Steinberg, G.R., and Kemp, B.E. (2009). AMPK in Health and Disease. Physiol. Rev. *89*, 1025–1078.

Stoppani, J., Hildebrandt, A.L., Sakamoto, K., Cameron-Smith, D., Goodyear, L.J., and Neufer, P.D. (2002). AMP-activated protein kinase activates transcription of the UCP3 and HKII genes in rat skeletal muscle. Am. J. Physiol. Endocrinol. Metab. *283*, E1239–1248.

Suter, M., Riek, U., Tuerk, R., Schlattner, U., Wallimann, T., and Neumann, D. (2006). Dissecting the role of 5'-AMP for allosteric stimulation, activation, and deactivation of AMP-activated protein kinase. J. Biol. Chem. *281*, 32207–32216.

Suzuki, A., Okamoto, S., Lee, S., Saito, K., Shiuchi, T., and Minokoshi, Y. (2007). Leptin stimulates fatty acid oxidation and peroxisome proliferator-activated receptor alpha gene expression in mouse C2C12 myoblasts by changing the subcellular localization of the alpha2 form of AMP-activated protein kinase. Mol. Cell. Biol. *27*, 4317–4327.

Swinnen, J.V., Vanderhoydonc, F., Elgamal, A.A., Eelen, M., Vercaeren, I., Joniau, S., Van Poppel, H., Baert, L., Goossens, K., Heyns, W., et al. (2000). Selective activation of the fatty acid synthesis pathway in human prostate cancer. Int. J. Cancer J. Int. Cancer *88*, 176–179.

Terunuma, M., Pangalos, M.N., and Moss, S.J. (2010). Functional modulation of GABAB receptors by protein kinases and receptor trafficking. Adv. Pharmacol. San Diego Calif *58*, 113–122.

Treebak, J.T., Glund, S., Deshmukh, A., Klein, D.K., Long, Y.C., Jensen, T.E., Jørgensen, S.B., Viollet, B., Andersson, L., Neumann, D., et al. (2006). AMPK-mediated AS160 phosphorylation in skeletal muscle is dependent on AMPK catalytic and regulatory subunits. Diabetes *55*, 2051–2058.

Um, J.H., Yang, S., Yamazaki, S., Kang, H., Viollet, B., Foretz, M., and Chung, J.H. (2007). Activation of 5'-AMP-activated kinase with diabetes drug metformin induces casein kinase Iepsilon (CKIepsilon)-dependent degradation of clock protein mPer2. J. Biol. Chem. *282*, 20794–20798.

Vernia, S., Solaz-Fuster, M.C., Gimeno-Alcañiz, J.V., Rubio, T., García-Haro, L., Foretz, M., de Córdoba, S.R., and Sanz, P. (2009). AMP-activated protein kinase phosphorylates R5/PTG, the glycogen targeting subunit of the R5/PTG-protein phosphatase 1 holoenzyme, and accelerates its down-regulation by the laforin-malin complex. J. Biol. Chem. *284*, 8247–8255.

Vingtdeux, V., Giliberto, L., Zhao, H., Chandakkar, P., Wu, Q., Simon, J.E., Janle, E.M., Lobo, J., Ferruzzi, M.G., Davies, P., et al. (2010). AMP-activated protein kinase signaling activation by resveratrol modulates amyloid-beta peptide metabolism. J. Biol. Chem. *285*, 9100–9113.

Vingtdeux, V., Chandakkar, P., Zhao, H., d' Abramo, C., Davies, P., and Marambaud, P. (2011). Novel synthetic small-molecule activators of AMPK as enhancers of autophagy and amyloid-β peptide degradation. FASEB J. Off. Publ. Fed. Am. Soc. Exp. Biol. *25*, 219–231.

Voet, D. (2011). Biochemistry (Hoboken, NJ: John Wiley & Sons).

Wang, M., and Unger, R.H. (2005). Role of PP2C in cardiac lipid accumulation in obese rodents and its prevention by troglitazone. Am. J. Physiol. Endocrinol. Metab. *288*, E216–221.

Wang, C., Mao, X., Wang, L., Liu, M., Wetzel, M.D., Guan, K.-L., Dong, L.Q., and Liu, F. (2007). Adiponectin sensitizes insulin signaling by reducing p70 S6 kinase-mediated serine phosphorylation of IRS-1. J. Biol. Chem. *282*, 7991–7996.

Wang, M.-Y., Orci, L., Ravazzola, M., and Unger, R.H. (2005). Fat storage in adipocytes requires inactivation of leptin's paracrine activity: implications for treatment of human obesity. Proc. Natl. Acad. Sci. U. S. A. *102*, 18011–18016.

Wang, W., Yang, X., Kawai, T., López de Silanes, I., Mazan-Mamczarz, K., Chen, P., Chook, Y.M., Quensel, C., Köhler, M., and Gorospe, M. (2004). AMP-activated protein kinase-regulated phosphorylation and acetylation of importin alpha1: involvement in the nuclear import of RNA-binding protein HuR. J. Biol. Chem. *279*, 48376–48388.

Watt, M.J., Holmes, A.G., Pinnamaneni, S.K., Garnham, A.P., Steinberg, G.R., Kemp, B.E., and Febbraio, M.A. (2006). Regulation of HSL serine phosphorylation in skeletal muscle and adipose tissue. Am. J. Physiol. Endocrinol. Metab. *290*, E500–508.

Webster, I., Friedrich, S.O., Lochner, A., and Huisamen, B. (2010). AMP kinase activation and glut4 translocation in isolated cardiomyocytes. Cardiovasc. J. Afr. *21*, 72–78.

Weisová, P., Concannon, C.G., Devocelle, M., Prehn, J.H.M., and Ward, M.W. (2009). Regulation of glucose transporter 3 surface expression by the AMP-activated protein kinase mediates tolerance to glutamate excitation in neurons. J. Neurosci. Off. J. Soc. Neurosci. *29*, 2997–3008.

Winder, W.W., and Hardie, D.G. (1999). AMP-activated protein kinase, a metabolic master switch: possible roles in type 2 diabetes. Am. J. Physiol. *277*, E1–10.

Won, J.-S., Im, Y.-B., Kim, J., Singh, A.K., and Singh, I. (2010). Involvement of AMP-activated-protein-kinase (AMPK) in neuronal amyloidogenesis. Biochem. Biophys. Res. Commun. *399*, 487–491.

Woods, A., Azzout-Marniche, D., Foretz, M., Stein, S.C., Lemarchand, P., Ferré, P., Foufelle, F., and Carling, D. (2000). Characterization of the role of AMP-activated protein kinase in the regulation of glucose-activated gene expression using constitutively active and dominant negative forms of the kinase. Mol. Cell. Biol. *20*, 6704–6711.

Woods, A., Johnstone, S.R., Dickerson, K., Leiper, F.C., Fryer, L.G.D., Neumann, D., Schlattner, U., Wallimann, T., Carlson, M., and Carling, D. (2003). LKB1 is the upstream kinase in the AMP-activated protein kinase cascade. Curr. Biol. CB *13*, 2004–2008.

Woods, A., Dickerson, K., Heath, R., Hong, S.-P., Momcilovic, M., Johnstone, S.R., Carlson, M., and Carling, D. (2005). Ca2+/calmodulin-dependent protein kinase kinase-beta acts upstream of AMP-activated protein kinase in mammalian cells. Cell Metab. *2*, 21–33.

Wu, Y., Song, P., Xu, J., Zhang, M., and Zou, M.-H. (2007). Activation of protein phosphatase 2A by palmitate inhibits AMP-activated protein kinase. J. Biol. Chem. *282*, 9777–9788.

Xiao, B., Heath, R., Saiu, P., Leiper, F.C., Leone, P., Jing, C., Walker, P.A., Haire, L., Eccleston, J.F., Davis, C.T., et al. (2007). Structural basis for AMP binding to mammalian AMP-activated protein kinase. Nature *449*, 496–500.

Xiao, B., Sanders, M.J., Underwood, E., Heath, R., Mayer, F.V., Carmena, D., Jing, C., Walker, P.A., Eccleston, J.F., Haire, L.F., et al. (2011). Structure of mammalian AMPK and its regulation by ADP. Nature *472*, 230–233.

Xie, M., Zhang, D., Dyck, J.R.B., Li, Y., Zhang, H., Morishima, M., Mann, D.L., Taffet, G.E., Baldini, A., Khoury, D.S., et al. (2006). A pivotal role for endogenous TGF-beta-activated kinase-1 in the LKB1/AMP-activated protein kinase energy-sensor pathway. Proc. Natl. Acad. Sci. U. S. A. *103*, 17378–17383.

Yamaguchi, S., Katahira, H., Ozawa, S., Nakamichi, Y., Tanaka, T., Shimoyama, T., Takahashi, K., Yoshimoto, K., Imaizumi, M.O., Nagamatsu, S., et al. (2005). Activators of AMP-activated protein kinase enhance GLUT4

translocation and its glucose transport activity in 3T3-L1 adipocytes. Am. J. Physiol. Endocrinol. Metab. *289*, E643–649.

Yang, W., Hong, Y.H., Shen, X.Q., Frankowski, C., Camp, H.S., and Leff, T. (2001). Regulation of transcription by AMP-activated protein kinase: phosphorylation of p300 blocks its interaction with nuclear receptors. J. Biol. Chem. *276*, 38341–38344.

Zaid, H., Antonescu, C.N., Randhawa, V.K., and Klip, A. (2008). Insulin action on glucose transporters through molecular switches, tracks and tethers. Biochem. J. *413*, 201–215.

Zhang, B.B., Zhou, G., and Li, C. (2009). AMPK: an emerging drug target for diabetes and the metabolic syndrome. Cell Metab. *9*, 407–416.

Zhou, G., Myers, R., Li, Y., Chen, Y., Shen, X., Fenyk-Melody, J., Wu, M., Ventre, J., Doebber, T., Fujii, N., et al. (2001). Role of AMP-activated protein kinase in mechanism of metformin action. J. Clin. Invest. *108*, 1167–1174.

PART 2

Aim of the project

Rationale of the project

Intracellular sensors of cellular energy and nutrient status are emerging as key players in the regulation of cell metabolism in health and disease. AMP-activated protein kinase (AMPK) has a central role in the regulation of cellular and whole body energy metabolism, and an ever increasing number of studies imply AMPK in major pathologies affecting modern societies such as cancer, cardiovascular and neurodegenerative diseases, diabetes and metabolic syndrome (Carling et al., 2012; Chuang et al., 2013; Zaha and Young, 2012). AMPK seems to become a promising drug target for these diseases, and particular efforts have been invested so far in the development of AMPK activators as anti-diabetic drugs (Zhang et al., 2009; Zhou et al., 2001). However, while the pleiotropic physiological actions of AMPK have favored its role as a putative therapeutic target, they also suggest that AMPK activators or inhibitors should be envisaged with caution for clinical therapy. This has been recognized for example for the use of AMPK activation in anti-cancer therapy (Chuang et al., 2013). Thus, targeting AMPK to cure diseases requires more fundamental research to understand the essential and pleiotropic roles of AMPK in cell metabolism.

Protein-protein interactions are essential for the majority of complex biological functions. Protein interactions include not only high affinity interactions leading to formation of stable protein complexes, but also lower affinity transient interactions, more frequent in signal transduction (e.g. ligand-receptor). In the latter case, interacting proteins can just provide a scaffold for another protein to recruit it to specific localizations, or they use the interaction to modify the interacting partner (e.g. via secondary modifications like phosphorylation). Indeed, proteins always have to interact to carry out their biological function.

Identification of AMPK interactors is essential to understand its upstream regulation and downstream function. Emergence of high throughput screening methods has largely facilitated such approaches. So far, few large-scale screens yielded information on AMPK interaction partners and substrates: *in vitro* phosphoscreens (e.g. Thali et al., 2010; Tuerk et al., 2007), chemical genetic screens (Banko et al., 2011) and peptide library/bioinformatics approaches (Gwinn et al., 2008) for AMPK substrates, as well as yeast-two-hybrid (Y2H) screens (Moreno et al., 2009) and large scale anti-bait co-immunoprecipitation (IP) follow by LC-ESI-MS/MS (e.g. Ewing et al., 2007) for interaction partners. However, only few of the

identified putative AMPK substrates and interactors were confirmed by a second method and/or *in vivo*. In particular co-IP studies do not allow confirming a direct interaction, so many of the identified proteins may interact only indirectly with AMPK.

Aim of the project

Different non-biased screening approaches for AMPK substrates (surface-plasmon-resonance (SPR) screening combined with LC-MS/MS and *in vitro* phosphorylation) and for AMPK interaction partners (Y2H screens), performed by our group, had yielded a number of candidate proteins. These screening procedures as well as some initial confirmation and characterization experiments for selected candidates, were carried out within the PhD thesis of Anna Brückner and the postdoctoral work of Cécile Polge and Alexandre Berthier. However, many molecular details (like e.g. interaction domains) and most importantly the physiological function of these interactions remained unclear. Other candidates were not yet characterized beyond the initial screening data.

Table 1. ***Confirmed AMPK interactors.***

	Biological functions	AMPK phosphorylation consensus-site[1]	Methods to confirm interaction: Split-ubiquitin	Split-trp	Biacore-SPR	Co-IP/ Pull-down
Glutathione-S-transferase (GST)	✓ Detoxification ✓ Antioxidant	1	x	x	x	x
Fumarate hydratase (FH)	✓ Mitochondrial: Krebs cycle ✓ Cytosolic: tumor suppressor	3	x		x	x
E3 ubiquitin-protein ligase NRDP1 (NRDP1)	✓ Protein degradation	1	x	x		
Vesicle associate membran protein (VAMP2/3)	✓ Endo & exocytose ✓ Glucose and fatty acid uptake	-	x	x	x	x

Interactions found by targeted analysis (green), SPR interaction/phosphorylation assays (red) and Y2H techniques (blue) were confirmed by at least two other, independent interaction methods. [1] Consensus sites were determined by sequence analysis

The goal of this thesis was therefore to further investigate some of the AMPK interactors and to understand the biological function of the interaction. From the list of putative AMPK interactors and substrates, four proteins have been selected based on their potential importance in metabolic pathways known to be regulated by AMPK (Table 1). The resulting sub-projects are presented in four separate chapters, followed by a general discussion:

- **Glutathione S-transferase (GST)**. Multiple evidence (Y2H, SPR and co-IP) demonstrated AMPK/GST interaction, and initial data suggested that this served to phosphorylate AMPK. However, subsequent mass spectrometry analysis indicated that the main phosphorylation occurred in the Strep-tag of the recombinant protein. Thus other putative functions AMPK/GST interaction had to be explored like GST-facilitated glutathionylation (Zmijewski et al., 2010) and glutathionylation-induced AMPK activation (Manevich et al., 2004; Ralat et al., 2006; Townsend et al., 2009), which were both, albeit separately, described in literature. The aim of this sub-project was thus to set-up glutathionylation assays and to look into GST-dependent glutathionylation of AMPK. The results have been published in the meantime (Klaus et al., 2013).

- **Fumarate hydratase (FH).** Initial Y2H and *in vitro* phosphorylation experiments had shown that FH interacts with and is phosphorylated by AMPK. The interaction was confirmed by SPR and another Y2H method. The aim of this sub-project was to further validate the interaction by co-IP, examine its consequences on FH activity *in vitro* and *in vivo* and identify the involved AMPK phospho-residue(s). Part of these results has been published (Klaus et al., 2012)

- **E3-ubiquitin-ligase** (**NRDP1).** NRDP1 was the only entirely soluble candidate interactor found in the initial Y2H screen. In addition, other E3-ubiquitin-ligases have been shown to be regulated by AMPK like MuRF1 and Atrogin-1 (Baskin and Taegtmeyer, 2011), or to regulate AMPK like malin in complex with laforin (Moreno et al., 2010). The aim of this sub-project was to produce for the first time the *full-length* NRDP1 protein and examine both putative regulations: of NRDP1 by AMPK, and of AMPK by NRDP1.

- **Vesicle-associated membrane proteins (VAMP2 and VAMP3).** VAMP proteins seemed the most attractive candidate interactors in the initial Y2H screen, since they are key elements of energy-dependent exocytotic processes, but on the other hand they also improve energy state by cell surface expression of nutrient transporters. However, VAMPs turned out not to be phosphorylated by AMPK. The aim of the sub-project was thus to further characterize the VAMP/AMPK interaction and to study its function by developing a strategy for its disruption *in vitro* and *in vivo*.

References

Banko, M.R., Allen, J.J., Schaffer, B.E., Wilker, E.W., Tsou, P., White, J.L., Villén, J., Wang, B., Kim, S.R., Sakamoto, K., et al. (2011). Chemical genetic screen for AMPKα2 substrates uncovers a network of proteins involved in mitosis. Mol. Cell *44*, 878–892.

Baskin, K.K., and Taegtmeyer, H. (2011). AMP-activated protein kinase regulates E3 ligases in rodent heart. Circ. Res. *109*, 1153–1161.

Carling, D., Thornton, C., Woods, A., and Sanders, M.J. (2012). AMP-activated protein kinase: new regulation, new roles? Biochem. J. *445*, 11–27.

Chuang, H.-C., Chou, C.-C., Kulp, S.K., and Chen, C.-S. (2013). AMPK As A Potential Anticancer Target - Friend or Foe? Curr. Pharm. Des.

Ewing, R.M., Chu, P., Elisma, F., Li, H., Taylor, P., Climie, S., McBroom-Cerajewski, L., Robinson, M.D., O'Connor, L., Li, M., et al. (2007). Large-scale mapping of human protein-protein interactions by mass spectrometry. Mol. Syst. Biol. *3*, 89.

Gwinn, D.M., Shackelford, D.B., Egan, D.F., Mihaylova, M.M., Mery, A., Vasquez, D.S., Turk, B.E., and Shaw, R.J. (2008). AMPK phosphorylation of raptor mediates a metabolic checkpoint. Mol. Cell *30*, 214–226.

Klaus, A., Polge, C., Zorman, S., Auchli, Y., Brunisholz, R., and Schlattner, U. (2012). A two-dimensional screen for AMPK substrates identifies tumor suppressor fumarate hydratase as a preferential AMPKα2 substrate. J. Proteomics *75*, 3304–3313.

Klaus, A., Zorman, S., Berthier, A., Polge, C., Ramirez, S., Michelland, S., Sève, M., Vertommen, D., Rider, M., Lentze, N., et al. (2013). Glutathione S-Transferases Interact with AMP-Activated Protein Kinase: Evidence for S-Glutathionylation and Activation In Vitro. PloS One *8*, e62497.

Manevich, Y., Feinstein, S.I., and Fisher, A.B. (2004). Activation of the antioxidant enzyme 1-CYS peroxiredoxin requires glutathionylation mediated by heterodimerization with pi GST. Proc. Natl. Acad. Sci. U. S. A. *101*, 3780–3785.

Moreno, D., Viana, R., and Sanz, P. (2009). Two-hybrid analysis identifies PSMD11, a non-ATPase subunit of the proteasome, as a novel interaction partner of AMP-activated protein kinase. Int. J. Biochem. Cell Biol. *41*, 2431–2439.

Moreno, D., Towler, M.C., Hardie, D.G., Knecht, E., and Sanz, P. (2010). The laforin-malin complex, involved in Lafora disease, promotes the incorporation of K63-linked ubiquitin chains into AMP-activated protein kinase beta subunits. Mol. Biol. Cell *21*, 2578–2588.

Ralat, L.A., Manevich, Y., Fisher, A.B., and Colman, R.F. (2006). Direct evidence for the formation of a complex between 1-cysteine peroxiredoxin and glutathione S-transferase pi with activity changes in both enzymes. Biochemistry (Mosc.) *45*, 360–372.

Thali, R.F., Tuerk, R.D., Scholz, R., Yoho-Auchli, Y., Brunisholz, R.A., and Neumann, D. (2010). Novel candidate substrates of AMP-activated protein kinase identified in red blood cell lysates. Biochem. Biophys. Res. Commun. *398*, 296–301.

Townsend, D.M., Manevich, Y., He, L., Hutchens, S., Pazoles, C.J., and Tew, K.D. (2009). Novel role for glutathione S-transferase pi. Regulator of protein S-Glutathionylation following oxidative and nitrosative stress. J. Biol. Chem. *284*, 436–445.

Tuerk, R.D., Thali, R.F., Auchli, Y., Rechsteiner, H., Brunisholz, R.A., Schlattner, U., Wallimann, T., and Neumann, D. (2007). New candidate targets of AMP-activated protein kinase in murine brain revealed by a novel multidimensional substrate-screen for protein kinases. J. Proteome Res. *6*, 3266–3277.

Zaha, V.G., and Young, L.H. (2012). AMP-activated protein kinase regulation and biological actions in the heart. Circ. Res. *111*, 800–814.

Zhang, B.B., Zhou, G., and Li, C. (2009). AMPK: an emerging drug target for diabetes and the metabolic syndrome. Cell Metab. *9*, 407–416.

Zhou, G., Myers, R., Li, Y., Chen, Y., Shen, X., Fenyk-Melody, J., Wu, M., Ventre, J., Doebber, T., Fujii, N., et al. (2001). Role of AMP-activated protein kinase in mechanism of metformin action. J. Clin. Invest. *108*, 1167–1174.

Zmijewski, J.W., Banerjee, S., Bae, H., Friggeri, A., Lazarowski, E.R., and Abraham, E. (2010). Exposure to hydrogen peroxide induces oxidation and activation of AMP-activated protein kinase. J. Biol. Chem. *285*, 33154–33164.

PART 3

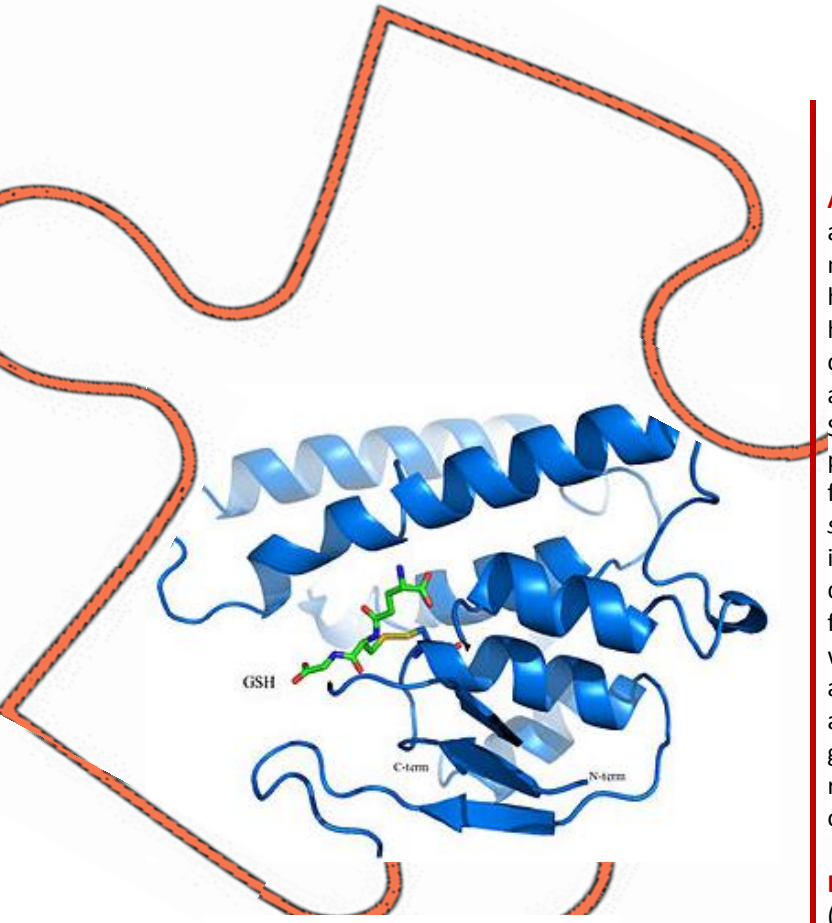

Glutathione S-transferase interacts with AMP-activated protein kinase: evidence for S-glutathionylation and activation *in vitro*

Abstract. AMP-activated protein kinase (AMPK) is a cellular and whole body energy sensor with manifold functions in regulating energy homeostasis, cell morphology and proliferation in health and disease. Here we apply multiple, complementary *in vitro* and *in vivo* interaction assays to identify several isoforms of glutathione S-transferase (GST) as direct AMPK binding partners: Pi-family member rat GSTP1 and Mu-family members rat GSTM1, as well as *schistosoma japonicum* GST. GST/AMPK interaction is direct and involves the N-terminal domain of the AMPK β-subunit. Complex formation of the mammalian GST-P1 and -M1 with AMPK leads to their enzymatic activation and in turn facilitates glutathionylation and activation of AMPK *in vitro*. GST-facilitated S-glutathionylation of AMPK may be involved in rapid, full activation of the kinase under mildly oxidative physiological conditions.

Résumé. La protéine kinase activée par l'AMP (AMPK) est un senseur métabolique de la cellule et de l'organisme avec diverses fonctions dans la régulation de l'homéostasie énergétique, ainsi que dans la morphologie et la prolifération cellulaires, que ce soit en conditions physiologiques ou pathologiques. Dans cette étude nous avons appliqué divers tests d'interaction *in vitro* et *in vivo* pour l'identification d'isoformes de la glutathion S-transferase (GST) interagissant directement avec l'AMPK: GSTP1 et GSTM1 (de rat) respectivement membre de la sous-famille Pi- et Mu-GST, et la GST de *schistosoma japonicum*. L'interaction GST/AMPK est directe et implique le domaine N-terminal de la sous-unité β de l'AMPK. La formation d'un complexe entre GSTP1 ou GSTM1 avec l'AMPK conduit à leur activation enzymatique, facilitant la glutathionylation et l'activation de l'AMPK *in vitro*. La S-glutathionylation de l'AMPK par GST peut être impliquée dans l'activation rapide et totale de la kinase en conditions physiologiques légèrement oxydatives.

This part has been published in PLoS One [Klaus, A., Zorman, S., Berthier, A., Polge, C., Ramirez, S., Michelland, S., Sève, M., Vertommen, D., Rider, M., Lentze, N., et al. (2013). Glutathione S-Transferases Interact with AMP-Activated Protein Kinase: Evidence for S-Glutathionylation and Activation In Vitro. PloS One *8*, e62497.]. **I am co-first author of this publication, I did the functional study that concerns AMPK gluthathionylation and activation by GST**

Introduction

AMP-activated protein kinase (AMPK) is an evolutionary conserved heterotrimeric serine/threonine kinase that plays a central role in sensing and regulating energy homeostasis at the cellular, organ and whole-body level (recently reviewed in (Carling et al., 2012; Hardie, 2011; Hardie et al., 2012; Neumann et al., 2003a; Steinberg and Kemp, 2009; Viollet et al., 2009; Zhang et al., 2009)). It exerts pleiotropic control of metabolic pathways and other physiological functions like cell growth, proliferation, motility or appetite control by affecting enzyme activities and transcription. This has made the kinase a prime pharmacological target for treating metabolic disorders or cancer (Fogarty and Hardie, 2010; Neumann et al., 2003b; Zhang et al., 2009). Activation of AMPK is triggered by a diverse array of external (e.g. hormones, cytokines, nutrients) and internal signals (e.g. AMP, ADP) linked to limited energy availability in physiological and pathological situations. Activation involves covalent phosphorylation of the α-subunit and allosteric binding of AMP or ADP to the γ-subunit. Covalent activation is complex, since it involves stimulated phosphorylation by upstream kinases (LKB1, CamKKβ) and inhibited dephosphorylation by phosphatases, both favored by binding of AMP and also ADP to different sites in the γ-subunit (Oakhill et al., 2011; Xiao et al., 2011) and myristoylation at the β-subunit (Oakhill et al., 2010).

Increasing evidence suggests that AMPK is also activated by reactive oxygen or nitrogen species (ROS, RNS), although the involved mechanisms are not entirely clear. The known inhibitory effect on mitochondrial ATP generation may simply increase cytosolic ADP/ATP and AMP/ATP ratios (Hawley et al., 2010), but also other, non-canonical activation mechanisms are conceivable. We and others have reported for example that ROS/RNS, in particular peroxynitrite, may interfere with AMPK upstream signaling (Xie et al., 2006, 2008; Zou et al., 2004). Vice versa, AMPK activation is involved in downstream redox regulation that can prolong cell survival (Jeon et al., 2012) and induces expression of anti-oxidative proteins like superoxide dismutase (SOD), catalase or thioredoxin (Colombo and Moncada, 2009; Kukidome et al., 2006; Wang et al., 2010).

More recently, S-glutathionylation of Cys299 and Cys304 in the AMPK α-subunit via exposure to the strong oxidant H_2O_2 was reported to activate AMPK (Zmijewski et al., 2010). This reversible posttranslational protein modification can act as a functional switch like the well-

known protein phosphorylation and also protect thiol groups against further oxidation (reviewed in (Pastore and Piemonte, 2012; Pimentel et al., 2012; Xiong et al., 2011)). In case of AMPK, it probably causes activating conformational changes similar to those provoked by AMP-binding (Chen et al., 2012; Riek et al., 2008). Protein S-glutathionylation is often induced non-enzymatically upon expose to strong oxidants, in particular *in vitro* in combination with high glutathione levels (Pastore and Piemonte, 2012; Pimentel et al., 2012; Xiong et al., 2011), as shown for AMPK in presence of 200 mM H_2O_2 (Zmijewski et al., 2010). Intracellular levels of H_2O_2, e.g. in human fibroblasts, may at best reach the low nanomolar range (Arbault et al., 1997), thus spontaneous S-glutathionylation *in vivo* would occur rather slowly and at low levels (Xiong et al., 2011). It may be more important in pathological, highly oxidative situations which change the cellular thiol redox state (ratio of reduced to oxidized glutathione, GSH/GSSG) and generate radical intermediates or oxidized cysteins. *In vivo*, protein glutathionylation is rather facilitated by specific enzymes that may constitute a dynamically regulated S-glutathionylation cycle (Anathy et al., 2012; Pimentel et al., 2012; Xiong et al., 2011). Sulfiredoxins (SRx) and glutaredoxins (Grx) can act in protein deglutathionylation, and the latter enzyme also catalyzes the inverse reaction. More recently, isoforms of glutathione S-transferase (GST (Townsend et al., 2009)), mainly GSTP1, were identified as catalysts of protein S-glutathionylation (de Luca et al., 2011; Manevich et al., 2004; Ralat et al., 2006; Townsend et al., 2009; Wetzelberger et al., 2010) confirming earlier models proposed by Townsend, Tew and colleagues (for recent reviews see (Tew and Townsend, 2011, 2012; Tew et al., 2011)).

GSTs occur as a large superfamily of mitochondrial and cytosolic proteins. In mammals, there are seven classes of cytosolic GSTs, including the Alpha-, Mu-, and Pi-families (Hayes et al., 2005), and lower eukaryotes express orthologs of these. A GST of the unicellular parasite Schistosoma japonicum belonging to the Mu-family is well known as the GST-tag used in fusion proteins to favor solubility and purification of proteins (Smith, 2000). Historically, GSTs were characterized as class II detoxification enzymes that react glutathione with electrophilic compounds like by-products of oxidative stress and xenobiotics, thus facilitating their elimination from the cell (reviewed in (Frova, 2006; Hayes et al., 2005; Lo and Ali-Osman, 2007)). However, some GSTs are now also emerging as ligands or modulators of signaling kinases like JNK, ASK1, PKC, PKA or EGFR, where either the interacting kinase or the GST is

modified, functionally altered or relocated within the cell (Adler et al., 1999; Cho et al., 2001; Gilot et al., 2002; Lo et al., 2004; Yin et al., 2000).

In particular GSTP1 was proposed to initiate a coordinated redox regulation of stress kinases to reduce cell death (Adler et al., 1999; Cho et al., 2001; Gilot et al., 2002; Lo et al., 2004; Yin et al., 2000). While this kind of redox regulation relies exclusively on GST protein interactions, the catalytic activity of GST is required for its role in protein glutathionylation. By hydrogen bonding of glutathione to their active site tyrosine, GST-Alpha, -Mu and -Pi enzymes decrease the pKa of the glutathione thiol group (R-SH) and thus favor thiol deprotonation to form the highly nucleophilic thiolate anion (R-S2) (Graminski et al., 1989; Nieslanik and Atkins, 2000; Pimentel et al., 2012). Such activated glutathione is used in various detoxification reactions, but also allows for S-glutathionylation of sulfenic acids (-SOH) on proteins with low pKa cysteines (Manevich et al., 2004; Townsend et al., 2009; Wetzelberger et al., 2010). Inversely, it has been speculated that low GST peroxidatic activity in presence of peroxides could generate glutathione sulfenic acid intermediates that would react with protein cysteine thiolates (Pimentel et al., 2012). The exact biochemical determinants of GST-catalyzed S-glutathionylation remain to be fully established. In particular, most studies so far were dedicated to the role of GSTP1 following expose to high concentrations of ROS or RNS, while few is known on its role under more physiological conditions and other GST isoforms (Xiong et al., 2011).

Here we describe an *in vitro* glutathionylation and activation of AMPK that is catalyzed by two mammalian GST isoforms, GSTM1 and -P1, and relies on close and direct interaction of these GSTs with the AMPK β-subunit as evidenced by multiple assays. Such AMPK/GST complexes may amplify kinase activation under mildly oxidative, physiological conditions.

Materials & Methods

Cloning and protein production

Cloning, expression and purification of GSTM1, GSTP1, GSTSj, CamKKβ, AMPK α2β2γ1 (221WT) and AMPK α2T172Dβ2γ1 mutant (221TD) is described in (Neumann et al., 2003b; Riek et al., 2009) and Methods S1. For phosphorylation assays, the N-terminal Strep-tag in GSTM1 and P1 was removed, since mass spectrometry identified a serine being phosphorylated by AMPK within this tag (peptide ASWpSHPQFEK, see Methods S1, *Figure S1*).

Yeast two-hybrid assays

Cytosolic yeast two-hybrid (Y2H) systems, Cyto-Y2H (Möckli et al., 2007) and Split-Trp-Y2H (Tafelmeyer et al., 2004), both as variants developed by Dualsystems Biotech (Schlieren, Switzerland), are described in Methods S1 and (Möckli et al., 2007). In short, GST and AMPK subunits were expressed as fusion proteins, in Cyto-Y2H with a membrane anchor and the C-terminal end of ubiquitin conjugated to a transcription factor (bait) or with the N-terminal end of ubiquitin (prey), and in Split-Trp-Y2H with the C-terminal (bait) or the N-terminal (prey) portion of Trp1p. Selective media to control the presence of bait and prey plasmid lacked tryptophan and leucine (SD-WL, Cyto-Y2H) or uracil and leucine (SD-UL, Split-Trp-Y2H), and additionally adenine and histidine (SD-AHWL, Cyto-Y2H) or tryptophan (SDUWL, Split-Trp-Y2H) for protein interaction analysis. Spotted plates were incubated 72 h at 30°C (Cyto-Y2H) or up to 9 days at 27°C (Split-Trp-Y2H).

Rat liver extracts, protein

Rat liver was obtained from animals anesthetized with sodium pentobarbital (40 mg/kg, i.p.) according to the protocol approved by the Grenoble Ethics Committee for Animal Experimentation (no. 36_LBFA-LK-01). Liver tissue was immediately extracted in 10 mM HEPES pH 7.4 (containing 220 mM mannitol, 70 mM sucrose, 0,1% bovine serum albumin (BSA), 0.2 mM EDTA) and centrifuged twice (1000 g and 12 000 g for 10 min each) to obtain soluble proteins in the supernatant for pull-down and immunoprecipitation. Protein concentrations

were determined according to Bradford (Bradford, 1976) with the Biorad microassay (Biorad, Reinach, Switzerland) and BSA as standard.

GST pull-down, immunoprecipitation and immunoblotting

For pull-down assays, either 30 mg of purified recombinant protein (GST-Sj, rat GSTM1 and -P1, or GST-tagged acetyl-CoA carboxylase, GST-ACC (Scott et al., 2002)) or 1 mg proteins from liver extract were incubated with 30 mg recombinant AMPK (α2β2γ1 wild type, 221WT; or T172Dα2β2γ1 mutant, 221TD) for 1 h in PD-buffer (20 mM HEPES pH 7.4, 50 mM NaCl, 2,5 mM MgCl2, 10% glycerol, 6 g/L BSA, 0,5% Tween 20, 0,02% NaN3) before addition of Glutathione Sepharose beads and incubation for an additional hour at 4°C. Where indicated, 1 mM glutathione was included. Sepharose beads were washed eight times and resuspended in SDS sample buffer. For immunoprecipitation, 1 mg protein from liver extracts were reacted with anti-GSTM (ab53942, Abcam) or GSTP1 (ab53943, Abcam) antibody (1:240) in PD-buffer overnight at 4°C. Protein A Sepharose was added, incubated for another hour at 4°C, and washed 8 times before being resuspended in SDS-PAGE sample buffer. Solubilized, denatured proteins were subjected to SDS-PAGE and immunoblotting using anti-AMPKα primary antibody (dilution 1: 1000, 2532, Cell Signaling Technology, Danvers, MA, USA) and anti-rabbit secondary antibody (1: 5000, NA934, GE Healthcare) for detection with a chemiluminescence kit (ECL plus, GE Healthcare) and a CCD camera (ImagerQuant LAS 4000, GE Healthcare). Bands were quantified densitometrically by Image J (imagej.nih.gov/ij) and normalized. Statistical analysis was done by students T-test. Where indicated, proteins stained in PAGE gels with colloidal Coomassie Blue were identified by MALDI-TOF/TOF mass spectrometry.

Surface Plasmon Resonance (SPR) and mass spectrometry (MS)

For SPR with BIAcore (GE Healthcare), GSTs were covalently immobilized by standard amine coupling (GE Healthcare) on the carboxylic functions of two different chips. Gold chips functionalized by mixed self-assembled monolayers as described (Boireau et al., 2009) were kindly provided by Wilfrid Boireau (FEMTO-ST, CNRS Besançon, France). They used 97% 11-mercapto-1-undecanol to reduce non-specific adsorption of proteins to the surface, and 3%

16-mercaptohexadecanoic acid for protein immobilization to obtain well controlled, low ligand densities as convenient for initial experiments with GST-Sj. CM5 chips (GE Healthcare) allowing higher ligand surface densities were used for sequential analyte injection during detailed kinetic analysis. GST (30 mg/ml) in 10 mM acetate buffer pH 6 (GST-Sj), pH 5 (GSTM1) or pH 4 (GSTP1) were injected at 5 ml/min to immobilize <2.5 ng GST/ mm2. Interaction measurements were carried out in running buffer (10 mM HEPES pH 7.4, 100 mM NaCl, 50 mM EDTA, 0.005% Surfactant P20) at a flow rate of 20 ml/min. AMPK diluted to different concentrations just prior to measurements was injected onto the GST surfaces for 180 to 300 s at 20 or 30 ml/min which excludes mass transfer limitations (not shown). Experimental curves were corrected for bulk refractive index changes. Fitting of association and dissociation curves for kinetic analysis was done with BIAevaluation software. GSTs were identified by MALDITOF/TOF and peptide mass fingerprinting, potential phosphosites by LC-MS/MS as described in Methods S1.

AMPK glutathionylation

AMPK 221WT (1 mM, stocks preserved at -80°C) in 0.1 M phosphate buffer pH 6.5 was incubated with or without 10 mM glutathione alone or together with GSTM1 or -P1 (0.5 mM) for 10 min at 30°C. Alternatively, AMPK (1 mM, reduced by overnight incubation with 1 mM ß-mercaptoethanol in phosphate buffer as above) was incubated with EDTA (1 mM) at 30°C alone or together with GSTM1 or -P1 (10 mM, added after 5 min). After 15 min, 0.1 mM glutathione was added for 2 or 4 min. The reaction was stopped by heating in SDS sample buffer and samples separated by non-reducing SDS-PAGE and immunoblotted using primary anti-glutathione antibody (1:1000, MAB5310, Millipore Corporation, Billerica, USA) and anti-mouse secondary antibody (1: 4000, 31430, Pierce, Rockford, USA) for luminescent detection and quantification as described above. Blotted proteins were also visualized by Ponceau staining to reveal M_r shifts due to glutathionylation.

AMPK phosphorylation

AMPK 221WT (25 nM) was incubated for 10 min at 30°C with or without glutathione (10 mM) and in presence or absence of GSTM1 or -P1 (125 nM) in kinase buffer containing 200 mM [γ-^{32}P]ATP (specific activity 400 mCi/mmol ATP), 50 mM AMP, 5 mM $MgCl_2$, 1 mM DTT, and 10 mM HEPES (pH 7.4). Recombinant CamKKβ (1.25 nM) was added and samples were incubated for 3 min at 30°C. The reaction was stopped by heating in SDS sample buffer and AMPK phosphorylation at Thr-172 as an indicator of AMPK activity was probed by SDS-PAGE and immunoblotting with anti-phospho-T172 AMPKα primary antibody (1: 1000, 2531, Cell Signaling Technology, Danvers, MA, USA) and anti-rabbit secondary antibody for luminescent detection and quantification as described above.

AMPK substrate phosphorylation

To analyze GST phosphorylation *in vitro*, AMPK 221WT (4 pmol) was activated by incubation with CamKKβ (1 pmol) for 20 min at 30°C in kinase buffer with cold ATP. Purified GSTs and ACC (Scott et al., 2002) (200 pmol each) were then incubated for 3–60 min at 37°C in the presence or absence of pre-activated AMPK 221WT (4 pmol) in kinase buffer. For negative controls, GSTs were incubated with 1 pmol CamKKβ alone without AMPK. To analyze effects of GST/AMPK complexes on *in vitro* phosphorylation of AMPK substrates, AMPK 221WT (4 pmol, reduced as above) was pre-activated with CamKKβ in kinase buffer with cold ATP and glutathionylated with 0;1 mM glutathione in presence or absence of GSTM1 or -P1, both as described above. Then, ACC (200 pmol) (Scott et al., 2002) and [γ-^{32}P]ATP were added and the mixture incubated for 2 min at 37°C. Kinase reactions were stopped as above, separated on SDS-PAGE and analyzed by Typhoon phosphoimager (GE Healthcare).

Results

GST-Mu and -Pi isoforms interact with AMPK *in vitro*

In the course of our interactomic research on AMPK, we repeatedly pulled down recombinant heterotrimeric AMPK with recombinant proteins fused to a GST-tag that is derived from S.japonicum GST (GST-Sj). In fact, GST-Sj alone can pull down AMPK 221WT (*Figure 1*). We first examined whether such heterologous interaction of GST-Sj with rat AMPK reflects an interaction that evolved with homologous rat GSTM1 (closest homologue of GST-Sj, 44% sequence identity) and GSTP1 (30% sequence identity). Both enzymes were cloned from a rat cDNA library, bacterially expressed and purified. In an assay with fivefold molar excess of GST, both GSTM1 and -P1 were able to pull down AMPK 221WT even after extensive washing (*Figure 1*). These results suggest that the GST/AMPK interaction evolved in at least two different eukaryotic GST classes: the Mu and Pi families.

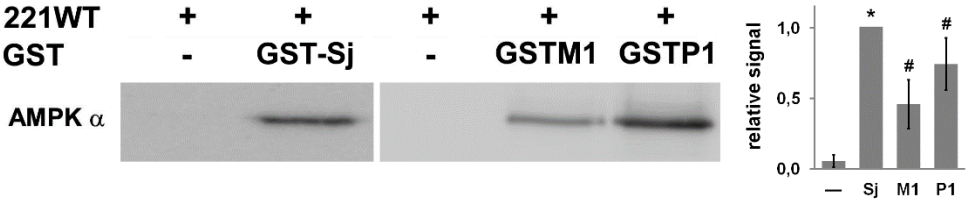

***Figure 1.* GST isoforms and GST-tag interact with full-length AMPK in pull-down assays.** Pull-down of recombinant AMPK 221WT with GST-Sj (S. japonicum), GSTM1 or GSTP1 (R. norvegicus). In all assays, AMPK (0.075 mg/ml) was incubated with or without (negative control) GST proteins (0.075 mg/ml). Pull-down with Glutathione Sepharose 4B was subjected to immunoblot analysis using anti-AMPKα antibody. Left: representative data; right: quantification (mean ± SD, n = 3; * $p<0.01$ and # $p<0.05$ versus no GST).

GST-Mu and -Pi isoforms directly interact with AMPK β-subunits in Y2H assays

A potential direct interaction of GSTs with AMPK *in vivo* was verified by two different last-generation Y2H assays (Brückner et al., 2009). Here, bait/prey interaction leads to reconstitution of split proteins in the yeast cytosol, either of ubiquitin (Cyto-Y2H) or an enzyme in tryptophan biosynthesis (Split-Trp-Y2H). Readout is provided via transcription factor release by ubiquitin-specific proteases that triggers transcription of reporter genes (Cyto-Y2H), or more directly by allowing growth on Trp-deficient medium (Split-Trp-Y2H) (Tafelmeyer et al., 2004). While the transcriptional amplification of the Cyto-Y2H read-out makes it very sensitive

to detect even weak or transient interactions, the direct readout of the Split-Trp-Y2H is more proportional to interaction strength.

The three examined GSTs (GST-Sj, GSTM1, GSTP1) did not interact with AMPK α -subunits in the sensitive Cyto-Y2H assay (*Figure 2*A). However, all three showed interaction with AMPK β-subunits: β1 and β2 in case of GST-Sj, and preferentially β2 in case of GSTM1 and -P1. The N-terminal domain of the β-subunits (Δβ1 or Δβ2, amino acids 1–54) was sufficient for GST/ AMPK binding, suggesting that it is part of the interaction domain. Control experiments confirmed expected GST homodimerization and AMPK α/β-subunit interaction, while no binding to unrelated protein Large T (LT) was detected. The Split-Trp-Y2H assay confirmed these data (*Figure 2*B), although the readout was weaker in some cases, as e.g. in case of the AMPK α-/β-subunit interaction. In both assays, results were similar, irrespective whether GST-Sj was used as bait or prey (not shown).

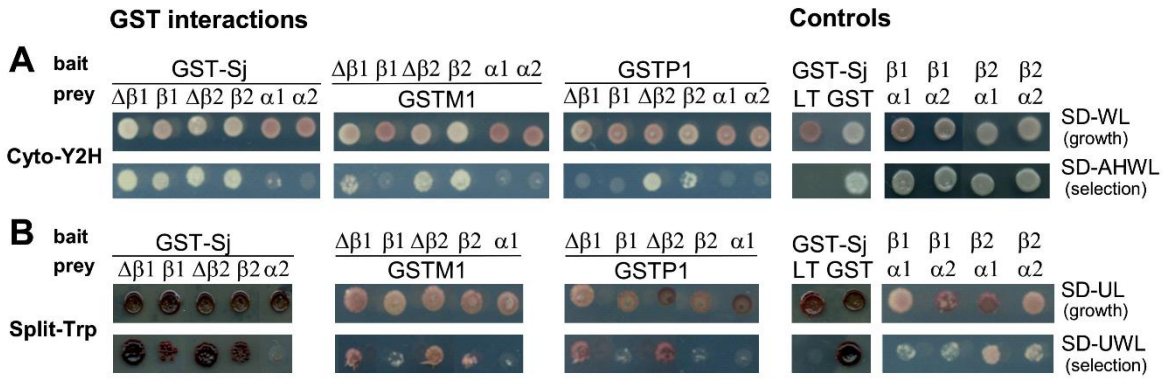

Figure 2. **Y2H analysis identifies GST isoforms as AMPK interaction partners and the AMPK interaction domain.** Two different cytosolic Y2H systems were applied to analyze interaction of AMPK with Schistosoma japonicum GST (GST-Sj) and mammalian (rat) GSTM1 and GSTP1. **(A)** Cyto-Y2H: interacting proteins lead to reconstitution of ubiquitin and a transcriptional readout allowing growth on medium lacking adenine and histidine (SD-AHWL). Spots represent yeast grown for 72 h at 30°C. **(B)** Split-Trp-Y2H: interacting proteins lead to reconstitution of Trp1p, an enzyme in tryptophan biosynthesis, and allow growth on medium lacking tryptophan (SD-UWL). Yeast was grown for 8–9 days at 27°C. Δβ, N-terminal domain of AMPK β-subunit. Controls: LT, Large T Antigen of Simian Virus (amino acids 84–704; negative control); GST, GST-Sj (positive control). A representative data set out of three independent experiments is shown. For more details see Materials and Methods and Supporting Information.

GST/AMPK interaction occurs in rat liver

To test whether also endogenous rat GST isoforms bind to AMPK, we used crude rat liver extracts for co-immunoprecipitation and GST pull-down assays. Liver contains mainly GST-Alpha and -Mu isoforms and few GST-Pi. Endogenous rat AMPK indeed co-immunoprecipitated with antibodies specific for GSTM1/2 and GSTP1 (*Figure 3A*) and pulled down together with three major endogenous GST isoforms, GSTA1, GSTA3 and GSTM1, as identified by MALDI mass spectrometry (*Figure 3B*). If glutathione is then added to the extract, the pull-down assay becomes more stringent. Mainly GSTM1 is now pulled down, while GSTA1 and GSTA3 are strongly reduced, without affecting the quantity of associated AMPK. Finally, when liver extracts were spiked with additional recombinant AMPK 221WT or 221TD, even more AMPK was pulled down (*Figure 3C*). More inactive AMPK 221WT was recovered as compared to AMPK 221TD, a mutant mimicking active AMPK (Stein et al., 2000).

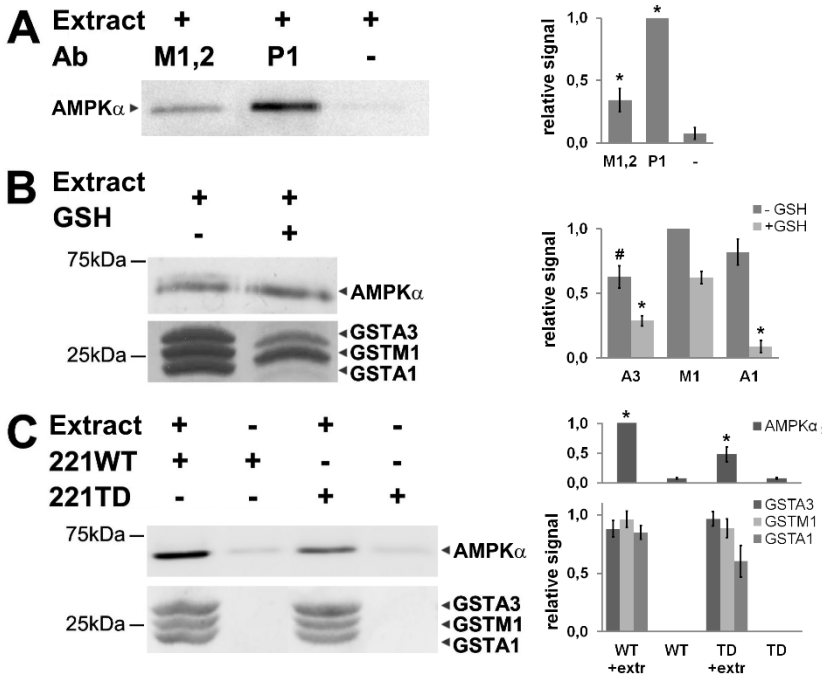

Figure 3. **AMPK interacts with endogenous GST isoforms in rat liver**. GST immunoprecipitation (A) or pull-downs (B, C) were performed with rat liver extract. AMPK in immunoprecipitates or pull-down fractions was detected by immunoblot analysis with anti-αAMPK antibody. The main liver GST isoforms in pull-down fractions were detected by Ponceau staining and mass spectroscopy**. (A)** Immunoprecipitation of endogenous AMPK by anti-GSTM1/2 or anti-GSTP1 antibodies. **(B)** GST pull-down of endogenous liver AMPK by liver GST isoforms in absence or presence of glutathione. Note: Addition of glutathione reduces pull-down of GSTA isoforms without affecting pull-down of AMPK. **(C)** GST pull-down of added AMPK 221WT or constitutively active 221TD. Left: representative data sets; right: quantification (mean ± SD, n = 3; * $p<0.01$ and # $p<0.05$ versus no GST (A), GSTM1 (B) or no extract (C)). Extr, liver extract.

GST/AMPK interaction is direct and rapid

To obtain quantitative data on the GST/AMPK interaction in respect to kinetics and affinity, we performed a series of *in vitro* experiments with surface plasmon resonance spectroscopy (SPR). The GST interaction partner was chosen for covalent immobilization since it appeared more stable in this setup. We first used a sensor chip where the gold surface had been functionalized with a self-assembled monolayer that reduces non-specific adsorption to the surface and allows immobilization of low ligand densities for analyzing GST-Sj. Sensorgrams with AMPK 221WT, 221TD or BSA (negative control) injected onto this surface confirmed a direct GST/AMPK interaction (*Figure 4A*) that was not affected by glutathione (not shown). The equilibrium response was 203641.5 RU for AMPK 221WT, which was reduced to 121627 RU for AMPK 221TD, as compared to 863.7 RU for BSA (*Figure 4B*). Conventional CM5 sensor chips were then used to confirm a specific interaction of rat GSTM1 or GSTP1 with rat AMPK (*Figure 4C*) and to extract affinity data for GSTM1 by injecting an AMPK concentration series (*Figure 4D*). The simple kinetics could be very well fitted to a Langmuir 1:1 model (*Figure 4D*) as seen by the very low residuals of the fit (<1 RU). The fast association ($k_a = 3.1.10^5$ M21 s21) and the very slow dissociation (kd= $1.6.10^{-3}$ s^{-1}) resulting in a KD of about 5 nM.

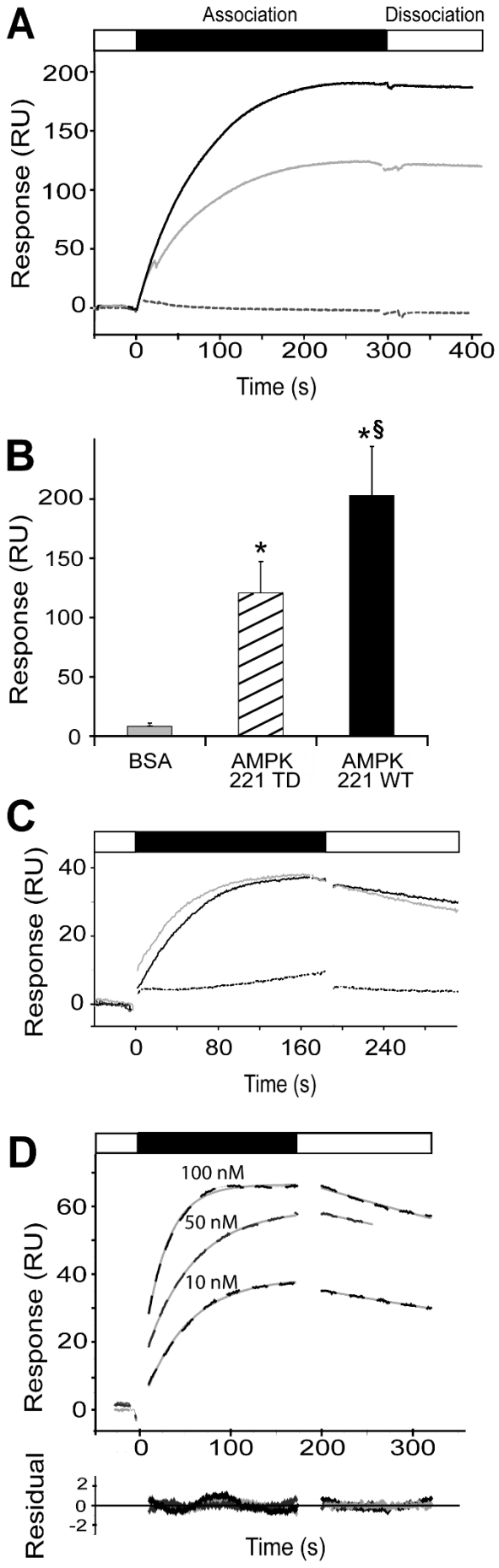

Figure 4. Surface plasmon resonance identifies high affinity interactions between GSTs and AMPK. Freshly diluted, recombinant full-length AMPK was injected onto immobilized GST. **(A)** GST-Sj binding of 10 nM AMPK 221WT (black full line), constitutive active AMPK 221TD (grey full line) or BSA (grey dotted line) at a flow rate of 20 ml/min (surface: self-assembled monolayer). **(B)** Equilibrium response from (A), mean ± SD, 12 (221TD), 6 (221WT) or 3 (BSA) independent experiments (* $p<0.01$ versus control; 1 $p<0.01$ versus AMPK-TD). **(C)** Comparison of GSTM1 (black) or GSTP1 (grey) association and dissociation kinetics of 10 nM AMPK 221WT (full lines) or 100 nM of BSA (dotted lines) and a flow rate of 30 ml/min (surface: CM5). **(D)** GSTM1 association and dissociation kinetics of AMPK 221WT at different concentrations (dashed black lines) and a flow rate of 30 ml/min (surface: CM5), single exponential fit of experimental data (grey lines) and corresponding residuals (to assess the quality of the fit, lower panel). Representative sensorgrams of at least two repetitions are shown. Bars on the top of sensorgrams indicate protein injection (association, black) or injection of running buffer (white).

GST/AMPK complexes do not lead to relevant GST phosphorylation but increase GST activity

To gain insight into the putative role(s) of GST/AMPK complexes, we first examined whether they lead to GST phosphorylation and/or affect GST activity. *In vitro* phosphorylation assays with CamKKβ-activated AMPK and a 50-fold excess of GSTs revealed no phosphorylation of GST-Sj and slow, very low level phosphorylation of GSTM1 and GSTP1 as compared to ACC (*Figure 5*), reaching less than 7% of the ACC phosphorylation level within 1 hour (*Figure S2*). Presence of glutathione did not further increase this phosphorylation (not shown) as it was reported for PKA and PKC (Lo et al., 2004), and no specific phosphosites could be identified by mass spectrometry (not shown). However, in an activity assay using the model substrate 1-chloro-2,4-dinitrobenzene (CDNB), addition of AMPK 221WT to GSTM1 or GSTP1 led to a moderate increase of v_{max} by about 25% at almost unchanged apparent K_m (Table 1, *Figure S3*). This increase occurred only after mixing GST with AMPK, not with BSA, and did not require addition of active AMPK 221TD (Table 1). Thus, GST activation is not due to unspecific stabilization by protein addition and unrelated to the faint and slow GST phosphorylation. Rather, specific GST/AMPK complex formation itself altered the catalytic properties of GST, since GST activation also depended on the amount of AMPK 221WT added (*Figure S3*).

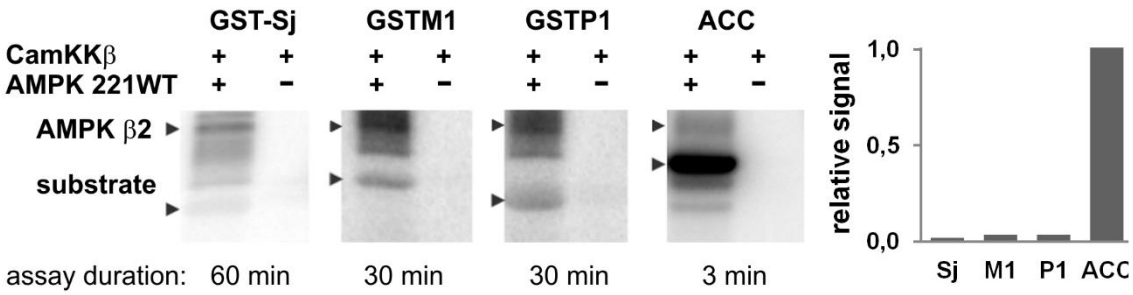

***Figure 5.* GST is a poor AMPK substrate.** AMPK 221WT (4 pmol) pre-activated by CamKKβ (1 pmol) does not phosphorylate GST-Sj and phosphorylates GSTM1 and -P1 only at low levels as compared to ACC (all at 200 pmol). *In vitro* phosphorylation assays were run for 3 min (GST-ACC), 30 min (GSTP1, GSTM1) or 60 min (GST-Sj) and analyzed by SDS-PAGE and Typhoon phosphoimager. Note the autophosphorylation of the AMPK β-subunit.Representative data with quantification are shown. Detailed phosphorylation kinetics is shown in *Figure S2*.

Table 1. ***Enzyme kinetic parameters of GSTP1 in presence or absence of AMPK or BSA.***

	V_{max}	k_{cat}	$K_{m(CDNB)}$
	(U mg^{-1})	*(s^{-1})*	*mM*
GSTM1	21.6±0.8	16.9±0.5	0.037±0.005
GSTM1 + BSA	20.9±0.8	16.4±0.5	0.033±0.006

GSTM1 + AMPK 221	25.5±0.7	20.0±0.5	0.045±0.005
GSTM1 + AMPK 221TD	25.9±0.9	20.3±0.6	0.043±0.006
GSTP1	20.4±2.9	16.0±2.3	1.9±0.4
GSTP1 + BSA	24.6±1.1	19.3±0.9	1.5±0.1
GSTP1 + AMPK221-P [1)]	26.8±0.5	21.0±0.8	1.7±0.1

GST enzyme activity was determined with variable concentrations of model substrate 1-chloro-2.4-dinitrobenzene at a fixed glutathione concentration (10 mM for GSTM1, 2 mM for GSTP1) at 25°C. V_{max} and K_m values were obtained by direct fitting of values to Michaelis-Menten kinetics. Enzyme activity given in U is equivalent to mmol/min. Values are means ± SD, n = 3. [1)] AMPK221 preactivated by phosphorylation with CamKKβ.

GST/AMPK complexes lead to AMPK glutathionylation and activation

It has previously been shown that GSTM1 and -P1 were able to modulate signal transduction through an interaction with JNK and/or other stress activated kinases ((Adler et al., 1999; Yin et al., 2000), reviewed in (Lo and Ali-Osman, 2007)). Hence, we hypothesized that GST could modulate AMPK activity by glutathionylation as it was shown recently (Zmijewski et al., 2010). At very high glutathione concentrations of 10 mM, spontaneous auto-glutathionylation occurred with AMPK 221WT already in absence of mammalian GSTs (*Figure 6A*). However, at more limiting conditions using 0.1 mM glutathione and AMPK pre-reduced with β-mercaptoethanol, auto-glutathionylation was almost absent (*Figure 6B*). In this case, presence of GSTM1 and -P1 increased glutathionylation of AMPK to immunodetectable levels, also visible as a partial shift of AMPK to a higher molecular mass (*Figure 6B*).

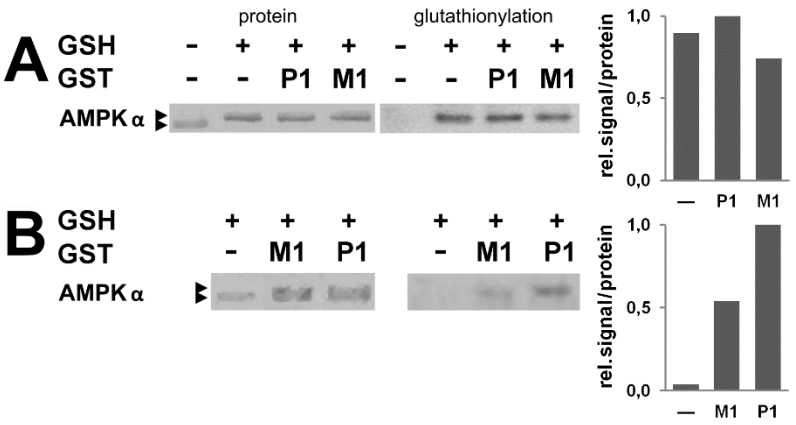

Figure 6. **Glutathionylation of AMPK is facilitated by GST.** Glutathionylation assays were performed **(A)** with AMPK 221WT (1 mM) in absence or presence of GSTM1 or -P1 (0.5 mM) and 10 mM glutathione or **(B)** with AMPK 221WT (1 mM, additionally pre-reduced with β-mercaptoethanol) in absence or presence of GSTM1 or -P1 (10 mM) and 0.1 mM glutathione. AMPK modification was detected either as a molecular mass shift of GST protein

in SDS-PAGE (see arrows in Ponceau protein stain, ‘‘protein’’) or by direct detection of glutathione by immunoblotting (‘‘glutathionylation’’). Note: As soon as glutathione is present, AMPK is almost quantitatively glutathionylated in (A), while additional presence of GST is needed for glutathionylation in (B). Left: representative data; right: quantification (mean, n = 2).

We then analyzed the effect of AMPK S-glutathionylation for AMPK signaling. *In vitro* phosphorylation of AMPK 221WT at αT172 by its upstream kinase CamKKβ was identical in presence or absence of glutathione, and also not further modified by GSTM1 or -P1 (*Figure 7A*). However, phosphorylation of the AMPK downstream substrate ACC was clearly increased with AMPK 221WT preparations that had been glutathionylated before in presence of glutathione by GSTM1 and -P1 as above, compared to controls lacking mammalian GSTs (*Figure 7B*). Activation of AMPK by CamKKβ was a prerequisite for this ACC phosphorylation. CamKKβ (*Figure 7B*) and AMPK alone (*Figure S4*) or combined with GSTs did not affect ACC phosphorylation. These results suggest that GST-dependent S-glutathionylation of AMPK *in vitro* indeed increases kinase activity in the same way as previously shown for H_2O_2-dependent AMPK glutathionylation (Zmijewski et al., 2010).

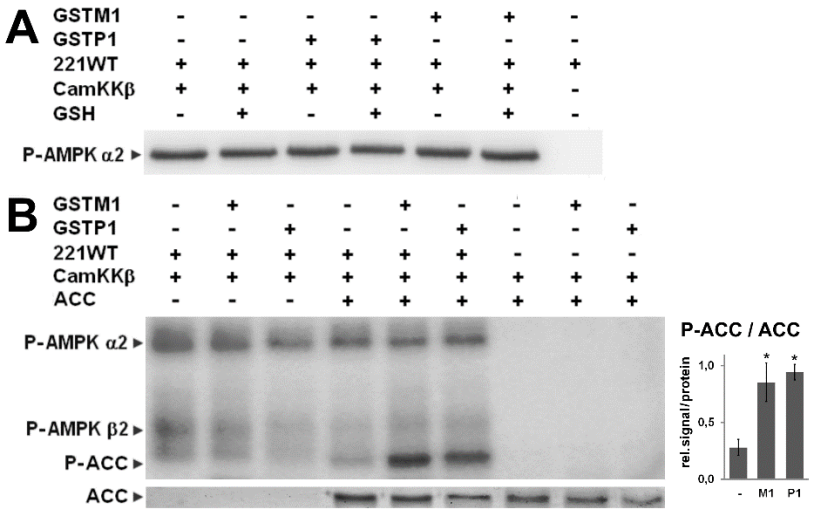

***Figure 7*. AMPK glutathionylation does not affect its phosphorylation by CamKKβ, but increases phosphorylation of downstream substrate**. **(A)** GSTM1 or -P1 (62.5 pmol) were pre-incubated with AMPK 221WT (12.5 pmol) with or without 10 mM glutathione, in presence of ATP prior to addition of CamKKβ (0.63 pmol). Phosphorylation assays were subjected to immunoblot analysis using anti-P-T172-α AMPK antibody. **(B)** AMPK 221WT pre-activated with CamKKβ in kinase buffer with cold ATP and glutathionylated with 0,1 mM glutathione in presence or absence of GSTM1 or -P1, both as described above and in *Figure 6*, were incubated with ACC (200 pmol) and [γ-^{32}P]ATP. *In vitro* phosphorylation assays were analyzed by SDS-PAGE, Ponceau protein staining (lower panel) and Typhoon phosphoimager (upper panel) are shown. Left: representative data; right:

quantification of lanes in presence of glutathione (mean ± SD, n = 4; * = $p<0.01$ versus no GST). A control experiment lacking CamKKβ is shown in *Figure S4*. Note: AMPK autophosphorylation of α- and β-subunits.

Discussion

The energy stress sensor AMPK can be activated by ROS and RNS, possibly via different AMP-dependent and -independent mechanisms (Hawley et al., 2010; Xie et al., 2006; Zou et al., 2004) and is involved in cellular redox regulation (Jeon et al., 2012) and antioxidative defense via induced expression of various antioxidative pathways (Colombo and Moncada, 2009; Kukidome et al., 2006; Wang et al., 2010). Exposure of AMPK to the strong oxidant hydrogen peroxide at high glutathione concentrations induces non-enzymatic S-glutathionylation of AMPK α- and β-subunits which in turn activates the kinase (Zmijewski et al., 2010). Our study adds another element to such redox regulation: activation of AMPK via GST-facilitated glutathionylation in the absence of exogenous oxidant that may be relevant to normal physiological conditions. We provide evidence that mammalian GSTM1 and -P1 can rapidly interact with AMPK, become enzymatically activated by this interaction, and assist in turn in glutathionylation and activation of AMPK as we show *in vitro*.

It has previously been demonstrated that GSTM1 and -P1 were able to modulate signal transduction through interactions with JNK and/or other stress activated kinases ((Adler et al., 1999; Yin et al., 2000), reviewed in (Lo and Ali-Osman, 2007)), and that this can involve GST phosphorylation or modification of the interacting kinase (Adler et al., 1999; Cho et al., 2001; Gilot et al., 2002; Lo et al., 2004; Yin et al., 2000). However, interaction with AMPK led only to slow and low-level phosphorylation of GSTM1 and -P1; its importance (if any) remains to be elucidated. By contrast, complex formation alone was sufficient to increase activity of bound GST and, importantly, to glutathionylate and activate AMPK under *in vitro* conditions where auto-glutathionylation is low, i.e. in the absence of strong oxidants. It is worth noting that protein interaction partners of GST were mostly also identified as targets for S-glutathionylation (e.g. (Cross and Templeton, 2004; Manevich et al., 2004; Wetzelberger et al., 2010)). The residues glutathionylated within AMPK, α-Cys299 and α-Cys304 (Zmijewski et al., 2010), activate AMPK rather due to direct conformational changes as those produced by allosteric AMP regulation. AMPK glutathionylation did not make AMPK a better substrate for the upstream kinase CamKKβ, at least with the recombinant enzymes in the reconstituted *in vitro* system applied here.

Reversible protein modification by cysteine glutathionylation is increasingly recognized as an important signaling mechanism by which cells can respond effectively and reversibly to redox inputs (Pastore and Piemonte, 2012; Xiong et al., 2011). S-glutathionylation inhibits or activates a number of protein kinases (PKA, PKC, MEKK1, ASK1) and phosphatases (reviewed in (Pastore and Piemonte, 2012)). Although the understanding of the S-glutathionylation cycle is still limited, there is evidence for the participation glutaredoxins and GST isoforms, including GSTM1 and -P1 (Tew and Townsend, 2011; Townsend et al., 2009; Wetzelberger et al., 2010). GSTP1P2 knockout mice and cells expressing dead mutants of GSTP have a diminished capacity to S-glutathionylate proteins (Townsend et al., 2009). GSTP plays an essential role in the S-glutathionylation of 1-cys peroxiredoxin (Manevich et al., 2004; Noguera-Mazon et al., 2006; Ralat et al., 2006). Even more, a glutathionylation cycle was recently described to regulate aldose reductase (Wetzelberger et al., 2010). Here, sequential glutathiolyation/ deglutathioylation is catalyzed by GSTP and GRx *in vitro* and *in vivo*, correlated with physical association of the reductase with either GSTP or GRx (Wetzelberger et al., 2010). Since the GST catalytic activity is necessary for lowering the pKa of the glutathione cysteine thiol (Graminski et al., 1989), altered catalytic properties as we observed with GSTM1 and -P1 in complex with AMPK may be relevant for the GST glutathionylation function.

These findings fit very well into the emerging role of AMPK as a redox switch in oxidative stress and redox signaling. AMPK is activated by ROS/RNS via different mechanisms: impaired mitochondrial ATP generation will translate into increased cytosolic AMP/ATP and ADP/ATP ratios that activate AMPK (Hawley et al., 2010), but ROS/RNS may also directly affect upstream mediators and kinases (Xie et al., 2006; Zou et al., 2004) or AMPK itself by glutathionylation (Zmijewski et al., 2010). Activated AMPK in turn up-regulates the cellular antioxidative defense machinery, mainly via the FOXO3 transcription factor: manganese superoxide dismutase (Colombo and Moncada, 2009; Kukidome et al., 2006; Wang et al., 2010), catalase (Colombo and Moncada, 2009; Wang et al., 2010), thioredoxin (Colombo and Moncada, 2009; Hou et al., 2010), metallothioneins (Greer et al., 2007), or uncoupling protein 2 (Xie et al., 2008). Among AMPK-FOXO3-induced genes are also γ-glutamylcysteine synthase, the first enzyme in glutathione biosynthesis (Colombo and Moncada, 2009), glutathione peroxidase (Wang et al., 2010) that uses glutathione to reduce lipid and hydrogen peroxides, as well as GSTM1 (Greer et al., 2007).

The interaction leading to GST/AMPK complexes seems to be rather specific for the GST-Mu and -Pi families, since it was not observed with GST-Alpha and -Omega isoforms (not shown). It does not involve the AMPK a-subunit, as we have recently reported for fumarate hydratase (Klaus et al., 2012), but the β-subunit, as also seen with several other putative mammalian AMPK interactors (IntAct database, (Aranda et al., 2010)) and the yeast and plants orthologs (Polge et al., 2008; Vincent and Carlson, 1999). Our data suggest interaction with the very N-terminal part of the β-subunit, a domain that is fairly well conserved across the AMPK protein family but lacks in the solved core structures of mammalian AMPK and its yeast ortholog ((Xiao et al., 2011); reviewed in (Sanz, 2008)), possibly due to its high flexibility. The physical interaction of AMPK with GST-Sj calls for a note of caution for using GST fusion proteins in pull-down assays to identify AMPK interaction partners.

GST-mediated glutathionylation and activation of AMPK may be considered a possible additional layer of AMPK regulation linking the energy-stress sensor to redox regulation and antioxidative defense. Our present data are novel in that they provide a mechanism for glutathionylation-dependent AMPK activation at low oxidative capacity, as compared to the highly oxidative conditions used in an earlier study (Zmijewski et al., 2010) which may not mimic peroxide concentrations generated intracellularly (Arbault et al., 1997; Pimentel et al., 2012). Further studies have to show the specific importance of this mechanism for *in vivo* regulation of AMPK activity.

Supplementary data

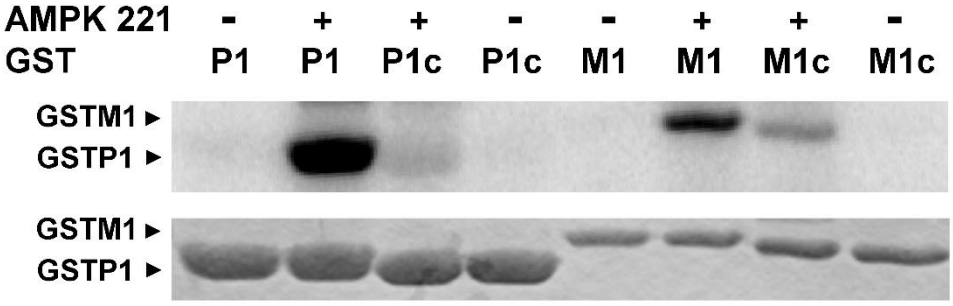

Figure S1. **The Strep-tag in Strep-GST constructs is phosphorylated by AMPK.** Phosphorylation of GSTP1 (200 pmol) and GSTM1 (40 pmol) in Strep-tagged (P1, M1) and Strep-tag-free forms (P1c, M1c) by AMPK221 (4 pmol) activated by CamKKβ (1 pmol). *In vitro* phosphorylation for 10 min at 37°C was analyzed by SDS-PAGE and Typhoon phosphoimager (top panel) and control Coomassie stain for protein loading (bottom panel). Control lanes lack AMPK221 but contain CamKKβ.

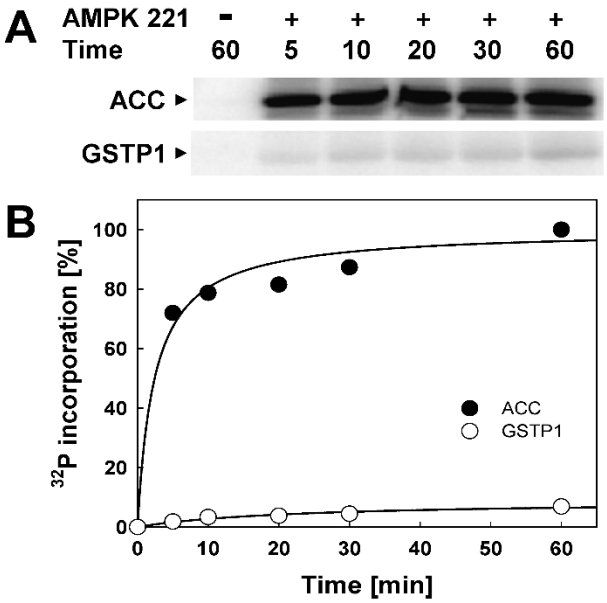

Figure S2. **Substoichiometric phosphorylation of GSTP1 by AMPK *in vitro*. (A)** Phosphorylation time course of GSTP1 or ACC (200 pmol each) by AMPK221 (4 pmol) activated by CamKKβ (1 pmol). *In vitro* phosphorylation for 5 to 60 min at 37°C was analyzed by SDS-PAGE and Typhoon phosphoimager. Control lanes lack AMPK221 but contain CamKKβ. **(B)** Quantification of (A) using Image Quant TL, using normalization to maximal ACC phosphorylation and fitting to phosphorylation enzyme kinetics.

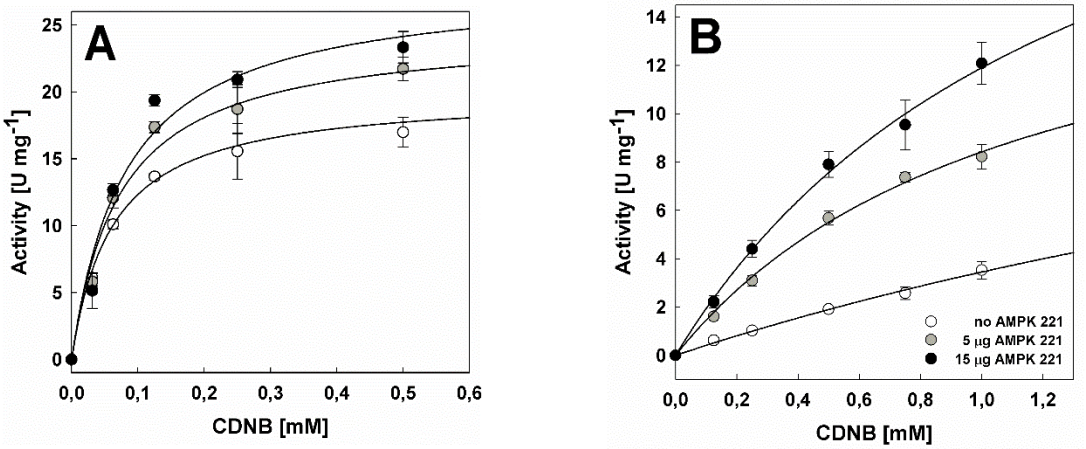

Figure S3. **GSTM1 and -P1 are activated in complexes with AMPK *in vitro*.** Enzyme activity of or 20 mg GSTM1 **(A)** or 30 mg GSTP1 **(B)** in absence or presence of 5 or 15 mg AMPK221WT at different concentrations of the model substrate CDNB and saturating glutathione concentrations.

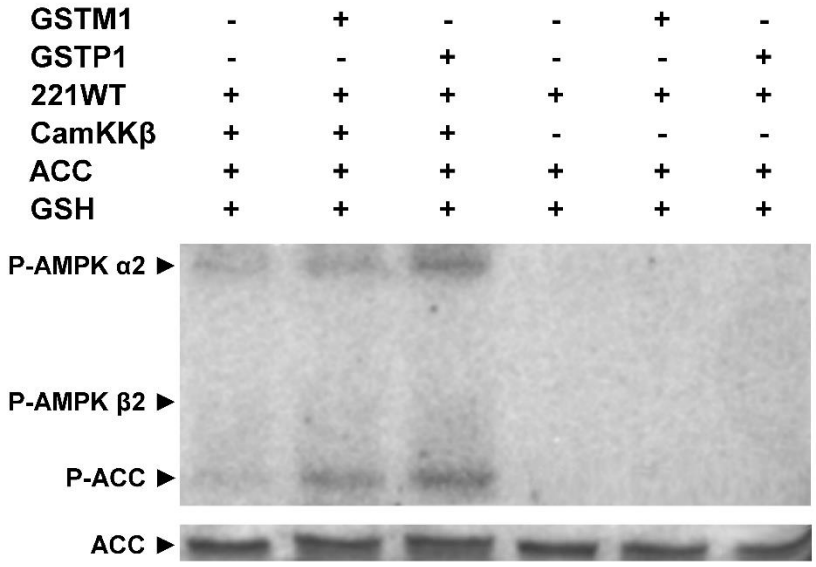

Figure S4. **Increased phosphorylation of AMPK downstream substrate depends on the presence of AMPK activating upstream kinase CamKKβ**. AMPK 221WT preactivated with CamKKβ in kinase buffer with cold ATP and glutathionylated with 0.1 mM glutathione in presence or absence of GSTM1 or -P1, both as described in *Figure 6* and *Figure 7*, were incubated with ACC (200 pmol) and [γ-^{32}P]ATP. *In vitro* phosphorylation assays were analyzed by SDS-PAGE, Ponceau protein staining (lower panel) and Typhoon phosphoimager (upper panel) are shown. Note: AMPK autophosphorylation in particular of the a-subunit.

References

Adler, V., Yin, Z., Fuchs, S.Y., Benezra, M., Rosario, L., Tew, K.D., Pincus, M.R., Sardana, M., Henderson, C.J., Wolf, C.R., et al. (1999). Regulation of JNK signaling by GSTp. EMBO J. *18*, 1321–1334.

Anathy, V., Roberson, E.C., Guala, A.S., Godburn, K.E., Budd, R.C., and Janssen-Heininger, Y.M.W. (2012). Redox-based regulation of apoptosis: S-glutathionylation as a regulatory mechanism to control cell death. Antioxidants Redox Signal. *16*, 496–505.

Aranda, B., Achuthan, P., Alam-Faruque, Y., Armean, I., Bridge, A., Derow, C., Feuermann, M., Ghanbarian, A.T., Kerrien, S., Khadake, J., et al. (2010). The IntAct molecular interaction database in 2010. Nucleic Acids Res. *38*, D525–531.

Arbault, S., Pantano, P., Sojic, N., Amatore, C., Best-Belpomme, M., Sarasin, A., and Vuillaume, M. (1997). Activation of the NADPH oxidase in human fibroblasts by mechanical intrusion of a single cell with an ultramicroelectrode. Carcinogenesis *18*, 569–574.

Boireau, W., Rouleau, A., Lucchi, G., and Ducoroy, P. (2009). Revisited BIA-MS combination: entire “on-a-chip” processing leading to the proteins identification at low femtomole to sub-femtomole levels. Biosens. Bioelectron. *24*, 1121–1127.

Bradford, M.M. (1976). A rapid and sensitive method for the quantitation of microgram quantities of protein utilizing the principle of protein-dye binding. Anal. Biochem. *72*, 248–254.

Brückner, A., Polge, C., Lentze, N., Auerbach, D., and Schlattner, U. (2009). Yeast two-hybrid, a powerful tool for systems biology. Int. J. Mol. Sci. *10*, 2763–2788.

Carling, D., Thornton, C., Woods, A., and Sanders, M.J. (2012). AMP-activated protein kinase: new regulation, new roles? Biochem. J. *445*, 11–27.

Chen, L., Wang, J., Zhang, Y.-Y., Yan, S.F., Neumann, D., Schlattner, U., Wang, Z.-X., and Wu, J.-W. (2012). AMP-activated protein kinase undergoes nucleotide-dependent conformational changes. Nat. Struct. Mol. Biol. *19*, 716–718.

Cho, S.G., Lee, Y.H., Park, H.S., Ryoo, K., Kang, K.W., Park, J., Eom, S.J., Kim, M.J., Chang, T.S., Choi, S.Y., et al. (2001). Glutathione S-transferase mu modulates the stress-activated signals by suppressing apoptosis signal-regulating kinase 1. J. Biol. Chem. *276*, 12749–12755.

Colombo, S.L., and Moncada, S. (2009). AMPKalpha1 regulates the antioxidant status of vascular endothelial cells. Biochem. J. *421*, 163–169.

Cross, J.V., and Templeton, D.J. (2004). Oxidative stress inhibits MEKK1 by site-specific glutathionylation in the ATP-binding domain. Biochem. J. *381*, 675–683.

Fogarty, S., and Hardie, D.G. (2010). Development of protein kinase activators: AMPK as a target in metabolic disorders and cancer. Biochim. Biophys. Acta *1804*, 581–591.

Frova, C. (2006). Glutathione transferases in the genomics era: new insights and perspectives. Biomol. Eng. *23*, 149–169.

Gilot, D., Loyer, P., Corlu, A., Glaise, D., Lagadic-Gossmann, D., Atfi, A., Morel, F., Ichijo, H., and Guguen-Guillouzo, C. (2002). Liver protection from apoptosis requires both blockage of initiator caspase activities and inhibition of ASK1/JNK pathway via glutathione S-transferase regulation. J. Biol. Chem. *277*, 49220–49229.

Graminski, G.F., Kubo, Y., and Armstrong, R.N. (1989). Spectroscopic and kinetic evidence for the thiolate anion of glutathione at the active site of glutathione S-transferase. Biochemistry (Mosc.) *28*, 3562–3568.

Greer, E.L., Oskoui, P.R., Banko, M.R., Maniar, J.M., Gygi, M.P., Gygi, S.P., and Brunet, A. (2007). The energy sensor AMP-activated protein kinase directly regulates the mammalian FOXO3 transcription factor. J. Biol. Chem. *282*, 30107–30119.

Hardie, D.G. (2011). AMP-activated protein kinase: an energy sensor that regulates all aspects of cell function. Genes Dev. *25*, 1895–1908.

Hardie, D.G., Ross, F.A., and Hawley, S.A. (2012). AMPK: a nutrient and energy sensor that maintains energy homeostasis. Nat. Rev. Mol. Cell Biol. *13*, 251–262.

Hawley, S.A., Ross, F.A., Chevtzoff, C., Green, K.A., Evans, A., Fogarty, S., Towler, M.C., Brown, L.J., Ogunbayo, O.A., Evans, A.M., et al. (2010). Use of cells expressing gamma subunit variants to identify diverse mechanisms of AMPK activation. Cell Metab. *11*, 554–565.

Hayes, J.D., Flanagan, J.U., and Jowsey, I.R. (2005). Glutathione transferases. Annu. Rev. Pharmacol. Toxicol. *45*, 51–88.

Hou, X., Song, J., Li, X.-N., Zhang, L., Wang, X., Chen, L., and Shen, Y.H. (2010). Metformin reduces intracellular reactive oxygen species levels by upregulating expression of the antioxidant thioredoxin via the AMPK-FOXO3 pathway. Biochem. Biophys. Res. Commun. *396*, 199–205.

Jeon, S.-M., Chandel, N.S., and Hay, N. (2012). AMPK regulates NADPH homeostasis to promote tumour cell survival during energy stress. Nature *485*, 661–665.

Klaus, A., Polge, C., Zorman, S., Auchli, Y., Brunisholz, R., and Schlattner, U. (2012). A two-dimensional screen for AMPK substrates identifies tumor suppressor fumarate hydratase as a preferential AMPKα2 substrate. J. Proteomics *75*, 3304–3313.

Klaus, A., Zorman, S., Berthier, A., Polge, C., Ramirez, S., Michelland, S., Sève, M., Vertommen, D., Rider, M., Lentze, N., et al. (2013). Glutathione S-Transferases Interact with AMP-Activated Protein Kinase: Evidence for S-Glutathionylation and Activation In Vitro. PloS One *8*, e62497.

Kukidome, D., Nishikawa, T., Sonoda, K., Imoto, K., Fujisawa, K., Yano, M., Motoshima, H., Taguchi, T., Matsumura, T., and Araki, E. (2006). Activation of AMP-activated protein kinase reduces hyperglycemia-induced mitochondrial reactive oxygen species production and promotes mitochondrial biogenesis in human umbilical vein endothelial cells. Diabetes *55*, 120–127.

Lo, H.-W., and Ali-Osman, F. (2007). Genetic polymorphism and function of glutathione S-transferases in tumor drug resistance. Curr. Opin. Pharmacol. *7*, 367–374.

Lo, H.-W., Antoun, G.R., and Ali-Osman, F. (2004). The human glutathione S-transferase P1 protein is phosphorylated and its metabolic function enhanced by the Ser/Thr protein kinases, cAMP-dependent protein kinase and protein kinase C, in glioblastoma cells. Cancer Res. *64*, 9131–9138.

De Luca, A., Moroni, N., Serafino, A., Primavera, A., Pastore, A., Pedersen, J.Z., Petruzzelli, R., Farrace, M.G., Pierimarchi, P., Moroni, G., et al. (2011). Treatment of doxorubicin-resistant MCF7/Dx cells with nitric oxide causes histone glutathionylation and reversal of drug resistance. Biochem. J. *440*, 175–183.

Manevich, Y., Feinstein, S.I., and Fisher, A.B. (2004). Activation of the antioxidant enzyme 1-CYS peroxiredoxin requires glutathionylation mediated by heterodimerization with pi GST. Proc. Natl. Acad. Sci. U. S. A. *101*, 3780–3785.

Möckli, N., Deplazes, A., Hassa, P.O., Zhang, Z., Peter, M., Hottiger, M.O., Stagljar, I., and Auerbach, D. (2007). Yeast split-ubiquitin-based cytosolic screening system to detect interactions between transcriptionally active proteins. BioTechniques *42*, 725–730.

Neumann, D., Schlattner, U., and Wallimann, T. (2003a). A molecular approach to the concerted action of kinases involved in energy homoeostasis. Biochem. Soc. Trans. *31*, 169–174.

Neumann, D., Woods, A., Carling, D., Wallimann, T., and Schlattner, U. (2003b). Mammalian AMP-activated protein kinase: functional, heterotrimeric complexes by co-expression of subunits in Escherichia coli. Protein Expr. Purif. *30*, 230–237.

Nieslanik, B.S., and Atkins, W.M. (2000). The catalytic Tyr-9 of glutathione S-transferase A1-1 controls the dynamics of the C terminus. J. Biol. Chem. *275*, 17447–17451.

Noguera-Mazon, V., Lemoine, J., Walker, O., Rouhier, N., Salvador, A., Jacquot, J.-P., Lancelin, J.-M., and Krimm, I. (2006). Glutathionylation induces the dissociation of 1-Cys D-peroxiredoxin non-covalent homodimer. J. Biol. Chem. *281*, 31736–31742.

Oakhill, J.S., Chen, Z.-P., Scott, J.W., Steel, R., Castelli, L.A., Ling, N., Macaulay, S.L., and Kemp, B.E. (2010). β-Subunit myristoylation is the gatekeeper for initiating metabolic stress sensing by AMP-activated protein kinase (AMPK). Proc. Natl. Acad. Sci. U. S. A. *107*, 19237–19241.

Oakhill, J.S., Steel, R., Chen, Z.-P., Scott, J.W., Ling, N., Tam, S., and Kemp, B.E. (2011). AMPK is a direct adenylate charge-regulated protein kinase. Science *332*, 1433–1435.

Pastore, A., and Piemonte, F. (2012). S-Glutathionylation signaling in cell biology: progress and prospects. Eur. J. Pharm. Sci. Off. J. Eur. Fed. Pharm. Sci. *46*, 279–292.

Pimentel, D., Haeussler, D.J., Matsui, R., Burgoyne, J.R., Cohen, R.A., and Bachschmid, M.M. (2012). Regulation of cell physiology and pathology by protein S-glutathionylation: lessons learned from the cardiovascular system. Antioxidants Redox Signal. *16*, 524–542.

Polge, C., Jossier, M., Crozet, P., Gissot, L., and Thomas, M. (2008). Beta-subunits of the SnRK1 complexes share a common ancestral function together with expression and function specificities; physical interaction with nitrate reductase specifically occurs via AKINbeta1-subunit. Plant Physiol. *148*, 1570–1582.

Ralat, L.A., Manevich, Y., Fisher, A.B., and Colman, R.F. (2006). Direct evidence for the formation of a complex between 1-cysteine peroxiredoxin and glutathione S-transferase pi with activity changes in both enzymes. Biochemistry (Mosc.) *45*, 360–372.

Riek, U., Scholz, R., Konarev, P., Rufer, A., Suter, M., Nazabal, A., Ringler, P., Chami, M., Müller, S.A., Neumann, D., et al. (2008). Structural properties of AMP-activated protein kinase: dimerization, molecular shape, and changes upon ligand binding. J. Biol. Chem. *283*, 18331–18343.

Riek, U., Ramirez, S., Wallimann, T., and Schlattner, U. (2009). A versatile multidimensional protein purification system with full internet remote control based on a standard HPLC system. BioTechniques *46*, ix–xii.

Sanz, P. (2008). AMP-activated protein kinase: structure and regulation. Curr. Protein Pept. Sci. *9*, 478–492.

Scott, J.W., Norman, D.G., Hawley, S.A., Kontogiannis, L., and Hardie, D.G. (2002). Protein kinase substrate recognition studied using the recombinant catalytic domain of AMP-activated protein kinase and a model substrate. J. Mol. Biol. *317*, 309–323.

Smith, D.B. (2000). Generating fusions to glutathione S-transferase for protein studies. Methods Enzymol. *326*, 254–270.

Stein, S.C., Woods, A., Jones, N.A., Davison, M.D., and Carling, D. (2000). The regulation of AMP-activated protein kinase by phosphorylation. Biochem. J. *345 Pt 3*, 437–443.

Steinberg, G.R., and Kemp, B.E. (2009). AMPK in Health and Disease. Physiol. Rev. *89*, 1025–1078.

Tafelmeyer, P., Johnsson, N., and Johnsson, K. (2004). Transforming a (beta/alpha)8--barrel enzyme into a split-protein sensor through directed evolution. Chem. Biol. *11*, 681–689.

Tew, K.D., and Townsend, D.M. (2011). Regulatory functions of glutathione S-transferase P1-1 unrelated to detoxification. Drug Metab. Rev. *43*, 179–193.

Tew, K.D., and Townsend, D.M. (2012). Glutathione-s-transferases as determinants of cell survival and death. Antioxidants Redox Signal. *17*, 1728–1737.

Tew, K.D., Manevich, Y., Grek, C., Xiong, Y., Uys, J., and Townsend, D.M. (2011). The role of glutathione S-transferase P in signaling pathways and S-glutathionylation in cancer. Free Radic. Biol. Med. *51*, 299–313.

Townsend, D.M., Manevich, Y., He, L., Hutchens, S., Pazoles, C.J., and Tew, K.D. (2009). Novel role for glutathione S-transferase pi. Regulator of protein S-Glutathionylation following oxidative and nitrosative stress. J. Biol. Chem. *284*, 436–445.

Vincent, O., and Carlson, M. (1999). Gal83 mediates the interaction of the Snf1 kinase complex with the transcription activator Sip4. EMBO J. *18*, 6672–6681.

Viollet, B., Lantier, L., Devin-Leclerc, J., Hebrard, S., Amouyal, C., Mounier, R., Foretz, M., and Andreelli, F. (2009). Targeting the AMPK pathway for the treatment of Type 2 diabetes. Front. Biosci. Landmark Ed. *14*, 3380–3400.

Wang, S., Dale, G.L., Song, P., Viollet, B., and Zou, M.-H. (2010). AMPKalpha1 deletion shortens erythrocyte life span in mice: role of oxidative stress. J. Biol. Chem. *285*, 19976–19985.

Wetzelberger, K., Baba, S.P., Thirunavukkarasu, M., Ho, Y.-S., Maulik, N., Barski, O.A., Conklin, D.J., and Bhatnagar, A. (2010). Postischemic deactivation of cardiac aldose reductase: role of glutathione S-transferase P and glutaredoxin in regeneration of reduced thiols from sulfenic acids. J. Biol. Chem. *285*, 26135–26148.

Xiao, B., Sanders, M.J., Underwood, E., Heath, R., Mayer, F.V., Carmena, D., Jing, C., Walker, P.A., Eccleston, J.F., Haire, L.F., et al. (2011). Structure of mammalian AMPK and its regulation by ADP. Nature *472*, 230–233.

Xie, Z., Dong, Y., Zhang, M., Cui, M.-Z., Cohen, R.A., Riek, U., Neumann, D., Schlattner, U., and Zou, M.-H. (2006). Activation of protein kinase C zeta by peroxynitrite regulates LKB1-dependent AMP-activated protein kinase in cultured endothelial cells. J. Biol. Chem. *281*, 6366–6375.

Xie, Z., Zhang, J., Wu, J., Viollet, B., and Zou, M.-H. (2008). Upregulation of mitochondrial uncoupling protein-2 by the AMP-activated protein kinase in endothelial cells attenuates oxidative stress in diabetes. Diabetes *57*, 3222–3230.

Xiong, Y., Uys, J.D., Tew, K.D., and Townsend, D.M. (2011). S-glutathionylation: from molecular mechanisms to health outcomes. Antioxidants Redox Signal. *15*, 233–270.

Yin, Z., Ivanov, V.N., Habelhah, H., Tew, K., and Ronai, Z. (2000). Glutathione S-transferase p elicits protection against H2O2-induced cell death via coordinated regulation of stress kinases. Cancer Res. *60*, 4053–4057.

Zhang, B.B., Zhou, G., and Li, C. (2009). AMPK: an emerging drug target for diabetes and the metabolic syndrome. Cell Metab. *9*, 407–416.

Zmijewski, J.W., Banerjee, S., Bae, H., Friggeri, A., Lazarowski, E.R., and Abraham, E. (2010). Exposure to hydrogen peroxide induces oxidation and activation of AMP-activated protein kinase. J. Biol. Chem. *285*, 33154–33164.

Zou, M.-H., Kirkpatrick, S.S., Davis, B.J., Nelson, J.S., Wiles, W.G., 4th, Schlattner, U., Neumann, D., Brownlee, M., Freeman, M.B., and Goldman, M.H. (2004). Activation of the AMP-activated protein kinase by the anti-diabetic drug metformin in vivo. Role of mitochondrial reactive nitrogen species. J. Biol. Chem. *279*, 43940–43951.

PART 4

Fumarate hydratase as AMPK substrate

Abstract. AMP-activated protein kinase (AMPK) is emerging as a central cellular signaling hub involved in energy homeostasis and proliferation. Here we apply an original two-dimensional *in vitro* screening approach for AMPK substrates that combines biophysical interaction based on surface plasmon resonance with *in vitro* phosphorylation. By enriching for proteins that interact with a specific AMPK isoform, we aimed to identify substrates that are also preferentially phosphorylated by this specific AMPK isoform. Application of this screen to full-length AMPK α2β2γ1 and soluble rat liver proteins identified the tumor suppressor fumarate hydratase (FH). FH was confirmed to interact with and to be preferentially phosphorylated by the AMPKα2 isoform by using yeast-two-hybrid and *in vitro* phosphorylation assays. In the second section we show that this phosphorylation occurs mainly at Ser19 in the amphiphatic N-terminal targeting peptide, and at a low level at Thr482 in the FH C-terminal domain 3. Out of some other mitochondrial proteins identified earlier as potential AMPK substrates by *in vitro* screening, also the pyruvate carboxylase prepeptide is phosphorylated by AMPK, suggesting that AMPK phosphorylations in prepeptides may occur more frequently with potential effects on mitochondrial protein import.

Résumé. La protéine kinase activée par l'AMP (AMPK) est un point clé de l'homéostasie énergétique et de la prolifération cellulaire. Dans cette étude nous avons appliqué une approche novatrice de criblage en deux dimensions *in vitro* ciblant des substrats de l'AMPK, combinant interaction biophysique basée sur la méthode de résonance plasmonique de surface avec des tests de phosphorylation *in vitro*. En utilisant un isoforme spécifique de l'AMPK, nous avions pour but d'identifier des substrats qui seraient aussi préférentiellement phosphorylés par ce même isoforme. L'application de ce système de criblage sur l'AMPK α2β2γ1 et sur des protéines solubles de foie de rat ont permis l'identification du suppresseur de tumeur, fumarate hydratase (FH). Le double hybride en levure et les essais de phosphorylation *in vitro* ont confirmé que FH interagit et est phosphorylé préférentiellement par l'isoforme α2 de l'AMPK. Dans la seconde section nous montrons que c'est essentiellement la Ser19 qui est phosphorylée, présente en N-terminal au niveau du peptide signal amphiphatique. Thr482 est phosphorylée plus faiblement. Parmi d'autres protéines mitochondriales identifiées plus tôt comme potentiels substrats de l'AMPK dans des criblages *in vitro*, le prépeptide de la pyruvate carboxylase est phosphorylé par l'AMPK. Ceci suggère que la phosphorylation de prépeptides par l'AMPK peut arriver plus fréquemment, avec un rôle potentiel dans l'import mitochondrial.

PART 4, SECTION 1

Fumarate hydratase is phosphorylated by AMPK

Section 1 of this part has been published in Journal of Proteomics [Klaus, A., Polge, C., Zorman, S., Auchli, Y., Brunisholz, R., and Schlattner, U. (2012). A two-dimensional screen for AMPK substrates identifies tumor suppressor fumarate hydratase as a preferential AMPKα2 substrate. J. Proteomics *75*, 3304–3313.]. **I did the Co-IP and the fumarate hydratase activity assays.**

Introduction

AMP-activated protein kinase (AMPK) is member of a Ser/Thr kinase family conserved across the eukaryotic kingdom, including SNF1 complex in yeast and SnRK1 in plants. These kinases function as heterotrimeric complexes composed of one catalytic α-type subunit and two regulatory β- and γ-type subunits (Bouly et al., 1999; Davies et al., 1994; Jiang and Carlson, 1997; Mitchelhill et al., 1994). Subunits of mammalian AMPK occur as different isoforms (α1, α2, β1, β2, γ1-3) and splice variants (of γ2 and 3), potentially generating multiple different heterotrimeric complexes.

In mammals, AMPK functions mainly as an energy sensor, integrating signals from inside the cell, the cellular environment, and the whole organism (for reviews see (Carling et al., 2011; Hardie, 2007; Mihaylova and Shaw, 2011; Neumann et al., 2003a)). The activation mechanism involves AMP-induced conformational changes, covalent activation by the upstream kinases LKB1 or CamKKβ (Riek et al., 2008; Woods et al., 1996), and AMP- and ADP-dependent inhibition of AMPK dephosphorylation. Altered AMPK signaling has been associated with different human pathologies like diabetes and cancer, and the kinase is a promising drug target for these pathologies (Fogarty and Hardie, 2010; Steinberg and Kemp, 2009). Two of the major drugs used for treating diabetes type II, metformin and thiazolidinediones, activate AMPK (Fryer et al., 2002; Zhou et al., 2001) and many of their therapeutic effects are mediated by AMPK signaling (Shaw et al., 2005). The identification of LKB1, a known tumor suppressor, as an upstream kinase of AMPK (Woods et al., 2003) and the effect of metformin reducing cancer incidence (Libby et al., 2009) have generated substantial interest for the role of AMPK in cancer development. Activated AMPK negatively regulates cell proliferation and the cell cycle, mostly mediated by mTOR and p53, respectively (Alessi et al., 2006; Jones et al., 2005; Kimura et al., 2003). However, treatments based on a systemic activation of AMPK may not only be beneficial, given the largely pleiotropic effects to be expected from a growing number of AMPK substrates.

Systemic activation may be avoided to some degree by targeting specific AMPK isoform combinations, since they show a partial tissue-specificity (Viollet et al., 2009) or may recognize specific substrates. However, information on putative determinants of kinase-substrate interaction is scarce. Few AMPK interactors have been independently verified by more than

one method (Polge et al., 2008; Vincent and Carlson, 1999; Woods et al., 2003), and most interaction data come from large-scale screening like immunoprecipitation-MS analysis with tagged AMPK (Ewing et al., 2007), which do even not proof direct interactions. The variable N-terminal region of the β-subunits has been proposed to mediate interaction of the kinase with its substrates in yeast (Kuramoto et al., 2007) and plants (Solaz-Fuster et al., 2006). In mammals, the α1 and α2 subunits were shown to exhibit subtle different substrate preferences when using variants of the SAMS peptide, suggesting that the two α isoforms could phosphorylate different substrates within the cell (Vernia et al., 2009), but this could not be confirmed so far for known AMPK substrates.

To identify substrates that interact with a specific AMPK isoform combination and thus potentially represent preferential substrates of this AMPK species, we have set up a protocol involving prefractionation and a two-dimensional *in vitro* screening. This combines biophysical interaction assays using surface plasmon resonance (SPR) with *in vitro* phosphorylation assays and protein identification by mass spectrometry (MS) as successfully applied already in an earlier study (Tuerk et al., 2007). This approach identified the tumor suppressor fumarate hydratase (FH) as an interactor and preferential substrate of α2-containing AMPK complexes, with phosphorylation leading to enzymatic activation.

Materials & Methods

Material

AICA-Riboside (AICAR) was from Biotrend Chemicals (Zurich, Switzerland), rabbit polyclonal anti-P-Thr172 AMPKα and anti-His-tag antibodies from Cell Signaling Technology (Danvers, MA, USA), goat polyclonal anti-GSTpi and rabbit polyclonal anti-FH antibody from Abcam (Cambridge, UK), secondary antibodies coupled to horseradish peroxidase were from GE Healthcare Life Science (Buckinghamshire, UK) for rabbit IgG and Thermo Scientific (Rockford, USA) for goat IgG.

Cloning and purification of proteins

Plasmids pγ1β1His-α1, pγ1β1His-α1T172D, pγ1β2His-α2 and pγ1β1His-α2T172D (Neumann et al., 2003b) were used for bacterial expression and purification as published previously (Neumann et al., 2003b; Riek et al., 2009). For Y2H experiments, PCR-amplified inserts were introduced into Y2H vectors pCab and pDSL (Dualsystems Biotech AG, Schlieren, Switzerland). FH (GeneID: 24368) and fatty acid binding protein 1 (FABP1, GeneID:24360) were amplified from rat liver cDNA and introduced into yeast two-hybrid vectors or bacterial expression vectors pET-52b (+) (Merck KGaA, Darmstadt, Germany) and pGEX-4T-1 (GE Healthcare). The fusion constructs Strep-FH, Strep-FABP1, GST-FH, GST-FABP1, GST-ACC (plasmid kindly provided by G. Hardie, Univ. of Dundee, UK) (Scott et al., 2002) and GST-CamKKβ (plasmid kindly provided by H. Tokumitsu, Kagawa Medical University, Japan) were bacterially expressed and purified according to standard procedures and the tag proteolytically removed where necessary. For further details see the online Supplementary Material 1.

Preparation and prefractionation of liver extract

Total liver from one rat was snap-frozen in liquid nitrogen and homogenized in 15 ml ice-cold extraction buffer A (20 mM HEPES, pH 7.4, 100 mM NaCl, 50 µM EDTA, and anti-protease cocktail, 1 tablet per 50 ml solution, Roche Diagnostics, Basel, Switzerland) using a Polytron PT 3000 homogenizer at 24 000 rpm for 20 s. After centrifugation at 15000 g for 30 min at 4°C,

the supernatant was filtered through a 0.22 µm filter. Prefractionation was carried out on an Äkta Explorer 100 Air HPLC system (GE Healthcare). Three ml of liver extract were applied to a Ni-NTA column (2 ml bed volume; Qiagen) preequilibrated in buffer A. The column was then washed at a flow rate of 1 ml/min with 2 column volumes (CV) of buffer A. Proteins were eluted with imidazole buffer (20 mM HEPES, pH 7.4, 100 mM NaCl and 250 mM imidazole) and the first 5 ml collected. This process was repeated 3 times. Between each load, the column was washed with 4 CV imidazole buffer, 1 CV water, 1 CV NaOH 0.5 M and 5 CV buffer A. To reduce the volume, collected proteins were precipitated with 80% (w/v) ammonium sulfate for 2 hours at 4°C. The pellet was resuspended in 5 ml buffer A and further centrifuged at 15 000 g for 10 min at 4 °C. The supernatant was filtered (0.22 mm filter) and applied to a Superdex 200 size exclusion column (separation range Mr 10 000-600 000; volume 120 ml; GE Healthcare) preequilibrated in buffer A. Proteins were then separated at a flow rate of 1 ml/min and collected in 12 fractions of 5 ml each (S1 to S12) supplemented with anti-protease cocktail (Roche, 1 tablet per 50 ml solution) was added.

Surface plasmon resonance interaction screening and yeast two-hybrid assays

The SPR screening was performed with a BIAcore 2000 (GE Healthcare) using a NTA sensor chip (GE Healthcare) and as running buffer 10 mM HEPES pH 7.4, 100 mM NaCl, 50 µM EDTA and 0.005 % Surfactant P20. In each measurement cycle, the NTA surface was activated by a 1 min-pulse of 500 µM NiCl2 and 50 nM His-tagged AMPK α2β2γ1 (AMPK221) was injected at 5 µl/min until reaching 4000 response units (RU) of immobilization. An HPLC fraction was then injected onto the AMP221 surface at 20 µl/min for 120 s. Interacting protein was quantified at a reporting point 80 s after dissociation start, since the association phase was biased by an SPR signal caused by the chromatography sample buffer. After 120 s of dissociation, a protein–free surface was regenerated by injection of 10 mM HEPES, pH 8.3, 150 mM NaCl, 350 mM EDTA and 0.005 % Surfactant P20. Binary protein-protein interactions were analyzed *in vivo* using the Cyto-Y2H system (Dualsystems Biotech) (Möckli et al., 2007) based on the split-ubiquitin system (Johnsson and Varshavsky, 1994; Stagljar et al., 1998) (see online Supplementary Material 1).

Co-immunoprecipitation

Strep-tagged FH (1µg) and His-tagged AMPK 221TD (1µg) were co-immunoprecipitated with anti-His-tag antibody (1:200) and protein G Sepharose (10% w/v) in IP buffer (30 mM Hepes pH 7.3, 300 mM NaCl, 6 g/l BSA, 0.5% w/v dodecylmaltoside) overnight at 4°C. Sepharose was washed twice (30 mM Hepes pH 7.3, 300 mM NaCl, 0.1% Tween 20) and resuspended in SDS-PAGE sample buffer. Proteins separated by SDS-PAGE were probed for FH by immunoblotting.

AMPK substrate phosphorylation screening

AMPK phosphorylation assays were performed at 37 °C in a final volume of 25 µl containing 12.5 µl of chromatography fractions and kinase buffer (200 µM [γ-32P]ATP (400 mCi/mmol ATP), 50 µM AMP, 5 mM MgCl2, 1 mM DTT and 10 mM HEPES pH 7.4), with or without recombinant constitutively active AMPK221 (50 pmol). The kinase reactions were stopped after 2 min by addition of 10 µl SDS sample buffer (105 mM Tris-HCl, pH 6.8, 4% (w/v) SDS, 15% (v/v) glycerol, 1.2 M β-mercaptoethanol, and 0.02% (w/v) bromophenol blue), heated to 95 °C for 5 min, and separated by SDS-PAGE. Following colloidal Coomassie staining, gels were air-dried and exposed to autoradiography films (GE Healthcare) for up to 2 weeks or to Typhoon imager (GE Healthcare).

Trypsin digestion and mass spectrometry

Radioactively labeled AMPK-specific bands were cut from the gels, in-gel trypsin-digested (Promega), and extracted peptides analyzed by MALDI MS and MALDI MS/MS using an Ultraflex TOF/TOF II (Bruker Daltonics, Bremen, Germany). Processed spectra were combined through BioTools software (Bruker Daltonics) to search the Uniref100 database (release 6.0), non-restricted to the taxonomy, using MASCOT software v. 2.0 (Matrix Science, London, UK). Probability-based MOWSE scores greater than 50 were considered significant. For details see the online Supplementary Material 2.

In vitro analysis of AMPK substrate phosphorylation

To compare phosphorylation kinetics, purified FABP1, FH and ACC Strep- or GST-constructs (200 pmol) were incubated for 5, 10, 20, 30 and 60 min at 37°C with 200 µM [γ-32P]ATP (specific activity 650 mCi/mmol ATP) and AMPK221 (4 pmol) previously activated by incubation with 1 pmol CamKKβ for 20 min at 30°C in kinase buffer (200 µM ATP, 50 µM AMP, 5 mM MgCl2, 1 mM DTT, 10 mM HEPES pH 7.4). To compare phosphorylation by different AMPK isoforms, purified Strep-FH and GST-ACC (200 pmol) were incubated for 8 min at 37°C in the presence or absence of 3 pmol previously activated AMPK (AMPK221, -211 or -111) in kinase buffer containing 200 µM [γ-32P]ATP (specific activity 650 mCi/m mol ATP). For negative controls, AMPK substrates were incubated with 1 pmol CamKKβ alone without AMPK. Kinase reactions were stopped by addition of SDS-PAGE sample buffer and subjected to SDS-PAGE and Typhoon phosphoimager (GE Healthcare).

AMPK activation in cell culture

HeLa cells were cultured in DMEM/F12 high glucose medium supplemented with 10% inactivated fetal calf serum (FCS) and 1% glutamate/streptomycine/penicillin. Endogenous AMPK of HeLa cells was activated by treatment with 1 mM AICAR for 1h at 37°C. Cells were then trypsinated, collected by centrifugation (1200 g, 5 min), and resuspended in lysis buffer (50 mM Tris/HCl pH 7.5, 100 mM NaCl, 5 mM MgCl2, 1 % NP-40, 0.1 % SDS) supplemented with protease (Roche) and phosphatase (Thermo Scientific) inhibitor cocktail. Cells were lysed by sonication and insoluble material was removed by centrifugation (10 min, 10 000 g, 4°C). AMPK activation was verified by immunoblotting using anti P-Thr172 AMPKα antibody. Immunoblot against GSTpi was used as a loading control.

Fumarate hydratase enzyme activity

AMPK221 was activated by CamKKβ and incubated with GST-FH in kinase buffer for 30 min at 37°C prior to activity measurements. Enzyme activity of FH and phospho-FH was then determined at 25°C by a spectrophotometric assay measuring fumarate formation (240 nm) in 0.1 M potassium phosphate buffer pH 7.6 using 0.5 to 8 mM malate. Data were analyzed by

direct fitting to Michaelis-Menten kinetics and secondary plots using SigmaPlot 10 (Systat Software, USA). FH activity of HeLa extracts was measured under the same conditions using 2.5 mM malate.

Results

Setup of an *in vitro* AMPK substrate screen

With the rationale to use the affinity between the kinase and its substrates as an additional parameter in a two-dimensional screening matrix for new substrates, we set out the following strategy (*Figure 1*): starting with soluble proteins within a cell extract of rat liver, we (i) eliminated proteins that non-specifically interact with Ni-NTA matrix, (ii) reduced complexity via size exclusion chromatography, (iii) screened for fractions containing AMPK interactors by using Biacore SPR with His-tagged AMPK221 immobilized on an NTA sensor chip, and finally (iv) screened SPR-positive fractions with *in vitro* phosphorylation assays using constitutively active AMPK221.

Preliminary experiments had revealed a high degree of non-specific protein binding to the NTA surface during SPR (not shown), which could be eliminated by an initial Ni-NTA chromatography step. Prefractionation with size exclusion chromatography on a Superdex 200 column had the additional advantage that eluted fractions contained proteins of similar size. This is an important prerequisite for the subsequent SPR experiments, since the SPR signal directly correlates with the mass bound at the chip surface, and thus not only with the number but also with the size of the bound protein. The unprocessed protein chromatography fractions were individually analyzed by Biacore SPR on surfaces covered with AMPK221 or left blank (*Figure 2*). Fractions were considered interaction positive when 80 s after dissociation start the SPR response on the AMPK221 surface was still higher as compared to the blank surface (fractions S1, S2, S3, S4, S10, S11 and S12). Fraction S1 contained mainly aggregates and was discarded; all other positive fractions were subjected to phosphorylation assays with or without constitutively active AMPK221 and separated by SDS-PAGE (*Figure 3*). Nine AMPK-specific bands could be identified in these interaction–positive fractions.

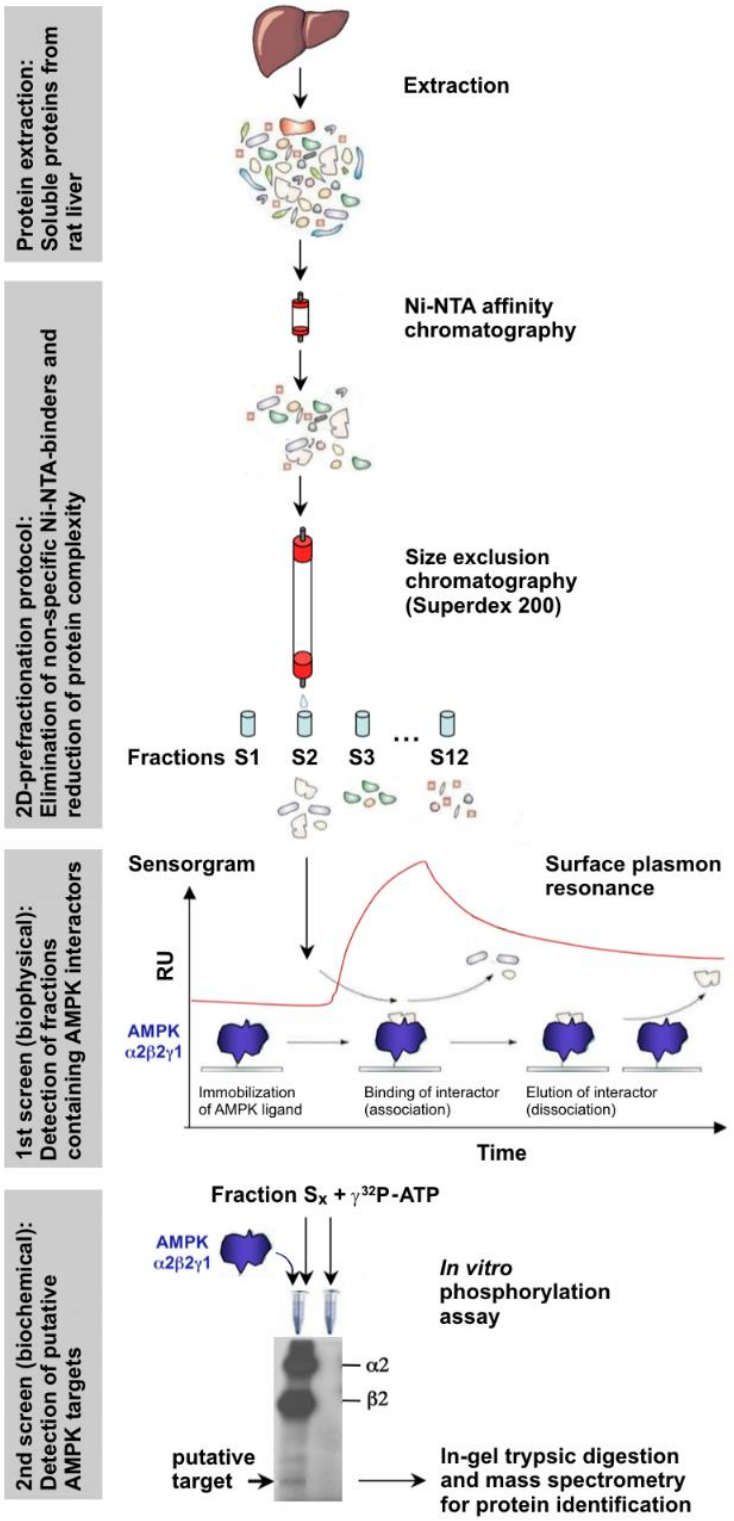

***Figure 1*. Flow chart of the *in vitro* screening procedure.** A tissue-derived extract containing soluble proteins is pre-fractionated by two step column chromatography with different sorbent chemistries. Each fraction is then analyzed by SPR for the presence of AMPK221 interacting proteins. Positive fractions are subjected to *in vitro* phosphorylation assays for detection of potential downstream substrates. After SDS-PAGE separation and autoradiography, positive lanes are excised and proteins identified by mass spectrometry.

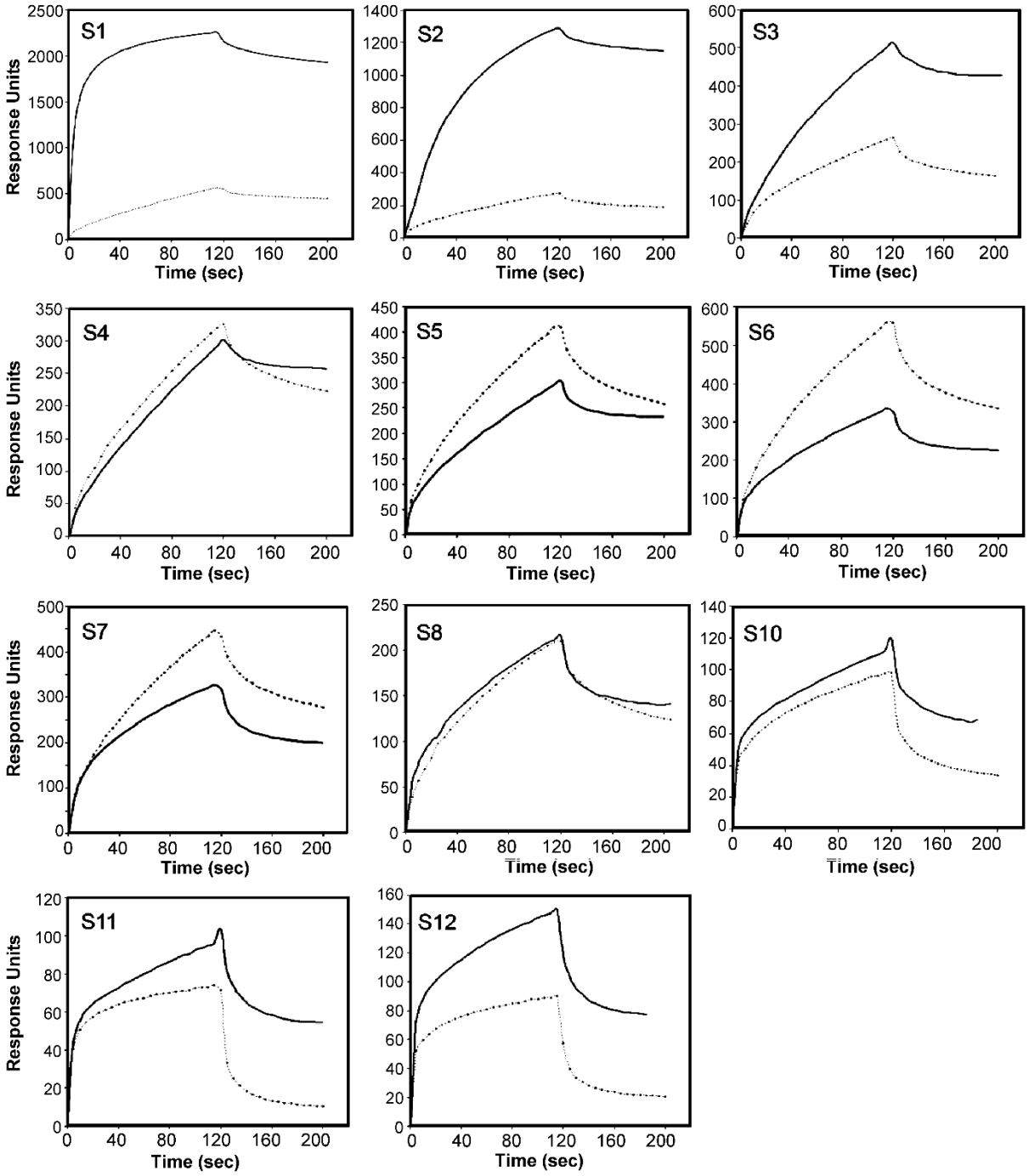

***Figure 2*. SPR interaction screening.** Representative association/dissociation kinetics of different fractions from size exclusion chromatography injected onto immobilized AMPK221 (full lines) or empty surface (control, dotted lines).

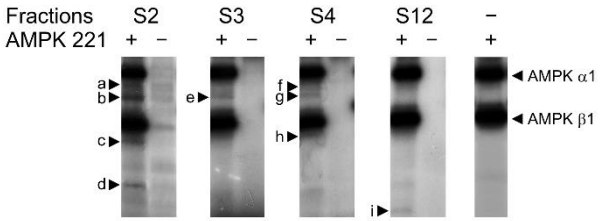

***Figure 3*. Phosphorylation assay screening.** SPR positive fractions were subjected to *in vitro* phosphorylation assays with or without constitutively active αT172D AMPK221 using incubation with [γ-32P]ATP for 2min at 37 °C. Assay mixtures analyzed by SDS-PAGE and Typhoon phospho-imager revealed AMPK auto-phosphorylation of α and β subunits and phosphorylation of putative AMPK substrates (bands indicated by small letters). Phosphorylation patterns of fractions S10 and S11 were similar to S12 and are not shown.

Identification of candidate substrates of AMPK

MALDI-MS/MS mass spectrometry of AMPK-specific phospho-bands identified several proteins with significant MASCOTT score (Table 1, online Supplementary Material 2). Three of them are at least partially localized in the cytosol and are thus the most likely candidate substrates of AMPK *in vivo*. The γ-actin was already identified as a putative AMPK substrate in our earlier *in vitro* AMPK substrate screen (Tuerk et al., 2007). Fumarate hydratase (FH) and fatty-acid binding protein 1 (FABP1 or FABPL) are newly identified AMPK candidate substrates. FH occurs in identical form in mitochondria and cytosol, but has different functions in the two compartments (Yogev et al., 2011). FABP1, a small protein of 14.6 kDa, is the liver isoform of a family of nine different FABPs in mammals (Storch and Corsico, 2008). These proteins were analyzed for putative AMPK phosphorylation sites, either corresponding to the stringent consensus motif (Scott et al., 2002) or to recognition sequences identified by peptide library profiling (Gwinn et al., 2008). While γ-actin did not contain a stringent AMPK site and was not further analyzed, FH preprotein and mature protein, as well as FABP1, contained at least one stringent AMPK site and additional less stringent sites.

Table 1. ***Protein identification by mass spectrometry.***

Fraction	Band	Identified protein	Accession no.[a]	Score [b]	Mass (kDa)	No. of peptides	Consensus sites [c]	Subcellular localization
S2	a	ATP synthase subunit α	P15999	281	60	5	Yes	Mitochondria
		Cytochrome P45O 2D26	P10634	150	57	3	Yes	Mitochondria
	b	3-ketoacyl-CoA thiolase	P13437	210	41	6	Yes	Mitochondria
S4	f	Aldehyde dehydrogenase	P11884	74	54	6	Yes	Mitochondria
	g	Fumarate hydratase	P14408	101	54	3	Yes	Cytosol and mitochondria
		γ-actin	P63259	104	42	2	No	Cytosol
S12	i	Fatty-acid-binding protein 1	P02692	53	15	1	Yes	Cytosol

Only vertebrate proteins identified with a significant MASCOTT score (>50) and different from AMPK subunits are shown. Candidate substrates (highlighted in grey) were selected due to cytosolic localization and presence of stringent AMPK consensus phosphorylation motifs: ϕ(X,β)XXS/TXXXϕ (ϕ, hydrophobic residue; β, basic residue, (Scott et al., 2002)). [a] UniProt accession number. [b] Probability-based MOWSE scores greater than 50 were considered significant and not a random event. [c] Presence of at least one stringent AMPK consensus site (Scott et al., 2002).

FH and FABP1 preferentially interact with AMPKα2

We next wanted to confirm whether FH and FABP1 are indeed those proteins that were directly interacting with AMPK221 in the first dimension and phosphorylated by AMPK221 in the second dimension of our screen. A cytosolic yeast two-hybrid (Y2H) assay, the Cyto-Y2H (Brückner et al., 2009; Möckli et al., 2007), confirmed a direct protein-protein interaction *in vivo* between FH and the α2 and β2 AMPK subunits, but not the α1 and β1 subunits (*Figure 4*).

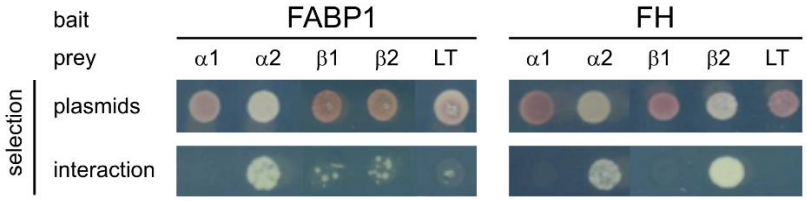

Figure 4. **FABP1 and FH directly interact with specific AMPK subunits in Y2H analysis.** Cytosolic Y2H analysis of interaction between the baits FABP1 or FH and the preys AMPK subunits (α1, α2, β1, β2) or LT (Large T Antigen of Simian Virus, aa 84-704; negative control). Spots represent yeast grown for 72 h at 30°C (1/10 dilution) either on medium selecting for the presence of bait and prey plasmids (upper row) and on medium selecting for bait/prey interaction (lower row). For more details see online Supplementary Material 1.

Direct interaction of AMPK221 with FH could be confirmed by co-immunoprecipiation (*Figure 5*). FABP1 showed the same specificity for α2, while it interacted only very weakly with both β1 and β2 (*Figure 4*). These results confirm that FH and FABP1 are true interactors of AMPK. Importantly, they show specific interactions with the AMPK subunits used in the initial SPR

screen: the AMPKα2 catalytic subunit (in case of FH and FABP) and the AMPKβ2 regulatory subunit (in case of FH).

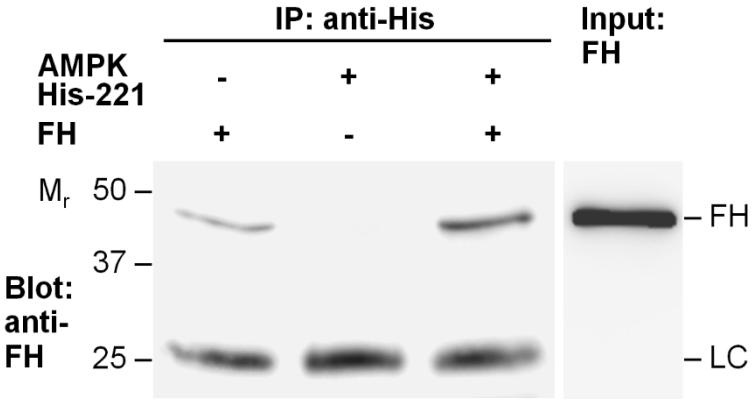

***Figure 5*. FH co-immunoprecipitates with AMPK221.** Strep-tagged FH and His-tagged AMPK221 were immunoprecipitated by using anti-His antibodies, and FH detected by immunoblot analysis with anti-FH antibodies. LC, primary antibody IgG light chain.

FH is directly phosphorylated by AMPK221

Direct phosphorylation of FH and FABP1 by AMPK was verified by *in vitro* phosphorylation assays with purified recombinant proteins. In principle, phosphorylation in complex mixtures could also occur by another protein kinase which is itself activated by AMPK. FH and FABP1 were therefore expressed in *E. coli* as GST- and Strep-tagged proteins. GST-FH incorporated γ-32P in presence of CamKKβ-activated AMPK221 in a time-dependent manner (*Figure 6*). Kinetics and extend of 32P incorporation were comparable to the reference AMPK substrate acetyl-CoA carboxylase (ACC). Similar results were obtained with Strep-tagged FH (Suppl. Fig. 1), showing that FH phosphorylation was not due to an interaction of AMPK with the GST-tag (Klaus & Schlattner, unpublished data). By contrast, FABP1 constructs were not phosphorylated under these conditions (not shown). Thus, the screen correctly identified FH as a true and direct substrate of AMPK *in vitro*.

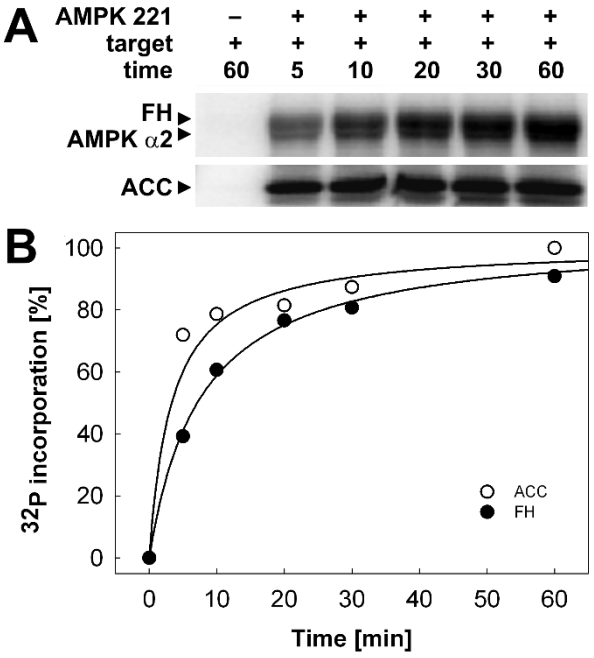

Figure 6. **FH is a direct AMPK substrate.** (A) Time course of FH phosphorylation by AMPK. AMPK221 (4pmol) first activated by CamKKβ (1 pmol) was incubated with purified GST-FH (100pmol) or GST-ACC (positive control, 100 pmol) for 5 to 60 min at 37°C. *In vitro* phosphorylation assays were analyzed by SDS-PAGE and Typhoon phosphoimager. (B) Quantification of the phosphorylation time course using Image Quant TL. Data is normalized to maximal ACC phosphorylation. Symbols: GST-ACC (○), GST-FH (●).

FH is preferentially phosphorylated by α2-containing AMPK complexes

We then wanted to know whether FH not only interacts specifically with AMPK221, but is also specifically phosphorylated by this AMPK isoform combination. Like above, *in vitro* phosphorylation assays were conducted with FH and ACC, using three different AMPK complexes: AMPK221, AMPK211, and AMPK111, all previously activated by CamKKβ. ACC phosphorylation served to account for different specific activities of the AMPK complexes, since the ACC-derived SAMS peptide is an equally good substrate for α1- and α2-containing AMPK complexes (Vernia et al., 2009). We first investigated the effect of different α-subunits on FH phosphorylation (*Figure 7*A). The ratio P-ACC$_{(221)}$/P-ACC$_{(111)}$ was 1.5, while the ratio P-FH$_{(221)}$/P-FH$_{(111)}$ was 5.0. If normalized to ACC, FH is still 3.3 times more phosphorylated by AMPKα2 as compared to AMPKα1. Complexes containing different β subunits (AMPK221 and AMPK211) phosphorylated both ACC and FH with similar efficiency (ratios of 1.1 for P-ACC$_{(221)}$/P-ACC$_{(211)}$ and 0.9 for P-FH$_{(221)}$/P-FH$_{(211)}$; *Figure 7*B). Thus, at least *in vitro*, AMPK β-subunits have no effect on FH phosphorylation. These results strongly suggest that AMPK

isoform composition can determine preference for specific substrates. FH interacts with AMPKα2 and is preferentially phosphorylated by α2-containing complexes. Although FH also interacts with the β2-subunit, this does not affect phosphorylation efficiency.

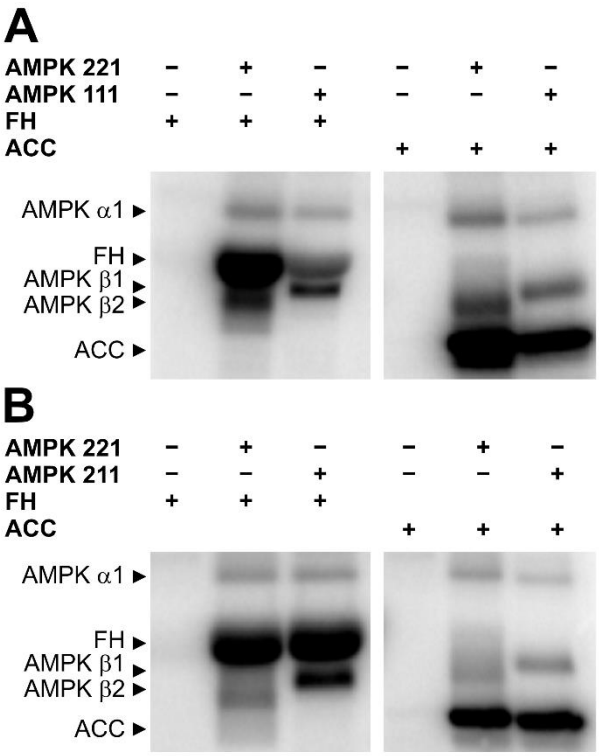

Figure 7. **AMPK isoform composition affects FH phosphorylation.** (A) AMPK221 phosphorylates FH more efficiently than AMPK111. (B) AMPK221 and AMPK211 phosphorylate FH and ACC with similar efficiency. Conditions: 3 pmol AMPK221, -211 or -111 first activated by CamKKβ (1 pmol) were incubated with purified FH or ACC (200 pmol) for 8 min at 37°C. *In vitro* phosphorylation assays were analyzed by SDS-PAGE and Typhoon phosphoimager.

FH phosphorylation by AMPK increases its enzyme activity *in vitro* and *in vivo*

We have finally addressed the effect of FH phosphorylation on its enzymatic function, which catalyzes the reversible hydration/dehydration of fumarate to malate. Enzyme kinetics of FH were determined before and after *in vitro* phosphorylation by CamKKβ-activated AMPK221, using malate as substrate and measuring fumarate formation by spectrophotometry. FH phosphorylation led to a 37 % increase in k_{cat} whereas the apparent K_m remained almost unaffected (*Figure 8*; Table 2).

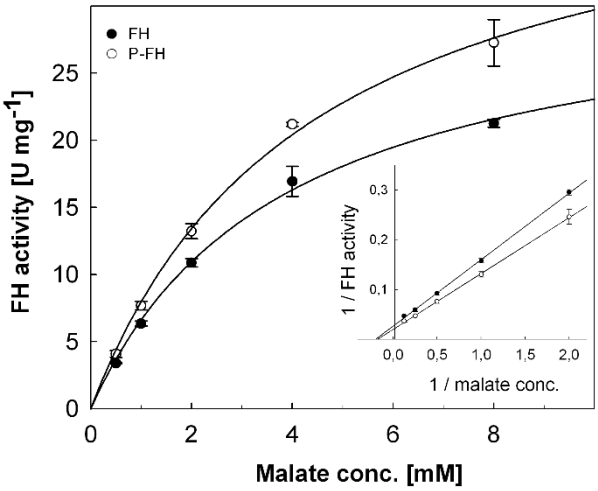

Figure 8. **AMPK-mediated phosphorylation affects enzymatic catalysis of FH.** Enzyme activity of phosphorylated (○) and non-phosphorylated (●) FH at different concentrations of malate, measured as described in material and methods. The direct fit to original data (large graph) and Lineweaver-Burk plot (insert graph) are shown. The derived catalytic constants are given in Table 2.

Table 2. ***Phosphorylation by AMPK activates FH.*** Enzyme kinetic parameters of recombinant FH before and after phosphorylation with AMPK221 activated by CamKKβ.

	V_{max} (U mg^{-1})	k_{cat} (s^{-1})	K_m (malate) (mM)	k_{cat}/ K_m (mM^{-1} s^{-})
FH	32,9 ± 0,4	110,0 ± 1,3	4,2 ± 0,1	26,2
P-FH	45,1 ± 1,4	150,8 ± 4,7	4,6 ± 0,3	32,8

Measurements with variable concentrations of malate at 25°C (see *figure 8*). Enzyme activity is given in U, equivalent to 1 µmol/min. Catalytic efficiency is calculated as k_{cat}/ K_m. Results are given as means ± SE (n=2) of two independent phosphorylation experiments.

To investigate whether AMPK could also affect FH activity *in vivo*, we examined the effect of AMPK activation by its pharmacological agonist AICAR on FH activity in HeLa cells. Treatment of HeLa cells with 1 mM AICAR for 1 h led to a strong increase in AMPK αThr172 phosphorylation (*Figure 9*A). This AMPK activation led to an average increase in FH activity by 31.3 ± 6.4 % (*Figure 9*B). Similar results were obtained by activating AMPK with the Abbott compound A-769662 (not shown).

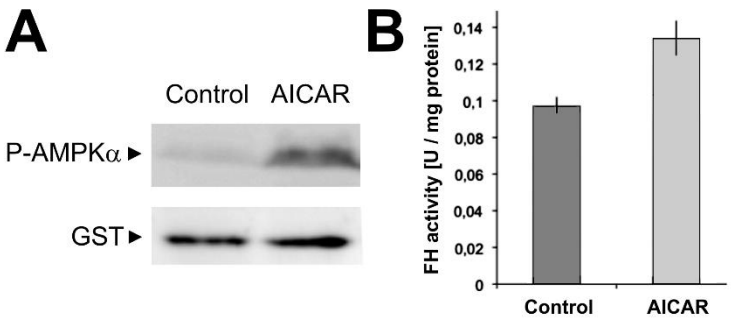

Figure 9. **Pharmacological AMPK activation increases FH enzyme activity in HeLa cells. (A)** Treatment of HeLa cells with 1 mM AICAR for 1 h increases AMPK activity as shown by immunoblotting for P-αThr172 AMPK with glutathione S-transferase pi (GST) as loading control. **(B)** FH activity in HeLa cells increases after AMPK activation as measured spectrophotometrically using malate as substrate (for details see material and methods). One representative experiment of three independent activation experiments is shown.

Discussion

The original two-dimensional *in vitro* screen for protein kinase substrates presented here combines biophysical interaction based on SPR with phosphorylation assays. Our data provide proof of principle that such a screening protocol can reveal AMPK substrates that are phosphorylated in an AMPK isoform-specific manner. We identified FH (or fumarase) as a novel AMPK substrate, and show that mainly the α2-subunit of AMPK is involved in FH interaction and recognition, as well as in FH phosphorylation. This phosphorylation increases FH enzymatic turnover *in vitro* and *in vivo*.

SPR technology has so far not been used to explore kinase/substrate interaction for screening of novel kinase substrates. It has only been applied as high-throughput readout device to measure interactions between phosphorylated kinase substrates and anti-phospho antibodies (Takeda et al., 2010). Highthoughput procedures have also been developed to screen for AMPK activators or inhibitors (e.g. (Anderson et al., 2004)). We show here that SPR can detect AMPK interactors in complex protein mixtures when different conditions are satisfied: (i) availability of highly pure, active kinase, as we have established by polycistronic bacterial expression of full-length AMPK complex (Neumann et al., 2003b); (ii) reversible, high density immobilization of the kinase on the chip surface for repeated use with fresh protein (e.g. by using Ni-NTA); (iii) the use of prefractionated extracts as source of soluble protein to reduce complexity; and in particular (iv) prior removal of proteins with non-specific affinity to the chip surface (especially relevant for Ni-NTA). We have assembled these conditions in a protocol (*Figure 1*) that provides useful data for AMPK and soluble liver proteins. The resolving power of the screen could be further improved by using multidimensional prefractionation (e.g. by additional ion exchange chromatography) or detection approaches (e.g. 2D-PAGE of interaction-positive fractions).

From SPR-positive fractions, FH and FABP1 were identified as direct AMPK221-interacting proteins. Another FABP family member, the epidermal FABP5, and FH were also part of AMPK-containing complexes in an earlier large-scale anti-bait co-immunoprecipitation study using AMPK-β1 (Ewing et al., 2007). However, here we show that both proteins exclusively interact with subunits used in our SPR screen: the α2- and (in case of FH) the β2-subunits. In addition, recombinant FH, but not FABP1, was also phosphorylated by AMPK *in vitro*. Possibly, FABP1

phosphorylation by AMPK requires additional factors (i.e. fatty acids) or secondary modifications missing in the bacterially expressed FABP1 but present in endogenous liver protein. Phosphorylation of FH constructs by AMPK221 occurred with kinetics and a degree of 32P-incorporation per mol of protein that were similar to the well characterized AMPK substrate ACC. Like for FH/AMPK interaction, FH was phosphorylated predominantly by complexes containing the α2-subunit as compared to α1-complexes. This is one of the first reports showing a clear preference of mammalian AMPK complexes for one of its substrates (Vernia et al., 2009). Such substrate specificity may contribute to tissue- and compartment-specific AMPK signaling whose mechanisms are so far largely unsolved.

FH or fumarase is encoded by a single gene, but dual-targeted to mitochondria and cytosol (reviewed in (Yogev et al., 2011)). As studied in yeast, after cleavage of the signal peptide in mitochondria, identical mature FH variants relocate in a metabolically regulated process either to the mitochondrial matrix or to the cytosol. In humans or yeast, cytosolic FH (cFH) represents about half of the cellular FH pool and is the likely substrate of AMPK *in vivo* (Yogev et al., 2011). While mitochondrial FH is well known for its participation in the tricarboxylic acid cycle (TCC), converting fumarate into malate, the role of cFH is emerging only more recently. Recent research is driven by the tumor suppressor function of FH which suggests that metabolic signals can regulate carcinogenesis (reviewed in (Raimundo et al., 2011)). Cancer incidence is linked to cFH inhibition and/or the resulting cytosolic fumarate accumulation, which may act via different mechanisms. These include induction of pseudohypoxia via stabilization of HIF-1α (O'Flaherty et al., 2010), signaling via serum responsive factor (Raimundo et al., 2009), up-regulation of antioxidant-response element-controlled genes (Ooi et al., 2011; Tong et al., 2011), or inhibition of DNA damage response (Yogev et al., 2010). In the latter mechanism, cellular stressors leading to DNA damage, induce cFH translocation to the nucleus, where its enzymatic activity is required to activate the DNA repair machinery, thus avoiding genomic instability. Our study together with literature data suggest that phosphorylation and activation of cFH by AMPK could play an important role in this sequence of events. AMPK signaling is known to respond to DNA damage and genotoxic stress transmitted via p53 and the p53 targets Sestrin1 and Sestrin2 (Budanov and Karin, 2008) or the cellular damage sensor ataxia-telangiectasia mutated protein (ATM) (Alexander et al., 2010). Furthermore, the nuclear functions of AMPK are mediated by α2-complexes (α1-

complexes are not localizing to the nucleus) (Salt et al., 1998), exactly the isoform that preferentially phosphorylates cFH.

In summary, we provide proof of concept that combining classical *in vitro* AMPK phosphorylation assays with SPR-based AMPK-protein interaction screening can not only identify novel AMPK substrates but also enrich for AMPK isoform-specific substrates. The newly identified AMPK substrate FH is exclusively interacting with and preferentially phosphorylated by α2-containing AMPK complexes. Both phosphorylation and activation of FH could contribute to the tumor suppressor function of FH.

References

Alessi, D.R., Sakamoto, K., and Bayascas, J.R. (2006). LKB1-dependent signaling pathways. Annu. Rev. Biochem. *75*, 137–163.

Alexander, A., Cai, S.-L., Kim, J., Nanez, A., Sahin, M., MacLean, K.H., Inoki, K., Guan, K.-L., Shen, J., Person, M.D., et al. (2010). ATM signals to TSC2 in the cytoplasm to regulate mTORC1 in response to ROS. Proc. Natl. Acad. Sci. U. S. A. *107*, 4153–4158.

Anderson, S.N., Cool, B.L., Kifle, L., Chiou, W., Egan, D.A., Barrett, L.W., Richardson, P.L., Frevert, E.U., Warrior, U., Kofron, J.L., et al. (2004). Microarrayed compound screening (microARCS) to identify activators and inhibitors of AMP-activated protein kinase. J. Biomol. Screen. *9*, 112–121.

Bouly, J.P., Gissot, L., Lessard, P., Kreis, M., and Thomas, M. (1999). Arabidopsis thaliana proteins related to the yeast SIP and SNF4 interact with AKINalpha1, an SNF1-like protein kinase. Plant J. Cell Mol. Biol. *18*, 541–550.

Brückner, A., Polge, C., Lentze, N., Auerbach, D., and Schlattner, U. (2009). Yeast two-hybrid, a powerful tool for systems biology. Int. J. Mol. Sci. *10*, 2763–2788.

Budanov, A.V., and Karin, M. (2008). p53 target genes sestrin1 and sestrin2 connect genotoxic stress and mTOR signaling. Cell *134*, 451–460.

Carling, D., Mayer, F.V., Sanders, M.J., and Gamblin, S.J. (2011). AMP-activated protein kinase: nature's energy sensor. Nat. Chem. Biol. *7*, 512–518.

Davies, S.P., Hawley, S.A., Woods, A., Carling, D., Haystead, T.A., and Hardie, D.G. (1994). Purification of the AMP-activated protein kinase on ATP-gamma-sepharose and analysis of its subunit structure. Eur. J. Biochem. FEBS *223*, 351–357.

Ewing, R.M., Chu, P., Elisma, F., Li, H., Taylor, P., Climie, S., McBroom-Cerajewski, L., Robinson, M.D., O'Connor, L., Li, M., et al. (2007). Large-scale mapping of human protein-protein interactions by mass spectrometry. Mol. Syst. Biol. *3*, 89.

Fogarty, S., and Hardie, D.G. (2010). Development of protein kinase activators: AMPK as a target in metabolic disorders and cancer. Biochim. Biophys. Acta *1804*, 581–591.

Fryer, L.G.D., Parbu-Patel, A., and Carling, D. (2002). The Anti-diabetic drugs rosiglitazone and metformin stimulate AMP-activated protein kinase through distinct signaling pathways. J. Biol. Chem. *277*, 25226–25232.

Gwinn, D.M., Shackelford, D.B., Egan, D.F., Mihaylova, M.M., Mery, A., Vasquez, D.S., Turk, B.E., and Shaw, R.J. (2008). AMPK phosphorylation of raptor mediates a metabolic checkpoint. Mol. Cell *30*, 214–226.

Hardie, D.G. (2007). AMP-activated/SNF1 protein kinases: conserved guardians of cellular energy. Nat. Rev. Mol. Cell Biol. *8*, 774–785.

Jiang, R., and Carlson, M. (1997). The Snf1 protein kinase and its activating subunit, Snf4, interact with distinct domains of the Sip1/Sip2/Gal83 component in the kinase complex. Mol. Cell. Biol. *17*, 2099–2106.

Johnsson, N., and Varshavsky, A. (1994). Split ubiquitin as a sensor of protein interactions in vivo. Proc. Natl. Acad. Sci. U. S. A. *91*, 10340–10344.

Jones, R.G., Plas, D.R., Kubek, S., Buzzai, M., Mu, J., Xu, Y., Birnbaum, M.J., and Thompson, C.B. (2005). AMP-activated protein kinase induces a p53-dependent metabolic checkpoint. Mol. Cell *18*, 283–293.

Kimura, N., Tokunaga, C., Dalal, S., Richardson, C., Yoshino, K., Hara, K., Kemp, B.E., Witters, L.A., Mimura, O., and Yonezawa, K. (2003). A possible linkage between AMP-activated protein kinase (AMPK) and mammalian target of rapamycin (mTOR) signalling pathway. Genes Cells Devoted Mol. Cell. Mech. *8*, 65–79.

Klaus, A., Polge, C., Zorman, S., Auchli, Y., Brunisholz, R., and Schlattner, U. (2012). A two-dimensional screen for AMPK substrates identifies tumor suppressor fumarate hydratase as a preferential AMPKα2 substrate. J. Proteomics *75*, 3304–3313.

Kuramoto, N., Wilkins, M.E., Fairfax, B.P., Revilla-Sanchez, R., Terunuma, M., Tamaki, K., Iemata, M., Warren, N., Couve, A., Calver, A., et al. (2007). Phospho-dependent functional modulation of GABA(B) receptors by the metabolic sensor AMP-dependent protein kinase. Neuron *53*, 233–247.

Libby, G., Donnelly, L.A., Donnan, P.T., Alessi, D.R., Morris, A.D., and Evans, J.M.M. (2009). New users of metformin are at low risk of incident cancer: a cohort study among people with type 2 diabetes. Diabetes Care *32*, 1620–1625.

Mihaylova, M.M., and Shaw, R.J. (2011). The AMPK signalling pathway coordinates cell growth, autophagy and metabolism. Nat. Cell Biol. *13*, 1016–1023.

Mitchelhill, K.I., Stapleton, D., Gao, G., House, C., Michell, B., Katsis, F., Witters, L.A., and Kemp, B.E. (1994). Mammalian AMP-activated protein kinase shares structural and functional homology with the catalytic domain of yeast Snf1 protein kinase. J. Biol. Chem. *269*, 2361–2364.

Möckli, N., Deplazes, A., Hassa, P.O., Zhang, Z., Peter, M., Hottiger, M.O., Stagljar, I., and Auerbach, D. (2007). Yeast split-ubiquitin-based cytosolic screening system to detect interactions between transcriptionally active proteins. BioTechniques *42*, 725–730.

Neumann, D., Schlattner, U., and Wallimann, T. (2003a). A molecular approach to the concerted action of kinases involved in energy homoeostasis. Biochem. Soc. Trans. *31*, 169–174.

Neumann, D., Woods, A., Carling, D., Wallimann, T., and Schlattner, U. (2003b). Mammalian AMP-activated protein kinase: functional, heterotrimeric complexes by co-expression of subunits in Escherichia coli. Protein Expr. Purif. *30*, 230–237.

O'Flaherty, L., Adam, J., Heather, L.C., Zhdanov, A.V., Chung, Y.-L., Miranda, M.X., Croft, J., Olpin, S., Clarke, K., Pugh, C.W., et al. (2010). Dysregulation of hypoxia pathways in fumarate hydratase-deficient cells is independent of defective mitochondrial metabolism. Hum. Mol. Genet. *19*, 3844–3851.

Ooi, A., Wong, J.-C., Petillo, D., Roossien, D., Perrier-Trudova, V., Whitten, D., Min, B.W.H., Tan, M.-H., Zhang, Z., Yang, X.J., et al. (2011). An antioxidant response phenotype shared between hereditary and sporadic type 2 papillary renal cell carcinoma. Cancer Cell *20*, 511–523.

Polge, C., Jossier, M., Crozet, P., Gissot, L., and Thomas, M. (2008). Beta-subunits of the SnRK1 complexes share a common ancestral function together with expression and function specificities; physical interaction with nitrate reductase specifically occurs via AKINbeta1-subunit. Plant Physiol. *148*, 1570–1582.

Raimundo, N., Vanharanta, S., Aaltonen, L.A., Hovatta, I., and Suomalainen, A. (2009). Downregulation of SRF-FOS-JUNB pathway in fumarate hydratase deficiency and in uterine leiomyomas. Oncogene *28*, 1261–1273.

Raimundo, N., Baysal, B.E., and Shadel, G.S. (2011). Revisiting the TCA cycle: signaling to tumor formation. Trends Mol. Med. *17*, 641–649.

Riek, U., Scholz, R., Konarev, P., Rufer, A., Suter, M., Nazabal, A., Ringler, P., Chami, M., Müller, S.A., Neumann, D., et al. (2008). Structural properties of AMP-activated protein kinase: dimerization, molecular shape, and changes upon ligand binding. J. Biol. Chem. *283*, 18331–18343.

Riek, U., Ramirez, S., Wallimann, T., and Schlattner, U. (2009). A versatile multidimensional protein purification system with full internet remote control based on a standard HPLC system. BioTechniques *46*, ix–xii.

Salt, I., Celler, J.W., Hawley, S.A., Prescott, A., Woods, A., Carling, D., and Hardie, D.G. (1998). AMP-activated protein kinase: greater AMP dependence, and preferential nuclear localization, of complexes containing the alpha2 isoform. Biochem. J. *334 (Pt 1)*, 177–187.

Scott, J.W., Norman, D.G., Hawley, S.A., Kontogiannis, L., and Hardie, D.G. (2002). Protein kinase substrate recognition studied using the recombinant catalytic domain of AMP-activated protein kinase and a model substrate. J. Mol. Biol. *317*, 309–323.

Shaw, R.J., Lamia, K.A., Vasquez, D., Koo, S.-H., Bardeesy, N., Depinho, R.A., Montminy, M., and Cantley, L.C. (2005). The kinase LKB1 mediates glucose homeostasis in liver and therapeutic effects of metformin. Science *310*, 1642–1646.

Solaz-Fuster, M.C., Gimeno-Alcañiz, J.V., Casado, M., and Sanz, P. (2006). TRIP6 transcriptional co-activator is a novel substrate of AMP-activated protein kinase. Cell. Signal. *18*, 1702–1712.

Stagljar, I., Korostensky, C., Johnsson, N., and te Heesen, S. (1998). A genetic system based on split-ubiquitin for the analysis of interactions between membrane proteins in vivo. Proc. Natl. Acad. Sci. U. S. A. *95*, 5187–5192.

Steinberg, G.R., and Kemp, B.E. (2009). AMPK in Health and Disease. Physiol. Rev. *89*, 1025–1078.

Storch, J., and Corsico, B. (2008). The emerging functions and mechanisms of mammalian fatty acid-binding proteins. Annu. Rev. Nutr. *28*, 73–95.

Takeda, H., Goshima, N., and Nomura, N. (2010). High-throughput kinase assay based on surface plasmon resonance. Methods Mol. Biol. Clifton NJ *627*, 131–145.

Tong, W.-H., Sourbier, C., Kovtunovych, G., Jeong, S.Y., Vira, M., Ghosh, M., Romero, V.V., Sougrat, R., Vaulont, S., Viollet, B., et al. (2011). The glycolytic shift in fumarate-hydratase-deficient kidney cancer lowers AMPK levels, increases anabolic propensities and lowers cellular iron levels. Cancer Cell *20*, 315–327.

Tuerk, R.D., Thali, R.F., Auchli, Y., Rechsteiner, H., Brunisholz, R.A., Schlattner, U., Wallimann, T., and Neumann, D. (2007). New candidate targets of AMP-activated protein kinase in murine brain revealed by a novel multidimensional substrate-screen for protein kinases. J. Proteome Res. *6*, 3266–3277.

Vernia, S., Solaz-Fuster, M.C., Gimeno-Alcañiz, J.V., Rubio, T., García-Haro, L., Foretz, M., de Córdoba, S.R., and Sanz, P. (2009). AMP-activated protein kinase phosphorylates R5/PTG, the glycogen targeting subunit of the R5/PTG-protein phosphatase 1 holoenzyme, and accelerates its down-regulation by the laforin-malin complex. J. Biol. Chem. *284*, 8247–8255.

Vincent, O., and Carlson, M. (1999). Gal83 mediates the interaction of the Snf1 kinase complex with the transcription activator Sip4. EMBO J. *18*, 6672–6681.

Viollet, B., Lantier, L., Devin-Leclerc, J., Hebrard, S., Amouyal, C., Mounier, R., Foretz, M., and Andreelli, F. (2009). Targeting the AMPK pathway for the treatment of Type 2 diabetes. Front. Biosci. Landmark Ed. *14*, 3380–3400.

Woods, A., Salt, I., Scott, J., Hardie, D.G., and Carling, D. (1996). The alpha1 and alpha2 isoforms of the AMP-activated protein kinase have similar activities in rat liver but exhibit differences in substrate specificity in vitro. FEBS Lett. *397*, 347–351.

Woods, A., Johnstone, S.R., Dickerson, K., Leiper, F.C., Fryer, L.G.D., Neumann, D., Schlattner, U., Wallimann, T., Carlson, M., and Carling, D. (2003). LKB1 is the upstream kinase in the AMP-activated protein kinase cascade. Curr. Biol. CB *13*, 2004–2008.

Yogev, O., Yogev, O., Singer, E., Shaulian, E., Goldberg, M., Fox, T.D., and Pines, O. (2010). Fumarase: a mitochondrial metabolic enzyme and a cytosolic/nuclear component of the DNA damage response. PLoS Biol. *8*, e1000328.

Yogev, O., Naamati, A., and Pines, O. (2011). Fumarase: a paradigm of dual targeting and dual localized functions. FEBS J. *278*, 4230–4242.

Zhou, G., Myers, R., Li, Y., Chen, Y., Shen, X., Fenyk-Melody, J., Wu, M., Ventre, J., Doebber, T., Fujii, N., et al. (2001). Role of AMP-activated protein kinase in mechanism of metformin action. J. Clin. Invest. *108*, 1167–1174.

PART 4, SECTION 2

Rat mitochondrial fumarate hydratase is phosphorylated by AMPK in the N-terminal targeting peptide

This section 2 will be submitted soon [Zorman, S., Tokarska-Schlattner, M., Michelland, S., Bourgoin-Voillard, S., Sève, M., Schlattner, U. Rat mitochondrial fumarate hydratase is phosphorylated by AMP activated protein kinase in the N-terminal targeting peptide]. **I did FH mutant constructs, phosphorylation assays, preparation for MS and mutational analysis.**

Introduction

AMP-activated protein kinase (AMPK) plays a central role in sensing and regulating energy homeostasis at the cellular, organ and whole-body level (Carling et al., 2012; Hardie, 2011; Hardie et al., 2012; Steinberg and Kemp, 2009). By regulating enzyme activity in metabolic pathways and transcription, it exerts pleiotropic control of metabolism and other physiological functions like cell growth, shape, motility and proliferation, including higher level functions such as appetite control. These functions suggested the kinase as a potential drug target for treating diabetes type II or cancer (Fogarty and Hardie, 2010; Viollet et al., 2009; Zhang et al., 2009). Kinase activation is triggered by a diverse array of external (e.g. hormones, cytokines, nutrients) and internal signals (e.g. AMP, ADP) linked to limited energy availability and other stress signals in physiological and pathological situations. The complex activation mechanism involves covalent phosphorylation of the α-subunit and allosteric binding of AMP or ADP to the γ-subunit.

In vitro screening that we carried out for novel substrates of AMPK repeatedly identified proteins that localize to mitochondria, in particular the mitochondrial matrix, like e.g. fumarate hydratae (fumarase, FH) (Klaus et al., 2012; Tuerk et al., 2007). Although the existence of different protein kinases within the mitochondrial compartment is emerging (Acin-Perez et al., 2009; Aponte et al., 2009; Padrão et al., 2013), AMPK has not yet been clearly localized with this organelle. An alternative possibility would be regulation of mitochondrial import of nascent protein that occurs already in the cytosol. It has been shown that phosphorylation of serine, threonine or tyrosine residues can either inhibit or promote mitochondrial targeting of nascent proteins, depending on the phosphorylated site and the nature of the targeting mechanism (Dasari et al., 2006; Robin et al., 2002, 2003). This would render subcellular localization dependent on dynamic signaling processes. Several studies provided evidence for phosphorylation within an N-terminal targeting sequence of mitochondrial proteins that reduces import efficiency (Chua et al., 2003; Lee et al., 2006; Merrill et al., 2013).

Here we examined in more detail the *in vitro* phosphorylation of rat mitochondrial FH and show that this secondary modification occurs mainly in the cleavable prepeptide at Ser19 and

only at a much lower level at Thr482. Out of other mitochondrial matrix proteins that our studies suggested as AMPK substrate candidates ((Klaus et al., 2012; Tuerk et al., 2007) and unpublished data), also the prepeptide of pyruvate carboxylase is AMPK-phosphorylated. Such phosphorylations, if occurring *in vivo*, must happen already in the cytosol before mitochondrial import, and may thus affect import efficiency.

Materials and Methods

Vectors

Plasmid pγ1β2His-α2AMPK was used for bacterial expression and purification as we have published previously (Neumann et al., 2003; Riek et al., 2009). FH (GeneID 24368) was amplified from rat liver cDNA and introduced into bacterial expression vector pET-52b (+) to obtain N-terminally tagged FH. Vectors for GST-ACC domain and GST-CamKKβ were kindly provided by G. Hardie (Univ. of Dundee, UK) (Scott et al., 2002) and H. Tokumitsu (Kagawa Medical University, Japan), respectively.

Site-directed mutagenesis of fumarate hydratase by sequence and ligation-independent cloning

FH plasmids were amplified by PCR using T4 DNA phusion polymerase (Thermo Scientific) and mutagenic primers listed in Table 1. After PCR amplification, 20 U DPN1 (New England BioLabs) were added to the reaction and the mixture was incubated at 37°C for 1 h to digest the template. Plasmid DNA was then purified by Nucleospin Extract II (Machinery-Nagel). 1 µg DNA was treated with 0.5 U T4 DNA polymerase (Invitrogen) in a 20 µl reaction mixture at 22°C for 30 min giving the exonuclease activity of T4 DNA polymerase 20 bp at both 3' end of the PCR product will be digested, forming sticky end between the two extremities of the PCR product to further recirculation of the plasmid. The reaction was stopped by purification with Nucleospin Extract II (Macherey-Nagel). Finally, 600 ng DNA, 2µl T4 DNA ligase buffer and 1µl T4 DNA ligase (New England BioLabs) were used in 20 µl reaction volume at room temperature for 2h for ligation. A 5µl aliquot of the annealing mix was used to transform 100 µl of competent MachT1 bacteria which were plated on Ampicillin plates. The sequence of all clones was verified by sequencing.

Table 1. ***Primers used for generating FH point mutations***

Mutation		Primers sequences : 5' → 3'
S19A	Fw	GTCGCTTCCCGCGGGTCCCCGCCGCCGGTGCTGTATTGTCAGGGGAAGCG
	Rev	GGCGGGGACCCGCGGGAAGCGAC
S43A	Fw	TCTATACGGAAGGAATTTTGCGCCGCTGCCATTCGCACGACG
	Rev	GCGCAAAATTCCTTCCGTATAGAATACGACACC
S155A	Fw	TGAATGTAAATGAAGTGATCGCCAACAGGGCAATCGAAATGCTAGG
	Rev	GGCGATCACTTCATTTACATTCATGTTCGTCTGG
T233A	Fw	TAAAAATTGGGCGGACTCATGCGCAGGACGCTGTCCCTCTTACTCTT
	Rev	CGCATGAGTCCGCCCAATTTTTATGAC
T482A	Fw	ACGGATCCACCTTAAAGAAAGCGGCTATTGAACTTGGCTATCTCACAG
	Rev	CGCTTTCTTTAAGGTGGATCCGTTCTTGTG
T482D	Fw	ACGGATCCACCTTAAAGAAAGACGCTATTGAACTTGGCTATCTCACAG
	Rev	GTC TTTCTTTAAGGTGGATCCGTTCTTGTG
T482G	Fw	ACGGATCCACCTTAAAGAAAGGGGCTATTGAACTTGGCTATCTCACAG
	Rev	CCCTTTCTTTAAGGTGGATCCGTTCTTGTG
T482V	Fw	ACGGATCCACCTTAAAGAAAGTGGCTATTGAACTTGGCTATCTCACAG
	Rev	CACTTTCTTTAAGGTGGATCCGTTCTTGTG

The sequence of the mutated amino acid is highlighted in grey; fw, forward primer; rev, reverse primer.

Expression and purification of GST-tagged proteins

All GST fusions protein constructs were transformed into competent BL21-Codon Plus (DE3)-RIL *E. coli* cells (Stratagene) and incubated overnight on LB agar containing 100 µg/ml ampicillin and 30 µg/ml chloramphenicol. Cultures were grown in LB containing antibiotics at 37°C with shaking until OD (600 nm) 0.7-0.9. Cells were then cooled down to 30°C and protein expression was induced for 4 hours with 2 mM isopropyl β-D-thiogalactopyranoside (IPTG) (Eurobio). Cells were harvested and suspended in lysis buffer: PBS (phosphate buffer saline) with complete EDTA-free protease inhibitor cocktail (Roche). After sonication, insoluble material was removed by centrifugation (40000 xg, 40 min at 4°C). Supernatant was applied to a Gluthatione Sepharose matrix (Qiagen) packed column, the column was washed with PBS, and proteins were eluted with 10 mM L-gluthatione reduced (Sigma-Aldrich) in 50 mM Tris-HCL, pH 8.

In vitro phosphorylation assays

Purified GST-tagged FH proteins (200 pmol each), including WT and mutants S19A, S43A, S155A, S233A, T482A, T482V, T482V, T482G and N-terminally truncated FH (amino acids 1-

41), as well as GST-tagged ACC domain (control) were incubated for 30 min at 37°C with 200 µM [γ-^{32}P]ATP (specific activity 6000 Ci/mmol ATP) and AMPK221 (4 pmol) previously activated by incubation with 1 pmol CamKKβ for 20 min at 30°C in kinase buffer (50 µM AMP, 5 mM $MgCl_2$, 1 mM DTT, 10 mM HEPES pH 7.4). For negative controls, AMPK substrates were incubated with 1 pmol CammKKβ without AMPK. Kinase reactions were stopped by addition of Laemmli buffer and subjected to SDS-PAGE and autoratiography by Typhoon phosphoimager (GE Healthcare).

Mass spectrometry

Phosphorylated samples were prepared with freshly purified AMPK221 to avoid the presence of glycerol normally needed for long term AMPK storage. FH-WT (100 pmol) was incubated for 30 min at 37°C with 2 pmol AMPK221 previously activated by incubation with 1 pmol CamKKβ for 20 min at 30°C in kinase buffer. As negative controls, ACC domain and FH-WT were incubated with 1 pmol CammKKβ without AMPK. The samples were conserved at 4°C.

Samples were dried and solubilized in 20 µl of ammonium bicarbonate (50 mM) before performing a reduction of disulfide bonds, an alkylation of thiols and trypsin digestion. Aliquots of the digest were either used directly for mass spectrometry analysis or phosphopeptides were enriched using the Pierce kits TiO_2 Phosphopeptide Enrichment or Fe-NTA Phosphopeptide enrichment (Thermo Scientific) and then purified with Graphit Clean-up kit (Thermo Scientific). Of each aliquot, 10 pmol were subjected to nanoLC-MS/MS using an ESI-QTrap mass spectrometer (4000QTRAP, AB Sciex) directly connected to a nano-chromatography system (3000 Ultimate nanoLC, Thermo Fischer). Bioinformatics analysis for identification of (phospho)peptides/proteins was performed using ProteinPilot 4 software (ABSciex) with both Paragon and Mascot algorithms and Swissprot (Rattus norvegicus species) as protein database. Validation of phosphopeptides was considered when their identification led to a high confidence level, i.e. confidence level >95% for Paragon algorithm and $p<0.05$ for Mascot algorithm.

Results

Fumarate hydratase contains different putative AMPK phosphorylation sites

Bioinformatics analysis of the full length sequence of rat mitochondrial FH suggested three AMPK sites, Ser19, Ser43 and Thr233, which correspond to the stringent AMPK phosphorylation motif. This motif is $\phi(X,\beta)XXS/TXXX\phi$, where ϕ is a hydrophobic residue (mostly M, V, L, I or F), β is a basic residue (R, K or H) and the parentheses indicate that the order of residues at the P-3 and P-4 positions is not critical (Dale et al., 1995).

We then performed LC-MS/MS analysis of *in vitro* phosphorylated full-length FH for unbiased identification of phosphosites, with or without additional enrichment of phosphopeptides (Table 2). Different experiments revealed either predominant phosphorylation in the sequence of the mature enzyme (Ser43, Ser155 and Thr482) or in the mitochondrial prepeptide (Ser19). The Ser43 site was identified at lower confidence, but retained for further analysis since it occurred in both phosphopeptide enrichment procedures. Ser155 and Thr482 both do not conform to a stringent AMPK motif (Dale et al., 1995); however, the latter may correspond to a less stringent AMPK motif as based on a peptide screen (Gwinn et al., 2008).

Table 2. ***Phosphorylation sites identified by mass spectrometry***

Phospho-site	Phosphorylation motif sequence	Identified phosphorylated peptides		
		Without enrichment	phosphopeptide enrichment with TiO_2	FeNTA
S19	RRFPRVPSAGAVLS	**V17-R33**	**V17-R33**	ND
S43	PNVVRMASQNSFRI	-	P36-R48	N37-R48 G21-R48 P36-R48
S155	MNVNEVISNRAIEM	**M148-K169**	-	-
T482	NGSTLKETAIELGY	**N475-K501** **K480-K501**	-	-

The stringent AMPK motif is $\phi(X,\beta)XXS/TXXX\phi$; ϕ is hydrophobic; β is basic (Dale et al., 1995). Bold Peptides in bold letters were identified with a high degree of confidence (>99%) via the paragon algorithm. ND, not determined.

AMPK phosphorylates fumarate hydratase mainly at Ser19

To unambiguously identify the FH phosphoresidues on the basis of the bioinformatic and MS data, all valid candidate Ser and Thr sites were mutated into a non-phosphorylatable alanine (Figure 1). Different mutations in the sequence of the mature enzyme, Ser43, Ser155 and Thr233, did not affect phosphorylation as compared to FH *wild-type* (WT). The T482A mutation reduced phosphorylation levels. This reduction was confirmed in some other Thr482 mutants (T482D, T482G and T482V) even if this phenomenon was less exacerbated in those mutants (Figure 1A). Surprisingly, the most important effect on phosphorylated level was observed on Ser19 in the N-terminal targeting peptide of FH that is cleaved after mitochondrial import (Figure 1B). Also in a truncation mutant lacking this targeting peptide (N-terminal 41 amino acids), phosphorylation by AMPK was strongly reduced.

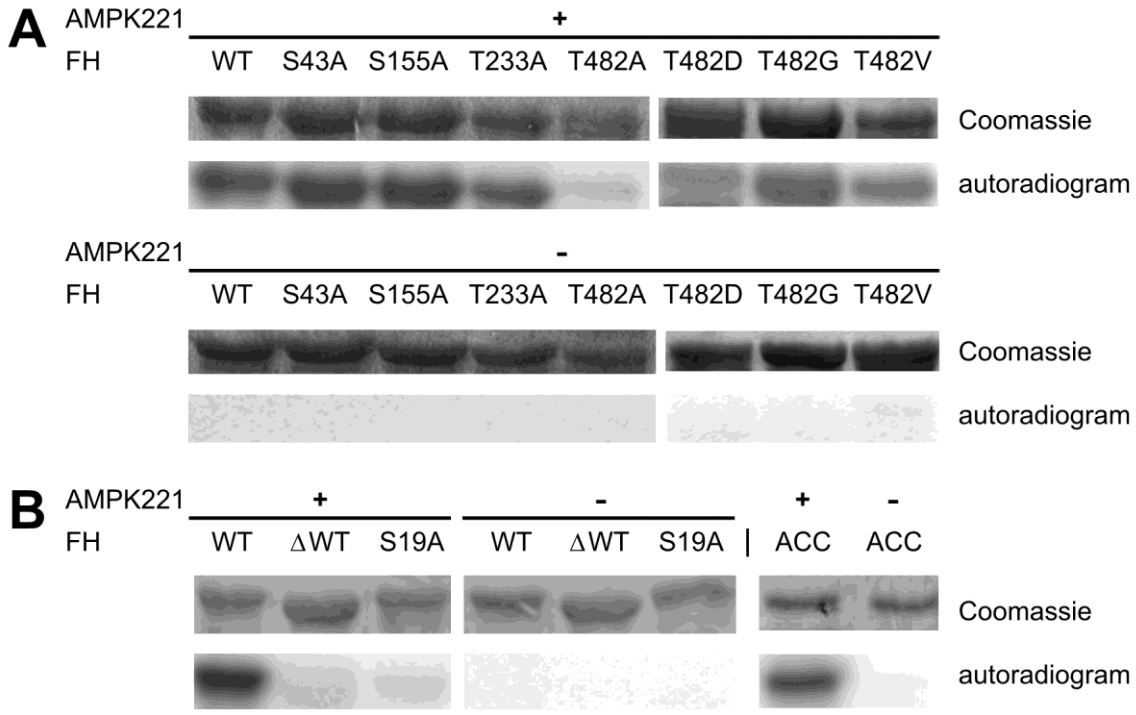

Figure 1. In vitro phosphorylation of fumarate hydratase wild type and mutant proteins. Mitochondrial FH wild-type (WT) together with (A) point mutants S43A, S155A, T233A, T482A, T482D, T482G, and T482V, or (B) truncated WT protein lacking the mitochondrial targeting peptide (amino acid 1-41, ΔWT) or point mutation S19A, as well as an acetyl-CoA carboxylase domain (ACC, positive control) were subjected to a standardized *in vitro* phosphorylation assay using AMPK221 heterotrimeric complex activated by CamKKβ (see Materials and Methods).

AMPK phosphorylates the prepeptide of pyruvate carboxylase

Mitochondrial prepeptides are amphiphatic and contain numerous hydrophobic and basic residues which are essential in the stringent AMPK motif ϕ(X,β)XXS/TXXXϕ (Dale et al., 1995). We therefore hypothesized that AMPK could also phosphorylate other mitochondrial prepeptides, at least *in vitro*. All mitochondrial matrix proteins suggested in our earlier studies as putative AMPK substrates ((Klaus et al., 2012; Tuerk et al., 2007) and unpublished data) were thus analyzed for potential AMPK phosphorylation sites. The AMPK motif was detected in addition to fumarate hydratase also in citrate synthase (CS) and pyruvate carboxylase (PC), when alanine and glycine were allowed as hydrophobic residues (Table 3). Less stringent forms of the AMPK motif (Gwinn et al., 2008) were found in several other mitochondrial matrix proteins (not shown). We then tested phosphorylation of synthetic CS and PC prepeptides in the same *in vitro* phosphorylation assay as used for FH. Heavy incorporation of ^{32}P label was observed in the prepeptide of PC, not of CS (*Figure 2*).

Table 3. ***Putative AMPK phosphorylation sites in mitochondrial prepeptides***

Protein	Uniprot	Name	localization	Prepeptide	Prepeptide sequence [4]
Fumarate hydratase [1]	P14408	FUMH	M, C	1-41	MNRAFCLLARSRRFPRVPSAGAVLSGEAATLPRCAPNVVRMASQN...
Citrate synthase [2]	O75390	CISY	M	1-27	MALLTAAARLLGTKNASCLVLAARHASASST...
Pyruvate carboxylase [3]	P11498	PYC	M	1-20	MLKFRTVHGGLRLLGIRRTSTAPAASPNVR...

[1] Klaus et al. 2012 (Klaus et al., 2012); [2] Tuerk et al 2007 (Tuerk et al., 2007); [3] Ramirez (2010) thesis Université de Grenoble no. 00641109; [4] Black letters indicate the N-terminal prepeptide, bold letters indicate the sequence used in *in vitro* phoisphorylation assays, colors indicate key residues in the AMPK motif ϕ(X,β)XXS/TXXXϕ; ϕ is hydrophobic; β is basic (Dale et al., 1995). Localization: M, matrix; IM, intermembrane space; C, cytosol.

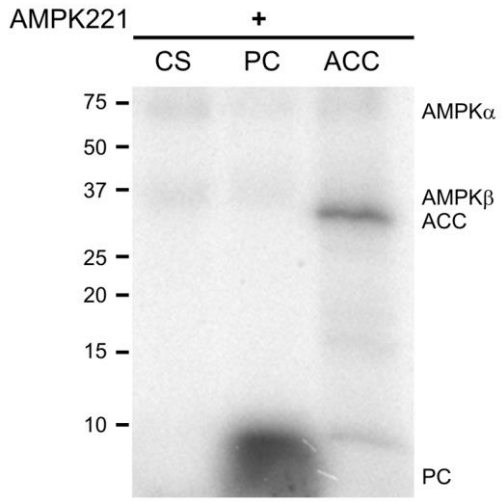

Figure 2. In vitro phosphorylation of mitochondrial prepeptides. Synthetic peptides corresponding to prepeptides of human citrate synthase (CS) or pyruvate carboxylase (PC), together with ACC domain (positive control) were subjected to a standardized *in vitro* phosphorylation assay using AMPK221 heterotrimeric complex activated by CamKKβ (see Materials and Methods). Note autophosphorylation of AMPKα and –β subunits.

Discussion

Several *in vitro* screens that we performed in recent years identified mitochondrial proteins, most in the matrix space, as candidates for AMPK substrates ((Klaus et al., 2012; Tuerk et al., 2007) and unpublished data). However, no relevant phosphorylation site has been reported so far for these proteins. Here we further analyzed the mitochondrial isoform of rat fumarate hydratase that we recently described as being phosphorylated by AMPK *in vitro* (Klaus et al., 2012). We identify Ser19 in the cleavable mitochondrial target peptide of FH as the main phosphorylated residue, and Thr482 as a putative secondary site.

Our MS analysis clearly pinpoints Ser19 as the by far most predominant site, thus responsible for the near stoichiometric phosphorylation of FH that we have observed earlier (Klaus et al., 2012). Although phosphorylation in the prepeptide is surprising at first glance, it could be physiologically relevant. Several studies have shown that phosphorylation within an N-terminal mitochondrial targeting sequence reduces protein import efficiency (Chua et al., 2003; Lee et al., 2006; Merrill et al., 2013). The amphiphatic cleavable presequences carry a net positive charge that is important for translocation into the negatively charged mitochondrial matrix by an electrophoretic mechanism (Neupert and Herrmann, 2007). Phosphorylation within this sequence reduces or neutralizes this positive charge and can retain the protein in the cytosol, leading to persistent cytosolic localization or degradation of the enzyme (Chua et al., 2003; Lee et al., 2006; Merrill et al., 2013). For example, phosphorylation of Ser9 and Ser22 in cNMP phosphodisesterase by PKC effectively inhibits targeting to the mitochondrial matrix and retains the protein in the cytosol (Lee et al., 2006). Also the actin-binding protein cofilin phosphorylated at Ser3 by LIM kinase is cytosolic, while dephosphorylation during apoptisis triggers mitochondrial import (Chua et al., 2003). Similarly, phosphorylation of so-called cryptic mitochondrial targeting signals, for example present in proteins with bimodal targeting to different compartments (Avadhani, 2011), can affect mitochondrial localization as in case of the cytochrome P450 family (Anandatheerthavarada et al., 1999; Dasari et al., 2006) or GSTA4-4 (Robin et al., 2003).

Phosphorylation of Thr482 occurs only at low levels *in vitro*, but a regulatory role *in vivo* cannot be excluded. The site is well exposed at the protein surface and situated in the C-terminal domain 3 of FH (Figure 3) which may have regulatory functions. Interestingly, this domain is

phosphorylated at multiple threonine and tyrosine residues in mouse liver (see (Villén et al., 2007) and www.phosphosite.org).

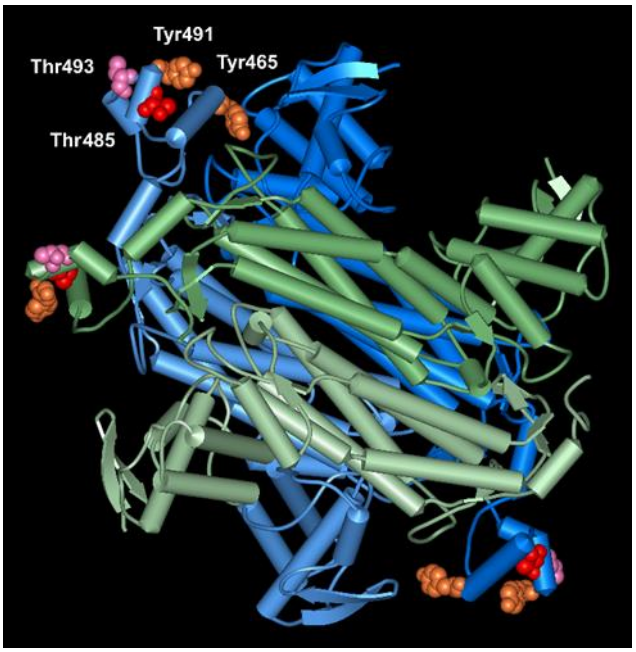

Figure 3. Phosphorylation sites in the fumarate hydratase domain 3. Tetrameric molecular structure of human fumarate hydratase (3E04, monomers in green and blue colors) showing the localization of the minor AMPK site Thr485 identified here (red, Thr482 in rat) within the domain 3 (C-terminal 65 residues). This domain habors also other Tyr (orange) and Thr (pink) phosphorylation sites reported elsewhere ((Villén et al., 2007) and www.phosphosite.org). Phosphorylated amino acids are given in spacefill representation. Structure prepared by WebLabVierwer Pro 4.0.

In conclusion, we unambiguously identify an AMPK phosphorylation site in the prepeptide of rat FH that targets the protein to mitochondria. Further studies will have to show whether this modification alters mitochondrial FH import.

References

Acin-Perez, R., Salazar, E., Kamenetsky, M., Buck, J., Levin, L.R., and Manfredi, G. (2009). Cyclic AMP produced inside mitochondria regulates oxidative phosphorylation. Cell Metab. *9*, 265–276.

Anandatheerthavarada, H.K., Biswas, G., Mullick, J., Sepuri, N.B., Otvos, L., Pain, D., and Avadhani, N.G. (1999). Dual targeting of cytochrome P4502B1 to endoplasmic reticulum and mitochondria involves a novel signal activation by cyclic AMP-dependent phosphorylation at ser128. EMBO J. *18*, 5494–5504.

Aponte, A.M., Phillips, D., Hopper, R.K., Johnson, D.T., Harris, R.A., Blinova, K., Boja, E.S., French, S., and Balaban, R.S. (2009). Use of (32)P to study dynamics of the mitochondrial phosphoproteome. J. Proteome Res. *8*, 2679–2695.

Avadhani, N.G. (2011). Targeting of the same proteins to multiple subcellular destinations: mechanisms and physiological implications. FEBS J. *278*, 4217.

Carling, D., Thornton, C., Woods, A., and Sanders, M.J. (2012). AMP-activated protein kinase: new regulation, new roles? Biochem. J. *445*, 11–27.

Chua, B.T., Volbracht, C., Tan, K.O., Li, R., Yu, V.C., and Li, P. (2003). Mitochondrial translocation of cofilin is an early step in apoptosis induction. Nat. Cell Biol. *5*, 1083–1089.

Dale, S., Wilson, W.A., Edelman, A.M., and Hardie, D.G. (1995). Similar substrate recognition motifs for mammalian AMP-activated protein kinase, higher plant HMG-CoA reductase kinase-A, yeast SNF1, and mammalian calmodulin-dependent protein kinase I. FEBS Lett. *361*, 191–195.

Dasari, V.R., Anandatheerthavarada, H.K., Robin, M.-A., Boopathi, E., Biswas, G., Fang, J.-K., Nebert, D.W., and Avadhani, N.G. (2006). Role of protein kinase C-mediated protein phosphorylation in mitochondrial translocation of mouse CYP1A1, which contains a non-canonical targeting signal. J. Biol. Chem. *281*, 30834–30847.

Fogarty, S., and Hardie, D.G. (2010). Development of protein kinase activators: AMPK as a target in metabolic disorders and cancer. Biochim. Biophys. Acta *1804*, 581–591.

Gwinn, D.M., Shackelford, D.B., Egan, D.F., Mihaylova, M.M., Mery, A., Vasquez, D.S., Turk, B.E., and Shaw, R.J. (2008). AMPK phosphorylation of raptor mediates a metabolic checkpoint. Mol. Cell *30*, 214–226.

Hardie, D.G. (2011). AMP-activated protein kinase: an energy sensor that regulates all aspects of cell function. Genes Dev. *25*, 1895–1908.

Hardie, D.G., Ross, F.A., and Hawley, S.A. (2012). AMPK: a nutrient and energy sensor that maintains energy homeostasis. Nat. Rev. Mol. Cell Biol. *13*, 251–262.

Klaus, A., Polge, C., Zorman, S., Auchli, Y., Brunisholz, R., and Schlattner, U. (2012). A two-dimensional screen for AMPK substrates identifies tumor suppressor fumarate hydratase as a preferential AMPKα2 substrate. J. Proteomics *75*, 3304–3313.

Lee, J., O'Neill, R.C., Park, M.W., Gravel, M., and Braun, P.E. (2006). Mitochondrial localization of CNP2 is regulated by phosphorylation of the N-terminal targeting signal by PKC: implications of a mitochondrial function for CNP2 in glial and non-glial cells. Mol. Cell. Neurosci. *31*, 446–462.

Merrill, R.A., Slupe, A.M., and Strack, S. (2013). N-terminal phosphorylation of protein phosphatase 2A/Bβ2 regulates translocation to mitochondria, dynamin-related protein 1 dephosphorylation, and neuronal survival. FEBS J. *280*, 662–673.

Neumann, D., Schlattner, U., and Wallimann, T. (2003). A molecular approach to the concerted action of kinases involved in energy homoeostasis. Biochem. Soc. Trans. *31*, 169–174.

Neupert, W., and Herrmann, J.M. (2007). Translocation of proteins into mitochondria. Annu. Rev. Biochem. *76*, 723–749.

Padrão, A.I., Vitorino, R., Duarte, J.A., Ferreira, R., and Amado, F. (2013). Unraveling the Phosphoproteome Dynamics in Mammal Mitochondria from a Network Perspective. J. Proteome Res.

Riek, U., Ramirez, S., Wallimann, T., and Schlattner, U. (2009). A versatile multidimensional protein purification system with full internet remote control based on a standard HPLC system. BioTechniques *46*, ix–xii.

Robin, M.-A., Anandatheerthavarada, H.K., Biswas, G., Sepuri, N.B.V., Gordon, D.M., Pain, D., and Avadhani, N.G. (2002). Bimodal targeting of microsomal CYP2E1 to mitochondria through activation of an N-terminal chimeric signal by cAMP-mediated phosphorylation. J. Biol. Chem. *277*, 40583–40593.

Robin, M.-A., Prabu, S.K., Raza, H., Anandatheerthavarada, H.K., and Avadhani, N.G. (2003). Phosphorylation enhances mitochondrial targeting of GSTA4-4 through increased affinity for binding to cytoplasmic Hsp70. J. Biol. Chem. *278*, 18960–18970.

Scott, J.W., Norman, D.G., Hawley, S.A., Kontogiannis, L., and Hardie, D.G. (2002). Protein kinase substrate recognition studied using the recombinant catalytic domain of AMP-activated protein kinase and a model substrate. J. Mol. Biol. *317*, 309–323.

Steinberg, G.R., and Kemp, B.E. (2009). AMPK in Health and Disease. Physiol. Rev. *89*, 1025–1078.

Tuerk, R.D., Thali, R.F., Auchli, Y., Rechsteiner, H., Brunisholz, R.A., Schlattner, U., Wallimann, T., and Neumann, D. (2007). New candidate targets of AMP-activated protein kinase in murine brain revealed by a novel multidimensional substrate-screen for protein kinases. J. Proteome Res. *6*, 3266–3277.

Villén, J., Beausoleil, S.A., Gerber, S.A., and Gygi, S.P. (2007). Large-scale phosphorylation analysis of mouse liver. Proc. Natl. Acad. Sci. U. S. A. *104*, 1488–1493.

Viollet, B., Lantier, L., Devin-Leclerc, J., Hebrard, S., Amouyal, C., Mounier, R., Foretz, M., and Andreelli, F. (2009). Targeting the AMPK pathway for the treatment of Type 2 diabetes. Front. Biosci. Landmark Ed. *14*, 3380–3400.

Zhang, B.B., Zhou, G., and Li, C. (2009). AMPK: an emerging drug target for diabetes and the metabolic syndrome. Cell Metab. *9*, 407–416.

PART 5

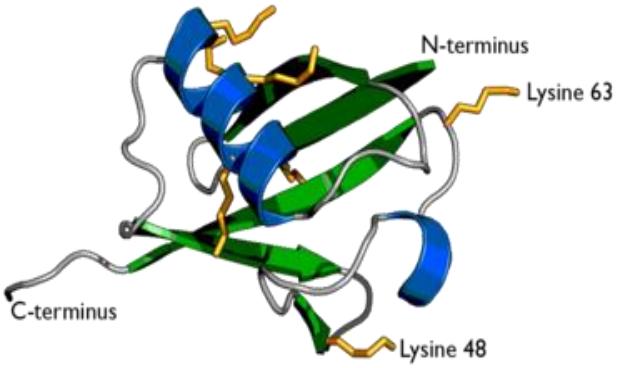

E3 ubiquitin ligase NRDP1 – high level expression of full-length protein and analysis of its interaction with AMPK

Abstract. NRDP1, an E3 ubiquitin ligase, has been shown to interact with AMP-activated protein kinase (AMPK) in cytosolic split-protein yeast-two hybrid screens (Y2H). Here we developed a method to produce NRDP1 full-length protein at high yield by avoiding formation of inclusion bodies. Recombinant NRDP1 can be phosphorylated by AMPK *in vitro*, but does not ubiquinate AMPK in HEK293 cells. Cellular overexpression of AMPK in HeLa cells increases NRDP1 proteasomal degradation, suggesting that AMPK affects cellular steady state levels of NRDP1 and thus NRDP1 functions.

Résumé. Un crible cytosolique de double hybride en levure (Y2H) a montré que l'E3 ubiquitine ligase NRDP1 interagit avec la protéine kinase activée par l'AMP (AMPK). Nous avons alors développé une méthode afin de produire la protéine NRDP1 à haut rendement en évitant la formation de corps d'inclusions. La protéine recombinante NRDP1 peut être phosphorylée par l'AMPK *in vitro*, en revanche elle n'ubiquitine pas l'AMPK dans les cellules HEK293. La surexpression d'AMPK dans les cellules HeLa augmente la dégradation de NRDP1 via le protéasome, ce qui suggère que l'AMPK affecte le niveau basal de NRDP1 et donc ses fonctions.

Research of this part was partially conducted in the group of Dr. Pascual Sanz, IBV, CSIC, Valencia, Spain. A manuscript based on this part [Zorman, S., Roma-Mateo, C., Sanz, P., Schlattner, U., High level expression and AMPK complex formation of E3 ubiquitin ligase NRDP] is submitted to Protein Expression and Purification.
I was involved in all experiments, data analysis and manuscript writing.

Introduction

The neuregulin receptor degradation protein 1 (NRDP1) is part of the E3 ubiquitin ligase family that is essential for the ubiquitination of proteins. This secondary protein modification, mostly known to target proteins to the proteasome for degradation (Hershko and Ciechanover, 1992) is among the most frequent in eukaryotes and occupies a pivotal role in regulating cell signaling and homeostasis (Dikic et al., 2009). The conjugation of an ubiquitin (Ub) moiety to a substrate protein serves as a recognition element for effector proteins. However, protein ubiquitination extends far beyond the well-known proteasome-linked protein degradation. It is critical for processes such as endocytosis, DNA repair, DNA damage tolerance, protein kinase regulation, autophagy, multivesicular bodies biogenesis or NF-κB activation and transcription (Dikic et al., 2009). Given the broad spectrum of ubiquitination events and substrates, it is not surprising that this modification is also involved in pathologies ranging from cancer to neurodegenerative disorders and infectious diseases, such as HIV (Weissman, 2013). Thus, there is intense interest in targeting enzymes involved in ubiquitination.

The ubiquitination system

Ub is a small, monomeric protein of 76 residues that is highly conserved in all eukaryotic organisms (except 3 amino acids, the sequence is identical between yeast and human proteins) (Ozkaynak et al., 1987). The lack of evolutionary divergence suggests that the entire sequence is functionally important. The conjugation of Ub to a substrate protein has been elucidated in detail by Avram Hershko & Aaron Ciechanover (Hershko and Ciechanover, 1998). It requires three enzyme subfamilies: E1, E2, and E3. ATP-dependent ubiquitin-activating enzyme E1 is a unique isoform in most organisms. It generates an activated E1-bound Ub able to be transferred to a cysteine in the active site of an E2 Ub conjugating enzyme. There are roughly 40 different E2 enzymes in mammals, working in conjunction with accessory E3 proteins. Ubiquitin-protein ligase E3, the last effector of the machinery, provides substrate specificity. By formation of E2-E3 complexes, E3 will transfer the Ub from E2 to a Lys ε-amino group of its target substrate protein, thereby forming an isopeptide bond. Mammalian cells contain over 600 type of E3 enzymes (Weissman, 2013), each of which mediating the

ubiquitination of a specific set of substrate proteins and thereby alter their fate or function. The known E3 enzymes form two unrelated families: the HECT domain E3 (**h**omologous to **E**6AP-**C**-**t**erminus) and the RING finger E3 (**r**eally **i**nteresting **n**ew **g**ene) (Ardley and Robinson, 2005). The HECT E3 enzymes have a 350 residue HECT domain that mediates E2 binding and catalyzes the ubiquitination reaction, and a unique N-terminal domain that interacts with its target substrate proteins. The ubiquitin moiety is first transferred from E2 to E3 before it is attached to the substrate. RING finger-containing E3s have a RING finger domain of 40 to 60 residues at their N-terminal tail which is thought to mediate a variety of protein-protein interactions and catalyzes a direct transfer of ubiquitin from E2 to a substrate protein (*Figure* 1).

In one round of ubiquitinylation, Ub is either directly bound to a lysine residue of a substrate protein, or to a lysine residue of protein-linked Ub, thus forming a polyUb chain. Ub has 7 internal Lys residues in positions 6, 11, 27, 29, 33, 48 and 63. Earlier studies suggested that only Lys48 was involved in the formation of Ub chains (Chau et al., 1989; Dammer et al., 2011), More recent studies showed that homogeneous chains could be also based on linkage of Lys6, 11, 27, and 29 (Dammer et al., 2011), and also Lys 33 (Bedford et al., 2009)and Lys 63 (Saeki et al., 2009). In addition, there are heterogeneous chains based on different internal linkages (Kirkpatrick et al., 2006), and more than one Ub can be linked to a proceeding Ub, thus creating branched Ub polymers (Kim et al., 2007). These different Ub structures are recognized by an Ub-binding domain (UBD) on the effector proteins. The entire Ub polymer structure is critical to condition the fate of the target protein (Husnjak and Dikic, 2012). This pattern seems to be a complex language which needs a better understanding to decode the numerous signals generated by these different chains and to discover the mechanisms that underlie the diversity of encoded functions.

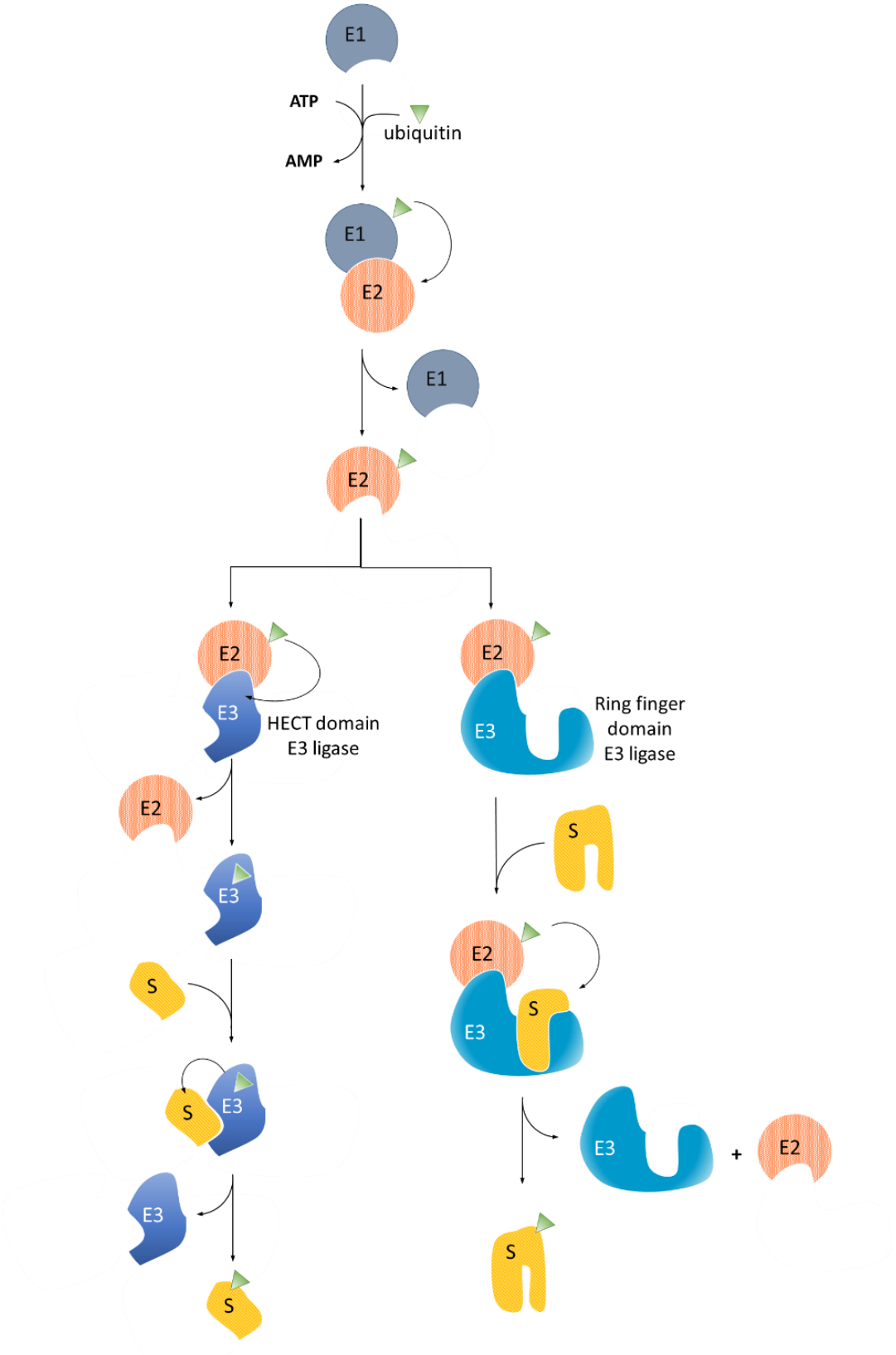

Figure 1. **Enzymatic reactions involved in the ubiquitination of proteins.** The ubiquitin-activating enzyme E1 binds ubiquitin to activate it for transfer to ubiquitin-conjugation enzyme E2. E2 is forming a complex with ubiquitin-ligase E3 which ubiquitinates substrate proteins and confers substrate specificity. The exact mechanism differs between the two E3 families, the HECT-domain E3 (left) and the ring finger-domain E3 enzymes (right).

The E3 ubiquitin ligase NRDP1

NRDP1 was first described in 2001, but only few publications are referring to it so far. This RING finger E3 ubiquitin ligase shows an ubiquitous expression in human adult tissues, with highest levels in heart, skeletal muscle and brain (Diamonti et al., 2002). Four different functions of NRDP1 have been described in literature:

1/ NRDP1 interacts with the cytoplasmic tail of ErbB3 (Bouyain and Leahy, 2007) receptor, thus stimulating Erb3 ubiquitination and degradation by the proteasome (Qiu and Goldberg, 2002; Sweeney and Carraway, 2004). ErbB3 is a component of the EGF receptor family that regulates cell survival, proliferation and differentiation. Overexpression of ErbB receptors is associated with the development of different types of human cancer (Berger et al., 1988; Gullick, 1996; Hynes, 2007; Press and Lenz, 2007; Sharma and Settleman, 2009). Moreover, human NRDP1 and ErbB3 genes co-localize at the chromosomal locus 12q13 which is frequently rearranged in human tumors (Abdullah et al., 2001), and NRDP1 is even lost in certain mammary tumors (Yen et al., 2006), both suggesting a putative role of NRDP1 in tumor progression via increased Erb signaling. Degradation of ErbB via NRDP1 would thus be an attractive target for cancer therapy.

2/ NRDP1 binds and catalyzes the ubiquitination of BRUCE, a member of the IAP (inhibitor of apoptosis proteins) family, thus targeting it to proteasomal degradation as shown by NRDP1 overexpression (Qiu et al., 2004) and siRNA knock-downs (Qiu et al., 2004). Such BRUCE degradation is critical for the initiation of apoptosis (Bartke et al., 2004).

3/ NRDP1 interacts with and regulates the stability of parkin, another E3 ubiquitin ligase. Loss of function in parkin causes accumulation and aggregation of its substrates and and inhibits mitophagy, leading to death of dopaminergic neurons in Parkinson disease (Mo et al., 2010; Yu and Zhou, 2008; Zhong et al., 2005).

4/ Finally, NRDP1 activity seems to be dependent on its antagonist USP8 (deubiquitinating enzyme 8) which is stabilizing both, NRDP1 and its target substrates, by deubiquitination (Avvakumov et al., 2006; De Ceuninck et al., 2013; Wu et al., 2004). This is important, since autoubiquitination of NRDP1 causes high cellular turnover of this protein (Qiu and Goldberg, 2002; Wu et al., 2004). The balanced reciprocal cross regulation between NRDP1 and USP8 thus decides about the fate of both proteins and their substrates.

NRDP1/AMPK interaction

An unbiased yeast-two-hybrid (Y2H) interaction screen performed in our laboratory has revealed another potential regulation of NRDP1: an interaction with the AMP-activated protein kinase (AMPK). AMPK is a key sensor and regulator of energy metabolism and represents a signaling hub in a large network that maintains cellular and organism energy homeostasis (Hardie and Carling, 1997; Winder and Hardie, 1999). AMPK is regulating its substrates by activatory or inhibory phosphorylations at serine or threonine residues. Activated AMPK is increasing the ATP-generating catabolism and reduces ATP-consuming anabolism. Among the various additional functions mostly related to spare cellular energy expenditure is the reduction of protein synthesis and cell growth. This is mediated by inhibition of the mammalian target of rapamycin complex 1 (mTORC1) pathway.

In this study, we report on the identification of AMPK as an NRDP1 interactor by two different Y2H screens. An NRDP1/AMPK interaction may have different, non-exclusive functional roles: (i) NRDP1 could be a putative substrate of AMPK, (ii) AMPK could be a putative substrate of NRDP1, or (iii) the interaction alone could affect NRDP1 or AMPK functions. Scaffolding, affecting conformation, stabilized or unstabilized one or both proteins.

To study the NRDP1/AMPK interaction *in vitro*, we established an efficient bacterial expression and purification protocol for full-length NRDP1. Recombinant protein used for *in vitro* assays, together with cellular overexpression systems, revealed an effect of the NRDP1/AMPK interaction on NRDP1 stability, independent of an observed low level NRDP1 phosphorylation by AMPK.

Materials & Methods

Cloning

NRDP1 (E3 ubiquitin-protein ligase NRDP1, Accession no. BC032637) was amplified from vector pCMV-SPORT6 (Thermo Fisher Scientific, Waltham, Massachusetts, USA) with NRDP1-fw (CAATGTATTGGCCATTACGGCCATGGGGTATGATGTAACCCGTTTC) and NRDP1-rev (CAATACATTGCAGGCCGAGGCGGCCCCTATCTCTTCCACGCCATGCGCAAATAT) primers containing sfi1 sites and introduced into yeast two-hybrid (Y2H) vectors pCab and pDSL (Dualsystems Biotech AG, Schlieren, Switzerland) for Y2H experiments or in bacterial expression vector pGEX-4T-1 (GE-Healthcare Life Sciences, Pittsburgh, PA, USA), all plasmids containing Sfi1 sites (more details can be found in the PhD thesis of A. Bruckner/Grenoble University). All construct were verify by sequencing (GATC-Biotech, Konstanz, Germany). The fusion constructs GST-NRDP1, GST-ACC (plasmid kindly provided by G.Hardie, Univ. of Dundee, UK) and GST-CamKKβ (plasmid kindly provided by H. Tokumitsu, Kagawa Medical University, Japan) all with GST-tag at n-terminal of the protein, were bacterially expressed as below.

Yeast-two-hybrid

Cytosolic yeast two-hybrid (Y2H) systems based on reconstitution of split proteins have been used for protein-protein interaction screening and pairwise protein-protein interaction analysis. The Cyto-Y2H (Möckli et al., 2007) (Dualsystems Biotech, Schlieren, Switzerland) is based on the split-ubiquitin system (Johnsson and Varshavsky, 1994; Stagljar et al., 1998). The membrane-anchored bait is fused to a reporter cassette composed of the C-terminal half of ubiquitin and the artificial transcription factor LexA-VP16, whereas the prey is fused to the N-terminal half of ubiquitin. Bait/prey interaction leads to ubiquitin reconstitution and cleavage by ubiquitin-specific proteases that liberate the transcription factor for classical transcriptional read-out. In contrast to the published ER-membrane-anchored (Ost4P) bait, we apply here a novel version using a plasma membrane anchor (Aβ-domain, transmembrane domain of the Type 1 membrane protein APP). Cloning procedures using Sfi1 sites, transformation of yeast cell line NMY51 (*MATa his3delta200 trp1-901 leu2-3,112 ade2 LYS2::(lexAop)4-HIS3 ura3::(lexAop)8-lacZ (lexAop)8-ADE2 GAL4*) and yeast spotting were

described earlier (Möckli et al., 2007). Selective media lacked either tryptophan and leucine (SD-WL) to control the presence of bait and prey plasmid, or additionally adenine and histidine (SD-AHWL) for protein interaction analysis. Spotted plates were incubated 72 h at 30°C. The Split-Trp is based on the split-protein sensor Trp1p (Tafelmeyer et al., 2004). A C-terminal part of Trp1p (CTrp) is fused to bait subunits and an N-terminal part of Trp1p (NTrp) is fused to prey. Upon interaction of bait and prey, active Trp1p is reconstituted from both domains, thus allowing growth of yeast strain CRY1 (*MATα ura3-1 trp1-1 his3-11,15 leu2-3,112 ade2-1 can1-100 GAL*) on medium lacking tryptophan. CRY1 transformation and spotting were similar as above. Selective media either lacked uracil and leucine (SD-UL, controls) or additionally tryptophan (SD-UWL, protein interaction analysis). Spotted plates were incubated up to 9 days at 27°C.

The Cyto-Y2H was used to screen a human brain cDNA library (preys) for interactors of the N-terminal domain of AMPK- β1 and - β2 subunits (Δβ1, Δβ2 amino acids 1-54 as baits). This domain was chosen to avoid interactions with other AMPK subunits, and because it has been identified as candidate AMPK interaction domain. About 6.2 × 106 and 3.4 × 106 clones were screened. Plasmids containing the cDNA sequence of putative interaction partners were extracted and reintroduced together with the corresponding Δβ -encoding bait vector into the reporter yeast strain in order to confirm the interaction. Reproducible interactors were sequenced and clones containing in-frame coding sequence ot known as false positives (Dualsystems, personal communication) were retained. To verify NRDP1/AMPK interactions, paired Y2H assays were performed using Δβ1 and Δβ2, full-length β1 and Δβ, as well as α1 and α2 subunits as baits and full-length NRDP1 as a prey. Interaction of GST with an unrelated bait, Large T antigen *(Simian virus)* was used as negative control.

Expression and purification of GST-fusion protein

All the GST fusions protein constructs were transformed into competent *E. coli* BL21-Codon Plus (DE3)-RIL cells (Stratagene, La Jolla, CA, USA) and incubated overnight on LB agar containing 100 µg/ml ampicillin and 30 µg/ml chloramphenicol. Cultures were routinely grown in standard LB medium containing antibiotics (100 µg/ml ampicillin and 30 µg/ml chloramphenicol) at 37°C in Erlenmeyer flasks with constant shaking until O.D. (600nm) 0.7-

0.9 (if not indicated otherwise). Cells were then cooled down to 30°C and protein expression was induced for 4 hours (if not indicated otherwise) with 2mM isopropyl β-D-thiogalactopyranoside (IPTG, Eurobio). Cells were centrifuged at 4000 g, 30 min at 4°C, harvested and suspended in PBS lysis buffer (phosphate buffer saline: 137 mM NaCl, 2.7 mM KCl, 10 mM Na_2HPO_4, 2 mM KH_2PO_4, pH 7.4). After 3x15s sonication at 85% of manual powered, insoluble material was removed by centrifugation (40000 g, 40 min at 4°C). All supernatant was applied by gravity flow to a 5 ml Gluthation Sepharose matrix (binding capacity up to 1g/ml, Qiagen, Hilden, Germany) self-packed in a column (diameter 1 cm). The column was washed with 3x5 column volumes PBS and proteins were eluted with 10 ml of 10 mM reduced L-glutathione (Sigma-Aldrich) in 50 mM Tris-HCl, pH 8. Ten µl of each elution fraction were mixed with Laemli sample buffer, separated by SDS-polyacrylamide gel electrophoresis (SDS-PAGE, 12% acrylamide), and stained with Coomassie. Protein concentrations were determined according to Bradford (Bradford, 1976) with the Biorad microassay (Biorad, Reinach, Switzerland) and BSA as standard.

Protein expression in bioreactor

GST-NRDP1 fusion protein constructs were transformed into competent *E. coli* BL21-Codon Plus (DE3)-RIL cells (stratagene, La Jolla, CA, USA) and incubated overnight on LB agar containing 100 µg/mL ampicillin and 30 µg/mL chloramphenicol. Precultures (30 mL) were grown in LB containing antibiotics at 37°C until $O.D_{600}$. 1. Bacteria were harvested by centrifugation and added to second preculture of 300 mL complement M9 medium (6.8 g/L $Na_2HPO_4.7H_2O$, 3 g/L KH_2PO_4, 1 g/L NH_4Cl, 0.5 g/L NaCl) containing antibiotics (100 µg/mL ampicillin and 30 µg/mL chloramphenicol), and grown overnight at 37°C and constant shaking. Cells were centrifuged (4000 g, 30 min at 4°C), resuspended in 20 mL M9 and injected with a 100 mL-syringe (sterile) into the bioreactor (Minifors, Infors HT) containing 3 L of complement M9 medium with antibiotics (100 µg/mL ampicillin and 30 µg/mL chloramphenicol). Bioreactor conditions were maintained constant at pH 7.4, 37°C and stirring speed of 500 rpm. Cells were grown until $O.D_{600}$. 8, cooled down to 16°C, and expression was induced by 2 mM IPTG (Eurobio, Courtaboeuf, France). Cells were harvested by centrifugation and treated as described above.

To follow bacteria growth, sample were taking every hour and O.D was measured at 600 nm.

In vitro analysis of AMPK substrate phosphorylation kinetics

Purified GST-ACC and GST-NRDP1 (200 pmol) were incubated for 5, 10, 20 and 40 min at 37°C with 200 µM [γ-^{32}P] ATP (specific activity 6000 Ci/mmol ATP) and AMPK221 (4 pmol) previously activated by incubation with 1 pmol CamKKβ for 20 min at 30°C in kinase buffer (50 µM AMP, 5mM $MgCl_2$, 1mM DTT, in 10 mM HEPES pH 7.4). For negative controls, AMPK substrates were incubated with 1 pmol CamKKβ without AMPK. Kinase reactions were stopped by addition of Laemli buffer and subjected to SDS-PAGE (12%) with Coomassie staining and analysis by Typhoon phosphoimager (GE Healthcare).

In vitro analysis of AMPK substrate phosphorylation stoichiometry

Different concentrations of purified GST-ACC and GST-NRDP1 (25, 50, 100, 200 pmol) were incubated 40 min at 37°C with 200 µM [γ-^{32}P] ATP (specific activity 6000 Ci/mmol ATP) and AMPK221 (4 pmol) previously activated by incubation with 1 pmol CamKKβ for 20 min at 30°C in kinase buffer. For negative controls, AMPK substrates were incubated with 1 pmol CamKKβ without AMPK. Kinase reactions were stopped by addition of Laemli buffer and subjected to SDS-PAGE. After Coomassie staining, the bands corresponding to the substrates (around 60 kDa) were cut and incubated in 5 ml scintillation solution and subjected to measurements in a liquid scintillation counter (Packard).

Sample preparation for mass spectrometry analysis

To find NRDP1 phosphorylation(s) site(s) by AMPK, GST-ACC, GST-NRDP1 (300 pmol) were incubated for 1 h at 37°C with 6 pmol of freshly purified AMPK-221 (to avoid the presence of glycerol needed for long term AMPK storage) previously activated by incubation with 3 pmol CamKKβ for 20 min at 30°C in kinase buffer. As negative controls, GST-ACC and GST-NRDP1 were incubated with 3 pmol CamKKβ without AMPK. The samples were conserved at 4°C.

Mass spectrometry to detect phosphosite(s)

Samples were dried and solubilized in 20 µL ammonium bicarbonate (50 mM), trypsin-digested. Part of them were enriched either in Pierce TiO_2 Phosphopeptide Enrichment (Thermo Scientific) or in Pierce Fe-NTA Phosphopeptide enrichment kit (Thermo Scientific) then purified with Graphit Clean-up kit (Thermo Scientific). 30 pmol of each assay were injected in LC-MS/MS. The analyses were proceed by a 4000QTrap mass spectrometer. Phosphopeptide identification was realized with ProteinPilot 4 (ABSciex) using Paragon and Mascot algorithms.

Cell culture conditions

Human embryonic kidney (HEK293) cells, were grown in DMEM supplemented with 100 units/ml penicillin, 100 µg/mL streptomycin, 2 mM glutamine, 10% inactivated fetal bovine serum (FBS, GIBCO). Hepitheloid cervix carcinoma (HeLa) cells, were cultured in DMEM/F12 high glucose medium supplemented with 10% inactivated fetal calf serum (FCS) and 1% glutamate/streptomycine/penicillin.

Analysis of *in vivo* ubiquitination

HEK293 cells cultured as describe above were transfected with one or several of the following plasmids (all gently provided by Pascual Sanz, IBV, Valencia, Spain): pCMV-His6xUbiq (encoding a modified ubiquitin, tagged in n-terminal with 6 His residues); pCMVmyc (encoding the different AMPK subunits α2, β2, and γ1 all tagged in N-terminal with myc), pcDNA3-HA-NRDP1 (encoding N-terminally HA-tagged NRDP1), by using the Lipofectamine 2000 reagent (Invitrogen) according to the manufacturer's instructions. After 36 h of transfection, medium was removed and cells were frozen in liquid nitrogen, then scrapped in lysis buffer A (6 M guanidinium-HCl, 0.1 M sodium phosphate, and 0.1 M Tris-HCl, pH 8.0). To purify His-tagged proteins, 4 mg protein of a clarified extract (CE; centrifuged at 12000 g for 15 min) was incubated in 100 µl of TALON resin (Clontech) in the presence of 10 mM imidazole, for 3 h at room temperature on a rocking platform. The resin was then successively washed with 2 mL each of buffer B (buffer A plus 10 mM imidazole), buffer C (buffer B but with 8 M urea instead

of 6 M guanidin-HCL), and four more times with buffer C adjusted to pH 6.0. Bound proteins were eluted with 50 µl of 2X Laemli's sample buffer and analyzed by Western blotting using appropriated antibodies.

AMPK or ubiquitin overexpression in cell culture

HeLa cells were transfected with one or several of the following plasmids (kindly provided by Pascual Sanz, IBV, Valencia, Spain): pCMV-myc (encoding the different AMPK subunit α2, β2, and γ1), pCMV-His6xUbiq (encoding a modified ubiquitin tagged with 6 His residues), and pCMV-His6xUbiqK48R or pCMV-HisxUbiqK63R (encoding mutated ubiquitin variants, were Lys48 and Lys63 is replaced by an arginine, by using the Lipofectamine 2000 reagent (Invitrogen) according to the manufacturer's instructions. 24 h after transfection, medium was removed and cells were frozen in liquid nitrogen. To extract proteins, HeLa cells were lysed in Tris-buffer (10 mM pH7 containing complete with EDTA-free protease inhibitor cocktail tablet (Roche), sonicated 3 X 10 s and centrifuged at 12000 g for 15 min at 4°C.

Proteasome inhibition in cell culture

HeLa cells were cultured as described above. Inhibitor MG132 (Sigma, Saint Louis, MO, USA) prepared in DMSO at 4 µM final concentration was added four hours before the medium was removed and cells were frozen in liquid nitrogen. Proteins were extracted as described above.

Immunoblotting

50 µg of total protein from the clarified extracts prepared as described above were analyzed by SDS-PAGE (12%) and Western blotting using appropriate antibodies: anti-myc (Sigma-Aldrich, diluted at 1/2000); anti-HA (Invitrogen, diluted at 1/1000); anti-NRDP1 (Bethyl dilute at 1/1000); anti-tubulin (Abcam diluted at 1/1000). All membranes were revealed at room temperature with ImageQuant CAS4000 CDD camera (GE Healthcare).

Results

Yeast-two-hybrid screening reveals an interaction between NRDP1 and AMPK

A Y2H screen using the AMPK- β1 and - β2 N-teminal domains (Δβ1, Δβ2 amino acids 1-54) as baits and a brain cDNA library as preys identified NRDP1 as a putative AMPK interactor. The applied novel cytosolic, split-ubiquitin-based system (Cyto-Y2H, (Möckli et al., 2007)) detects protein-protein interactions in a cytosolic environment, with bait and prey anchored to the plasma membrane, and uses a very sensitive transcriptional read-out that detects also weak or transient interactions. The identified NRDP1 clone contained the C-terminal domain of NRDP1, which also associates with receptor tyrosine-protein kinase ErbB3 to trigger its degradation (Diamonti et al., 2002; Yen et al., 2006).

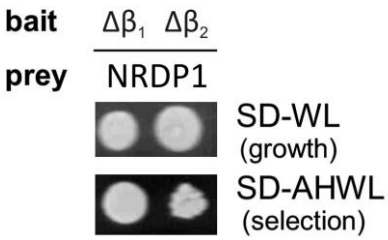

Figure 2. **Cyto-Y2H reveals interaction of NRDP1 with AMPK β-subunits.** Representative results of a cyto-Y2H assay to analyze interaction of AMPK-Δβ subunits with the C-terminal domain of NRDP1 (amino acids 136-316). Presence of bait and prey plasmids are verified on selective media (SD-WL). Bait/prey interaction leads to reconstitution of ubiquitin and a transcriptional readout allowing growth on medium lacking in addition adenine and histidine (SD-AHWL). Spots represent yeast grown for 48h at 30°C. Δβ: N-terminal domain of AMPK β-subunit used for Y2H screening. For more details see Material and Methods.

The NRDP1/AMPK interaction was then confirmed by different paired Y2H assays. First, in Cyto-Y2H, the identified NRDP1 clone interacted with both Δβ1 and Δβ2 subunits, (*Figure 2*). In another cytosolic Y2H assay, the Split-Trp-Y2H, protein-protein interaction reconstitutes an enzyme in tryptophane biosynthesis, allowing a direct readout that is more proportional to interaction strength (*Figure 3*). This assay confirmed interaction of NRDP1 with both truncated and full-length β subunits although interaction seemed to be less strong with full-length β1. When α-subunits were tested in this Y2H assay, NRDP1 interacted weakly with α2 and more strongly with α2TD (a constitutive active α2 mutant), but not with α1.

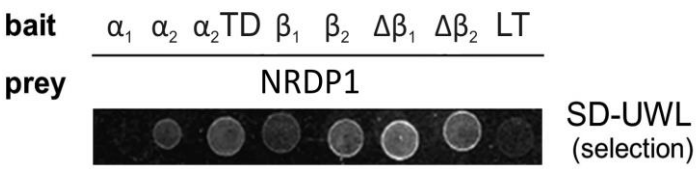

Figure 3. **Split-Trp Y2H confirms interaction between NRDP1 and AMPK β subunits but also α2 subunit.** Representative results of a Split-Trp-Y2H assay to analyze interaction of AMPK subunits with full-length NRDP1. Bait/prey interaction leads to reconstitution Trp1P essential for tryptophan synthesis, thus allowing growth on medium lacking tryptophan (SD-UWL). Spots represent yeast grown for 9 days at 27°C. α1, α2, β1, β2: AMPK subunits; α2TD: constitutive α subunit; Δβ: N-terminal domain of AMPK β-subunit used for Y2H screening. For more details see Material and Methods.

Production of NRDP1 full-length protein

Since our goal was to proceed with *in vitro* characterization of the NRDP1/AMPK interaction without prior knowledge of the involved domain(s), our primary aim was to produce recombinant full-length NRDP1. Previous publications have shown the difficulties to produce full-length NRDP1 (Wu et al., 2004), although it is a cytosolic and thus an *a priori* soluble protein. So far, only a C-terminally truncated version (amino acids 134 to 317) could be produced at low quantities (Qiu and Goldberg, 2002). We thus generated a NRDP1 construct carrying a GST-tag at the N-terminus for bacterial expression.

Bacterial expression in shaking flask cultures

First, a standard protocol for production of GST-tagged protein was applied, where bacteria were grown at 37°C until $O.D_{600}$. 1 before expression was induced by IPTG (2 mM) for 4 h at 30°C. Under these conditions, a predominant band at the size of full-length GST-NRDP1 (around 60 kDa) appeared in *E. coli* lysates, reaching a maximum after about 3 hours (*Figure* 4). Further bands between 25 and 50 kDa also increased during induction, possibly as a consequence of proteolytic degradation or incomplete translation.

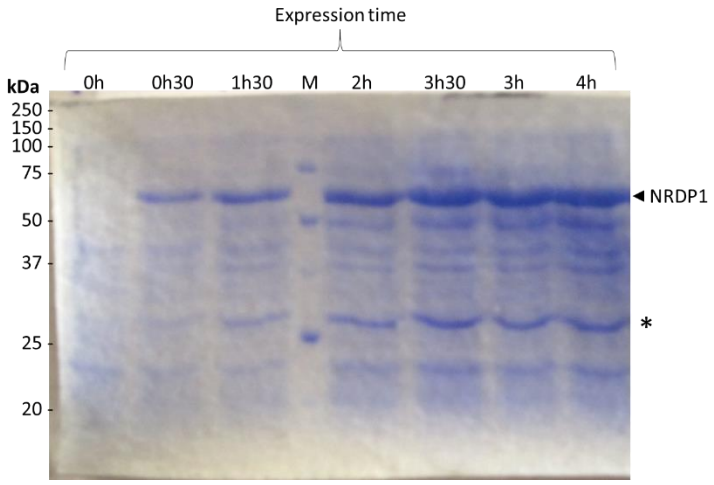

Figure 4. **Effect of expression time on quantity and quality of expressed NRDP1 (expression at 30°C).** Expression profile of NRDP1 at 30°C after induction by IPTG (2 mM). Coomassie staining of a SDS-PAGE gel. Culture of BL21 bacteria transformed with pABGSTn-NRDP1 was done in 400 ml LB. At O.D. 1, expression was induced with IPTG for 4 hours at 30°C. 20 µL aliquots were taken at different expression time (0-4 h). **M:** molecular mass markers.

However, when soluble protein of these expressions was subjected to affinity purification, full-length GST-NRDP1 around 60 kDa occurred only as minor band as compared to the lower molecular mass bands (*Figure 5*), in particular the 23 kDa band that corresponds to the size of the GST-tag domain. A commercial protease inhibitor mix in the lysis buffer did not improve this result and was therefore not added in further experiments. The yield of these purifications reached only 0.12 mg/L, a too low value considering the small fraction of full-length protein in this preparation. Further analysis of lysate preparation revealed that it is not the sonication procedure itself that degrades NRDP1, but the presence of mainly insoluble full-length NRDP1 that remains in the pellet after sonication (*Figure 6*). Thus, recombinant full-length NRDP1 tends to form insoluble inclusion bodies in *E. coli.*

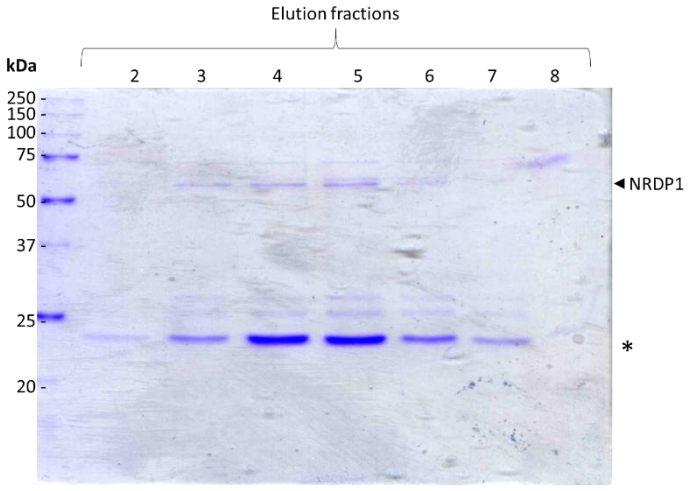

Figure 5. **Quantity and quality of purified NRDP1 (expression at 30°C).** Elution profile of the NRDP1 peak from a glutathione sepharose column. Coomassie staining of a SDS-PAGE gel. Induction of expression at O.D. 1 for 4 hours at 30°C. Bacterial lyses buffer: PBS pH.7.4 complemented with 20% glycerol and 1% Triton X-100. **2, 3, 4, 5, 6, 7, 8:** NRDP1 peak elution fractions; NRDP1: full-length NRDP1; *: main band, possibly corresponding to a NRDP1 degradation product.

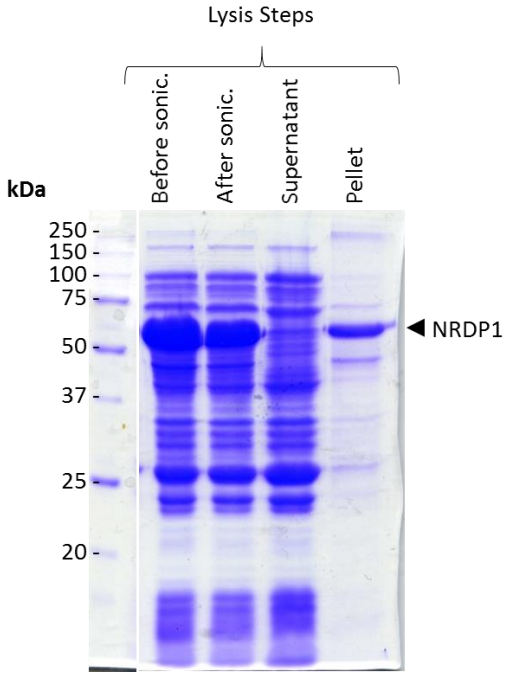

Figure 6. **Full-length NRDP1 in soluble and insoluble fractions (expression at 30°C).** Coomassie staining of a SDS-PAGE gel. Induction of expression at O.D. 1 for 4 hours at 30°C. The bacteria were lysed in PBS pH 7.4, 20% glycerol and 1% Triton X-100, sonicated 7x10 s and centrifuged 40 min at 25000 g. NRDP1: full-length NRDP1.

Inclusion bodies are the consequence of incorrect or insufficient protein folding. We therefore modified the expression protocol by (i) repeating 4 times the sonication-centrifugation step, (ii) inducing expression at different O.D., and (iii) using growth at only 25°C to slow down the bacterial metabolism Repeated sonication rather solubilized preferentially the contaminating lower Mr bands in expressions induced at O.D. 0.8 and grown at 25°C and was not retained (*Figure 7*).

Then, expression was induced at 25°C at different moments during growth: late lag phase (O.D. 0.5), exponential phase (O.D. 0.8) and early stationary phase (O.D. 1.5). The soluble fractions were directly applied to a glutathione Sepharose column to compare purity (*Figure 8*) and protein yield. All these expressions increased protein yield by about 3-fold as compared to expressions at 30°C. In addition, expressions induced at O.D. 0.8 and 1.5 each increased protein yield by another 10% each, and these two preparations also contained a higher fraction of full-length NRDP1 as compared to early induction (O.D. 0.5) (*Figure 8*). Thus, late expression appears to be preferable for maximal quantity and quality of full-length NRDP1.

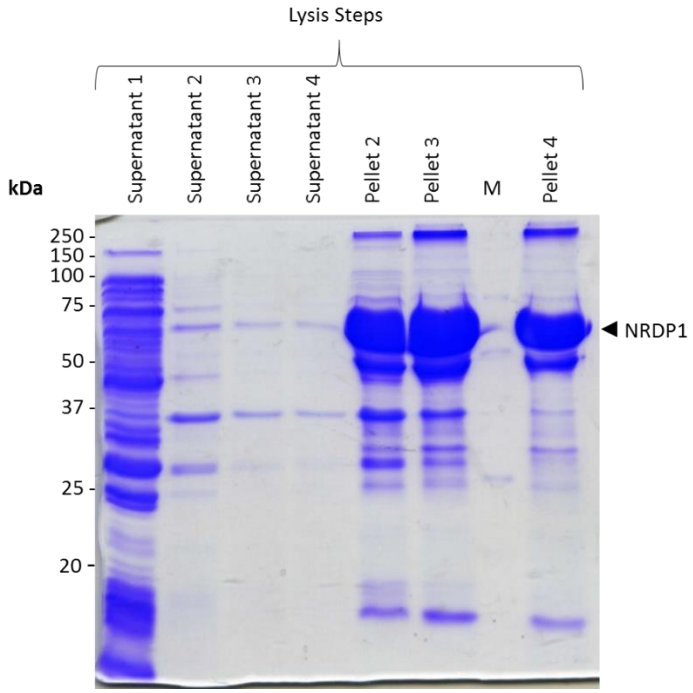

Figure 7. **Full-length NRDP1 in soluble and unsoluble fractions (expression at 25°C).** Coomassie staining of a SDS-PAGE gel. Induction of expression at O.D. 0.8 for 4h at 25°C. Protein extraction by consecutive sonication-centrifugation steps. Supernatants (supernatant 1 to 4) as well as resuspension of corresponding pellets in lysis buffer (pellet 2, 3 and 4) are shown. **M:** molecular mass markers; NRDP1: full-length NRDP1.

Table 1. **Effect of temperature and induction time point on the yield of purified NRDP1**

O.D.	**1.0**	**0.5**	**0.8**	**1.5**	**4.3**
Temperature	30°C	25°C	25°C	25°C	10°C
Expression	4h	4h	4h	4h	16h
Yield (mg protein/L)	0.12	0.30	0.35	0.39	0.71

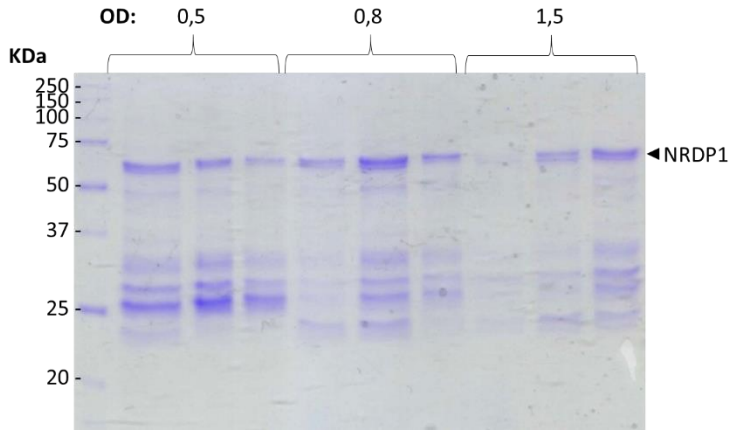

Figure 8. **Effect of induction time point on quality of purified NRDP1 (expression at 25°C).** NRDP1 elution profiles from a glutathione Sepharose column using *E. coli* lysates from different induction growth phases. Coomassie staining of a SDS-PAGE gel. The expression was induced at O.D. 0.5, 0.8 or 1.5 at 25°C for 4 h. The fractions collected after purification represent the NRDP1 elution peaks. NRDP1: full-length NRDP1.

Since lower temperature seemed to be the major factor driving production of soluble full-length NRDP1, bacteria were grown at 10°C and expression time was concomitantly increased to reach stationary phase as optimized above (*Figure 8*).

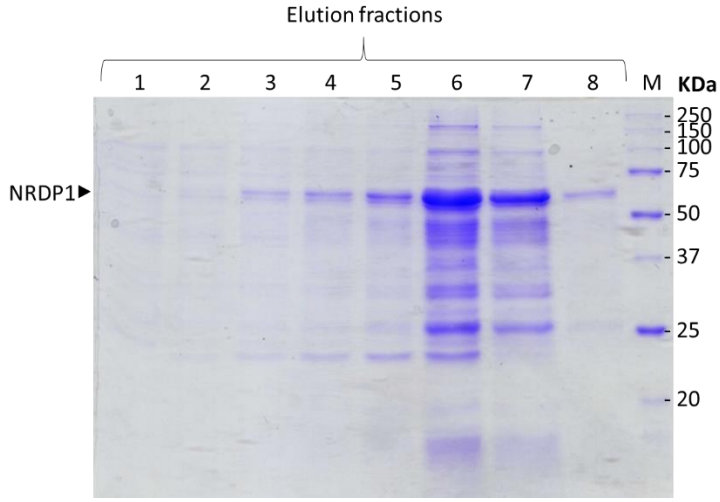

Figure 9. **Effect of low-temparture expression at 10°C on quality of purified NRDP1.** Elution profile of a glutathione Sepharose column. Coomassie staining of a SDS-PAGE gel. Expression was inducted at O.D. 4.3 at 10°C for 16 h. 1 to 8: fractions representing the NRDP1 elution peak; NRDP1: full-length NRDP1.

Under these conditions, protein yield doubled to 0.71 mg/L as compared to expressions at 25°C (table 1). Also purity seemed to improve slightly, although there still remained contaminating bands (*Figure 9*). Thus, late induction combined with very slow expression at 10°C clearly increased production of soluble full-length NRDP1.

<u>Bacterial expression of NRDP1 in a bioreactor</u>

A bioreactor allows control of bacterial growth conditions by regulation of nutriment, pO_2, pH and temperature of the medium. Such controlled conditions require however the use of a minimal medium which prolongs the lag phase as compared to complete LB medium.

With NRDP1-transfected bacteria, a 2 L-bioreactor allowed to reach O.D. 27 (*Figure 10*) instead of O.D. 4 in batch culture.

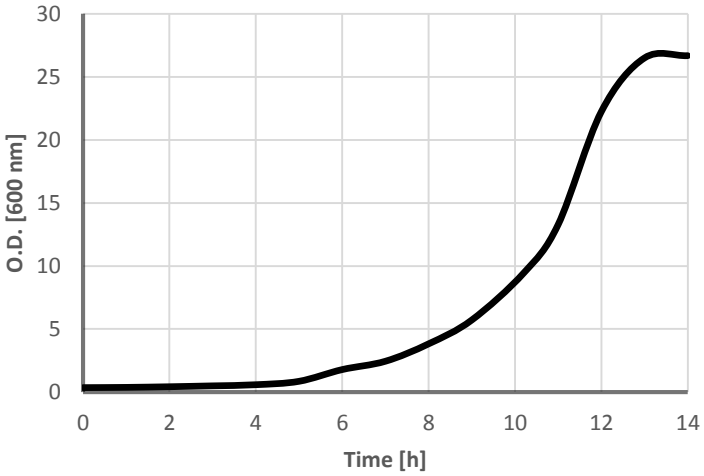

Figure 10. **Typical bacterial growth curve in the bioreactor.** Samples were taken every hour and O.D. was measured at 600 nm.

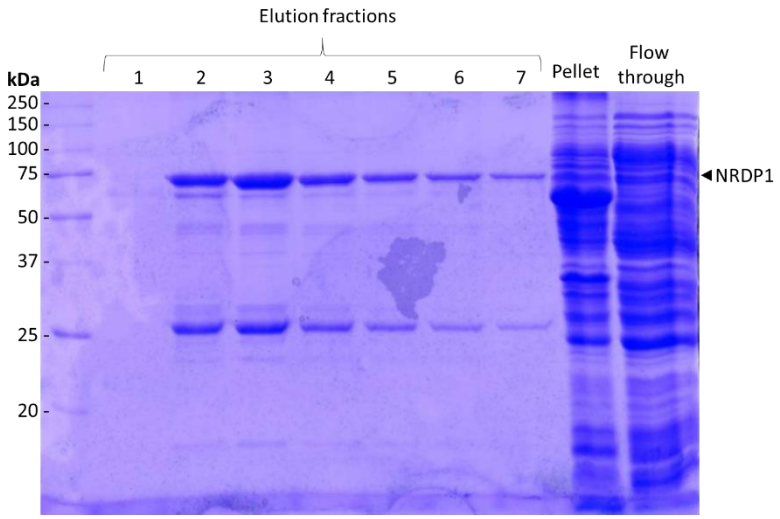

Figure 11. **Effect of bioreactor expression on quality of purified NRDP1.** Elution profile of a glutathione Sepharose column following production in bioreactor. Coomassie staining of a SDS-PAGE gel. Expression was inducted at O.D. 8 at 16°C for 12 h. 1 to 7: fractions representing the NRDP1 elution peak; pellet: insoluble protein after first sonication step, flow through: protein not binding to the column.

According to the data obtained in batch culture, expression was induced at the rather high O.D. of 8, corresponding to early exponential growth phase, and continued for 12 h at the low temperature of 16°C. Full length NRDP1 was mostly soluble and appeared in the pellet only at low levels (*Figure 11*). The yield was 3.1 mg/L, meaning that a single run of the bioreactor followed by a single purification step yielded 6.2 mg of protein

NRDP1 is directly phosphorylated by AMPK 221

With recombinant protein we first tested whether NRDP1 could be directly phosphorylated by AMPK. An *in vitro* phosphorylation assay revealed that NRDP1 can be directly phosphorylated by AMPK 221 in a time-dependent manner, although at low levels (*Figure 12*). Incorporation of ^{32}P into NRDP1 calculated by phosphoimager and scintillation counter reached about 30-40% of what was seen with the AMPK reference substrate acetyl-CoA carboxylase (ACC). Also the time course of NRDP1 phosphorylation was much slower than with ACC, reaching maximal activation only after 20 minutes (as compared to <5 min with ACC).

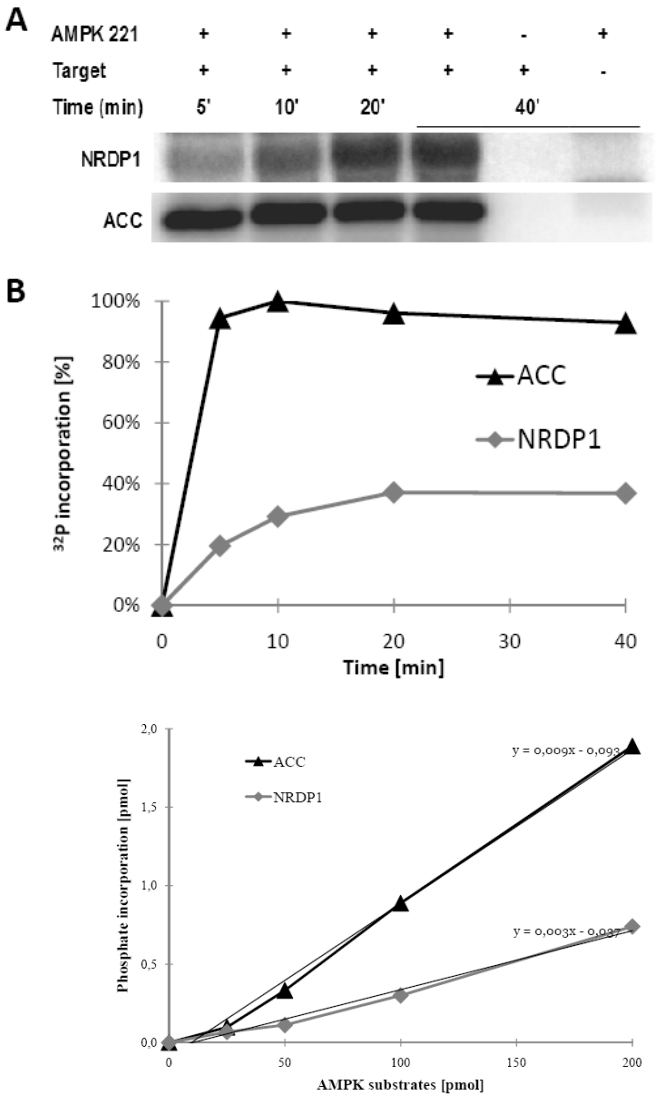

***Figure 12*. NRDP1 is a direct AMPK substrate *in vitro*. (A)** Time course of NRDP1 phosphorylation by AMPK. AMPK 221WT (4 pmol) first activated by CamKKβ (1 pmol) was incubated with purified NRDP1 (200 pmol) or ACC (positive control, 200 pmol) for 5 to 40 min at 37°C. *In vitro* phosphorylation was analyzed by SDS-PAGE and Typhoon phosphoimager. **(B)** Quantification of the phosphorylation time course using ImageJ. Data are normalized to maximal ACC phosphorylation. **(C)** Incorporation of ^{32}P into ACC and NRDP1 by AMPK. Assay as above, but using varying amounts of purified NRDP1 or ACC (50-200 pmol) and analyzing bands in SDS-PAGE by scintillation counting. Lines and values of a linear regression fit is indicated.

In silico analysis of the NRDP1 sequence identified Ser77 as a putative AMPK phosphorylation consensus sequence. However, mass spectrometry of *in vitro* phosphorylated NRDP1 did not

yield conclusive data. Thus, the significance of the observed phosphorylation remains to be shown.

AMPK is not ubiquinated by NRDP1

We therefore tested whether the NRDP1/AMPK complex could serve NRDP1 to ubiquitinate AMPK. We compared the effect of overexpression of two E3 ubiquitin ligases, NRDP1 and MDM2, on AMPK 221 ubiquitination in HEK293 cells. MDM2 served as a negative control for unspecific ubiquitination induced by ubiquitin and ubiquitin ligase overexpression. Experiments with both E3 ubiquitin ligases revealed AMPK γ_1 as a highly ubiquitinated subunit, while AMPK α_2 was ubiquitinated only at a low level and AMPK β_2 seemed not to be ubiquitinated under these conditions (*Figure 13*). Ubiquitination by NRDP1 was however identical or even lower as with MDM2 control, indicating that NRDP1 is not a specific ubiquitin ligase of AMPK subunits in HEK293 cells. The AMPK/NRDP1 interaction would thus have no function in AMPK ubiquitination.

A

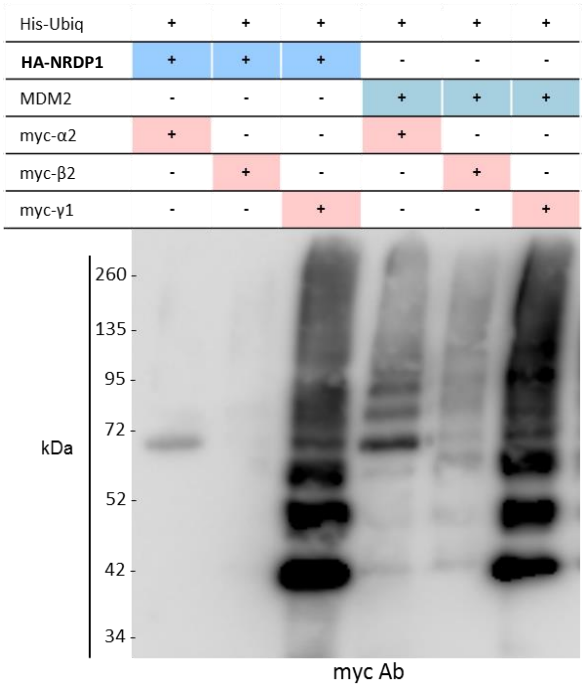

Figure 13. **AMPK is not ubiquitinated by NRDP1.** *In vivo* ubiquitination assay using overexpression of proteins (+) in HEK293 cells and corresponding control experiments for construct expression. **(A)** Pull-down for His-tagged ubiquitin with Ni-NTA resin analyzed by Western blot for AMPK subunits with anti-Myc Ab. **(B)** Overexpression of AMPK subunits (α_2, β_2, γ_1) analyzed by Western blot with anti-Myc Ab. **(C)** Overexpression of E3 ubiquitin ligase (NRDP1 and MDM2) analyzed by Western blot with anti-HA and anti-MDM2 Ab.

B

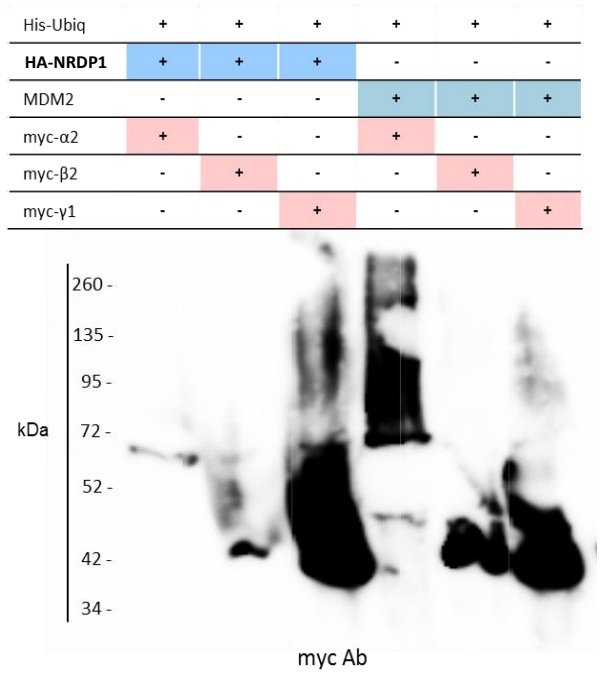

C

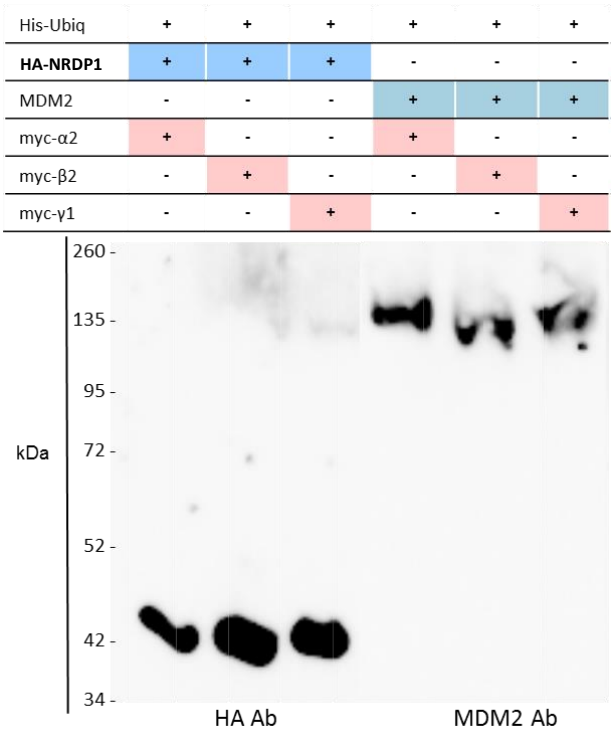

NRDP1 proteasome targeting inactive ubiquitination of both lysine 48 and 63

Independent of NRDP1/AMPK complexes, NRDP1 is rapidly auto-ubiquitinated for proteasomal degradation, but it is unknown how this occurs. We therefore applied a similar ubiquitination assay but using ubiquitin constructs mutated at specific lysine residues to address this question (*Figure 14*). Overexpression of ubiquitin wild-type in HeLa cells induced degradation of full-length NRDP1 *via* the proteasome since this decrease could be rescued by the proteasome inhibitor MG132. In case of overexpressed ubiquitin mutants K48R and K63R, unable to link ubiquitin moieties to Lys48 or Lys63, respectively, partial degradation in absence of MG132 still occurred. This result suggests that both lysine residues are involved to target NRDP1 to the proteasome.

Figure 14. **Ubiquitination NRDP1 topology for it proteasome degradation.** Representative Western blot for NRDP1 levels in HeLa cells overexpressing wild-type or mutant (K48R, K63R) ubiquitin in absence or presence of protease inhibitor MG132. *One representative out of four experiments is show.*

AMPK decreases NRDP1 levels

We finally tested whether the high NRDP1 turnover due to auto-ubiquitination is modulated by AMPK (*Figure 15*). Two genuine NRDP1 bands can be detected in HeLa cells with NRDP1-specific antibody (*https://www.bethyl.com*): a full-length NRDP1 at 36 kDa and a short form of NRDP1 (sNRDP1) at around 30 kDa. Overexpression of individual AMPK subunits (α,β or γ) had no significant impact on the levels of the two NRDP1 forms. However, co-expression of all three subunits supposed to form heterotrimeric complex decreased full-length NRDP1 levels by about 30%.

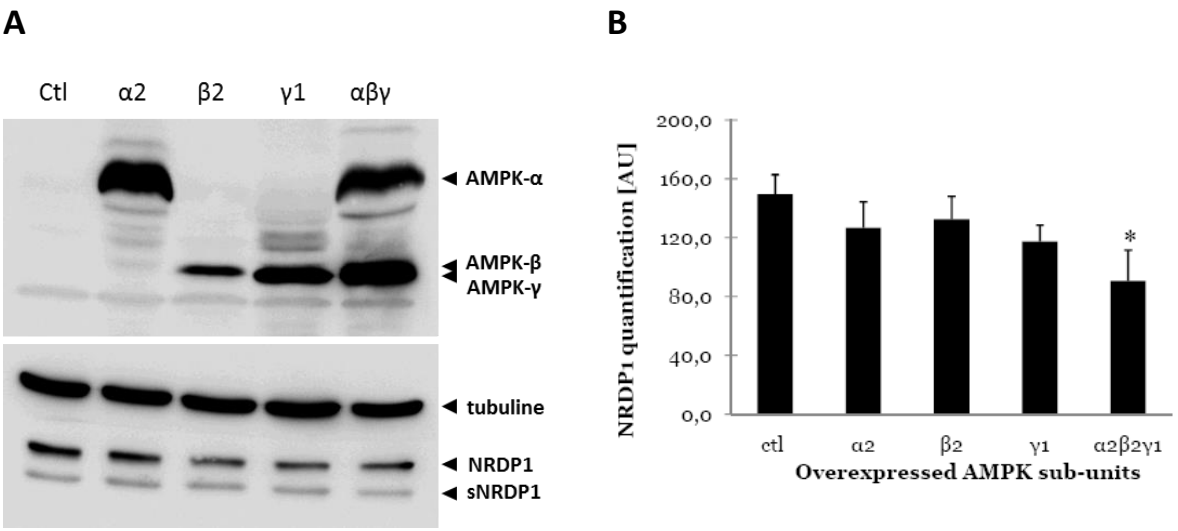

Figure 15. **Overexpressions of AMPK221 decreases NRDP1 levels. (A)** Representative Western blot of NRDP1 levels (bottom) under conditions of AMPK subunit overexpression (top) in HeLa cells for 24 h, Anti-myc Ab is used to verify overexpression of myc-tagged AMPK subunits α2, β2 and γ1 . NRDP1, full-length NRDP1; sNRDP1, lower Mr NRDP1. **(B)** Western blot quantification of full-length NRDP1 from four independent experiments by Image J, normalized to the level of tubulin.*p<0.05 versus ctl; *n=4.*

When expressing increasing levels of AMPK heterotrimer, levels of full-length NRDP1 decreased, while sNRDP1 rather increased (*Figure 16*). These data suggest that sNRDP1 results from NRDP1 degradation and that AMPK/NRDP1 interaction plays a role in regulating cellular NRDP1 levels.

To further test this hypothesis, we applied the proteasome inhibitor MG132 which reduces degradation of ubiquitin-conjugated proteins.

In presence of MG132, as expected, NRDP1 levels increased in both controls and AMPK221 overexpressing HeLa cells (*Figure 17*). Importantly, the decrease of NRDP1 by AMPK221 overexpression is rescued by MG132 to levels comparable to control, suggesting that an AMPK-induced NRDP1 degradation *via* the proteasome pathway is operating here.

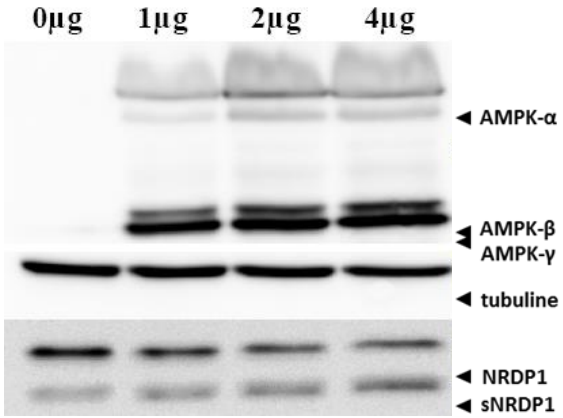

Figure 16. **Full-length NRDP1 levels are inversely correlated with AMPK levels. (A)** Representative Western blot of AMPK221 and NDRP1 levels in HeLa cells transfected with different amounts of AMPK vector. Anti-myc Ab is used to verify overexpression of myc-tagged AMPK subunits α2, β2 and γ1 NRDP1, full-length NRDP1; sNRDP1, lower Mr NRDP1. **(B)** Western blot quantification of full-length NRDP1. **(C)** Western blot quantification of sNRDP1 Data in (B) and (C) were obtained by ImageJ, normalized to tubulin and AMPK control (0 µg AMPK plasmid). */°p<0.05 versus 0 µg and 1 µg, respectively; *n=4.*

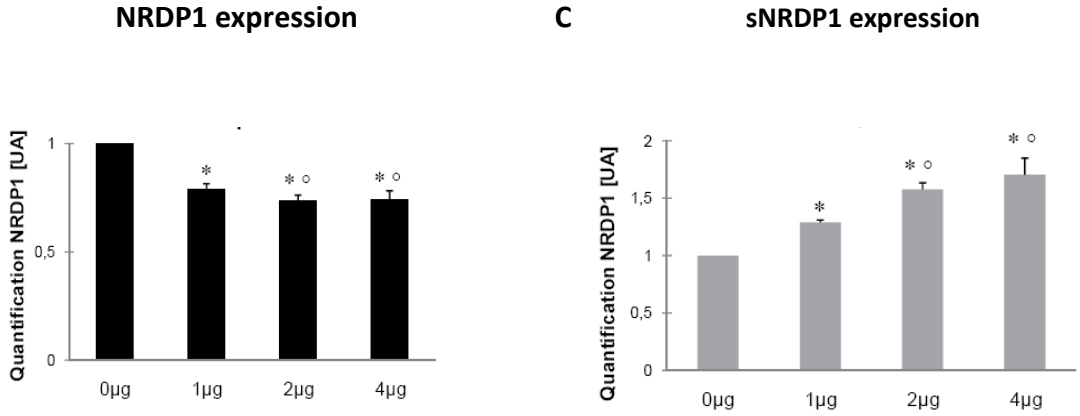

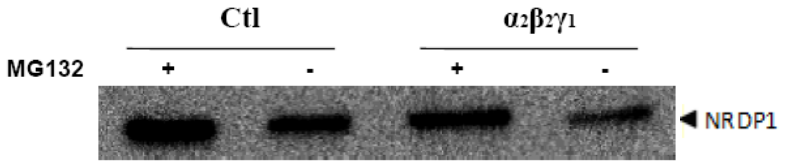

Figure 17. **Induction of NRDP1 degradation by AMPK via proteasome.** Representative Western blot of full-length NRDP1 in HeLa cells overexpressing AMPK221, Cells were treated for 4h with MG132 (4µM) before lysis and analysis of NRDP1 levels by Western blot. *One representative out of four experiments is show.*

AMPK activity is not required for NRDP1 degradation

AMPK-induced NRDP1 degradation could involve the above described NRDP1 phosphorylation. We therefore overexpressed AMPK221 wild type (*wt*) or dominant negative AMPK221 mutant (T172A, an α_2 subunit that cannot be activated). Both AMPKs (wt and T172A) caused a similar, significant degradation of NRDP1 (*Figure 18*). Thus, the kinase activity of AMPK is not required for NRDP1 degradation.

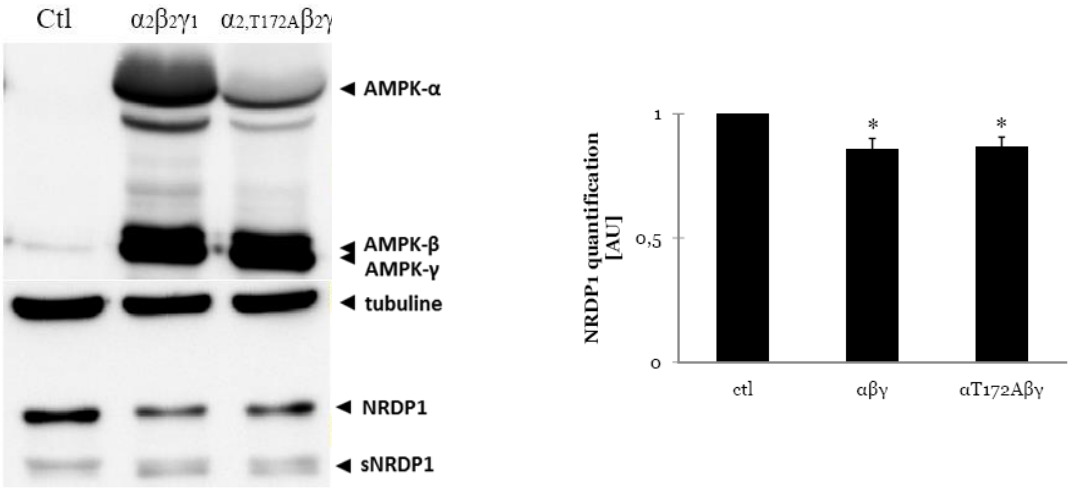

Figure 18. **Kinase activity of AMPK is not required for NRDP1 degradation. (A)** Representative Western blot of NRDP1 levels (bottom) under conditions of overexpressing AMPKwt or dominant negative AMPK mutant (top) in HeLa cells for 24 h, Anti-myc Ab is used to verify overexpression of myc-tagged AMPK. **(B)** Western blot quantification of full-length NRDP1 by Image J, normalized to the level of tubulin. *p<0.05 versus ctl; *n=4*

Discussion

NRDP1 is an E3 ubiquitin ligase for which information is still scarce. Here we provide a bacterial expression protocol that yields as much as 3.1 mg/L full-length NRDP1 for *in vitro* studies. Further, we present evidence for a direct interaction of NRDP1 with the energy sensor and regulator AMPK. This interaction involves the C-terminal domain of NRDP1 (amino acids 136 to 317) and the N-terminal tail of AMPK β-subunits (amino acids 1 to 54). Complex formation increases NRDP1 turnover, independent of low-level phosphorylation by AMPK, but *vice versa* does not induce specific ubiquitination of AMPK by NRDP1.

In the first part of this study, we describe highly efficient conditions for bacterial expression and purification of full-length NRDP1. So far, bacterial production of this protein was hampered by predominant formation of insoluble protein in bacterial inclusion bodies (Wu et al., 2004). Only a C-terminally truncated version (amino acids 135 to 317 aa) could be prepared at a satisfying yield (Qiu and Goldberg, 2002). In *E.coli*, host protein misfolding is not uncommon. It may result from premature termination of translation, failure of a newly synthesized chain to reach a correct conformation or loss of structural integrity triggered by environmental stress (Baneyx and Mujacic, 2004). Attempts to correlate the probability of inclusion body formation with particular properties of the recombinant protein, the expression system, or the host cell have for the most part been unsuccessful (Schein, 1990). It seems that overproduction by itself is sufficient to induce formation of inclusion bodies of cytosolic proteins (Gribskov and Burgess, 1983). Based on this finding a kinetic model was proposed that shows that the yield of native protein depends only on the rate of folding, the rate of aggregation, and the rate of protein synthesis (Kiefhaber et al., 1991). This model implies that the yield of native protein increases with a decreasing rate of protein expression. Thus, reducing growth rate by slowing down metabolism increases yield of native, soluble protein (Cabilly, 1989; Kopetzki et al., 1989; Schein, 1990). In our batch culture experiments, a decreased in expression temperature from 30°C to 10°C had the most pronounced effect, leading to a 6-fold higher yield of soluble full-length NRDP1. Induction at a later growth phase also slightly increased yield, but mainly had a positive effect by reducing co-purifying low molecular mass contaminants. This may be also due to more growth-limiting conditions (nutrient deprivation, acidification etc.). Up-scaling batch cultures to a bioreactor further

increased yield by at least 4-fold. Apparently, controlled bioreactor conditions provide all the benefits of slowing down metabolism by growth at 16°C, while avoiding potential disadvantages of batch cultures by keeping all growth conditions constant. Efficiency and reproducibility of a bioreactor culture thus allows maximum yield for a given volume of medium, particularly important in case of an expensive additions (e.g. carbon-14 labeled medium).

In the second part of the study, we concentrated on the interaction of NRDP1 with AMPK that we have detected and confirmed by Y2H analysis. In an attempt to identify a functional role of this interaction, we primarily analyzed phosphorylation and ubiquitination events. Although NRDP1 can be phosphorylated by AMPK *in vitro*, it appeared to be a poorer substrate as compared to the AMPK reference substrate ACC, seen by both kinetic and stoichiometric measurements. Mass spectrometry (MS) did neither reveal any phosphorylated residue. The *in vivo* significance of NDRP1 phosphorylation remains to be clarified.

Vice versa, in HEK293 cells, AMPK was not specifically ubiquinated by NRDP1, although it is known that AMPK can be ubiquitinated *in vivo* (Zungu et al., 2011) and some involved E3 ubiquitin ligase have been identified (e.g. WWP1 and malin) (Lee et al., 2013; Moreno et al., 2010). However, NRDP1 is also heavily autoubiquitinated, resulting in proteasomal degradation and concomitant high turnover rate (Wu et al., 2004) which are the key regulators of cellular activity of this protein. Our data with HeLa cells suggest that NRDP1/AMPK interaction accelerates proteasomal NRDP1 degradation. First, I*n vivo* AMPK overexpression reduces levels of full-length NRDP1 while increasing levels of a shorter NRDP1 species, probably a first product of NRDP1 degradation. Second, such reduced NRDP1 levels do not occur when proteasomal protein degradation is inhibited. AMPK-dependent proteasomol NRDP1 degradation does not involve putative NRDP1 phosphorylation, since it occurs also with inactive AMPK. A similar regulation has been reported for other E3 ubiquitin ligases. Auto-ubiquitination and proteasomal degradation of certain inhibitor of apoptosis (IAP) is stimulated by interaction with SMAC/DIABLO (Dueber et al., 2011; Varfolomeev et al., 2007). The role of AMPK in NRDP1 autoubiquitination may involve activating conformational changes, a NRDP1 scaffolding function (bringing different NRDP1 proteins close to each other), or disrupting interaction of NRDP1 with ubiquitin carboxyl-terminal hydrolase 8 (USP8), a major stabilizing NRDP1 protein (Avvakumov et al., 2006).

One consequence of AMPK-dependent NRDP1 degradation would be increased levels of known NRDP1 substrates like ErbB3. ErbB3 is the first effector of the ErbB3-PI3K-Akt-TSC2-mTOR cascade, whose activation leads to cell survival, proliferation and differentiation, but also higher susceptibility for certain types of cancer (Gwinn et al., 2008; Inoki et al., 2003). Thus, formation of AMPK/NRDP1 complexes would activate ErbB3 signaling and proliferation which could be in contradiction with the well-described AMPK tumor suppressor effect, but since few years it clearly appear that AMPK also play a role in helping tumor cell survival (Banko et al., 2011; Frigo et al., 2011; Laderoute et al., 2006).

This work establishes a link between AMPK and NRDP1. However, more research is needed to fully clarify its functional significance.

References

Abdullah, J.M., Li, X., Nachtman, R.G., and Jurecic, R. (2001). FLRF, a novel evolutionarily conserved RING finger gene, is differentially expressed in mouse fetal and adult hematopoietic stem cells and progenitors. Blood Cells. Mol. Dis. *27*, 320–333.

Ardley, H.C., and Robinson, P.A. (2005). E3 ubiquitin ligases. Essays Biochem. *41*, 15–30.

Avvakumov, G.V., Walker, J.R., Xue, S., Finerty, P.J., Jr, Mackenzie, F., Newman, E.M., and Dhe-Paganon, S. (2006). Amino-terminal dimerization, NRDP1-rhodanese interaction, and inhibited catalytic domain conformation of the ubiquitin-specific protease 8 (USP8). J. Biol. Chem. *281*, 38061–38070.

Baneyx, F., and Mujacic, M. (2004). Recombinant protein folding and misfolding in Escherichia coli. Nat. Biotechnol. *22*, 1399–1408.

Banko, M.R., Allen, J.J., Schaffer, B.E., Wilker, E.W., Tsou, P., White, J.L., Villén, J., Wang, B., Kim, S.R., Sakamoto, K., et al. (2011). Chemical genetic screen for AMPKα2 substrates uncovers a network of proteins involved in mitosis. Mol. Cell *44*, 878–892.

Bartke, T., Pohl, C., Pyrowolakis, G., and Jentsch, S. (2004). Dual role of BRUCE as an antiapoptotic IAP and a chimeric E2/E3 ubiquitin ligase. Mol. Cell *14*, 801–811.

Bedford, L., Paine, S., Rezvani, N., Mee, M., Lowe, J., and Mayer, R.J. (2009). The UPS and autophagy in chronic neurodegenerative disease: six of one and half a dozen of the other--or not? Autophagy *5*, 224–227.

Berger, M.S., Locher, G.W., Saurer, S., Gullick, W.J., Waterfield, M.D., Groner, B., and Hynes, N.E. (1988). Correlation of c-erbB-2 gene amplification and protein expression in human breast carcinoma with nodal status and nuclear grading. Cancer Res. *48*, 1238–1243.

Bouyain, S., and Leahy, D.J. (2007). Structure-based mutagenesis of the substrate-recognition domain of Nrdp1/FLRF identifies the binding site for the receptor tyrosine kinase ErbB3. Protein Sci. Publ. Protein Soc. *16*, 654–661.

Bradford, M.M. (1976). A rapid and sensitive method for the quantitation of microgram quantities of protein utilizing the principle of protein-dye binding. Anal. Biochem. *72*, 248–254.

Cabilly, S. (1989). Growth at sub-optimal temperatures allows the production of functional, antigen-binding Fab fragments in Escherichia coli. Gene *85*, 553–557.

De Ceuninck, L., Wauman, J., Masschaele, D., Peelman, F., and Tavernier, J. (2013). Reciprocal cross-regulation between RNF41 and USP8 controls cytokine receptor sorting and processing. J. Cell Sci. *126*, 3770–3781.

Chau, V., Tobias, J.W., Bachmair, A., Marriott, D., Ecker, D.J., Gonda, D.K., and Varshavsky, A. (1989). A multiubiquitin chain is confined to specific lysine in a targeted short-lived protein. Science *243*, 1576–1583.

Dammer, E.B., Na, C.H., Xu, P., Seyfried, N.T., Duong, D.M., Cheng, D., Gearing, M., Rees, H., Lah, J.J., Levey, A.I., et al. (2011). Polyubiquitin linkage profiles in three models of proteolytic stress suggest the etiology of Alzheimer disease. J. Biol. Chem. *286*, 10457–10465.

Diamonti, A.J., Guy, P.M., Ivanof, C., Wong, K., Sweeney, C., and Carraway, K.L., 3rd (2002). An RBCC protein implicated in maintenance of steady-state neuregulin receptor levels. Proc. Natl. Acad. Sci. U. S. A. *99*, 2866–2871.

Dikic, I., Wakatsuki, S., and Walters, K.J. (2009). Ubiquitin-binding domains — from structures to functions. Nat. Rev. Mol. Cell Biol. *10*, 659–671.

Dueber, E.C., Schoeffler, A.J., Lingel, A., Elliott, J.M., Fedorova, A.V., Giannetti, A.M., Zobel, K., Maurer, B., Varfolomeev, E., Wu, P., et al. (2011). Antagonists induce a conformational change in cIAP1 that promotes autoubiquitination. Science *334*, 376–380.

Frigo, D.E., Howe, M.K., Wittmann, B.M., Brunner, A.M., Cushman, I., Wang, Q., Brown, M., Means, A.R., and McDonnell, D.P. (2011). CaM kinase kinase beta-mediated activation of the growth regulatory kinase AMPK is required for androgen-dependent migration of prostate cancer cells. Cancer Res. *71*, 528–537.

Gribskov, M., and Burgess, R.R. (1983). Overexpression and purification of the sigma subunit of Escherichia coli RNA polymerase. Gene *26*, 109–118.

Gullick, W.J. (1996). The c-erbB3/HER3 receptor in human cancer. Cancer Surv. *27*, 339–349.

Gwinn, D.M., Shackelford, D.B., Egan, D.F., Mihaylova, M.M., Mery, A., Vasquez, D.S., Turk, B.E., and Shaw, R.J. (2008). AMPK phosphorylation of raptor mediates a metabolic checkpoint. Mol. Cell *30*, 214–226.

Hardie, D.G., and Carling, D. (1997). The AMP-activated protein kinase--fuel gauge of the mammalian cell? Eur. J. Biochem. FEBS *246*, 259–273.

Hershko, A., and Ciechanover, A. (1992). The ubiquitin system for protein degradation. Annu. Rev. Biochem. *61*, 761–807.

Hershko, A., and Ciechanover, A. (1998). The ubiquitin system. Annu. Rev. Biochem. *67*, 425–479.

Husnjak, K., and Dikic, I. (2012). Ubiquitin-binding proteins: decoders of ubiquitin-mediated cellular functions. Annu. Rev. Biochem. *81*, 291–322.

Hynes, N.E. (2007). Targeting ERBB receptors in cancer. Recent Results Cancer Res. Fortschritte Krebsforsch. Progrès Dans Rech. Sur Cancer *172*, 45–57.

Inoki, K., Zhu, T., and Guan, K.-L. (2003). TSC2 mediates cellular energy response to control cell growth and survival. Cell *115*, 577–590.

Johnsson, N., and Varshavsky, A. (1994). Split ubiquitin as a sensor of protein interactions in vivo. Proc. Natl. Acad. Sci. U. S. A. *91*, 10340–10344.

Kalender, A., Selvaraj, A., Kim, S.Y., Gulati, P., Brûlé, S., Viollet, B., Kemp, B.E., Bardeesy, N., Dennis, P., Schlager, J.J., et al. (2010). Metformin, independent of AMPK, inhibits mTORC1 in a rag GTPase-dependent manner. Cell Metab. *11*, 390–401.

Kim, H.T., Kim, K.P., Lledias, F., Kisselev, A.F., Scaglione, K.M., Skowyra, D., Gygi, S.P., and Goldberg, A.L. (2007). Certain pairs of ubiquitin-conjugating enzymes (E2s) and ubiquitin-protein ligases (E3s) synthesize nondegradable forked ubiquitin chains containing all possible isopeptide linkages. J. Biol. Chem. *282*, 17375–17386.

Kirkpatrick, D.S., Hathaway, N.A., Hanna, J., Elsasser, S., Rush, J., Finley, D., King, R.W., and Gygi, S.P. (2006). Quantitative analysis of in vitro ubiquitinated cyclin B1 reveals complex chain topology. Nat. Cell Biol. *8*, 700–710.

Kopetzki, E., Schumacher, G., and Buckel, P. (1989). Control of formation of active soluble or inactive insoluble baker's yeast alpha-glucosidase PI in Escherichia coli by induction and growth conditions. Mol. Gen. Genet. MGG *216*, 149–155.

Laderoute, K.R., Amin, K., Calaoagan, J.M., Knapp, M., Le, T., Orduna, J., Foretz, M., and Viollet, B. (2006). 5'-AMP-activated protein kinase (AMPK) is induced by low-oxygen and glucose deprivation conditions found in solid-tumor microenvironments. Mol. Cell. Biol. *26*, 5336–5347.

Lee, J.O., Lee, S.K., Kim, N., Kim, J.H., You, G.Y., Moon, J.W., Jie, S., Kim, S.J., Lee, Y.W., Kang, H.J., et al. (2013). E3 ubiquitin ligase, WWP1, interacts with AMPKα2 and down-regulates its expression in skeletal muscle C2C12 cells. J. Biol. Chem. *288*, 4673–4680.

Mo, X., Liu, D., Li, W., Hu, Z., Hu, Y., Li, J., Guo, J., Tang, B., Zhang, Z., Bai, Y., et al. (2010). Genetic screening for mutations in the Nrdp1 gene in Parkinson disease patients in a Chinese population. Parkinsonism Relat. Disord. *16*, 222–224.

Möckli, N., Deplazes, A., Hassa, P.O., Zhang, Z., Peter, M., Hottiger, M.O., Stagljar, I., and Auerbach, D. (2007). Yeast split-ubiquitin-based cytosolic screening system to detect interactions between transcriptionally active proteins. BioTechniques *42*, 725–730.

Moreno, D., Towler, M.C., Hardie, D.G., Knecht, E., and Sanz, P. (2010). The laforin-malin complex, involved in Lafora disease, promotes the incorporation of K63-linked ubiquitin chains into AMP-activated protein kinase beta subunits. Mol. Biol. Cell *21*, 2578–2588.

Ozkaynak, E., Finley, D., Solomon, M.J., and Varshavsky, A. (1987). The yeast ubiquitin genes: a family of natural gene fusions. EMBO J. *6*, 1429–1439.

Press, M.F., and Lenz, H.-J. (2007). EGFR, HER2 and VEGF pathways: validated targets for cancer treatment. Drugs *67*, 2045–2075.

Qiu, X.-B., and Goldberg, A.L. (2002). Nrdp1/FLRF is a ubiquitin ligase promoting ubiquitination and degradation of the epidermal growth factor receptor family member, ErbB3. Proc. Natl. Acad. Sci. U. S. A. *99*, 14843–14848.

Qiu, X.-B., Markant, S.L., Yuan, J., and Goldberg, A.L. (2004). Nrdp1-mediated degradation of the gigantic IAP, BRUCE, is a novel pathway for triggering apoptosis. EMBO J. *23*, 800–810.

Saeki, Y., Kudo, T., Sone, T., Kikuchi, Y., Yokosawa, H., Toh-e, A., and Tanaka, K. (2009). Lysine 63-linked polyubiquitin chain may serve as a targeting signal for the 26S proteasome. EMBO J. *28*, 359–371.

Schein, C.H. (1990). Solubility as a function of protein structure and solvent components. Biotechnol. Nat. Publ. Co. *8*, 308–317.

Sharma, S.V., and Settleman, J. (2009). ErbBs in lung cancer. Exp. Cell Res. *315*, 557–571.

Stagljar, I., Korostensky, C., Johnsson, N., and te Heesen, S. (1998). A genetic system based on split-ubiquitin for the analysis of interactions between membrane proteins in vivo. Proc. Natl. Acad. Sci. U. S. A. *95*, 5187–5192.

Sweeney, C., and Carraway, K.L., 3rd (2004). Negative regulation of ErbB family receptor tyrosine kinases. Br. J. Cancer *90*, 289–293.

Tafelmeyer, P., Johnsson, N., and Johnsson, K. (2004). Transforming a (beta/alpha)8--barrel enzyme into a split-protein sensor through directed evolution. Chem. Biol. *11*, 681–689.

Varfolomeev, E., Blankenship, J.W., Wayson, S.M., Fedorova, A.V., Kayagaki, N., Garg, P., Zobel, K., Dynek, J.N., Elliott, L.O., Wallweber, H.J.A., et al. (2007). IAP antagonists induce autoubiquitination of c-IAPs, NF-kappaB activation, and TNFalpha-dependent apoptosis. Cell *131*, 669–681.

Weissman, A.M. (2013). Ubiquitin and Drug Discovery: Challenges and Opportunities. Cell Biochem. Biophys.

Winder, W.W., and Hardie, D.G. (1999). AMP-activated protein kinase, a metabolic master switch: possible roles in type 2 diabetes. Am. J. Physiol. *277*, E1–10.

Wu, X., Yen, L., Irwin, L., Sweeney, C., and Carraway, K.L., 3rd (2004). Stabilization of the E3 ubiquitin ligase Nrdp1 by the deubiquitinating enzyme USP8. Mol. Cell. Biol. *24*, 7748–7757.

Yen, L., Cao, Z., Wu, X., Ingalla, E.R.Q., Baron, C., Young, L.J.T., Gregg, J.P., Cardiff, R.D., Borowsky, A.D., Sweeney, C., et al. (2006). Loss of Nrdp1 enhances ErbB2/ErbB3-dependent breast tumor cell growth. Cancer Res. *66*, 11279–11286.

Yu, F., and Zhou, J. (2008). Parkin is ubiquitinated by Nrdp1 and abrogates Nrdp1-induced oxidative stress. Neurosci. Lett. *440*, 4–8.

Zhong, L., Tan, Y., Zhou, A., Yu, Q., and Zhou, J. (2005). RING finger ubiquitin-protein isopeptide ligase Nrdp1/FLRF regulates parkin stability and activity. J. Biol. Chem. *280*, 9425–9430.

PART 6

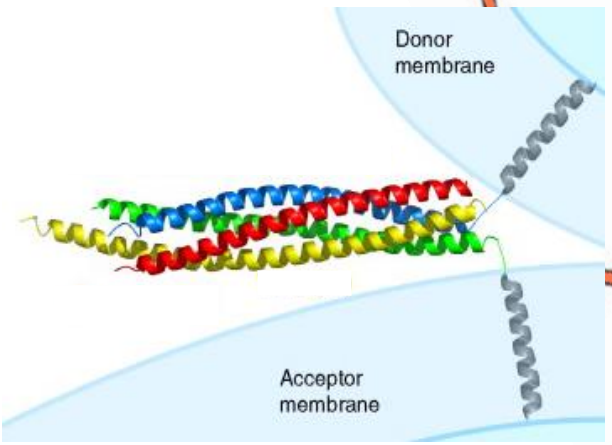

AMPK interacts with vesicle-associated proteins VAMP2 and VAMP3 – a role in exocytosis?

Abstract. AMP-activated protein kinase (AMPK) and the vesicle-associated membrane proteins VAMP2 and VAMP3 are involved in exocytotic translocation of e.g. nutrient transporters GLUT4 and CD36 to the cell surface to increase glucose and fatty acid uptake, respectively. The exact molecular mechanism is still unclear. We found that VAMP2 and VAMP3 both interact with AMPK by using yeast two hybrid (Y2H) approaches, co-immunoprecipitation, pull-down and surface plasmon resonance (SPR). VAMP does not serve as AMPK substrate, but could be a scaffold for AMPK to recruit it to exocytotic vesicles. In support of this, we show direct AMPK/VAMP interaction of medium affinity as typical for reversible interactions, and the presence of putative AMPK substrates in exocytotic vesicles. The mapped AMPK and VAMP3 interaction domains enabled the generation of an inhibitory construct. This construct is able to decrease AMPK-VAMP interaction *in vitro* and will be suitable for *in vivo* applications, in particular to study effects on the translocation of GLUT4 and CD36.

Résumé. La protéine kinase activée par l'AMP (AMPK) ainsi que les protéines membranaires associées aux vésicules VAMP2 et VAMP3 sont impliquées dans l'exocytose et la translocation des transporteurs de nutriments à la surface cellulaire, tels GLUT4 et CD36 qui permettent respectivement l'entrée de glucose et d'acides gras dans la cellule. Le mécanisme moléculaire reste pour le moment indéfini. Par un système de double hybride en levures nous avons découvert que VAMP2 et VAMP3 interagissent avec l'AMPK, résultats confirmés également par co-immunoprécipitation, pull-down et résonance plasmon de surface. VAMP n'est pas un substrat de l'AMPK, mais pourrait être une protéine de recrutement (scaffold) d'AMPK vers les vésicules exocytotiques. Allant dans ce sens, nous avons montré qu'AMPK et VAMP interagissent de façon directe avec une affinité moyenne, typique des interactions réversibles. Nous avons aussi montré la présence de substrats putatifs de l'AMPK dans des vésicules exocytotiques. La détermination du domaine d'interaction entre AMPK et VAMP3 a permis la production d'une construction inhibant leur interaction. Cette construction est capable de diminuer l'interaction AMPK-VAMP *in vitro* et adaptée pour des expériences *in vivo*, en particulier pour étudier son effet sur la translocation de GLUT4 et CD36.

I was involved in all experiments following the yeast-two hybrid and VAMP phosphorylation assays data analysis and manuscript writing.

Introduction

Vesicular transport mediates a continuous exchange of components between membrane enclosed distinct compartments. Since cells segregate proteins into separate membrane domains by assembling a special protein coat (which is a cage of protein covering the cytosolic face, (Kirchhausen, 2000)), a transport mechanism is necessary that extracts specific components from a compartment for delivery to another one. Transport vesicles will dock to the target membrane and fuse with it to deliver their cargo (Bonifacino and Glick, 2004). These vesicles are classified according to their origin and type of cargo (Rothman and Wieland, 1996). Vesicle-stored cargo could be a chemical element as neurotransmitter (synaptic vesicle), hormone (endocrine tissue), but also receptors or transporters present at the vesicular membrane which will incorporate into the target membrane during membrane fusion.

To ensure an orderly flow of vesicular traffic, transport vesicles must be highly selective in recognizing the correct target membrane to fuse with. A vesicle is likely to encounter many potential target membranes because of the large diversity of membrane systems. To select the correct one, all transport vesicles display surface markers ensuring targeting specificity (Pfeffer, 1999). Target membranes display the complementary receptors that recognize the appropriate vesicle markers. However the precise mechanism for the specificity of this crucial process is still not entirely clear; it depends on two major types of proteins: Rab proteins that direct the vesicle towards the correct target membrane for a preliminary docking (Grosshans et al., 2006), and the soluble NSF attachment receptor (SNARE) proteins that catalyze the fusion of the lipid bilayers (Jahn and Scheller, 2006), (*Figure 1*).

Rab proteins are the largest subfamily of monomeric GTPases with over 60 known members (Grosshans et al., 2006). Each Rab protein is associated with one or more membrane enclosed organelles, and each one of these organelles has at least one Rab protein on its cytosolic surface. Thus Rab proteins are ideal molecular markers for identifying membrane types and guiding vesicular traffic between them. Finally, Rab proteins bind to proteins called Rab effectors, which facilitate vesicle transport, membrane tethering, and fusion (Mizuno-Yamasaki et al., 2012; Pfeffer, 2012).

SNARE proteins are transmembrane protein that catalyze the membrane fusion reactions in vesicular transport (Jahn and Scheller, 2006). Once a transport vesicle has been tethered to its target membrane, complementary sets of v-SNAREs and t-SNAREs, respectively found on vesicle membrane and target membranes (McNew et al., 2000), will be able to form complexes (Sutton et al., 1998). The resulting SNARE complexes lock the two membranes together and mediate membrane fusion by bringing the lipid bilayers of two membranes close enough so that they can join (Fasshauer, 2003). SNAREs also provide an additional layer of specificity, helping to ensure that only correctly targeted vesicles fuse (Scales et al., 2000).

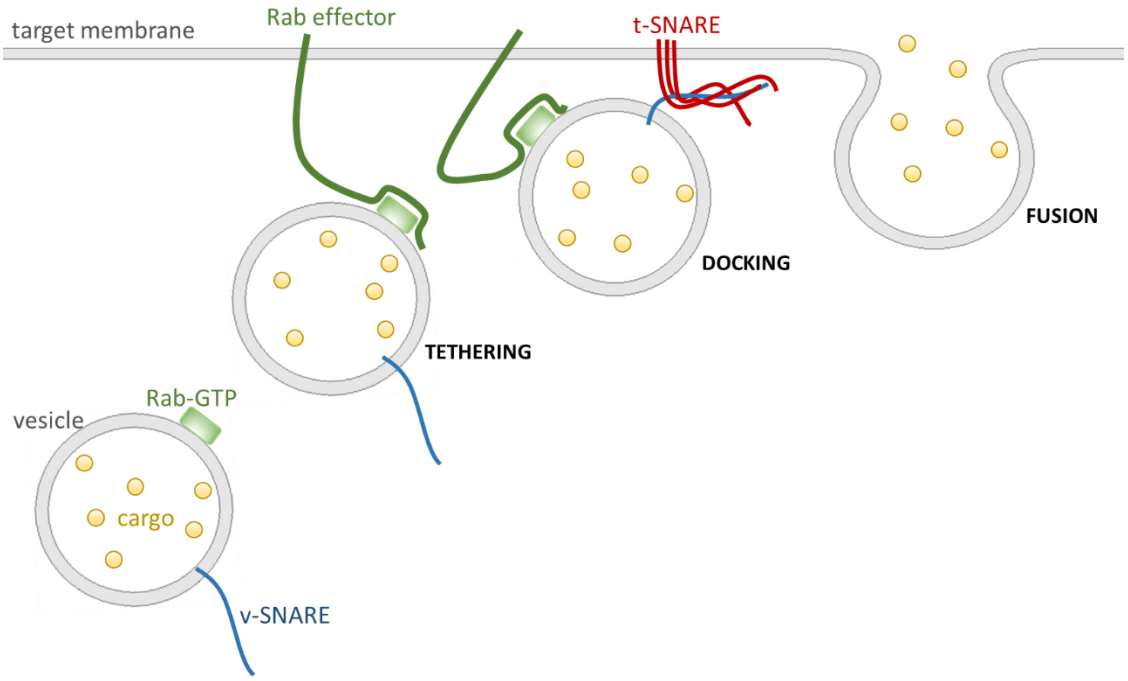

Figure 1. **Process preceding membrane fusion.** Tethering: Rab effector proteins tether a vesicle via interaction with active Rab protein (Rab-GTP) located on the vesicle membrane. Docking: the v-SNARE and t-SNARE assemble into a four-helix bundle forming a trans-SNARE complex. Fusion: Formation of multiple trans-SNARE complexes between vesicle and target membrane catalyzes the fusion of the two apposed lipid bilayers.

Fusion does not always immediately follow v-SNARE- t-SNAREs pairing. In fact, to allow for additional regulation, fusion is delayed until e.g. secretion of cargo is triggered by a specific intra- or extracellular signal (Varlamov et al., 2004). These will cause the release of inhibitory proteins that prevent the complete zipping-up of the SNARE complexes. Rab proteins and Rab-effectors are involved in the release of such SNARE inhibitory proteins (Pfeffer, 1999).

The vesicle-associated membrane proteins VAMP2 (or synaptobrevin) and its closest homolog VAMP3 (or cellubrevin) are two major members of the v-SNARE family. They are both involved in many exocytotic processes as e.g. neurotransmitter release from synaptic vesicles in neuron synapses (Mochida, 2000; Procino et al., 2008; Sai et al., 2013), or cell surface expression of nutrient transporters such as glucose transporter GLUT4 and long chain fatty acid (LCFA) transporter CD36. The latter occurs by translocation of storage vesicles from intracellular stores to the plasma membrane, followed by membrane fusion that inserts the transporters into the cell membrane (Holman and Cushman, 1994; Karylowski et al., 2004; Martin et al., 1998; Schwenk et al., 2010). This is the rate-limiting step for cellular uptake of glucose and fatty acids, the predominant substrates for cellular energy conversion into ATP. Fusion of GLUT4 storage vesicles (GSVs) with the plasma membrane to trigger glucose uptake can occur insulin-dependent, e.g. under hyperglycemic conditions (Lizunov et al., 2005) in different peripheral organs, or insulin-independent, e.g. after physical exercise in muscle (Hayashi et al., 1997).

The AMP-activated protein kinase (AMPK) is a key sensor and regulator of cellular energy homeostasis (Hardie and Carling, 1997). AMPK is activated to maintain cellular ATP level, increasing ATP-producing pathways while decreasing ATP-consuming pathways (Carling, 2005; Hardie et al., 2006). Thus it is strongly implicated in transformation of the two major cellular sources of free energy, carbohydrates and fatty acids. Among many others, it regulates the cellular uptake of these nutriments. AMPK is implicated in exercise-induced GLUT4 and CD36 translocation to the plasma membrane (Kurth-Kraczek et al., 1999; Luiken et al., 2003; Webster et al., 2010). However the exact mechanism of how AMPK regulates GLUT4/CD36 translocation is not entirely clear.

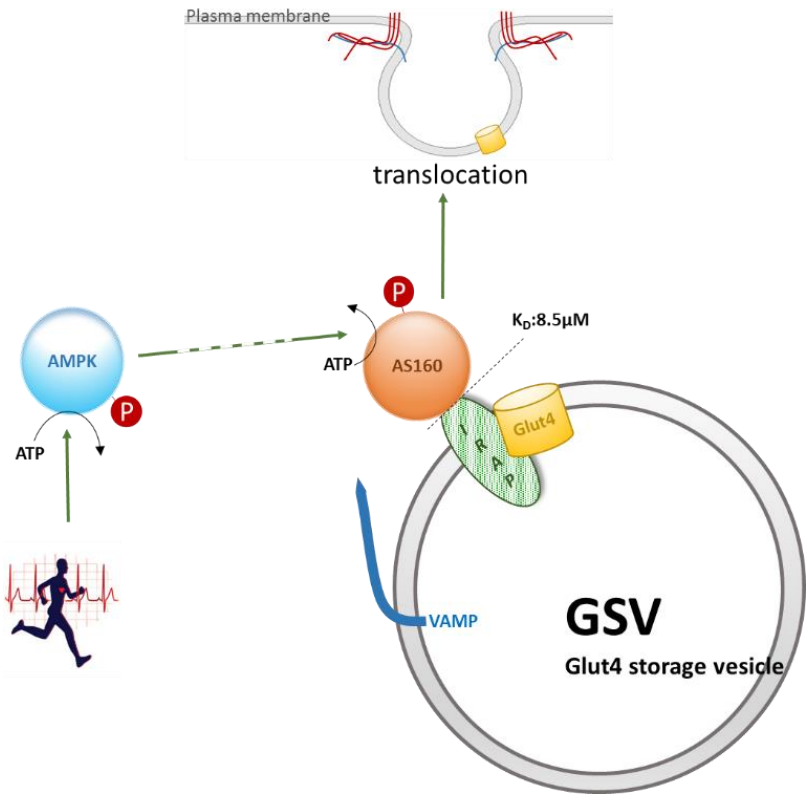

Figure 2. **Regulation of glucose uptake by AMP-activated protein kinase (AMPK).** Exercise activates AMPK by a multiple pathways. Activated AMPK causes direct or indirect phosphorylation of the Akt substrate AS160 (Geraghty et al., 2007; Treebak et al., 2006). AS160 interacts with IRAP (insulin-regulated aminopeptidase) (Park et al., 2012; Peck et al., 2006), a marker of Glut4 storage vesicles (GSV), which interacts itself directly with glucose transporter 4 (GLUT4) (Martin et al., 1997; Ross et al., 1996). Phosphorylation of AS160 triggers translocation of GSV to the plasma membrane, leading to incorporation of GLUT4 into the latter and increased glucose uptake.

Both insulin-dependent and -independent pathways of GLUT4 translocation seem to involve Akt substrate of 160 kDa (AS160) (Cartee and Wojtaszewski, 2007; Sakamoto and Holman, 2008; Zaid et al., 2008). This downstream effector protein is anchored to the GSV via cargo proteins like insulin-regulated amino peptidase (IRAP) (Larance et al., 2005), (*Figure 2*). AS160 is a Rab GTPase-activating protein (RabGAP) that keeps the corresponding Rab in an inactive, GDP bound state (Mîinea et al., 2005). In response to insulin, AS160 is phosphorylated at Thr642 and other sites by protein kinase B/Akt (Baus et al., 2008; Kane et al., 2002). This leads to binding of AS160 to inhibitory 14-3-3 protein that relieves AS160 inhibition of Rab, thus triggering Rab-mediated GSV translocation and docking to the plasma membrane, where VAMP proteins initiate membrane fusion process (Sano et al., 2003). VAMP2 was identified in GSV membranes already in 1992 (Cain et al., 1992), later also VAMP3 and VAMP5 were implicated in translocation of GLUT4 and CD36 (Schwenk et al., 2010). The exocytotic process

thus finally leads to cell surface localization of GLUT4, CD36, IRAP and other cargo membrane proteins (Martin et al., 1997; Ross et al., 1996). More recently, AS160 was found phosphorylated by several protein kinases other than Akt. It has been suggested as a downstream effector of AMPK in response to exercise/contractile activity. The pharmacological AMPK-activator AICAR increases AS160 phosphorylation and contraction-mediated AS160 phosphorylation is impaired in α_2-AMPK knock-out (KO) and knock-down mice (Treebak et al., 2006). During post-exercise recovery in vivo, increased muscle AMPKα2 activity correlates with AS160 phosphorylation state and muscle glucose uptake (Dreyer et al., 2008). Consistent with this, AS160 has been shown to be phosphorylated by AMPK *in vitro* at Ser570 and Ser588 (Geraghty et al., 2007). Even though less is known for CD36 trafficking, there seems to be much similarity to GLUT4, suggesting a very similar mechanism (Schwenk et al., 2010).

In the present study, we describe an interaction between AMPK and VAMP2 and -3 that we originally discovered in a yeast-two-hybrid (Y2H) screen for interacting proteins of the AMPK β-subunit and that we confirmed by co-immunoprecipitation, pull-down and surface plasmon resonance (SPR) with full-length AMPK complexes. We show that interaction does not involve VAMP phosphorylation by AMPK, but that VAMP may rather serve as a scaffold to recruit AMPK to exocytotic vesicles e.g. involved in cell surface expression of nutrient transporters like CD36 or GLUT4. In support of this, we show direct AMPK/VAMP interaction of medium affinity as typical for reversible interactions, and the presence of putative AMPK substrates in exocytotic vesicles. Finally, we map the involved interaction domains and present data on an inhibitory construct that is able to decrease AMPK-VAMP interaction *in vitro*.

Materials & Methods

Yeast-two-hybrid assay: Cyto-Y2H

Cytosolic yeast-two-hybrid (Y2H) systems based on reconstitution of split proteins have been used for protein interaction screening. The cytoY2H (Möckli et al., 2007) (Dualsystems Biotech, Schlieren, Switzerland) is based on the split ubiquitin system (Johnsson and Varshavsky, 1994; Stagljar et al., 1998). The membrane-anchored bait is fused to a reporter cassette composed of the C-terminal half of ubiquitin half and the artificial transcription factor LexA-VP16 whereas the prey is fused to the N-terminal half of ubiquitin. Bait/prey interaction leads to ubiquitin reconstitution and cleavage by ubiquitin-specific protease that liberate the transcription factor thus leading to a classical transcriptional read-out. While the original system used an ER-membrane anchor (Ost4P) for the bait, we applied here a version that uses a plasma membrane anchor (Aβ-domain). Cloning procedures using Sfi1 sites, transformation of yeast cell line NMY51 (MATa his3delta200 trp1-901 leu2-3,112 ade2 lys2: (lexAop)4-HIS3 ura3: (lexAop)8-ADE2 GAL4) with the lithium acetate method (Gietz and Woods, 2006) and yeast spotting were performed as described earlier (Möckli et al., 2007). Different dilutions (1, 1/10, 1/100, 1/1000) of overnight yeast cultures were spotted on selective medium lacking tryptophan and leucine (SD-WL) for growth verification and on medium lacking tryptophan, leucine, adenine, and histidine (SD-AHWL) for protein interaction analysis. In some cases up to 5 mM 3 Amino-triazole (3-AT; Applichem, Darmstadt, Germany) was added to increase selection stringency (see also Y2H cDNA library screening procedures). The spotted plates were incubated 48-72 h at 30°C.

The Cyto-Y2H was used to screen a human brain cDNA library (preys) for interactors of the N-terminal domain of AMPK- β1 and - β2 subunits (Δβ1, Δβ2; amino acids 1-54 as baits). This domain was chosen to avoid interactions with other AMPK subunits, and because it has been suggested as a putative AMPK interaction domain. A 3-AT concentration of 2.5 mM was determined by a pilot screen testing autoactivation by using empty library vector. About 6.2 × 106 and 3.4 × 106 clones were screened. Plasmids containing the cDNA sequence of putative interaction partners were extracted and reintroduced together with the corresponding Δβ -encoding bait vector into the reporter yeast strain in order to confirm the interaction. Reproducible interactors were sequenced and clones containing in-frame coding sequence

and not known as false positives (Dualsystems, personal communication) were retained. To verify VAMP2,3/AMPK interactions, paired Y2H assays were performed using Δβ1 and Δβ2, full-length β1 and Δβ, as well as α1 and α2 subunits as baits and VAMP2,3 as a prey. Interaction with an unrelated bait, Large T antigen (Simian virus), was used as negative control.

Yeast-two-hybrid assay: Split-Trp-Y2H

The Split-Trp Y2H is based on the split-protein sensor Trp1p (Tafelmeyer et al., 2004). A C-terminal part of Trp1p (CTrp) is fused to bait subunits and an N-terminal part of Trp1p (NTrp) is fused to prey. Upon interaction of bait and prey, active Trp1p is reconstituted from both domains, thus allowing growth of yeast strain CRY1 (MATa ura3-1 trp1-1 his3-11,15 leu2-3,112 ade2-1 can1-100 GAL) on medium lacking tryptophan. CRY1 transformation and spotting were similar as above. Selective media either lacked uracil and leucine (SD-UL, controls) or additionally tryptophan (SD-UWL, protein interaction analysis). Spotted plates were incubated up to 9 days at 27°C.

Expression and purification of GST-fusion protein

All the GST fusions protein constructs were transformed into competent *E. coli* BL21-Codon Plus (DE3)-RIL cells (Stratagene, La Jolla, CA, USA) and incubated overnight on LB agar containing 100 µg/ml ampicillin and 30 µg/ml chloramphenicol. Cultures were routinely grown in standard LB medium containing antibiotics (100 µg/ml ampicillin and 30 µg/ml chloramphenicol) at 37°C in Erlenmeyer flasks with constant shaking until O.D. (600nm) 0.7-0.9 (if not indicated otherwise). Cells were then cooled down to 30°C and protein expression was induced for 4 hours (if not indicated otherwise) with 2mM isopropyl β-D-thiogalactopyranoside (IPTG, Eurobio). Cells were harvested by centrifugation at 4000 g, 30 min at 4°C, harvest and suspended in lysis buffer: PBS (phosphate buffer saline: 137 mM NaCl, 2.7 mM KCl, 10 mM Na_2HPO_4, 2 mM KH_2PO_4, pH7.4). After 3x15s sonication at 85% of manual powered, insoluble material was removed by centrifugation (40000 g, 40 min at 4°C). All supernatant was applied by gravity flow to a 5ml Gluthation Sepharose matrix (binding up to 1 g/mL) (Qiagen, Hilden, Germany) self-packed in a column (diameter 1cm). The column was

washed with 3x5 column volumes of PBS and proteins were eluted with 10 ml of 10 mM L-glutathione reduced (Sigma-Aldrich) in 50mM Tris-HCl, pH 8. Ten µl of each elution fraction were mixed with Laemli sample buffer, separated by SDS-polyacrylamide gel electrophoresis (SDS-PAGE, 12% acrylamide), and stained with Coomassie. Protein concentrations were determined according to Bradford (Bradford, 1976) with the Biorad microassay (Biorad, Reinach, Switzerland) and BSA as standard.

Preparation of synaptic vesicles

Synaptic vesicles were obtained from Wistar rat forebrains by differential centrifugation and a density gradient procedure (Whittaker et al., 1964). Rat forebrains were homogenized in sucrose buffer (0.32 M sucrose, 4 mM HEPES pH 7.4) and separated into fraction P1 (nuclei, large myelin fragments, tissue debris), P2 (mitochondria, synaptosomes, small myelin fragments, some microsomes) and S2 (microsomes, some small mitochondria and synaptosomes, and soluble proteins). The synaptosomal fraction (P2) was washed two times with sucrose buffer and re-suspended in water (2 ml/mg tissue) to disrupt synaptosomal membranes and liberate synaptic vesicles. Synaptic vesicles were then purified on a discontinuous sucrose density gradient composed of 20 mL 0.6 M sucrose, 5 mL 0.4 M sucrose and 5 mL sample. After centrifugation for 2 h at 53500 g (4°C), vesicles were located in the 0.4 M sucrose phase. Enrichment of synaptic vesicles was verified by immunoblotting using anti-VAMP2 antibody (1:3000, Pierce Biotechnology, Rockford, IL, USA). All protein concentrations of biological samples were determined using the BCA Protein Assay Kit according to provider's instruction (Thermo Scientific, Rockford, IL, USA).

***In vitro* analysis of AMPK phosphorylation on VAMP2/3 and synaptic fractions**

AMPK 221TD was activated by incubation in kinase buffer (200 µM ATP, 50 µM AMP, 5 mM $MgCl_2$, 1 mM DTT, in 10 mM HEPES pH 7.4) for 20 min at 30°C. Purified GST-ACC (200 pmol) and GST-VAMP2 (200 pmol), GST-VAMP3 (200 pmol), synaptosomal proteins (20 µg) and vesicular proteins (1.3 or 2.6 µg) were incubated for 2-8 min at 37°C with 200 µM [γ-^{32}P] ATP (specific activity 6000 Ci/mmol ATP) in presence or absence of 221TD (30 pmol) previously

activated by incubation with 1 pmol CamKKβ for 20 min at 30°C in kinase buffer. Kinase reactions were stopped by addition of Laemli buffer and subjected to SDS-PAGE (12%) with Coomassie staining and analysis by Typhoon phosphoimager (GE Healthcare).

Co-immunoprecipitation of AMPK and VAMP2

VAMP2 was immunoprecipitated from synaptic vesicle fractions (20 µg protein) incubated with 1 µg recombinant His-tagged AMPK (221TD) using anti-His-tag antibody (1:200, 2366, Cell Signaling Technology, Danvers, MA, USA) and protein A sepharose (10%) in IP-buffer (10 mM HEPES pH 7.3, 100 mM NaCl, 6 g/L BSA, 0.5 % dodecylmaltoside) overnight at 4°C. The Sepharose was washed 4 times with wash-buffer (10 mM HEPES pH 7.3, 100 mM NaCl, 0.1 % Tween 20), re-suspended in SDS-PAGE sample buffer, and the solubilized denatured proteins were subjected to SDS-PAGE and immunoblotting using anti-VAMP2 antibody (1:3000, Pierce Biotechnology, Rockford, IL, USA).

Co-pull down of AMPK and VAMP2

20 µg vesicle fraction were incubated with or without 1 µg recombinant His-tagged AMPK (221TD) overnight at 4°C in IP-buffer containing 10 mM imidazole and 10 % nickel-nitrilotriacetic acid (NTA) Sepharose (Qiagen, Hilden, Germany). The Sepharose was washed 5 times with wash-buffer containing 10 mM imidazole and proteins bound to the Sepharose beads were directly re-suspended and denatured in SDS-PAGE sample buffer and subjected to SDS-PAGE and immunoblotting, using anti-VAMP2 antibody as above.

Cloning of VAMP3 and AMPK constructs

Truncated constructs of VAMP 3 (Q15836) were amplified from vector pDSL20-V3 obtained in our Y2H screen library (Dualsystems Biotech AG, Schlieren, Switzerland) using PCR with specific primers (Table 1).

Table 1. ***Primers used for amplification of VAMP3 clones***.

VAMP3	*fw*	CAATGTATTGGCCATTACGGCC**ATGTCTACAGGTCCAACTGCTGC**
	rev	CAATACATTGCAGGCCGAGGCGGCCCC**TGAAGAGACAACCCACACGATG**
SNARE-domain	*fw*	CAATGTATTGGCCATTACGGCC**ATGAGACTTCAGCAGACACAAAATC**
	Rev	CAATACATTGCAGGCCGAGGCGGCCCC**CTTCCACCAATATTTCCTCTTC**
Ct-V3	*Fw*	CAATGTATTGGCCATTACGGCC**GACGCACTGCAGGCAGGCGCTTCTCAA**
	Rev	CAATACATTGCAGGCCGAGGCGGCCCC**TGAAGAGACAACCCACACGATG**
Nt-V3	*Fw*	CAATGTATTGGCCATTACGGCC**ATGTCTACAGGTCCAACTGC**
	rev	CAATACATTGCAGGCCGAGGCGGCCCC**CTTGCAATTCTTCCACC**

Green:sfi1 restriction enzyme site/ ***Bold:*** *hybridization site*

Amplified PCR sequences containing Sfi1 sites on 3' and 5' ends of the coding sequence were introduced into yeast two-hybrid (Y2H) vectors pCab and pDSL20 (Dualsystems Biotech AG, Schlieren, Switzerland) containing two additional Sfi1 sites for Y2H experiments.

The Nter-GBD domain of AMPK β2 comprising the N-terminal VAMP interaction domain (amino acids 1-71) and the glycogen binding domain (amino acids 72-168) was PCR-amplified (Table 2) to be inserted into bacterial expression vector pAB52s (derived from pET52b(+), Novagen, by insertion of a second Sfi1 site and a N-terminal Strep-tag in the coding sequence), and in vector pcDNA3.1(-) (Invitrogen) for eukaryotic expression.

Table 2. ***Primers used for PCR-amplification of Nter-GBD β2 AMPK domain.***

To be inserted in pAB52s			
	fw	Sfi1	CAATGTATTGGCCATTACGGCC**ATGGGAAACACCACCAGCGA**
	rev	Sfi1	CAATACATTGCAGGCCGAGGCGGCCCC**CTATAACTTTAAAGCATCGAACACCTCAAAATCA**
To be inserted in pcDNA3.1			
	fw	Hind3	CAATGTATTCTCGAG**ATGGGAAACACCACCAGCGA**
	rev	Xho1	CAATACATTGCAAAGCTT**CTATAACTTTAAAGCATCGAACACCTCAAAATCA**

Green: restriction enzyme site/ ***Bold:*** *hybridization site*

Expression and purification of Strep-GBD Nter β2 domain

The fusion protein construct Strep-GBDNter β2 domain was transformed into competent *E.coli* BL21-Codon Plus (DE3)-RIL cells (Stratagene) and incubated overnight on LB agar containing 100 µg/ml ampicillin and 30 µg/ml chloramphenicol. Cultures were grown in LB containing antibiotics at 37°C with shaking until OD (600 nm) 0.7-0.9. Cells were then cooled down to 30°C and protein expression was induced for 4 hours with 2 mM isopropyl β-D-thiogalactopyranoside (IPTG, Eurobio). Cells were harvested and suspended in lysis buffer: PBS (phosphate buffer saline) with complete EDTA-free protease inhibitor cocktail (Roche). After

sonication, insoluble material was removed by centrifugation (40000 g, 40 min at 4°C). The supernatant was applied to a Strep Tactin Superflow column (Merck KGaA, Darmstadt, Germany) and Strep-fusion proteins were purified according to the purification protocol provided by the manufacturer.

In vitro activation of AMPK by CamKKβ

AMPK221 (4 pmol) was activated by incubation with 1 pmol CamKKβ for 20 min at 30°C in kinase buffer (200 µM ATP, 50 µM AMP, 5 mM $MgCl_2$, 1 mM DTT, in 10 mM HEPES pH 7.4).

Surface plasmon resonance

Binding of inactive AMPK221 to the soluble, cytosolic domain of VAMP2 (amino acids 1-94, kind gift of Rothman lab, Yale University, USA) was analyzed by surface plasmon resonance (SPR) with a Biacore T100 instrument (GE Healthcare). The SPR signal is expressed in arbitrary response units (RU) which are proportional to the amount of material bound at a sensorchip surface. All experiments were carried out at 25°C in running buffer containing 10 mM HEPES (pH 7.4), 50 mM K-acetate, and 0.005 % Surfactant P20 (GE Healthcare), using stock solutions of VAMP2 domain (3.34 mg/mL in 25mM HEPES pH7.8 containing 100 µM TCEP, 200 mM KCl, 10% glycerol and 400 mM Imidazole) and AMPK221 (3.1 mg/ml in phosphate buffer 50 mM pH8 containing 50 mM NaCl, 250 mM imidazole. Soluble VAMP2 domain was randomly immobilized on a carboxy-methylated dextran sensorchip (CM5; GE Healthcare) using routine covalent amine coupling according to the manufacturer's instructions. Control lanes were only treated with amine coupling reagents without protein. A defined immobilization level of VAMP2 domain was achieved by multiple injections of VAMP2 onto the activated chip at a flow rate of 5 µl/min. AMPK association and dissociation kinetics (300 s each) were recorded at a flow rate of 30 µl/min. The initial baseline was recovered by injection of 150 µl 0.5 M NaCl.

For determination of binding parameters, 400 RU VAMP2 were immobilized. AMPK221 stock solution, inactive or activated *in vitro* by CamKKβ, were diluted into running buffer to different concentrations (7.5 and 12.5 µM) just prior to injection. At lower or higher AMPK concentrations there was an unacceptable signal/noise ratio, possibly because AMPK became

unstable or bulk refractive index change was too important, respectively. Binding curves of inactive or active AMPK with VAMP2 domain were calculated as the difference between VAMP2-containing channels and control channels. Kinetic data were subjected to a global fit with a simple Langmuir 1:1 kinetics (Biacore software, GE Healthcare). The affinity K_D (dissociation equilibrium constant) was derived from rate constants as $K_D = k_{off} / k_{on}$.

For competition binding experiments, 900 RU VAMP2 were immobilized, and the buffer of AMPK221 stock solution was exchanged against Biacore running buffer by 20 concentration-dilution cycles using a Amicon-30 device (Merck Millipore). A constant concentration of 4 µM AMPK221 was pre-mixed with a concentration series (0, 1, 2, 4, 8, and 16 µM) of AMPK β-subunit N-terminal domain (AMPK-βN; stock solution of 0.4 mg/ml in Tris-buffer 50 mM pH8). Control-corrected AMPK221 binding levels at a reporting point 150 s after injection were recalculated into percentage of bound AMPK221 *vs.* AMPK-βN using a calibration curve based on their different molecular mass (135 kDa *vs.* 20 kDa) and assuming a fixed number of binding sites shared by both proteins (*Figure 3*). These data were fitted to a sigmoidal dose-response curve using using Sigma Plot 10.0 (Systat Software).

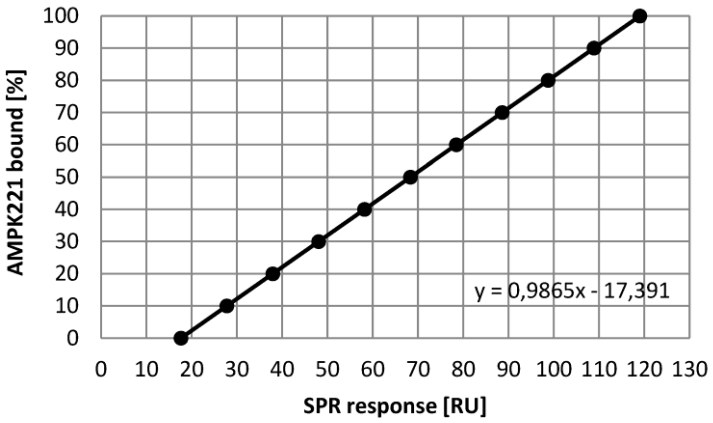

***Figure 3.* Calibration curve for competition binding assay of AMPK221/VAMP2 interaction and AMPK-βN as competitive inhibitor.** Data given in *Figure 13* were recalculated into percentage of bound AMPK221 vs. AMPK-βN based on their different molecular mass (135 kDa vs. 20 kDa) and assuming a single binding site shared by both proteins. For further details see Materials & Methods.

Membrane fusion assay

Full length t-SNARE and v-SNARE protein expression and purification were performed as described (Parlati et al., 1999; Weber et al., 1998). All lipids for proteoliposome preparation were obtained from Avanti Polar Lipids. For white vesicles, 100 µL of a 15 mM premixed lipid solution in chloroform (POPC (1-plamitoyl, 2-oleoyl phosphatidylcholine):DOPS (1,2-dioleoyl phosphatidylserine), in an 85:15 mol ratio), and for fluorescent (red) donor vesicles 100 µL of a 3 mM premixed lipid solution in chloroform (POPC (1-plamitoyl, 2-oleoyl phosphatidylcholine):DOPS (1,2-dioleoyl phosphatidylserine):rhodamine-DOPE (1,2-dioleoyl-sn-glycero-3-phosphoethanolamine: PE-NBD (phosphatidylethanolamine), in a 82:15:1.5:1.5 mol ratio), were dried down in 10x75 mm glass test tubes by a gentle stream of nitrogen (15 min), and any remaining traces of chloroform were then removed under vacuum for 1 h, leaving a pure lipid film. Then t-SNARE (SNAP25) (200 lipids/FLT) is added to the white lipid film and volume adjusted with 1% octyl-β-D-glucopyranoside (OG) in buffer A (25 mM Hepes-KOH (pH7.4), 3 M KCl, 10% glycerol, 1 mM DTT) in order to have a final solution of 500 µL (3mM lipids), and v-SNARE (VAMP2) (40 lipids/FLV) is added to the red lipid film and volume adjusted with OG 1% in buffer A in order to have a final solution of 100 µL (3 mM lipids). In both cases, the lipids were dissolved by gentle agitation for 15 min at room temperature. Vesicles were then formed from these samples by rapid dilution followed by extensive dialysis as follows. While vortexing vigorously, the sample was diluted with twice the sample volume of buffer A (at room temperature), thereby diluting the detergent OG below its critical micellar concentration and promoting vesicle formation. Then detergent was removed by dialysis (in Spectrapore 6-8 kDa cut-off dialysis tubing) against 3 L of buffer overnight at 4°C (2-3 mL/min).

For free protein removal, 1.5 mL of t-liposomes were mixed with 1.5 mL of HistoDenz 80% and poured into a MLS50 Beckman centrifuge tube (5 mL UltraClear) and overlayed with 1.5 mL of 30% HistoDenz and 900 µL of buffer A. This was centrifuged 5 h at 46000 g, and twice 240µL were collected from each tube (~ 6.25 mM lipids). In analogy, 300 µL of v-liposomes were mixed with 300 µL of HistoDenz 80% and poured into a MLS50 Beckman centrifuge tube (0.8 mL UltraClear) and overlaid with 100 µL of HistoDenz 30% and 75µL of buffer A. This was centrifuged 5 h at 46000 g, and twice 40 µL were collected from each tube (~ 7.5 mM lipids).

Standard fusion assays were performed in white 96-well FluoroNunc plates (Nunc). 45 µL unlabeled t-liposome (white) were prewarmed in the plate at 37°C in presence or absence of

AMPK, then 5 µL of labeled v-liposomes (red) were added. The plates were then placed in the Fluorimeter (Fluoroskan II, Labsystems) equilibrated to 37°C. NBD fluorescence was followed with filters set at 460nm (excitation, half band width 25 nm) and 538 nm (emission, half band width 25 nm). NBD fluorescence was monitored every minute for 140 min. To obtain maximum intensity of fluorescence for normalization, 10 µL n-Dodecyl-β-maltoside (10%) was added.

Results

Yeast-two-hybrid screen for AMPK interactors identifies VAMP3

Putative interaction partners of the N-terminal domain of AMPK β-subunits (Δβ) were identified in a Y2H screen using a human brain cDNA library. The applied novel split-ubiquitin cyto-Y2H system (Möckli et al., 2007) detects protein-protein interactions occurring in the cytosol. It is coupled to a transcriptional read-out that allows growth on nutrient-deficient medium that detects also weak or transient interactions. About 6.2×10^6 and 3.4×10^6 clones were screened for AMPK-Δβ1 and -Δβ2 subunits, respectively, yielding 102 primary interacting clones, including 38 that reproducibly interacted with Δβ in paired Y2H assays as compared to a negative control, the unrelated bait *Simian virus* large T antigen (Table 3). Sequencing confirmed 5 clones containing in-frame coding sequences not known or not supposed to be false positives in Cyto-Y2H (Dualsystems, personal communication) and corresponding to different proteins (Table 4). Sequencing of these clones identified mainly transmembrane proteins, including the vesicle associated membrane protein (VAMP) family member 3.

Table 3: ***Cyto-Y2H screen for interactors of AMPK β1 or β2 N-terminal domain in a human cDNA library*****.**

	Δβ1	**Δβ2**
Library	human brain cDNA library	human brain cDNA library
Transformation efficiency	2.2×10^5clones/ug library	1.2×10^5clones/ug library
Clones, total number	ca. 6.2×10^6	ca. 3.4×10^6
Clones, selected on SD-AHTL	69	33
Clones, bait dependent [1]	26	12
Clones, selected [2]	4 different	2 different

[1)] Clones interacting with Δβ but not with LT. [2)] Clones with in-frame CDS not corresponding to known false positives, corresponding to different proteins. In addition, known interactors of APP were excluded, since the transmembrane domain of APP is used as a membrane anchor in the Cyto-Y2H screen.

Table 4. ***Putative AMPK interactors identified in the Cyto-Y2H screen.***

Bait	**Gene name**	**Encoded protein**	**SwissProt entry**	**Identified part (amino acids)**
Δβ2	VAMP3	Vesicle-associated membrane protein 3	Q15836	22-80
Δβ2	C14orf1	Probable ergosterol biosynthetic protein 28	Q9UKR5	1-140
Δβ1	NRDP1/RNF41	E3 ubiquitin-protein ligase Nrdp1	Q9H4P4	136-316
Δβ1	JWA/ARL6IP5	JWA protein or PRA1 family protein 3	O75915	1-188
Δβ1	CLDND1	Claudin domain-containing protein 1	Q9NY35	203-253

VAMP 2 and 3 are interacting with AMPK beta

We further concentrated on VAMP proteins because of the apparent functional link between vesicle exocytosis and AMPK activation. We first checked whether VAMP3 can interact with both Δβ constructs and also with full-length β-subunits, and whether such interactions are preserved in the highly homologous VAMP2 isoform. VAMP3 indeed interacted with both truncated and full-length β1 and β2, but not with isolated SNARE domain common to all VAMPs (amino acids 31-91 in VAMP2, 14-74 in VAMP3). All these interactions were conserved in VAMP2 (*Figure 4*). These results were confirmed by an independent Y2H assay, the Split-Trp system (data not shown), as well as co-immunoprecipitation and pull-down of VAMP2 from synaptic vesicles by heterotrimeric full-length AMPK (*Figure 5*).

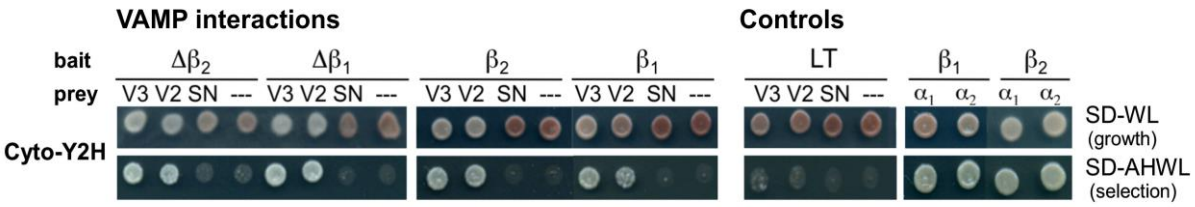

Figure 4. **Two major VAMP isoforms interact with the AMPK β-subunit.** Paired Cyto-Y2H was performed with Δβ1, Δβ2, β1 and β2 as baits and VAMP2 or 3 (V2, V3) or the shared SNARE domain (SN, VAMP2 amino acids 31-91) as preys. Presence of bait and prey plasmids are verified on selective media (SD-WL). Bait/prey interaction leads to reconstitution of ubiquitin and a transcriptional readout allowing growth on medium lacking in addition adenine and histidine (SD-AHWL). Spots represent yeast grown for 72h at 30°C. Negative controls: LT, Large T Antigen of *Simian Virus* (aa 84-704) and empty prey vector (---). Positive controls: AMPK α-β dimerization. For more details see Materials and Methods.

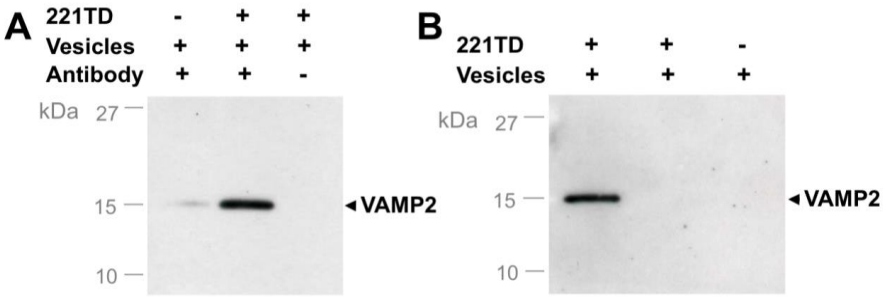

Figure 5. **AMPK/VAMP2 interaction is confirmed by immunoprecipitation and pull-down.** (A) Immuno-precipitation of VAMP2 from purified synaptic vesicles with added constitutively active AMPK αT172D-Hisβ2γ1 (221TD) using anti-His-tag antibody. (B) Pull-down of VAMP2 from purified synaptic vesicles by added 221TD using Ni-NTA Sepharose. VAMP2 was detected by immunoblot analysis with anti-VAMP2 antibody.

VAMP is not a substrate for AMPK

For further *in vitro* assays, the soluble N-terminal domains of VAMP2 and -3 fused to an N-terminal GST-tag (GST-ntVAMP3, GST-ntVAMP2) were produced in *E. coli* and purified. When these proteins were subjected to an *in vitro* phosphorylation assay, neither of both VAMPs was phosphorylated (*Figure 6*). The same negative results were obtained when Strep-ntVAMP3 or a constitutive active AMPK 221TD mutant were used in such *in vitro* experiments (data not shown). Thus, at least the soluble, N-terminal VAMP domain is not an AMPK substrate. This coincides with the lack of any consensus AMPK phosphorylation recognition sites in both VAMP2 and VAMP3 (Prosite Scan for [MLIFV]-[XRKH]-[XRKH]-X-X-[ST]-X-X-X-[MLIFV]; (Dale et al., 1995; Scott et al., 2002)).

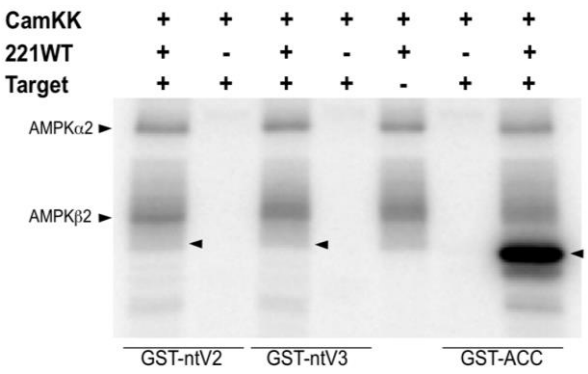

***Figure 6*. VAMPs are not AMPK substrates.** AMPK 221WT (4 pmol) previously activated by CamKK (1 pmol) was incubated with GST-ntVAMP3 or GST-ntVAMP2 (200 pmol) or with GST-ACC (100 pmol) for 8 min at 37°C. *In vitro* phosphorylation assays were analyzed by SDS-PAGE and Typhoon phosphoimager. Note the AMPK autophosphorylation of α and β subunits.

VAMP is not directly regulated by AMPK-binding

Since the v-SNARE VAMPs did not serve as an AMPK substrate, we hypothesized that the interaction alone could affect VAMP-mediated membrane fusion. In an *in vitro* assay for SNARE-complex induced membrane fusion, we tested whether addition of AMPK affects fusion of two vesicle populations containing either the v-SNARE VAMP2 or a t-SNARE SNAP25 (*Figure 7*). However, the interaction of VAMP2 and AMPK did not affect SNARE-complex function in membrane fusion.

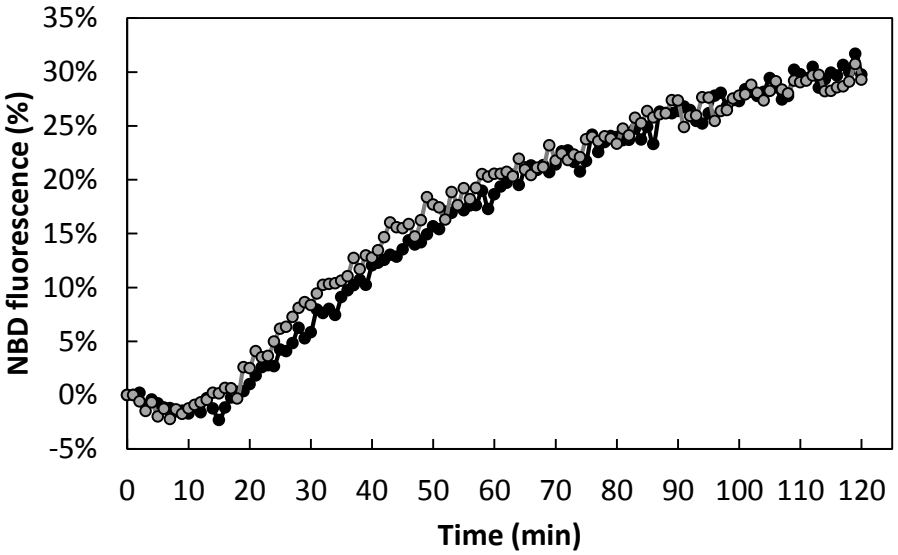

Figure 7. **AMPK/VAMP interaction does not affect vesicle fusion.** Mixing of two vesicle populations containing either v-SNARE (VAMP2) or a t-SNARE (SNAP25) together with NBD- and rhodamine-labelled lipids leads to SNARE-mediated vesicle fusion, dilution of the fluorescent labels and thus loss of FRET between NBD and rhodamine. This is monitored by the increase in NBD fluorescence at 538 nm. Grey and black symbols represent, respectively, membrane fusion in absence and in presence of AMPK. For further details see Materials & Methods.

Determination of the AMPK-VAMP interaction domain

Since VAMPs were not phosphorylated by AMPK, we considered the possibility that they could act as scaffolding proteins to recruit AMPK to exocytotic vesicles, which could facilitate phosphorylation of vesicle-bound AMPK substrates. In support of this model, we could detect AMPK together with at least two putative AMPK substrates in a purified fraction of synaptic vesicles from rat brain (*Figure 8*, see arrow in B).

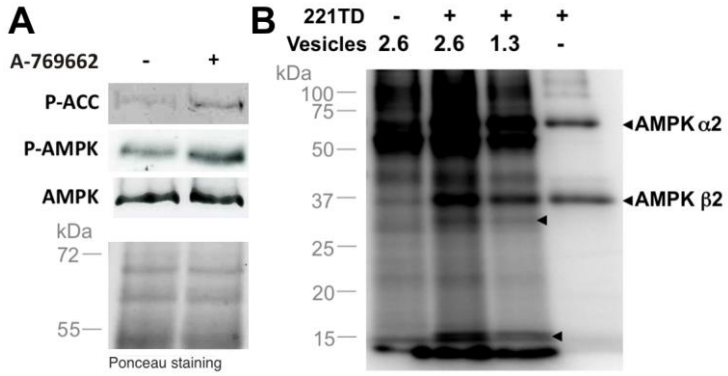

Figure 8. **AMPK and putative AMPK substrates in synaptic vesicles.** (A) Representative immunoblots showing that AMPK is present in synaptosome fractions and can be activated. Synaptosomes were treated (+) or not (-) with AMPK activator A-769662 for 30 min at 37°C. Immunoblotting of 50 µg synaptosomal proteins probed with anti-phospho-ACC, anti-P172 AMPK (Ponceau staining as loading control) or anti-total AMPK antibodies. (B) *In vitro* phosphorylation assay for AMPK substrates. AMPK 221TD (30 pmol) was incubated with synaptic vesicles (2.6 or 1.3 µg) for 2 min at 37°C. *In vitro* phosphorylation assays were analyzed by SDS-PAGE and Typhoon phosphoimager. Note the AMPK autophosphorylation of α and β subunits.

To further tackle such scaffolding function of VAMPs, we mapped the interaction domains situated in VAMP3 and the AMPK β2 subunit by applying Y2H analysis to different VAMP3 and AMPK β2 truncation constructs. Y2H data revealed that the very N-terminal domain of AMPK β ($\Delta\beta_{1/2,}$ amino acids 1-54) is sufficient for interaction with full-length VAMP3 (*Figure 9*). However, the N-terminal truncation construct $\Delta_{1\text{-}54}\beta2$ is still able to interact with VAMP3, and N-terminal truncation up to the glycogen-binding domain (amino acid 72; construct $\Delta_{1\text{-}72}\beta2$) is necessary to suppress the interaction (*Figure 9*). These results clearly show that the entire N-terminal sequence of AMPK β2 (amino acids 1-72) can interact with VAMP, and that sequences 1-54 and 55-72 are sufficient for this interaction.

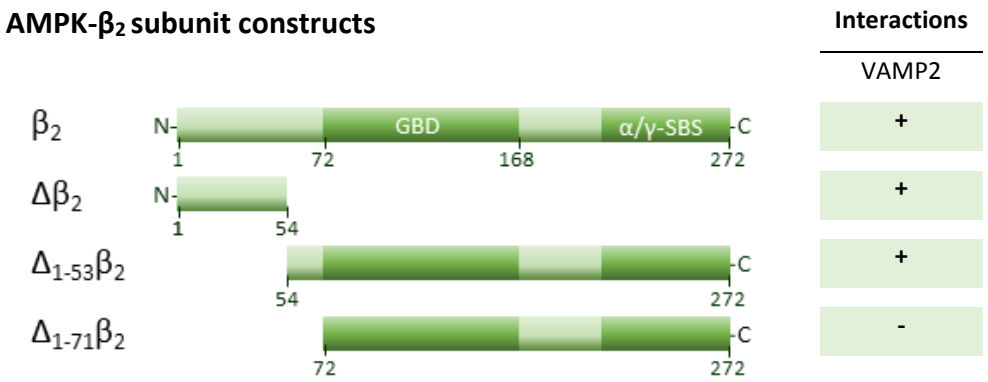

Figure 9. **Mapping of the AMPK-β2 domain interacting with VAMP2.** Paired Cyto-Y2H was carried out as described in *Figure 4*. AMPK β2 subunit constructs used: β2, full length subunit; Δβ2, N-terminal amino acids 1-54; $\Delta_{1\text{-}53}$β2, C-terminal amino acids 54-272;$\Delta_{1\text{-}71}$β2, C-terminal amino acids 72-272; GBD, glycogen binding domain; α/γ-SBS , C-terminal α/γ-subunit binding sequence. (+) proteins interact, (-) no interaction between proteins, (ND) not determined.

The mapping occurred to be more complex for VAMP. The VAMP3 clone identified in the original Y2H screen corresponds to a truncated version comprising amino acids 22-80, thus spanning a large part of the SNARE domain (amino acids 14-74). However, isolated SNARE domain did not interact with AMPK-β1/-β2 (*Figure 4*) or did so only more weakly with AMPK-β2 and somewhat more weakly (*Figure 10*).

We therefore checked separately the C-terminal 50 amino acids of VAMP3 bearing the transmembrane domain and a minor part of the SNARE domain, as well as the VAMP3 C-terminal 14 amino acids which are VAMP-isoform-specific (*Figure 10*). No interactions were detectable with these constructs. Thus, the SNARE domain (in particular the region between amino acids 22 and 50) is necessary, but it does not seem to be sufficient for interaction. Most likely, the SNARE domain requires the context of a more extended VAMP structure, as in case of the identified Y2H clone (amino acids 22-80), possibly for reaching a proper folding.

We finally also tested VAMP interaction with the catalytic subunits α_1, and α_2. VAMP 3 interacted with AMPK catalytic subunit α_2, but not with the α_1 isoform (*Figure 10B*). AMPK-α_1 and -α_2 have only 74% sequence homology which may explain these differences. The AMPK γ subunit does not correctly express in yeast and cannot be used in Cyto-Y2H.

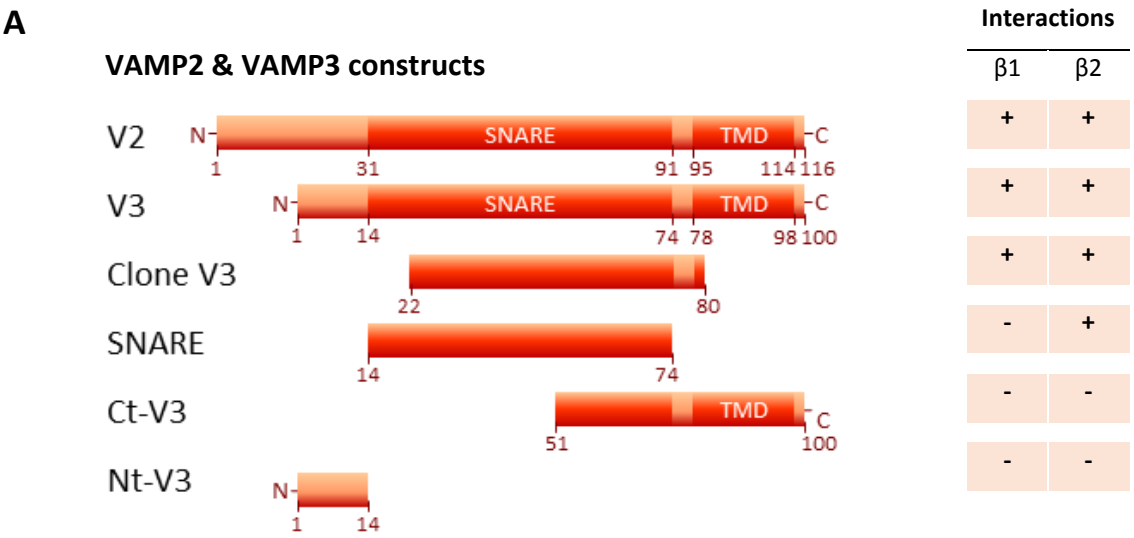

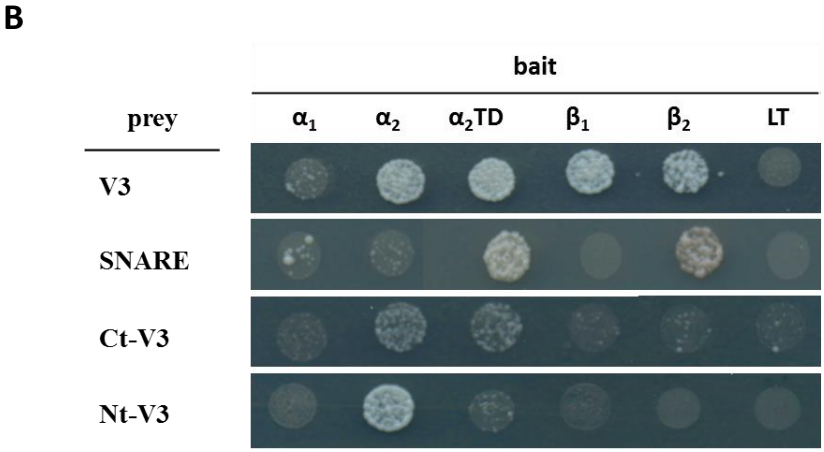

Figure 10. **VAMP3 interaction with AMPK.** (A) Mapping of the VAMP3 domain interacting with AMPK β1 and β2. Paired Cyto-Y2H was carried out as described in *Figure 4*. (+) proteins interact, (-) no interaction between proteins (see (B)). (B) Interaction of VAMP3 with different AMPK subunits. Paired Cyto-Y2H with different AMPK subunits or Large T (LT) as negative control (baits) and VAMP3 constructs (preys). Spots represent yeast grown for 48h at 30°C on selective medium lacking tryptophan, leucine, adenine, and histidine (SD-AHWL). Different VAMP constructs used: V3, full-length VAMP3; SNARE, common SNARE domain of VAMP proteins (amino acids 14-74); Ct-V3, C-terminal 50 amino acids of VAMP3 bearing a part of the SNARE domain and the C-terminal transmembrane domain (TMD); Nt-V3, VAMP3 N-terminal 14 amino acids; α_1, $\alpha_{2,,}$, β_1, $\beta_{2,}$ AMPK subunits; α_2TD, a constitutively active AMPK subunit.

Determination of AMPK-VAMP binding kinetics

To further verify a function of VAMP in recruiting AMPK to transport vesicles, we applied surface plasmon resonance (SPR) spectroscopy to (i) test whether AMPK/VAMP interaction is direct, (ii) measure the kinetic and equilibrium binding parameters, and (iii) analyze how to experimentally interfere with AMPK/VAMP interaction.

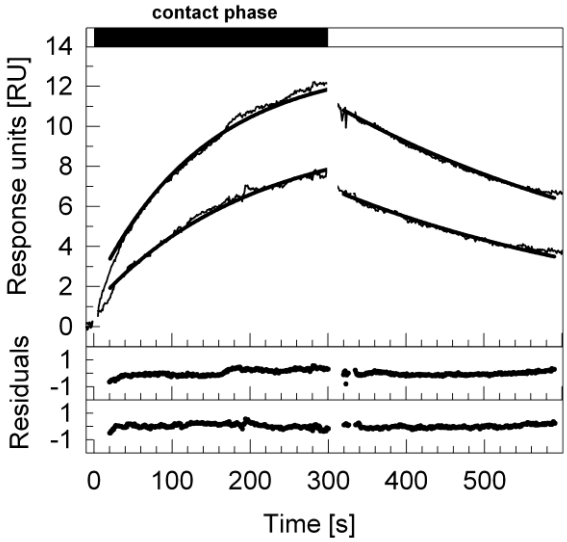

***Figure 11*. Surface plasmon resonance identifies interaction of AMPK221 with VAMP2.** Representative SPR traces of association (contact) and dissociation phase of 7.5 and 12.5 µM AMPK221 with soluble VAMP2 domain (thin lines). Global fitting of traces to 1:1 Langmuir kinetics (bold lines) and the corresponding residuals (below) are given. Data were recorded at 25°C and 30 µl/min flow rate. The calculated interaction parameters are: $k_a=2.5\cdot10^2$ M^{-1} s^{-1}, $k_d=2.2\cdot10^{-3}$ s^{-1}, and $K_D=8.5\cdot10^{-6}$ M. For further details see Materials & Methods.

For SPR, we used an immobilized soluble N-terminal VAMP2 domain (amino acids 1 to 94) and injected AMPK221 heterotrimer in the flow (*Figure 11*). The data show that AMPK and VAMP interact directly with an affinity constant (K_D) of 8.5µM. This rather low affinity argues for a more transient type of interaction, although in *vivo* additional factors may increase this affinity. We further tested whether VAMP interaction is different between AMPK in an active or inactive conformation by activating AMPK with CamKKβ prior to SPR experiments (*Figure 12*). Activation of AMPK caused a slightly faster association rate without affecting dissociation, thus increasing affinity.

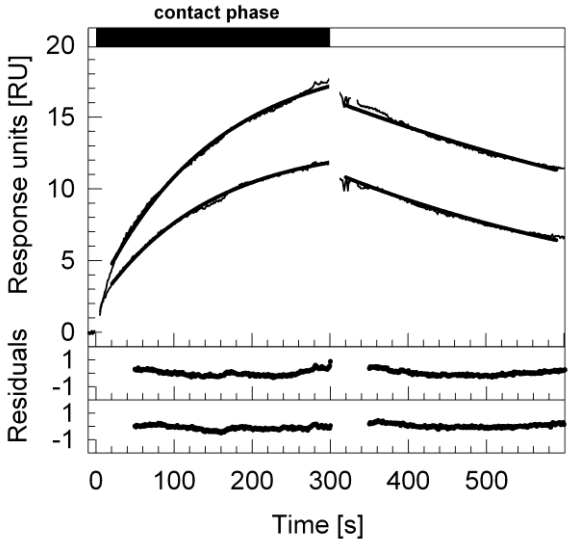

***Figure 12*. Surface plasmon resonance identifies differences between active and inactive AMPK in VAMP2 interaction.** Representative SPR traces of association (contact) and dissociation phase (thin lines) of AMPK at 12,5 µM, either activated *in vitro* by CamKKβ (top trace) or inactive (bottom trace), with soluble VAMP2 domain. Data were recorded at 25°C and 30 µl/min flow rate. Traces were fitted individually to 1:1 Langmuir kinetics (bold lines) and the corresponding residuals (below) are given. The calculated interaction parameters are: k_a=4,5·10^2 M^{-1} s^{-1}, k_d=1,5·10^{-3} s^{-1}, and K_D=3,2·10^{-6} M (for active AMPK), and k_a=2,5·10^2 M^{-1} s^{-1}, k_d=1,8·10^{-3} s^{-1}, and K_D=7,4·10^{-6} M (for inactive AMPK). For further details see Materials & Methods.

Inhibition of AMPK-VAMP interaction

In the next step, we wanted to disrupt the interaction between VAMP and AMPK. Based on the mapping of the interaction domains (*Figure 9* and *Figure 10*), we decided to generate an AMPK β2 construct comprising the N-terminal VAMP interaction domain (amino acids 1-71) and the glycogen binding domain (amino acids 72-168). This construct should be able (i) to fold correctly (with the GBD domain being successfully crystallized), (ii) to competitively inhibit the AMPK/VAMP interaction, while (iii) being unable to interact with α- and γ-subunits. In a competition assay, using again soluble VAMP domain immobilized at the chip surface, we co-injected both, AMPK221 complex and AMPK-βN domain. The assay clearly showed a decrease in AMPK221 binding with increasing concentrations of AMPK-βN in the lower micromolar range (*Figure 13*).

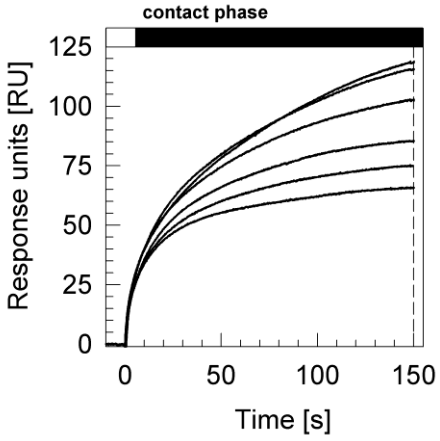

Figure 13. **Competition binding assay of AMPK221/VAMP2 interaction and AMPK-βN as competitive inhibitor.** Representative SPR traces of association (contact) phase with 4 µM AMPK221 and (from top to bottom) 0, 1, 2, 4, 8, or 16 µM AMPK-βN. Data were recorded at 25°C and 30 µl/min flow rate. For further details see Materials & Methods.

The percentage of bound AMPK was then calculated from the binding response by correcting for bound AMPK-βN (which has much lower molecular mass) and assuming a fixed number of binding sites shared by both proteins. These data were fitted to a sigmoidal dose-response curve (*Figure 14*). They demonstrate that at an equimolar concentration of 4 µM of both proteins, AMPK221 and AMPK-βN, the interaction is inhibited by about 35%. Inhibition reaches 80% at higher AMPK-βN concentrations. Possibly, the remaining AMPK-βN-resistant AMPK/VAMP interaction is due to the interacting α subunit (*Figure 10*). The SPR study allowed

us to confirm a direct interaction between AMPK221 and VAMP2 that can be inhibited by a AMPK-βN construct.

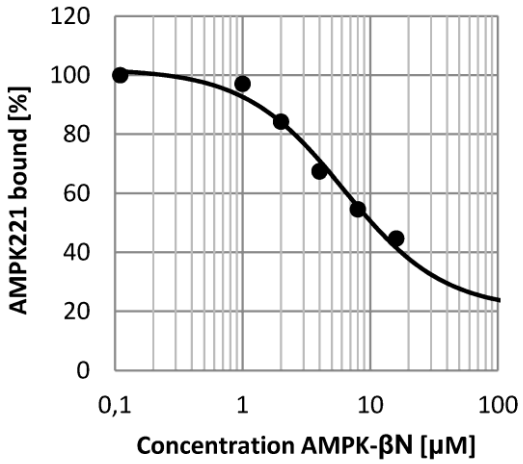

***Figure 14*. AMPK221 β-subunit N-terminal domain competes with AMPK221 for VAMP2 binding.** Competition binding assay showing the effect of AMPK221 β-subunit N-terminal domain (AMPK-βN) on AMPK221/VAMP2 interaction. SPR binding kinetics of 4 µM AMPK221 to soluble VAMP2 domain were determined as a function of the presence of 0, 1, 2, 4, 8, or 16 µM AMPK-βN. Reporting points taken at 150 s of association from *Figure 13* were used for calculation of data presented here. For further details see Materials & Methods.

Discussion

One of the most interesting putative AMPK interactors identified in our Y2H assays were members of the large VAMP family, VAMP2 and VAMP3, both essential players in exocytosis. Localized at different intracellular storage vesicles, they are involved in their correct sorting and fusion with specific target membranes (Mochida, 2000; Procino et al., 2008; Sai et al., 2013). Regulation of many of these exocytotic processes seems to involve also AMPK. The most prominent example is cell surface expression of the nutrient transporters GLUT4 (glucose uptake) and CD36 (fatty acid uptake), playing a central role in regulating glucose and lipid uptake (Heather et al., 2013; Holman and Cushman, 1994; Karylowski et al., 2004). However, also the release of neurotransmitters like glutamate from synaptic vesicles in synapses is controlled by AMPK (Cunningham et al., 2012). In this study we provide insight into the molecular properties of the AMPK/VAMP interaction, and develop tools to further study its functional role *in vitro* and *in vivo*. Taken together with published data, our study suggests an AMPK scaffolding function for VAMP2 and VAMP3.

The interaction between AMPK and VAMP2/3 found in Y2H assays was confirmed by multiple, independent interaction assays, including co-immunoprecipitation, pull-down and SPR. Thus the VAMP/AMPK interaction has been established *in vivo.* We could also map the interaction domains to a central portion of VAMP3 and more precisely to the N-terminal 72 amino acids of the AMPK β-subunit. In addition, an N-terminal AMPK-β domain was able to competitively inhibit AMPK/VAMP interaction in SPR assays. This domain could thus be used to disturb VAMP/AMPK interaction *in vivo* to study e.g. effects on exocytosis. Addition of the GBD-β domain (73-168 amino acids) which is an autonomously folding domain should help to correctly structure the entire N-terminal AMPK-β domain of 168 amino.

There is ample evidence that both interaction partners, AMPK and VAMP2/3, are acting sequentially in the same signaling pathway of exocytosis. However, so far they have been involved at very different stages. In the best studied case, which is the exocytosis of GLUT4-containg storage vesicles (GSV), AMPK acts upstream by phosphorylating AS160 at Ser570/588 to trigger GSV release and translocation to the cell surface, the key event in exercise-stimulated glucose uptake. In contrast, VAMP2 and VAMP3 seem to act very much more downstream in the docking and membrane fusion processes. Our data however suggest that

both proteins have a more intimate role to play here. This role does not include direct regulation of VAMPs by AMPK. As our *in vitro* data suggest, VAMPs are neither a direct substrate of AMPK nor are they regulated in their membrane fusion activity by bound AMPK. By contrast, VAMPs may represent a type of scaffolding protein that allows recruitment of a fraction of AMPK to the surface of storage vesicles. In support of this, our SPR experiments confirmed a direct interaction between both proteins with an affinity in the lower µM-range, increasing when AMPK was activated. Such affinities are typical for interactions mapped at the surface of GSVs, such as the interaction between the RabGAP AS160 and the insulin regulated amino peptidase (IRAP; Park et al., 2012). Interestingly, the GLUT4-interacting IRAP is like VAMP a transmembrane protein (Martin et al., 1997; Ross et al., 1996), and both may share a common functional feature: they represent scaffolds to recruit the "true" signaling molecules, AS160 and AMPK, respectively, to the storage vesicles.

We would thus propose a model (*Figure 15*) in which VAMP2 and VAMP3 have an additional role at the initiation step of exocytosis. By interacting with AMPK or even more the activated form of AMPK, they would bring the kinase in close vicinity of its substrate AS160 for triggering downstream exocytosis. This concept may be generally true for exocytotic translocation processes which involve VAMP2 and VAMP3 as v-SNAREs. In addition to GLUT4 and CD36 translocation to the plasma membrane, this could also concern the release of neurotransmitters from synaptosomes, which involves VAMP2-containing storage vesicles and possibly also activation by AMPK (Cunningham et al., 2012). In support of this, we found that synaptic vesicles (i) contain considerable amounts of AMPK, (ii) contain different putative AMPK substrates that could act similar to AS160, and (iii) fuse with the synaptosome membrane for glutamate release depending on the AMPK activation state (not shown).

In summary, our data support formation of transient AMPK/VAMP complexes *in vitro* and *in vivo*. They suggest a role of VAMP2 and VAMP3 upstream of vesicle docking and membrane fusion, in form of a scaffolding function that recruits AMPK to storage vesicles for phosphorylation of vesicle-located substrates such as AS160. It has still to be tested whether such a model applies *in vivo*, either in case of nutrient transporter externalization or neurotransmitter release. Such experiments will employ the N-terminal AMPK β_2-construct for which we have shown competitive inhibition of the AMPK/VAMP interaction. Its expression in cells should for example reduce AS160 phosphorylation and GLUT4 or CD36

appearance at the cell surface. It also remains to be established whether this novel function of VAMPs is a general feature of exocytotic processes.

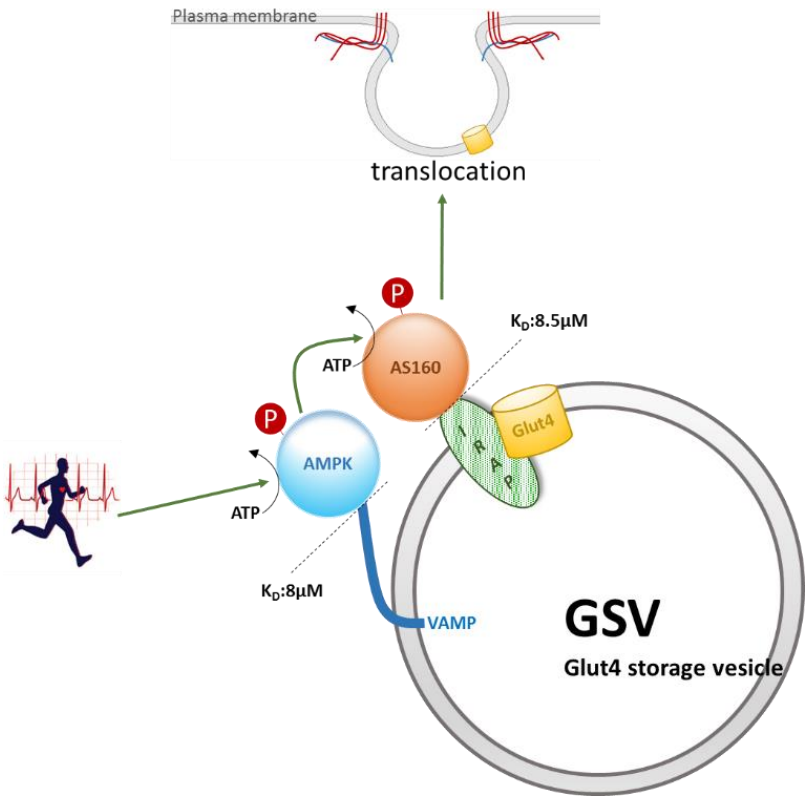

Figure 15. **VAMP as a scaffold to recruit AMPK to glucose storage vesicles.** Exercise causes AMPK activation. Interaction of AMPK with the VAMP scaffold then recruits AMPK transiently to the vicinity of its substrate AS160, anchored via the IRAP scaffold to the same GSVs. Thus, AMPK could easily phosphorylate AS160, which triggers translocation of GSVs to the plasma membrane, integration of cargo like GLUT4 and IRAP into the plasma membrane, and finally an increase in glucose uptake.

References

Baus, D., Heermeier, K., De Hoop, M., Metz-Weidmann, C., Gassenhuber, J., Dittrich, W., Welte, S., and Tennagels, N. (2008). Identification of a novel AS160 splice variant that regulates GLUT4 translocation and glucose-uptake in rat muscle cells. Cell. Signal. *20*, 2237–2246.

Bonifacino, J.S., and Glick, B.S. (2004). The mechanisms of vesicle budding and fusion. Cell *116*, 153–166.

Bradford, M.M. (1976). A rapid and sensitive method for the quantitation of microgram quantities of protein utilizing the principle of protein-dye binding. Anal. Biochem. *72*, 248–254.

Cain, C.C., Trimble, W.S., and Lienhard, G.E. (1992). Members of the VAMP family of synaptic vesicle proteins are components of glucose transporter-containing vesicles from rat adipocytes. J. Biol. Chem. *267*, 11681–11684.

Carling, D. (2005). AMP-activated protein kinase: balancing the scales. Biochimie *87*, 87–91.

Cartee, G.D., and Wojtaszewski, J.F.P. (2007). Role of Akt substrate of 160 kDa in insulin-stimulated and contraction-stimulated glucose transport. Appl. Physiol. Nutr. Metab. Physiol. Appliquée Nutr. Métabolisme *32*, 557–566.

Cunningham, K.A., Hua, Z., Srinivasan, S., Liu, J., Lee, B.H., Edwards, R.H., and Ashrafi, K. (2012). AMP-activated kinase links serotonergic signaling to glutamate release for regulation of feeding behavior in C. elegans. Cell Metab. *16*, 113–121.

Dale, S., Wilson, W.A., Edelman, A.M., and Hardie, D.G. (1995). Similar substrate recognition motifs for mammalian AMP-activated protein kinase, higher plant HMG-CoA reductase kinase-A, yeast SNF1, and mammalian calmodulin-dependent protein kinase I. FEBS Lett. *361*, 191–195.

Dreyer, H.C., Drummond, M.J., Glynn, E.L., Fujita, S., Chinkes, D.L., Volpi, E., and Rasmussen, B.B. (2008). Resistance exercise increases human skeletal muscle AS160/TBC1D4 phosphorylation in association with enhanced leg glucose uptake during postexercise recovery. J. Appl. Physiol. Bethesda Md 1985 *105*, 1967–1974.

Geraghty, K.M., Chen, S., Harthill, J.E., Ibrahim, A.F., Toth, R., Morrice, N.A., Vandermoere, F., Moorhead, G.B., Hardie, D.G., and MacKintosh, C. (2007). Regulation of multisite phosphorylation and 14-3-3 binding of AS160 in response to IGF-1, EGF, PMA and AICAR. Biochem. J. *407*, 231–241.

Gietz, R.D., and Woods, R.A. (2006). Yeast transformation by the LiAc/SS Carrier DNA/PEG method. Methods Mol. Biol. Clifton NJ *313*, 107–120.

Grosshans, B.L., Ortiz, D., and Novick, P. (2006). Rabs and their effectors: achieving specificity in membrane traffic. Proc. Natl. Acad. Sci. U. S. A. *103*, 11821–11827.

Hardie, D.G., and Carling, D. (1997). The AMP-activated protein kinase--fuel gauge of the mammalian cell? Eur. J. Biochem. FEBS *246*, 259–273.

Hardie, D.G., Hawley, S.A., and Scott, J.W. (2006). AMP-activated protein kinase--development of the energy sensor concept. J. Physiol. *574*, 7–15.

Hayashi, T., Wojtaszewski, J.F., and Goodyear, L.J. (1997). Exercise regulation of glucose transport in skeletal muscle. Am. J. Physiol. *273*, E1039–1051.

Heather, L.C., Pates, K.M., Atherton, H.J., Cole, M.A., Ball, D.R., Evans, R.D., Glatz, J.F., Luiken, J.J., Griffin, J.L., and Clarke, K. (2013). Differential Translocation of FAT/CD36 and GLUT4 Coordinates Changes in Cardiac Substrate Metabolism During Ischemia and Reperfusion. Circ. Heart Fail.

Holman, G.D., and Cushman, S.W. (1994). Subcellular localization and trafficking of the GLUT4 glucose transporter isoform in insulin-responsive cells. BioEssays News Rev. Mol. Cell. Dev. Biol. *16*, 753–759.

Jahn, R., and Scheller, R.H. (2006). SNAREs--engines for membrane fusion. Nat. Rev. Mol. Cell Biol. *7*, 631–643.

Johnsson, N., and Varshavsky, A. (1994). Split ubiquitin as a sensor of protein interactions in vivo. Proc. Natl. Acad. Sci. U. S. A. *91*, 10340–10344.

Kane, S., Sano, H., Liu, S.C.H., Asara, J.M., Lane, W.S., Garner, C.C., and Lienhard, G.E. (2002). A method to identify serine kinase substrates. Akt phosphorylates a novel adipocyte protein with a Rab GTPase-activating protein (GAP) domain. J. Biol. Chem. *277*, 22115–22118.

Karylowski, O., Zeigerer, A., Cohen, A., and McGraw, T.E. (2004). GLUT4 is retained by an intracellular cycle of vesicle formation and fusion with endosomes. Mol. Biol. Cell *15*, 870–882.

Kirchhausen, T. (2000). Three ways to make a vesicle. Nat. Rev. Mol. Cell Biol. *1*, 187–198.

Kurth-Kraczek, E.J., Hirshman, M.F., Goodyear, L.J., and Winder, W.W. (1999). 5' AMP-activated protein kinase activation causes GLUT4 translocation in skeletal muscle. Diabetes *48*, 1667–1671.

Larance, M., Ramm, G., Stöckli, J., van Dam, E.M., Winata, S., Wasinger, V., Simpson, F., Graham, M., Junutula, J.R., Guilhaus, M., et al. (2005). Characterization of the role of the Rab GTPase-activating protein AS160 in insulin-regulated GLUT4 trafficking. J. Biol. Chem. *280*, 37803–37813.

Lizunov, V.A., Matsumoto, H., Zimmerberg, J., Cushman, S.W., and Frolov, V.A. (2005). Insulin stimulates the halting, tethering, and fusion of mobile GLUT4 vesicles in rat adipose cells. J. Cell Biol. *169*, 481–489.

Luiken, J.J.F.P., Coort, S.L.M., Willems, J., Coumans, W.A., Bonen, A., van der Vusse, G.J., and Glatz, J.F.C. (2003). Contraction-induced fatty acid translocase/CD36 translocation in rat cardiac myocytes is mediated through AMP-activated protein kinase signaling. Diabetes *52*, 1627–1634.

Martin, L.B., Shewan, A., Millar, C.A., Gould, G.W., and James, D.E. (1998). Vesicle-associated membrane protein 2 plays a specific role in the insulin-dependent trafficking of the facilitative glucose transporter GLUT4 in 3T3-L1 adipocytes. J. Biol. Chem. *273*, 1444–1452.

Martin, S., Rice, J.E., Gould, G.W., Keller, S.R., Slot, J.W., and James, D.E. (1997). The glucose transporter GLUT4 and the aminopeptidase vp165 colocalise in tubulo-vesicular elements in adipocytes and cardiomyocytes. J. Cell Sci. *110 (Pt 18)*, 2281–2291.

McNew, J.A., Parlati, F., Fukuda, R., Johnston, R.J., Paz, K., Paumet, F., Söllner, T.H., and Rothman, J.E. (2000). Compartmental specificity of cellular membrane fusion encoded in SNARE proteins. Nature *407*, 153–159.

Mîinea, C.P., Sano, H., Kane, S., Sano, E., Fukuda, M., Peränen, J., Lane, W.S., and Lienhard, G.E. (2005). AS160, the Akt substrate regulating GLUT4 translocation, has a functional Rab GTPase-activating protein domain. Biochem. J. *391*, 87–93.

Mizuno-Yamasaki, E., Rivera-Molina, F., and Novick, P. (2012). GTPase networks in membrane traffic. Annu. Rev. Biochem. *81*, 637–659.

Mochida, S. (2000). Protein-protein interactions in neurotransmitter release. Neurosci. Res. *36*, 175–182.

Möckli, N., Deplazes, A., Hassa, P.O., Zhang, Z., Peter, M., Hottiger, M.O., Stagljar, I., and Auerbach, D. (2007). Yeast split-ubiquitin-based cytosolic screening system to detect interactions between transcriptionally active proteins. BioTechniques *42*, 725–730.

Park, S., Kim, K.Y., Kim, S., and Yu, Y.S. (2012). Affinity between TBC1D4 (AS160) phosphotyrosine-binding domain and insulin-regulated aminopeptidase cytoplasmic domain measured by isothermal titration calorimetry. BMB Reports *45*, 360–364.

Parlati, F., Weber, T., McNew, J.A., Westermann, B., Söllner, T.H., and Rothman, J.E. (1999). Rapid and efficient fusion of phospholipid vesicles by the alpha-helical core of a SNARE complex in the absence of an N-terminal regulatory domain. Proc. Natl. Acad. Sci. U. S. A. *96*, 12565–12570.

Peck, G.R., Ye, S., Pham, V., Fernando, R.N., Macaulay, S.L., Chai, S.Y., and Albiston, A.L. (2006). Interaction of the Akt substrate, AS160, with the glucose transporter 4 vesicle marker protein, insulin-regulated aminopeptidase. Mol. Endocrinol. Baltim. Md *20*, 2576–2583.

Pfeffer, S.R. (1999). Transport-vesicle targeting: tethers before SNAREs. Nat. Cell Biol. *1*, E17–22.

Pfeffer, S.R. (2012). Rab GTPase localization and Rab cascades in Golgi transport. Biochem. Soc. Trans. *40*, 1373–1377.

Procino, G., Barbieri, C., Tamma, G., De Benedictis, L., Pessin, J.E., Svelto, M., and Valenti, G. (2008). AQP2 exocytosis in the renal collecting duct -- involvement of SNARE isoforms and the regulatory role of Munc18b. J. Cell Sci. *121*, 2097–2106.

Ross, S.A., Scott, H.M., Morris, N.J., Leung, W.Y., Mao, F., Lienhard, G.E., and Keller, S.R. (1996). Characterization of the insulin-regulated membrane aminopeptidase in 3T3-L1 adipocytes. J. Biol. Chem. *271*, 3328–3332.

Rothman, J.E., and Wieland, F.T. (1996). Protein sorting by transport vesicles. Science *272*, 227–234.

Sai, Y., Chen, J., Ye, F., Zhao, Y., Zou, Z., Cao, J., and Dong, Z. (2013). Dopamine Release Suppression Dependent on an Increase of Intracellular Ca(2+) Contributed to Rotenone-induced Neurotoxicity in PC12 Cells. J. Toxicol. Pathol. *26*, 149–157.

Sakamoto, K., and Holman, G.D. (2008). Emerging role for AS160/TBC1D4 and TBC1D1 in the regulation of GLUT4 traffic. Am. J. Physiol. Endocrinol. Metab. *295*, E29–37.

Sano, H., Kane, S., Sano, E., Mîinea, C.P., Asara, J.M., Lane, W.S., Garner, C.W., and Lienhard, G.E. (2003). Insulin-stimulated phosphorylation of a Rab GTPase-activating protein regulates GLUT4 translocation. J. Biol. Chem. *278*, 14599–14602.

Scales, S.J., Chen, Y.A., Yoo, B.Y., Patel, S.M., Doung, Y.C., and Scheller, R.H. (2000). SNAREs contribute to the specificity of membrane fusion. Neuron *26*, 457–464.

Schwenk, R.W., Dirkx, E., Coumans, W.A., Bonen, A., Klip, A., Glatz, J.F.C., and Luiken, J.J.F.P. (2010). Requirement for distinct vesicle-associated membrane proteins in insulin- and AMP-activated protein kinase (AMPK)-induced translocation of GLUT4 and CD36 in cultured cardiomyocytes. Diabetologia *53*, 2209–2219.

Scott, J.W., Norman, D.G., Hawley, S.A., Kontogiannis, L., and Hardie, D.G. (2002). Protein kinase substrate recognition studied using the recombinant catalytic domain of AMP-activated protein kinase and a model substrate. J. Mol. Biol. *317*, 309–323.

Stagljar, I., Korostensky, C., Johnsson, N., and te Heesen, S. (1998). A genetic system based on split-ubiquitin for the analysis of interactions between membrane proteins in vivo. Proc. Natl. Acad. Sci. U. S. A. *95*, 5187–5192.

Sutton, R.B., Fasshauer, D., Jahn, R., and Brunger, A.T. (1998). Crystal structure of a SNARE complex involved in synaptic exocytosis at 2.4 A resolution. Nature *395*, 347–353.

Tafelmeyer, P., Johnsson, N., and Johnsson, K. (2004). Transforming a (beta/alpha)8--barrel enzyme into a split-protein sensor through directed evolution. Chem. Biol. *11*, 681–689.

Treebak, J.T., Glund, S., Deshmukh, A., Klein, D.K., Long, Y.C., Jensen, T.E., Jørgensen, S.B., Viollet, B., Andersson, L., Neumann, D., et al. (2006). AMPK-mediated AS160 phosphorylation in skeletal muscle is dependent on AMPK catalytic and regulatory subunits. Diabetes *55*, 2051–2058.

Varlamov, O., Volchuk, A., Rahimian, V., Doege, C.A., Paumet, F., Eng, W.S., Arango, N., Parlati, F., Ravazzola, M., Orci, L., et al. (2004). i-SNAREs: inhibitory SNAREs that fine-tune the specificity of membrane fusion. J. Cell Biol. *164*, 79–88.

Weber, T., Zemelman, B.V., McNew, J.A., Westermann, B., Gmachl, M., Parlati, F., Söllner, T.H., and Rothman, J.E. (1998). SNAREpins: minimal machinery for membrane fusion. Cell *92*, 759–772.

Webster, I., Friedrich, S.O., Lochner, A., and Huisamen, B. (2010). AMP kinase activation and glut4 translocation in isolated cardiomyocytes. Cardiovasc. J. Afr. *21*, 72–78.

Whittaker, V.P., Michaelson, I.A., and Kirkland, R.J. (1964). The separation of synaptic vesicles from nerve-ending particles ('synaptosomes'). Biochem. J. *90*, 293–303.

Zaid, H., Antonescu, C.N., Randhawa, V.K., and Klip, A. (2008). Insulin action on glucose transporters through molecular switches, tracks and tethers. Biochem. J. *413*, 201–215.

PART 7

Conclusions & Outlook

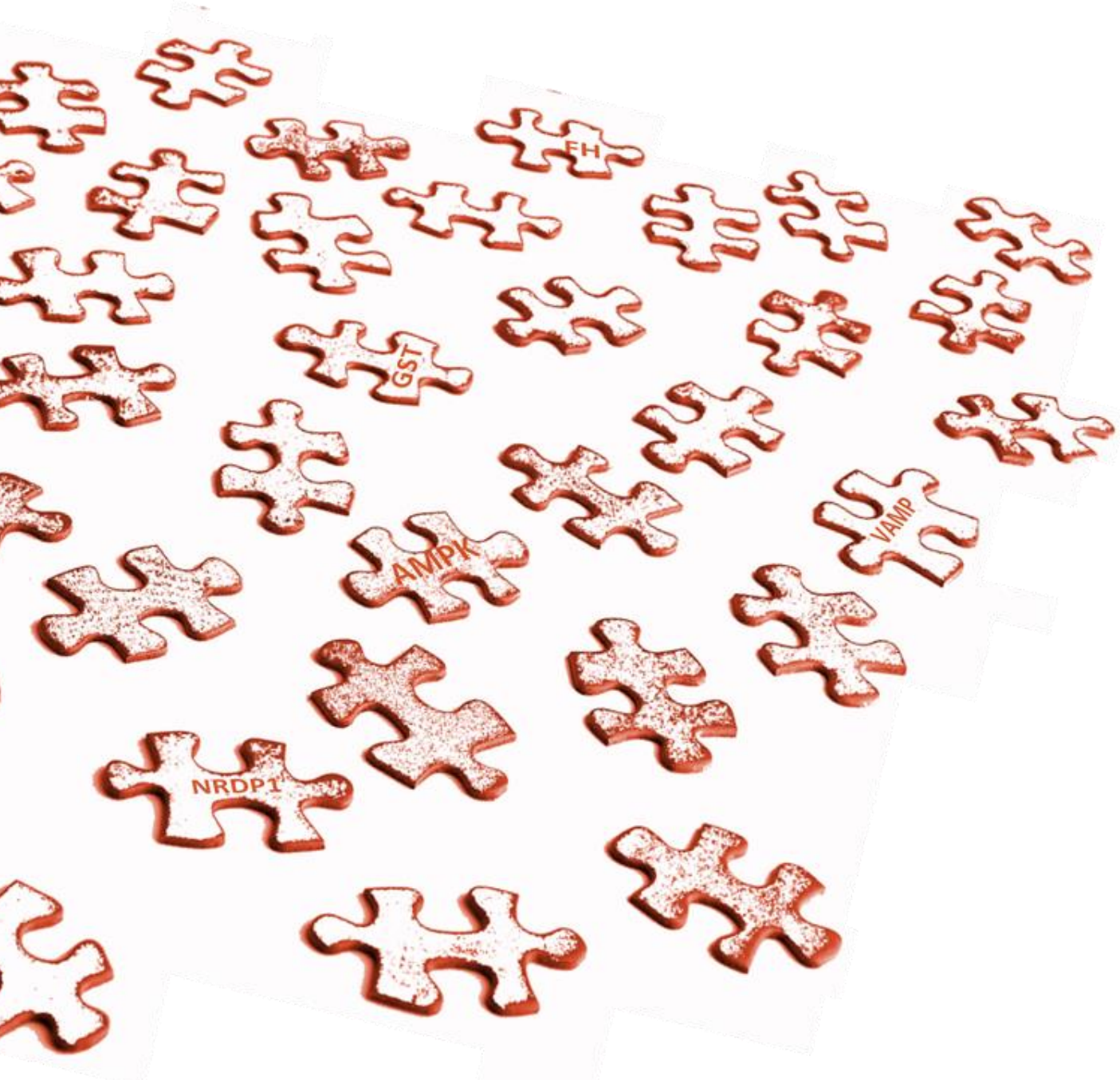

Conclusions and outlook

During the three-year work on this thesis, over 4000 articles have been published about AMPK. Although some of them identified new AMPK interaction partners and substrates (Liu et al., 2013; Um et al., 2013; Zhang et al., 2012), few have applied large scale screening to characterize the AMPK signaling network (Banko et al., 2011; Thali et al., 2010). This thesis provides confirmation and further functional characterization of several novel AMPK interaction partners and substrates which emerged from two large scale screens performed in the laboratory. First, a two dimensional *in vitro* screen combining surface plasmon resonance (SPR) with *in vitro* phosphorylation assays allowed identification fumarate hydratase (FH) as new putative AMPK substrate. Second, split-ubiquitin based cytosolic yeast two-hybrid (Y2H) systems combined with complementary interaction methods (split-Trp1 based Y2H, co-immunoprecipitation, SPR) led to the identification of two protein interaction partners of AMPK: E3 ubiquitin-ligase NRDP1 and vesicle-associated membrane proteins 2 and 3 (VAMP2/3). Finally, glutathione S-transferase (GST) was found to interact with AMPK during our interactomics research on AMPK. The kinase was pulled-down with recombinant proteins fused to a GST-tag and we could show that GST alone is sufficient to interact with AMPK. During this thesis, several of these putative AMPK interaction partners and substrates could be characterized in more detail, in particular concerning their functional role in the AMPK signaling network.

Analysis of the AMPK interactome

New protein interaction partners of the AMPK complex were identified in two large scale screening interactomic strategies: (1) A novel procedure combining SPR and phosphorylation assay, which revealed new AMPK-interacting substrates such as FH. (2) A cyto-Y2H screen for new interactions partners of AMPKβ1 and AMPKβ2, which led to identification of five putative AMPK protein interaction partners. The latter approach seems particularly interesting since it is not limited to AMPK substrates. Most work in this thesis was done with two candidates that emerged from this screen: NRDP1 and VAMP3.

Both screens yielded less candidates than anticipated. Probably, this relates to the high stringency that we applied, but also screening protocols could be improved. All investigated proteins occurred to be true positive interaction candidates. Our approach also indicates that high throughput interactomic methods, although giving valuable new insight, should be followed by targeted studies to verify the actual relationships e.g. between two interaction partners in a complex network. This may reveal very different roles of a given interaction, going from pure scaffolding functions to different kinds of mutual modifications involving one or both interacting proteins.

Glutathione S-transferase (GST)

The GST of *Schistosoma japonicum* (GST-Sj) commonly used as GST-tag, and the rat GST isoforms GSTM1 and GSTP1 were shown to interact with heterotrimeric AMPK via the N-terminal domain of the AMPK β-subunit in initial Y2H assays. Here we have confirmed the interaction between AMPK and GST by several independent procedures, such as pull-down and co-immunoprecipitation, SPR and Y2H. We have further investigated possible functions of this interaction, including putative phosphorylation and activation of GST by AMPK or glutathionylation and activation of AMPK by GST. We could show that formation of a GST/AMPK complex slightly increases GST activity and in turn GST glutathionylates AMPK, which increases AMPK activity. Such S-glutathionylation of AMPK leading to non-canonical full activation of AMPK under certain conditions could represent an additional layer of AMPK regulation. It would link AMPK signaling to redox regulation and position AMPK as a redox sensor. It has previously been shown *in vivo* that under highly oxidative conditions AMPK is glutathionylated and activated (Zmijewski et al., 2010). Here, we demonstrate *in vitro* that already under mildly oxidative conditions, GSTM1 and –P1 are able to catalyze AMPK glutathionylation. It is well established that reversible protein modification by glutathionylation could play a protective role against irreversible protein thiol oxidation which is usually associated with permanent loss of protein function and leads to protein degradation (Giustarini et al., 2004). Thus glutathionylation of AMPK in mildly oxidative conditions could be important for protecting AMPK. Further work should be done to demonstrate the significance of AMPK glutathionylation *in vivo* and to confirm the role of GST in this mechanism. To analyze the importance of AMPK glutathionylation, GST inhibitors like

ethacrynic acid (EA) or the peptidomimetic glutathione analog TLK199 ([γ-glutamyl-*S*-(benzyl)cysteinyl-*R*-phenyl glycine diethyl ester]) (Tew, 2007) could be used in cells *in vivo* under different oxidative conditions, followed by pull-down of glutathionylated proteins and Western blot analysis to detect AMPK.

Fumarate hydratase (FH)

Among the five putative AMPK substrates found by combining SPR and *in vitro* phosphorylation screening, fumarate hydratase (FH) was confirmed by co-immunoprecipitation and *in vitro* phosphorylation assays as AMPK interactor and substrate. FH phosphorylation by AMPK also affects its activity *in vitro* and in HeLa cells. However, after thorough phosphosite analysis by mass spectrometry (MS) and site-directed mutagenesis it appears that FH is primarily phosphorylated at serine 19 located in the cleavable mitochondrial transit or targeting peptide. FH is encoded by one unique nuclear gene and could be localized both to mitochondria or to cytosol (Yogev et al., 2011), and in mammals only the mitochondrial form contains the transit peptide. Phosphorylation of FH in the targeting peptide could thus affect its mitochondrial translocation and reduce the amount of mitochondrial FH. Activation of FH due to phosphorylation, as we initially observed, has to be reconsidered, since the phophorylatable residue is not present in the mature protein. Production of an antibody against phosphorylated serine 19 could provide a tool to study this process *in vivo*, but since lifetime of the native protein containing the targeting peptide is probably short, the phosphorylation may be difficult to observe. In addition, overexpression of wild type and S19A mutant FH could already give information on mitochondrial import efficiency by observation of FH localization (e.g. accumulation of FH-S19A in the cytosol).

E3 ubiquitin-ligase NRDP1 (NRDP1)

We describe here the first successful production of full-length NRDP1 protein. Previous attempts always yielded insoluble protein (Wu et al., 2004). We have also noticed the formation of a large proportion of inclusion bodies during NRDP1 production, but could reduce their formation and increase yield of soluble protein by reducing the temperature during

expression and applying bioreactor conditions. Bioreactor production yielded 3.1 mg of soluble NRDP1 protein per liter of culture.

Y2H analysis led to detection and confirmation of an interaction between NRDP1 and AMPK, and allowed to identify the C-terminal domain of NRDP1 and the N-terminal tail of the AMPK β-subunit as interaction domains. In an attempt to clarify the functional consequences of this interaction, we primarily analyzed phosphorylation and ubiquitination events. Ubiquitination assays in HEK293 cells showed that even though AMPK can be ubiquitinated *in vivo* (Zungu et al., 2011), this is no specific function of NRDP1. In contrast, NRDP1 is phosphorylated *in vitro*, but the low level as compared to the AMPK reference substrate acetyl-CoA carboxylase (ACC) makes it uncertain whether this is of physiological relevance.

Considering the high NRDP1 turnover rate caused by its strong autoubiquitination leading to proteasomal degradation, we have finally also investigated the effect of AMPK on cellular NRDP1 levels. We could show that in HeLa cells *in vivo*, AMPK overexpression reduces levels of NRDP1 by increasing its proteasomal degradation, probably via enhanced NRDP1 autoubiquitination, independent of phosphorylation by AMPK. These results suggest a role of AMPK in NRDP1 turnover, which might be due to (i) activating conformational changes within NRDP1, (ii) a NRDP1 scaffolding function of AMPK which recruits several NRDP1 proteins close to each other, or (iii) a role for AMPK in disrupting NRDP1 interactions with ubiquitin carboxyl-terminal hydrolase 8 (USP8), a major stabilizing NRDP1 protein (Avvakumov et al., 2006). At present, our work suggests a functional link between AMPK and NRDP1. However more work is needed to understand its putative function in NRDP1 down-regulation. Immunocytochemistry combined with confocal microscopy could be used to analyze NRDP1 localization in situations of AMPK overexpression. In addition work should be done to analyze the impact of NRDP1 downregulation on its targets.

Vesicle associate membrane protein (VAMP)

Interaction of VAMP2 and VAMP3 with AMPK was first shown by us in Y2H assays, and then confirmed by pull-down, co-immunoprecipitation and SPR. However VAMPs occurred not to be AMPK substrates. Further work on functional consequences of VAMP/AMPK interaction was less straight forward, since activity of VAMPs is relatively difficult to assess due to the fact

that VAMPs have no simple enzymatic activity but cellular sorting functions. To be able to investigate VAMP/AMPK interaction, we have mapped the interaction domain with the idea to disrupt the interaction *in vivo* and to analyze the effect at the cellular level.

Based on the mapping of the interaction domain, we decided to generate an AMPK β2 construct comprising the N-terminal VAMP interaction domain (amino acids 1-71) and the glycogen binding domain (amino acids 72-168), that we call the AMPK-βN domain. SPR confirmed the interaction between VAMP and AMPK and in addition demonstrated that the AMPK-βN domain is able to competitively inhibit the interaction. *In vitro*, a membrane fusion assay involving VAMP2 and its *in vivo* partner t-SNARE (SNAP25) showed that the AMPK/VAMP interaction does not interfere with the final VAMP-mediated fusion of vesicles with the plasma membrane, indicating that the role of VAMPs in AMPK interaction may be situated further upstream.

AMPK and VAMP2/3 are both implicated in translocation of glucose transporter GLUT4 and the long chain fatty acid (LCFA) transporter CD36 to the plasma membrane (Kurth-Kraczek et al., 1999; Martin et al., 1998; McGee et al., 2003; Schwenk et al., 2010; Webster et al., 2010). The mechanism of how AMPK regulates the translocation of these nutrient transporters is not entirely elucidated to date, and the interaction between VAMP and AMPK could be a major key to understand it. Therefore, the hypothesis should be tested whether VAMP represents a scaffold for AMPK, recruiting it to exocytotic vesicles. This would facilitate phosphorylation of AMPK substrates at the vesicle surface, such as AS160 (at serine 570 and 588 (Geraghty et al., 2007)), to induce vesicle transfer to the cellular periphery. According to this model, overexpression of AMPK-βN domain in eukaryotic cells should inhibit AMPK/VAMP interaction, reduce AS160 phosphorylation and thus reduce translocation of CD36 or GLUT4, observable by combining immunohistochemistry and confocal microscopy.

In addition to its implication in GLUT4 and CD36 translocation, AMPK/VAMP interaction could be of importance for other exocytotic processes that involve VAMP2 or VAMP3 like e.g. neurotransmitter release, and possibly also for other VAMPs that have not been tested for AMPK interaction. Such scaffolding mechanisms are relevant for understanding the role of AMPK localization which was first thought to be diffuse within the cytosol. AMPK secondary modifications have already been shown to localize AMPK in certain cellular compartment

(McGee et al., 2003; Oakhill et al., 2010; Suzuki et al., 2007); here we present a mechanism by which AMPK may be localized at specific sites via its interaction with another protein.

Novel AMPK interactors in the context of the known AMPK signaling network

The analysis of the four putative AMPK interacting proteins, GSTM1/GSTP1, FH; NRDP1 and VAMP2/VAMP3 confirmed all four as actual AMPK interactors, although the roles of the interactions seem to be very different in the four cases examined. The only interactor that is clearly downstream of AMPK is FH. Phosphorylation of FH within the mitochondrial targeting sequence strongly suggests a role of AMPK in FH translocation into mitochondria. Changing the charge of the transit peptide could influence its ability to pass through the mitochondrial membrane (part 4, p.79). Another interactor, GSTM1/GSTP1, is clearly upstream of AMPK, since it glutathionylates and activates the kinase. GST-facilitated-glutathionylation of AMPK adds a novel layer of complexity to AMPK activation, depending on the cellular redox state (part 3, p.49). The two other candidates, which were identified in the Y2H screen, NRDP1 and VAMP2/3, turned out not to be classical substrates. NRDP1 presents an example of a “cross-talk” protein; this cross-talk would affect cellular levels of NRDP1 (part 5, p.123). Finally, VAMP2/VAMP3 (part 6, p.157) may function as scaffold protein to recruit AMPK, thus possibly adding yet another layer of complexity to AMPK signaling by introducing specific cellular localization of AMPK. This interaction proposes a novel model for the role of AMPK in regulating nutrient uptake.

Taken together, the studies give new insight into regulation and role of AMPK and open several new perspectives for research in AMPK signaling.

References

Avvakumov, G.V., Walker, J.R., Xue, S., Finerty, P.J., Jr, Mackenzie, F., Newman, E.M., and Dhe-Paganon, S. (2006). Amino-terminal dimerization, NRDP1-rhodanese interaction, and inhibited catalytic domain conformation of the ubiquitin-specific protease 8 (USP8). J. Biol. Chem. *281*, 38061–38070.

Banko, M.R., Allen, J.J., Schaffer, B.E., Wilker, E.W., Tsou, P., White, J.L., Villén, J., Wang, B., Kim, S.R., Sakamoto, K., et al. (2011). Chemical genetic screen for AMPKα2 substrates uncovers a network of proteins involved in mitosis. Mol. Cell *44*, 878–892.

Geraghty, K.M., Chen, S., Harthill, J.E., Ibrahim, A.F., Toth, R., Morrice, N.A., Vandermoere, F., Moorhead, G.B., Hardie, D.G., and MacKintosh, C. (2007). Regulation of multisite phosphorylation and 14-3-3 binding of AS160 in response to IGF-1, EGF, PMA and AICAR. Biochem. J. *407*, 231–241.

Giustarini, D., Rossi, R., Milzani, A., Colombo, R., and Dalle-Donne, I. (2004). S-glutathionylation: from redox regulation of protein functions to human diseases. J. Cell. Mol. Med. *8*, 201–212.

Kurth-Kraczek, E.J., Hirshman, M.F., Goodyear, L.J., and Winder, W.W. (1999). 5' AMP-activated protein kinase activation causes GLUT4 translocation in skeletal muscle. Diabetes *48*, 1667–1671.

Liu, Y., Lai, Y.-C., Hill, E.V., Tyteca, D., Carpentier, S., Ingvaldsen, A., Vertommen, D., Lantier, L., Foretz, M., Dequiedt, F., et al. (2013). Phosphatidylinositol 3-phosphate 5-kinase (PIKfyve) is an AMPK target participating in contraction-stimulated glucose uptake in skeletal muscle. Biochem. J.

Martin, L.B., Shewan, A., Millar, C.A., Gould, G.W., and James, D.E. (1998). Vesicle-associated membrane protein 2 plays a specific role in the insulin-dependent trafficking of the facilitative glucose transporter GLUT4 in 3T3-L1 adipocytes. J. Biol. Chem. *273*, 1444–1452.

McGee, S.L., Howlett, K.F., Starkie, R.L., Cameron-Smith, D., Kemp, B.E., and Hargreaves, M. (2003). Exercise increases nuclear AMPK alpha2 in human skeletal muscle. Diabetes *52*, 926–928.

Oakhill, J.S., Chen, Z.-P., Scott, J.W., Steel, R., Castelli, L.A., Ling, N., Macaulay, S.L., and Kemp, B.E. (2010). β-Subunit myristoylation is the gatekeeper for initiating metabolic stress sensing by AMP-activated protein kinase (AMPK). Proc. Natl. Acad. Sci. U. S. A. *107*, 19237–19241.

Schwenk, R.W., Dirkx, E., Coumans, W.A., Bonen, A., Klip, A., Glatz, J.F.C., and Luiken, J.J.F.P. (2010). Requirement for distinct vesicle-associated membrane proteins in insulin- and AMP-activated protein kinase (AMPK)-induced translocation of GLUT4 and CD36 in cultured cardiomyocytes. Diabetologia *53*, 2209–2219.

Suzuki, A., Okamoto, S., Lee, S., Saito, K., Shiuchi, T., and Minokoshi, Y. (2007). Leptin stimulates fatty acid oxidation and peroxisome proliferator-activated receptor alpha gene expression in mouse C2C12 myoblasts by changing the subcellular localization of the alpha2 form of AMP-activated protein kinase. Mol. Cell. Biol. *27*, 4317–4327.

Tew, K.D. (2007). Redox in redux: Emergent roles for glutathione S-transferase P (GSTP) in regulation of cell signaling and S-glutathionylation. Biochem. Pharmacol. *73*, 1257–1269.

Thali, R.F., Tuerk, R.D., Scholz, R., Yoho-Auchli, Y., Brunisholz, R.A., and Neumann, D. (2010). Novel candidate substrates of AMP-activated protein kinase identified in red blood cell lysates. Biochem. Biophys. Res. Commun. *398*, 296–301.

Um, J.-H., Brown, A.L., Singh, S.K., Chen, Y., Gucek, M., Lee, B.-S., Luckey, M.A., Kim, M.K., Park, J.-H., Sleckman, B.P., et al. (2013). Metabolic sensor AMPK directly phosphorylates RAG1 protein and regulates V(D)J recombination. Proc. Natl. Acad. Sci. U. S. A. *110*, 9873–9878.

Webster, I., Friedrich, S.O., Lochner, A., and Huisamen, B. (2010). AMP kinase activation and glut4 translocation in isolated cardiomyocytes. Cardiovasc. J. Afr. *21*, 72–78.

Wu, X., Yen, L., Irwin, L., Sweeney, C., and Carraway, K.L., 3rd (2004). Stabilization of the E3 ubiquitin ligase Nrdp1 by the deubiquitinating enzyme USP8. Mol. Cell. Biol. *24*, 7748–7757.

Yogev, O., Naamati, A., and Pines, O. (2011). Fumarase: a paradigm of dual targeting and dual localized functions. FEBS J. *278*, 4230–4242.

Zhang, L., Yi, Y., Guo, Q., Sun, Y., Ma, S., Xiao, S., Geng, J., Zheng, Z., and Song, S. (2012). Hsp90 interacts with AMPK and mediates acetyl-CoA carboxylase phosphorylation. Cell. Signal. *24*, 859–865.

Zmijewski, J.W., Banerjee, S., Bae, H., Friggeri, A., Lazarowski, E.R., and Abraham, E. (2010). Exposure to hydrogen peroxide induces oxidation and activation of AMP-activated protein kinase. J. Biol. Chem. *285*, 33154–33164.

Zungu, M., Schisler, J.C., Essop, M.F., McCudden, C., Patterson, C., and Willis, M.S. (2011). Regulation of AMPK by the ubiquitin proteasome system. Am. J. Pathol. *178*, 4–11.

PART 7

Conclusions & Perspectives

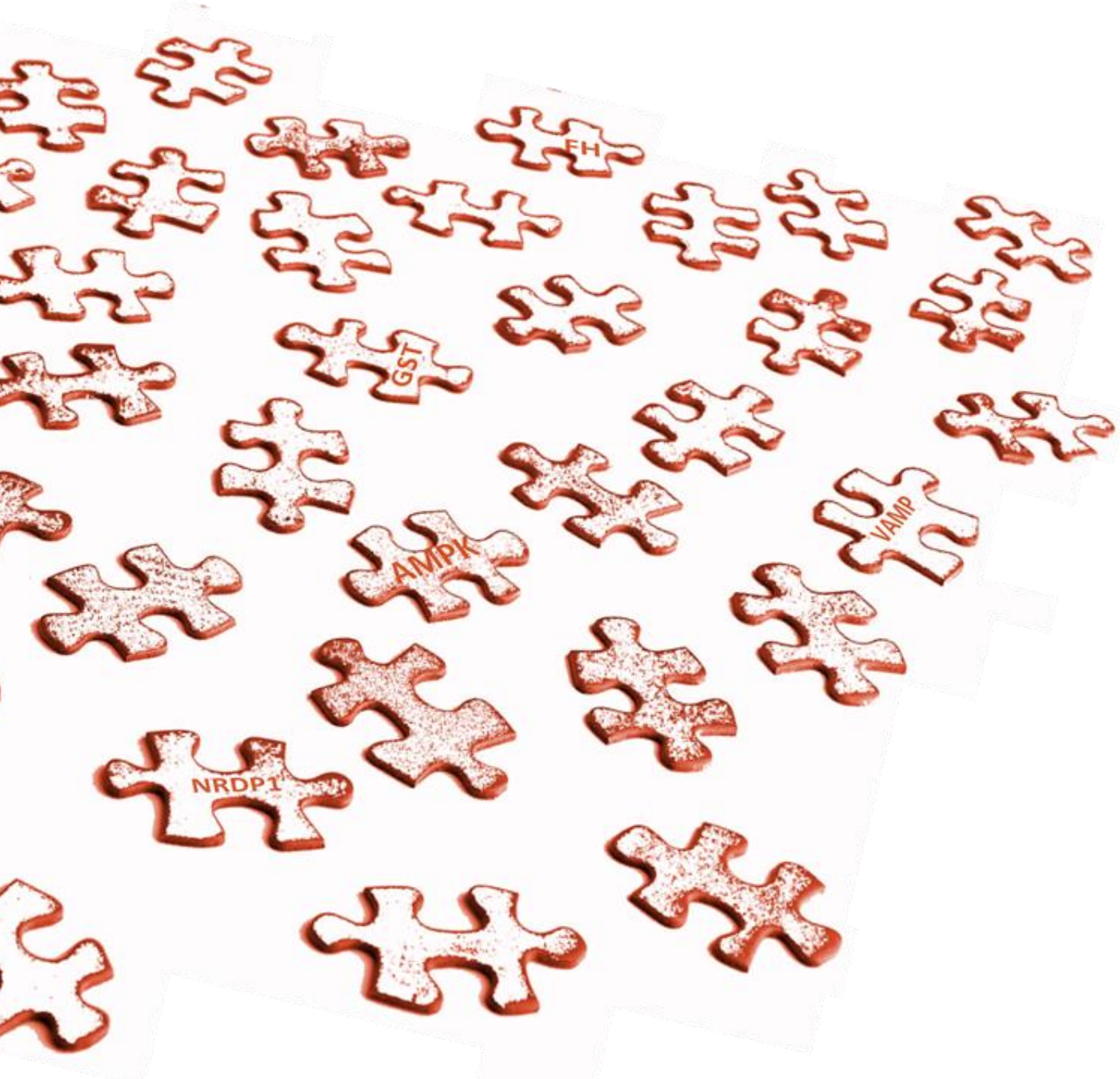

Conclusions et perspectives

Durant les trois ans qu'a duré ce travail de thèse, plus de 4000 articles en lien avec l'AMPK ont été publiés. Même si quelques-uns ont permis l'identification de nouveaux interacteurs et substrats de l'AMPK (Liu et al., 2013; Um et al., 2013; Zhang et al., 2012), peu ont appliqué des criblages à grande échelle afin de caractériser les voies de signalisation de l'AMPK (Banko et al., 2011; Thali et al., 2010). Cette thèse a permis la confirmation ainsi que la caractérisation fonctionnelle de nouveaux partenaires d'interactions et substrats de l'AMPK provenant de deux criblages interactomique sans à priori réalisé dans le laboratoire. Premièrement, un criblage *in vitro* à deux dimensions combinant résonance plasmon de surface (SPR) avec des essais de phosphorylation *in vitro* a permis l'identification de nouveaux substrats putatifs de l'AMPK tel que la fumarate hydratase (FH). Par la suite, un système de double hybride cytosolique en levure (Y2H, basé sur une split-ubiquitine) combiné avec des méthodes complémentaires de confirmation d'interactions protéine/protéine (Y2H basé sur un split-Trp1, co-immunoprecipitation, SPR) a conduit à la découverte de deux partenaires d'interaction de l'AMPK : l'E3 ubiquitine-ligase NRDP1 et les protéines associées à la membrane des vésicules VAMP2 et VAMP3. Finalement, la gluthation S-transferase (GST) a été identifiée comme interacteur de l'AMPK au cours de recherches interactomiques dans lesquelles nous avons fait des pull-down entre l'AMPK et des protéines recombinantes contenant un tag GST. Nous avons alors montré que le tag GST interagissait directement avec l'AMPK. Au cours de cette thèse, ces partenaires d'interaction et substrats de l'AMPK ont été caractérisés en détail, en particulier pour leurs fonctions dans les voies de signalisation de l'AMPK.

Analyse de l'interactome d'AMPK

De nouvelles protéines partenaire d'interaction de l'AMPK ont été identifiées par deux stratégies de criblage interactomique : (1) une nouvelle procédure combinant SPR et essais de phosphorylation a permis la détection de nouveaux substrats interagissant avec l'AMPK tel que FH ; (2) un criblage Y2H cytosolique à la recherche de nouveaux partenaires de AMPKβ1 et AMPKβ2 a conduit à l'identification de 5 interacteurs putatifs de l'AMPK. Cette deuxième

approche fut particulièrement intéressante, car ne se limitant pas à la recherche de substrats d'AMPK. Une grosse partie du travail de cette thèse est basée sur deux candidats établis par ce criblage : NRDP1 et VAMP3.

Les deux criblages ont conduit à peu de candidats par rapport à ce que nous attendions. La sélectivité avec laquelle nous avons validé les candidats explique pour partie leur faible nombre, même si les protocoles appliqués pour le criblage pourraient également être améliorés. Toutes les protéines sélectionnées ont été confirmées comme réels interacteurs de l'AMPK. De plus, nos données montrent aussi que l'analyse ne peut pas se limiter à des approches d'interactomique à haut débit mais doivent être suivies par des études ciblées afin de vérifier la relation comme par exemple celle entre deux partenaires d'interaction au sein d'un réseau complexe de signalisation. Ces études ciblées peuvent révéler des rôles très différents pour une interaction, allant d'une fonction de recrutement à différents types de modifications venant de l'une ou même des deux protéines interagissant.

Glutathion S-transferase (GST)

Nous avons montré par un premier essai de Y2H que la protéine GST de *Schistosoma japonicum* (GST-Sj), communément utilisée comme tag GST, et les isoformes GST de rat GSTM1 et GSTP1 interagissent avec l'hétérotrimère AMPK via le domaine N-terminal de la sous-unité β de l'AMPK. Ici nous avons confirmé l'interaction entre l'AMPK et GST par plusieurs procédures indépendantes telles que par pull-down et co-immunoprecipitation, mais également par SPR et Y2H. Nous avons ensuite recherché les fonctions possibles de l'interaction, notamment la possible phosphorylation et activation de GST par l'AMPK ainsi que la possible glutathionylation et activation de l'AMPK par GST. Nous avons pu montrer que la formation du complexe GST/AMPK augmente légèrement l'activité GST, en retour GST glutathionyle AMPK, augmentant ainsi son activité. Une telle S-glutathionylation de l'AMPK conduit à son activation de façon non-canonique, dans certaines conditions rajoute un niveau de complexité liant la régulation AMPK à la signalisation redox, et possiblement positionne AMPK comme senseur du stress oxydant. Une étude *in vivo* a précédemment montré que dans des conditions fortement oxydatives l'AMPK est glutathionylée et activée (Zmijewski et al., 2010). Ici nous démontrons qu'in *vitro* dans des conditions d'oxydation moyenne, GSTM1 et

GSTP1 favorisent une glutathionylation d'AMPK. De plus, la glutathionylation (qui est une modification réversible) peut jouer un rôle protecteur contre d'irréversibles oxydations des thiols de la protéine, qui sont en général associées avec une perte permanente de la fonction et qui conduisent à sa dégradation (Giustarini et al., 2004). Ainsi la glutathionylation de l'AMPK dans des conditions moyennes d'oxydation peut être essentielle pour protéger l'AMPK. Un travail plus poussé est nécessaire pour démontrer l'importance du mécanisme de glutathionylation d'AMPK *in vivo* et pour confirmer l'implication de GST dans ce mécanisme. Pour ce faire des inhibiteurs de GST (l'acide ethacrynique et l'analogue peptidomimétique du glutathion TLK199 [γ-glutamyle-*S*-(benzyl)cysteinyle-*R*-phenyle glycine diethyle ester]) (Tew, 2007) pourraient être utilisés sur des cellules *in vivo* dans différentes conditions oxydatives, suivi par le pull-down de protéines glutathionylées et Western blot pour la détection de l'AMPK.

Fumarate hydratase (FH)

Parmi les cinq substrats putatifs de l'AMPK trouvés en combinant SPR et par criblage de phosphorylation *in vitro*, fumarate hydratase (FH) a été confirmée par co-immunoprecipitation et phosphorylation *in vitro* comme interacteur et substrat direct de l'AMPK. La phosphorylation de FH par l'AMPK affecte son activité *in vitro* et dans les cellules HeLa. Cependant, la recherche minutieuse de phosphosites par spectrométrie de masse (MS) et mutagenèse dirigée a révélé que FH est principalement phosphorylée au niveau de la serine 19, localisée au niveau du peptide signal mitochondrial clivé dans la protéine mature. FH est codée par un unique gène nucléaire et peut être localisée aussi bien au niveau de la mitochondrie que du cytosol (Yogev et al., 2011). Chez les mammifères, seule la forme mitochondriale contient le peptide signal. La phosphorylation de FH au niveau du peptide signal pourrait affecter la translocation mitochondriale, en réduisant par exemple la quantité de FH mitochondriale. D'un autre côté, l'activation de FH due à la phosphorylation doit être reconsidérée en tenant compte de l'absence du résidu phosphorylable dans la protéine mature. La production d'un anticorps contre la serine 19 phosphorylée serait un outil pour son étude *in vivo*, mais considérant que la durée de vie de la protéine native contenant le peptide signal est probablement très courte, la phosphorylation est surement difficile à observer. De plus La surexpression de FH sauvage et d'un mutant FH en S19A pourrait donner

de premières informations sur l'implication de S19 dans l'import mitochondrial par l'observation de la localisation (ex. : accumulation de FH-S19A dans le cytosol).

E3 ubiquitine-ligase NRDP1 (NRDP1)

Nous donnons ici pour la première fois un protocole pour la production de la protéine NRDP1 complète qui avait jusque-là toujours été décrite comme conduisant à la production de protéine insoluble (Wu et al., 2004). Nous avons également remarqué la formation en grande proportion de corps d'inclusions lors de la production de NRDP1, mais nous avons pu réduire leur formation et augmenter le rendement de protéine soluble en baissant la température durant l'expression, et par l'utilisation d'un bioréacteur. La production en bioréacteur permet d'obtenir 3,1 mg de protéine NRDP1 soluble par litre de culture.

L'analyse en Y2H a conduit à la détection et la confirmation de l'interaction entre NRDP1 et AMPK, et permet de déterminer les domaines d'interaction telle que le domaine C-terminal pour NRDP1 et le domaine N-terminal de la sous-unité β de l'AMPK. Dans le but de découvrir les conséquences fonctionnelles de cette interaction, nous avons premièrement analysé la phosphorylation et l'ubiquitination. Les essais d'ubiquitination dans les cellules HEK293 ont montré que bien qu' AMPK puisse être ubiquitinylée *in vivo* (Zungu et al., 2011) cette fonction n'est pas régulée de façon spécifique par NRDP1. D'un autre côté, NRDP1 est phosphorylée *in vitro* mais a un faible niveau comparé à l'acetyl-CoA carboxylase (ACC) – substrat de référence de l'AMPK – ce qui rend sa pertinence physiologique incertaine.

En considérant le haut taux de renouvellement de NRDP1 du à son importante autoubiquitination (qui conduit à sa dégradation par le protéasome) nous avons finalement étudié l'effet de l'AMPK sur le niveau cellulaire de NRDP1. *In vivo*, la surexpression d'AMPK dans les cellules HeLa réduit le niveau de NRDP1 en augmentant sa dégradation par le protéasome, probablement en augmentant l'autoubiquitination de NRDP1. Ce phénomène est indépendant de la phosphorylation par l'AMPK. Ces résultats suggèrent un rôle de l'AMPK dans le renouvellement de NRDP1, qui peut être causé par (i) des changements conformationnels de NRDP1 causant son activation ; (ii) un recrutement de NRDP1 par l'AMPK, positionnant les protéines NRDP1 proches les unes des autres ; (iii) la perturbation *via* l'AMPK de l'interaction entre NRDP1 et l'ubiquitine carboxyl-terminal hydrolase 8 (USP8, une protéine

majeure pour la stabilisation de NRDP1) (Avvakumov et al., 2006). Notre travail suggère un lien entre AMPK et NRDP1, même si plus de travail est nécessaire pour comprendre son rôle *in vivo* et la fonction de cette diminution du niveau NRDP1. L'immunohistochimie combinée avec de la microscopie confocale pourrait être utilisée pour l'analyse de la localisation de NRDP1 dans différentes conditions de surexpression AMPK. De plus, un travail d'analyse de l'impact de la diminution du niveau NRDP1 sur ses cibles serait très intéressant.

Protéine associée à la membrane des vésicules (VAMP)

Nous avons pour la première fois montré l'interaction entre VAMP2, VAMP3 et l'AMPK par un essai Y2H, confirmés ensuite par pull-down, co-immunoprecipitation et SPR. VAMPs ne sont pas des substrats de l'AMPK. Un travail plus poussé sur les conséquences fonctionnelles de l'interaction VAMP/AMPK est complexifié du fait que VAMP n'ait pas d'activité enzymatique mais plutôt des fonctions de tri. Afin de pouvoir étudier l'interaction VAMP/AMPK, nous avons cartographié le domaine d'interaction avec l'idée de pouvoir gêner l'interaction *in vivo* et d'analyser l'effet au niveau cellulaire.

En se basant sur la cartographie des domaines d'interaction, nous avons décidé de générer une construction à partir de la sous-unité β2 de l'AMPK comprenant le domaine N-terminal interagissant avec VAMP (acides aminés 1-71) et le « glycogen binding domain » (acides aminés 72-168), construction que nous avons appelée « domaine AMPK-βN ». La SPR confirme l'interaction entre VAMP et AMPK et démontre également que notre domaine AMPK-βN est capable d'inhiber de façon compétitive cette interaction. *In vitro*, un essai de fusion de membrane impliquant VAMP2 et son partenaire *in vivo* t-SNARE (SNAP25) montre que l'interaction AMPK/VAMP n'interfère pas avec l'étape finale de fusion prise en charge par VAMP, indiquant que le rôle de VAMPs dans son interaction avec AMPK se trouve surement en amont.

AMPK et VAMP2/3 sont impliquées dans la translocation à la membrane plasmique du transporteur de glucose GLUT4 et du transporter CD36 (long chain fatty acid, LCFA; Kurth-Kraczek et al., 1999; Martin et al., 1998; McGee et al., 2003; Schwenk et al., 2010; Webster et al., 2010). Le mécanisme par lequel AMPK régule la translocation de ces transporteurs de nutriments n'est pour le moment pas entièrement élucidé, et l'interaction entre VAMP et

AMPK pourrait jouer un rôle majeur. A ce niveau, l'hypothèse à tester est que VAMP serait une protéine de recrutement (« scaffold ») de l'AMPK vers les vésicules en exocytose, facilitant ainsi la phosphorylation de substrat de l'AMPK tel que AS160 (sur la serine 570 et 588 (Geraghty et al., 2007)) au niveau de ces vésicules pour induire leur transfert à la périphérie cellulaire. En se basant sur ce modèle, la surexpression du domaine AMPK-βN dans des cellules eucaryotes (inhibant l'interaction AMPK/VAMP) devrait réduire la phosphorylation d'AS160 et ainsi réduire la translocation de CD36 et GLUT4, observable en combinant immunocytochimie et microscopie confocale.

Finalement, en plus de son implication dans la translocation GLUT4 et CD36, l'interaction AMPK/VAMP peut être importante pour d'autre procédés exocytotiques impliquant VAMP2 et VAMP3 (par exemple la libération de neurotransmetteurs) et ceci pourrait aussi inclure d'autres VAMPs que nous n'avons pour le moment pas testées pour leur interaction avec AMPK. Un tel mécanisme de recrutement de l'AMPK est important pour comprendre le rôle de sa localisation, qui était en premier lieu considérée diffuse dans le cytosol. Des modifications secondaires de l'AMPK ont déjà été montrées comme localisant AMPK dans certains compartiments cellulaires (McGee et al., 2003; Oakhill et al., 2010; Suzuki et al., 2007). Nous présentons ici un mécanisme par lequel AMPK serait localisée à des sites spécifiques *via* son interaction avec une autre protéine.

De nouveaux interacteurs de l'AMPK dans le contexte de ses voies de signalisation

L'analyse des quatre interacteurs putatifs de l'AMPK, GSTM1/GSTP1, FH, NRDP1 and VAMP2/3 les a confirmés comme interacteurs avérés de l'AMPK, avec pour les quatre interactions un rôle extrêmement différent. Le seul interacteur clairement en aval d'AMPK est FH. La phosphorylation de FH au niveau du peptide signal suggère fortement un rôle d'AMPK dans la translocation FH mitochondrial. En changeant la charge du peptide signal, AMPK peut influencer sa propension à passer à travers la membrane mitochondriale (partie 4, p.79). L'interacteur GSTM1/P1 est clairement en amont d'AMPK, étant donné qu'il glutathionyle et active la kinase. La glutathionylation d'AMPK, facilitée par GST, ajoute un nouveau niveau de complexité dans l'activation de l'AMPK dépendant de l'état redox de la cellule (partie 3, p.49). Les deux autres candidats tirés du criblage Y2H, NRDP1 et VAMP2/3, se sont révélés ne pas

être des substrats classiques de l'AMPK. NRDP1 présente un exemple de protéine « cross-talk », ce dernier affecterait le niveau cellulaire de NRDP1 (partie 5, p.123). Finalement, VAMP2/3 (partie 6, p.159) aurait une fonction de protéine « scaffold » recrutant l'AMPK, ainsi probablement ajoutant un niveau de complexité à la signalisation AMPK en introduisant un aspect de localisation cellulaire. Cette dernière interaction supporte un nouveau mécanisme pour la régulation de l'assimilation des nutriments via l'AMPK.

Globalement, ces études donnent un nouvel aperçu dans la régulation et le rôle de l'AMPK et ouvrent plusieurs nouvelles perspectives pour la recherche sur la signalisation AMPK.

Références

Avvakumov, G.V., Walker, J.R., Xue, S., Finerty, P.J., Jr, Mackenzie, F., Newman, E.M., and Dhe-Paganon, S. (2006). Amino-terminal dimerization, NRDP1-rhodanese interaction, and inhibited catalytic domain conformation of the ubiquitin-specific protease 8 (USP8). J. Biol. Chem. *281*, 38061–38070.

Banko, M.R., Allen, J.J., Schaffer, B.E., Wilker, E.W., Tsou, P., White, J.L., Villén, J., Wang, B., Kim, S.R., Sakamoto, K., et al. (2011). Chemical genetic screen for AMPKα2 substrates uncovers a network of proteins involved in mitosis. Mol. Cell *44*, 878–892.

Geraghty, K.M., Chen, S., Harthill, J.E., Ibrahim, A.F., Toth, R., Morrice, N.A., Vandermoere, F., Moorhead, G.B., Hardie, D.G., and MacKintosh, C. (2007). Regulation of multisite phosphorylation and 14-3-3 binding of AS160 in response to IGF-1, EGF, PMA and AICAR. Biochem. J. *407*, 231–241.

Giustarini, D., Rossi, R., Milzani, A., Colombo, R., and Dalle-Donne, I. (2004). S-glutathionylation: from redox regulation of protein functions to human diseases. J. Cell. Mol. Med. *8*, 201–212.

Kurth-Kraczek, E.J., Hirshman, M.F., Goodyear, L.J., and Winder, W.W. (1999). 5' AMP-activated protein kinase activation causes GLUT4 translocation in skeletal muscle. Diabetes *48*, 1667–1671.

Liu, Y., Lai, Y.-C., Hill, E.V., Tyteca, D., Carpentier, S., Ingvaldsen, A., Vertommen, D., Lantier, L., Foretz, M., Dequiedt, F., et al. (2013). Phosphatidylinositol 3-phosphate 5-kinase (PIKfyve) is an AMPK target participating in contraction-stimulated glucose uptake in skeletal muscle. Biochem. J.

Martin, L.B., Shewan, A., Millar, C.A., Gould, G.W., and James, D.E. (1998). Vesicle-associated membrane protein 2 plays a specific role in the insulin-dependent trafficking of the facilitative glucose transporter GLUT4 in 3T3-L1 adipocytes. J. Biol. Chem. *273*, 1444–1452.

McGee, S.L., Howlett, K.F., Starkie, R.L., Cameron-Smith, D., Kemp, B.E., and Hargreaves, M. (2003). Exercise increases nuclear AMPK alpha2 in human skeletal muscle. Diabetes *52*, 926–928.

Oakhill, J.S., Chen, Z.-P., Scott, J.W., Steel, R., Castelli, L.A., Ling, N., Macaulay, S.L., and Kemp, B.E. (2010). β-Subunit myristoylation is the gatekeeper for initiating metabolic stress sensing by AMP-activated protein kinase (AMPK). Proc. Natl. Acad. Sci. U. S. A. *107*, 19237–19241.

Schwenk, R.W., Dirkx, E., Coumans, W.A., Bonen, A., Klip, A., Glatz, J.F.C., and Luiken, J.J.F.P. (2010). Requirement for distinct vesicle-associated membrane proteins in insulin- and AMP-activated protein kinase (AMPK)-induced translocation of GLUT4 and CD36 in cultured cardiomyocytes. Diabetologia *53*, 2209–2219.

Suzuki, A., Okamoto, S., Lee, S., Saito, K., Shiuchi, T., and Minokoshi, Y. (2007). Leptin stimulates fatty acid oxidation and peroxisome proliferator-activated receptor alpha gene expression in mouse C2C12 myoblasts by changing the subcellular localization of the alpha2 form of AMP-activated protein kinase. Mol. Cell. Biol. *27*, 4317–4327.

Tew, K.D. (2007). Redox in redux: Emergent roles for glutathione S-transferase P (GSTP) in regulation of cell signaling and S-glutathionylation. Biochem. Pharmacol. *73*, 1257–1269.

Thali, R.F., Tuerk, R.D., Scholz, R., Yoho-Auchli, Y., Brunisholz, R.A., and Neumann, D. (2010). Novel candidate substrates of AMP-activated protein kinase identified in red blood cell lysates. Biochem. Biophys. Res. Commun. *398*, 296–301.

Um, J.-H., Brown, A.L., Singh, S.K., Chen, Y., Gucek, M., Lee, B.-S., Luckey, M.A., Kim, M.K., Park, J.-H., Sleckman, B.P., et al. (2013). Metabolic sensor AMPK directly phosphorylates RAG1 protein and regulates V(D)J recombination. Proc. Natl. Acad. Sci. U. S. A. *110*, 9873–9878.

Webster, I., Friedrich, S.O., Lochner, A., and Huisamen, B. (2010). AMP kinase activation and glut4 translocation in isolated cardiomyocytes. Cardiovasc. J. Afr. *21*, 72–78.

Wu, X., Yen, L., Irwin, L., Sweeney, C., and Carraway, K.L., 3rd (2004). Stabilization of the E3 ubiquitin ligase Nrdp1 by the deubiquitinating enzyme USP8. Mol. Cell. Biol. *24*, 7748–7757.

Yogev, O., Naamati, A., and Pines, O. (2011). Fumarase: a paradigm of dual targeting and dual localized functions. FEBS J. *278*, 4230–4242.

Zhang, L., Yi, Y., Guo, Q., Sun, Y., Ma, S., Xiao, S., Geng, J., Zheng, Z., and Song, S. (2012). Hsp90 interacts with AMPK and mediates acetyl-CoA carboxylase phosphorylation. Cell. Signal. *24*, 859–865.

Zmijewski, J.W., Banerjee, S., Bae, H., Friggeri, A., Lazarowski, E.R., and Abraham, E. (2010). Exposure to hydrogen peroxide induces oxidation and activation of AMP-activated protein kinase. J. Biol. Chem. *285*, 33154–33164.

Zungu, M., Schisler, J.C., Essop, M.F., McCudden, C., Patterson, C., and Willis, M.S. (2011). Regulation of AMPK by the ubiquitin proteasome system. Am. J. Pathol. *178*, 4–11.